# Cellular Processes in the Induction of Embryonic Stem Cell Differentiation into Neural Crest Cell Derivatives

Stuart John Fielding

A thesis submitted in partial fulfilment of the requirements of the Manchester Metropolitan University for the degree of Doctor of Philosophy

School of Healthcare Science the Manchester Metropolitan University

October 2015

## Chapter 2: Materials and Methods



## Chapter 3: Growth and Differentiation of E14 Mouse Embryonic Stem Cells.

## Chapter 4: Transcriptional Analysis of Neural Crest Derived Peripheral Neuron Differentiation from Mouse Embryonic Stem Cells.



## Chapter 5: Characterisation of Neural Crest Derived Peripheral Neurons Differentiated from Mouse Embryonic Stem Cells



## Chapter 6: Proteomic Analyses and Noggin Inhibition of BMP-4 in the Differentiation of E14 Mouse Embryonic Stem Cells

## List of abbreviations

| | |
|---|---|
| APS | ammonium persulphate |
| ATP | adenosine triphosphate |
| BLAST | basic local alignment search tool |
| BMP protein) | bone morphogenetic protein (sometimes bone morphogenic |
| BDGF | brain derived growth factor |
| BSA | bovine serum albumin |
| cDNA | complimentary deoxyribonucleic acid |
| CHARGE | coloboma, heart defect, atresia choanae (also known as choanal atresia), retarded growth and development, genital abnormality, and ear abnormality |
| CIL | contact inhibition of locomotion |
| CM | complete media |
| DAPI | 4', 6-diamidino-2-phenylindole |
| DMSO | dimethyl sulphoxide |
| DNA | deoxyribonucleic acid |
| DNMT3B | DNA methyltransferase 3B |
| dNTP | deoxynucleotide triphosphate |
| Dppa | developmental pluripotency associated |
| (D)PBS | (Dulbecco's) phosphate buffered saline |
| EBI | European Bioinformatics Institute |
| EDTA | Ethylenediaminetetraacetic acid |
| EMT | epithelial to mesenchymal transition |
| ESC | embryonic stem cell(s) |
| FCS | foetal calf serum |
| FGF | fibroblast growth factor |
| FGFR | fibroblast growth factor receptor |
| GABA | gamma amino-butyric acid |
| GFAP | glial fibrillary acidic protein |
| GP-130 | glycoprotein 130 |
| HAT | histone acetyl transferase |

| | |
|---|---|
| HDAC | histone deacetylase |
| Hox | homeobox |
| IM | inhibition media |
| IPSC | induced pluripotent stem cell(s) |
| KEGG | Kyoto Encyclopaedia of Genes and Genomes |
| (KO) DMEM | (knockout) Dulbecco's modified eagle's medium |
| LIF | leukaemia inhibitory factor |
| MACS | magnetic activated cell sorting |
| MEA | microelectrode array |
| MSC | myelinating Schwann cell |
| MPNST | malignant peripheral nerve sheath tumours |
| MRTFB | Myocardin-related transcription factor B |
| MUSCLE | multiple sequence alignment by log expectation |
| NC | neural crest |
| NCBI | National Centre for Biotechnology Information |
| NCC | neural crest cell(s) |
| NEAA | non-essential amino acids |
| NGR | neuregulin |
| NMDA | N-methyl-D-aspartate |
| NMSC | non-myelinating Schwann cell |
| NT | neurotrophin |
| PAGE | polyacrylamide gel electrophoresis |
| Pax | paired box |
| PBS | phosphate buffered saline |
| PCA | principle component analysis |
| PCR | polymerase chain reaction |
| PI | propidium iodide |
| PIM | primary induction media |
| PSC | perisynaptic Schwann cell |
| PNS | peripheral nervous system |
| PcG | polycomb group |
| QC | quality control |

| | |
|---|---|
| RIPA | radioimmunoprecipitation assay |
| RNA | ribonucleic acid |
| Rt-qPCR | real time quantitative PCR |
| SostC1 | Sclerostin Domain Containing 1 |
| SDS | sodium dodecyl sulphate |
| SEM | standard error of the mean |
| Shh | Sonic Hedgehog |
| SIM | secondary induction media |
| Sox | sex determining high mobility group box |
| SM | smooth muscle media |
| SSEA | stage specific embryonic antigen |
| STAT | signal transducer and activator of transcription |
| SDIA | stromal derived inducing activity |
| SNP | single nucleotide polymorphism |
| TBE | tris-boric acid-EDTA |
| TEMED | tetramethylethylenediamine |
| TGF | transforming growth factor |
| TrK | tyrosine kinase |

## List of Figures

## List of Tables

# Abstract

Neural crest induction and migration is the culmination of an intricate network of signalling from both the ectoderm and underlying mesoderm. Due to the transient nature of the neural crest, little is known about the specific interactions of growth factors and morphogens required for correct patterning.

Neural crest stem cells were differentiated from embryonic stem cells in serum-free feeder-free culture conditions. Cells were further differentiated into functional peripheral neurons, expressing the synaptic protein neurexin3, able to spontaneously generate action potentials and showing responses to the neuroactive compounds GABA and NMDA.

Microarray analyses and subsequent RT-qPCR experiments revealed that gene expression of the key pluripotency associated factor *Oct-4* was initially downregulated upon differentiation before expression levels increased as cells developed into a neural crest phenotype. Further experiments indicated an intrinsic role for bone morphogenetic protein-4 (BMP-4) in mediating this resurgence of expression. In addition to BMP-4 influenced expression of *Nanog*, members of the developmental pluripotency associated *family* of genes and important adhesion molecules with roles in the epithelial to mesenchymal transition of the neural crest.

Global gene expression profiling of differentiating functional neurons offers new insights into BMP-4 mediated patterning of the neural crest and peripheral nervous system during development. This study implicates BMP-4 as a key factor in neural crest differentiation, with a role in diverse cellular processes including proliferation, fate determination and cell migration. The role of BMP-4 in mediating expression of pluripotency and adhesion factors highlights a potential role in oncogenesis; neural crest cells share many phenotypic traits with cancer cells. Finally, the generation of functional peripheral neurons in feeder free culture conditions offers a reliable method for the recapitulation of these tissues and the possibility of use in future tissue replacement therapy.

## Declaration

I declare that no portion of the work referred to in this thesis has been submitted in support of an application for another degree or qualification of this or any other university or institute of learning.

# Acknowledgements

First and foremost, I would like to thank my supervisory team. Profound thanks to my director of studies Dr. Qiuyu Wang for giving me the opportunity to pursue my studies, supporting me and advising me throughout my time at MMU and for patiently reading the endless drafts of my thesis. I would also like to extend my thanks to Dr. Lisa Lee Jones for her encouragement, advice and occasional haranguing when the situation demanded. I am grateful for the technical advice and support offered to me by Dr. Chris Murgatroyd whose insights were of great help. Thanks are due to Professor Shant Kumar for providing me with the opportunity and for the advice and encouragement throughout the course of my studies and Professor William Gilmore for his technical advice.

I would like to thank Dr. Michael Carrol and Professor Mark Slevin both for their advice and for introducing me to the dubious delights of Fab Café. Dr. Louise Melling and Dr. Ruth Shepherd for equipment loans, random chats and sharing your technical knowledge. Special thanks must go to Glenn Ferris without who I (and probably every other research student) would have floundered in the laboratories. I would like to thank Dr. Llwyd Orton for his advice on electrophysiology and for his seamless integration into our squad.

I would like to offer my appreciation to Manal and Ali who were so welcoming when I first arrived in the lab as well as Kamella for being such a delight, Yasmin for the green tea, Donghui for trying to teach me Mandarin, Fiona, Ria and Catherine for advice and encouragement.

Finally the Science Squad, the reprobates who have shared the highs and lows in the life of a research student. Nicola (with me in this from the start), Clare (our social conscience), Steve (PCR boys forever), Yoann (king of the mountains), Jonathan (for bringing the crazy), Sander (lunch games champion), Arjun (for being even worse than I am at bowling and pool), María (For invaluable formatting assistance), Alex (for the family picture).

Special thanks to Jade “Little Vesuvius” Lai and Mia “Baroness Smaug” Tomova for (amongst other things). Fab Fridays, radgeball, oink joy, poetry, adventures, minesweeping, the inviable rules of RC, gains, raiderschlager and helping me maintain my sanity.

# Chapter 1: Introduction

## 1.1 Embryonic Stem Cells

Embryonic stem cells (ESCs) are derived from the inner cell mass of late stage blastocysts (Figure 1.1). It is possible to culture these cells indefinitely in an undifferentiated state, either by growing on a feeder layer of murine embryonic fibroblast cells, or in the presence of leukaemia inhibitory factor (LIF) and serum (Martin, 1981; Williams, *et al*., 1988; Thomson, *et al*., 1998). Embryonic stem cells are capable of recapitulating any tissue in the mammalian body and as such are described as being pluripotent. (Martin, 1981)

Leukaemia inhibitory factor mediated maintenance of pluripotency occurs through interaction with low affinity receptors coupled to the GP-130 (glycoprotein-130) transmembrane protein. A signal transduction cascade is subsequently activated culminating in the dimerization of a pair of phosphorylated signal transducer and activator of transcription (STAT) 3 proteins. Concomitant activation of the mitogen-activated protein kinase and the phosphatidylinositol-3 phosphate kinase pathways results in the activation of genes responsible for survival and self-renewal (Graf *et al*, 2011).

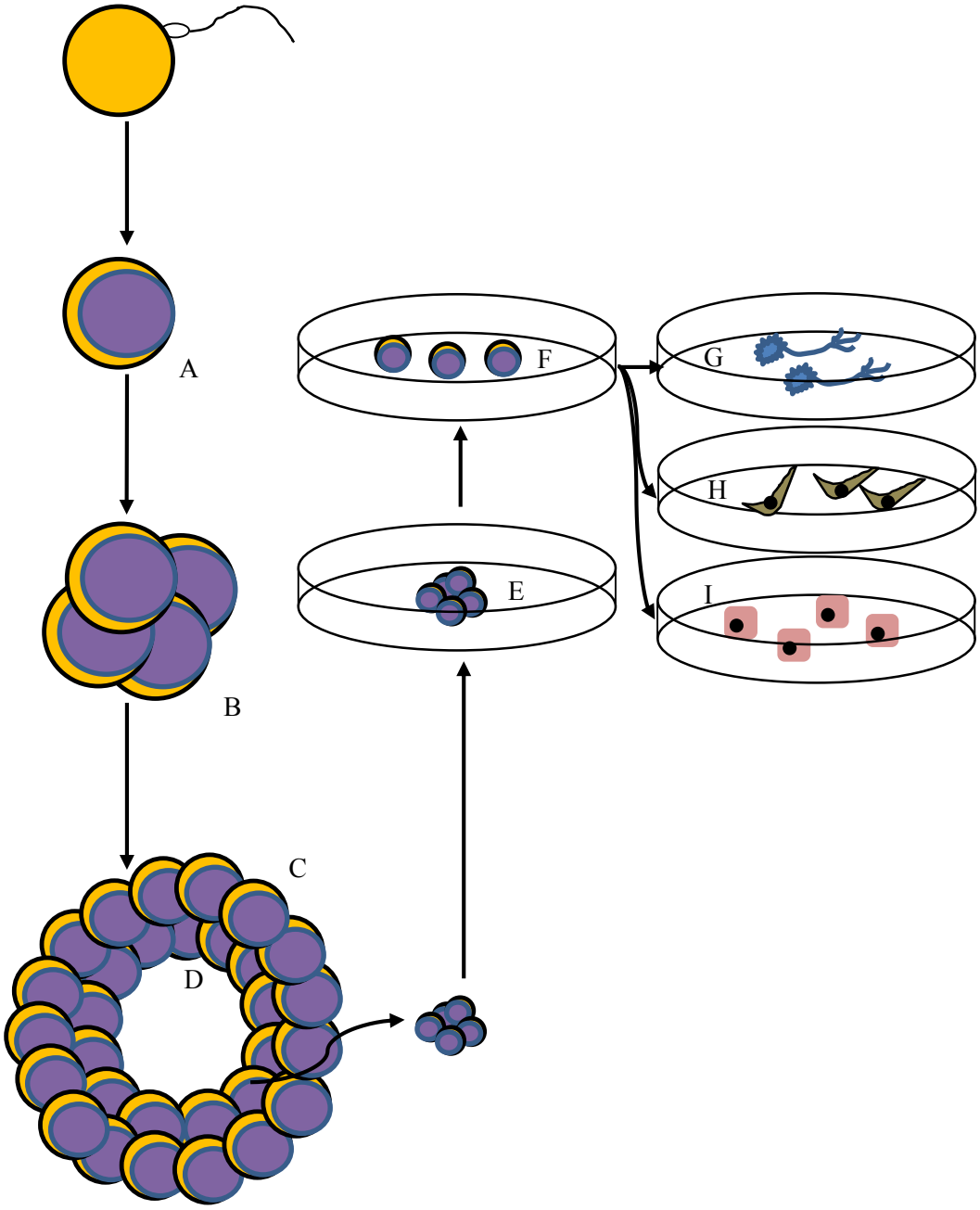


**Fig. 1.1 Isolation of Embryonic Stem Cells.** A four-cell embryo (B) generated from a fertilised egg (A) develops into a blastocyst (C). The inner cell mass (D) is isolated and plated onto inactivated murine embryonic fibroblast (MEF) cells (E). Upon subsequent culture on MEF cells (F) embryonic stem cell lines capable of differentiating into tissues from the three germ layers (ectoderm (G), mesoderm (H) and endoderm (I) can be derived.

In their natural environment stem cells are capable of remaining quiescent – a state which describes cells in a dormant state, neither dividing nor differentiating whilst remaining in the stem cell pool. Upon appropriate signals from the surrounding tissues, stem cells are known to divide in two distinct fashions, symmetrical in which two identical daughter cells arise from a single progenitor and asymmetrical in which a parent cell produces one identical and one differentiated cell. Alternatively, stem cells can be induced to differentiate without replenishment of the stem cell pool. ESCs in this manner populate the three germ layers (endoderm, mesoderm and ectoderm) during early development (Thomson, *et al*., 1998; Biehl and Russel, 2009).

The mechanics of stem cell differentiation are regulated by a complex series of cellular and molecular interactions. Significant variability in gene expression within differentiating cells governed by a number of epigenetic changes occurs (Lunyak and Rosenfield, 2008). Such changes act to promote either gene silencing or the activation of specific transcription factors (Dai and Rosenfield, 2007). Since the 1980's when ESCs were first isolated (Martin 1981) a large body of work has been undertaken in order to maximise their therapeutic potential. Embryonic stem cells have been proposed as a source for tissue replacement therapy in a range of neurological, cardiovascular and orthopaedic conditions (Goldman and Windrem, 2006; Caspi, *et al*., 2007; Fisher, *et al*., 2012), as well as for disease modelling to enable better understanding of the aetiology of conditions such as Huntington's disease (Niclis, *et al*., 2009).

### 1.1.2 Directed Differentiation of Embryonic Stem Cells

Removal of LIF from cultured embryonic stem cells has shown to result in the reduction of pluripotency markers such as *Oct-4, Nanog* and *Sox2* (Murgatroyd and Spengler, 2014). However in order to be used in clinical, diagnostic or investigative applications, controlled protocols are required to direct stem cell differentiation towards particular somatic lineages. Removal of LIF results in unpredictable ESC differentiation to the three germ layers, although evidence suggests ectodermal lineages are less well represented than mesodermal or endodermal lineages (Jeonghoon, *et al.*, 2005). Directed differentiation experiments have resulted in the generation of cells types such as peripheral neurons, Schwann cells and glia (Aihara, *et al*., 2010), cardiac tissue such as arterial and venous endothelial cells and myogenic cardiomyocytes (Narazaki, *et al*., 2008).

## 1.2 The Neural Crest

### 1.2.1 Characteristics of the Neural Crest

The neural crest is a transitory population of stem cells capable of forming numerous terminally differentiated lineages found in all vertebrate embryos, in which it is a unique feature. As the cells comprising the neural crest are self-renewing and multipotent, they are defined as stem cells (Teng, 2006). Since its initial description in the latter half of the nineteenth century, significant efforts have been made to determine the mechanisms and processes contributing to neural crest development from populations of embryonic progenitor cells and its migration and differentiation into numerous somatic cells throughout the vertebrate body (His, 1868; Huang and Siant-Jeannet, 2004; Simões-Costa and Bronner, 2013).

Due to the wide array of terminally differentiated progeny arising from neural crest stem cells, the neural crest has sometimes been termed the fourth germ layer (Hall, 2008). The neural crest presents a significant contribution to the physiology of the developing embryo with neural crest derived cells being found throughout the body, forming the bulk of the peripheral and sympathetic nervous system as well as cranio-facial cartilage, tooth dentine, melanocytes and cardiac smooth muscle (Anderson, 2006; Chai, *et al*., 2000; Henderson and Chaudrey, 2012). Recent experiments have recorded the presence of neural crest derived cells in the cornea of mice (Osei-Bempong, *et al.*, 2012). Subpopulations of neural crest cells (NCCs) have been identified and it is known that their position along the rostral-caudal axis *in vivo* is of utmost importance in determining ultimate cell fate. However, *in vitro* NCCs derived from different populations can be programmed to differentiate into any of the

somatic cell lines associated with their multipotent state (Olapoa and Conway, 2012).

Although the neural crest is exclusive to vertebrates, sensory neurons in ascidians derive from a population of cells discrete from those forming the central nervous system. Like the neural crest, these require signals from fibroblast growth factors and bone morphogenetic proteins to co-ordinate spatial and temporal patterning. However, unlike NCCs they display less plasticity and contribute only to the formation of peripheral nerves. Nonetheless, comparisons of non-chordate, invertebrate chordate and vertebrate development offers an insight into the contribution of the neural crest towards vertebrate evolution (Ohtsuka, *et al*, 2014).

The wide range of tissue types demonstrated to be of neural crest origin infer that there is a great potential for these cells to find therapeutic use, underpinned by recent research on tissue engineering strategies (Wang, *et al.,* 2011). However, despite numerous advances, a full understanding of the cellular and molecular mechanisms governing both initial and terminal differentiation as well as migration has remained elusive.

The inherent difficulties imposed on neural crest investigation by its transient nature is exacerbated by the fact that *in vivo* the neural crest is not a clearly delineated structure, being formed at the border of the non-neural and neural ectoderm and displaying characteristics associated with both (Sargent, 2006). Although populations of adult neural crest stem cells have been identified, they are rare and difficult to extract in numbers suitable for analysis (Jiang, *et al*., 2009). *In vivo* techniques such as stromal derived inducing activity have found success in the recapitulation of NCCs from embryonic precursors in both murine and primate

systems (Mizuseki, *et al*., 2003). However, there is evidence that the cells forming the feeder layer used in these protocols may have an influence on cell fate selection potentially obfuscating important data; as such, protocols using serum free, defined media were developed in order to derive neural crest stem cells in constant, controlled condition (Aihara, *et al*., 2010). Finally induced pluripotent stem cells (IPSCs) have been proposed as a potential source of NCCs. Briefly, somatic cells transfected with certain transcription factors have been shown to revert to an embryonic state as originally demonstrated by the pioneering work of Takahashi and his co-workers (Takahashi, *et al*., 2007). However question marks remain as to the suitability of IPSCs as a model for differentiation studies and a potential source of replacement tissue for clinical practice, most notably differences in cytosine methylation patterns between IPSCs and their embryonic counterparts persisting into terminally differentiated tissues derived from both have been reported. These differences are significant enough that they can be used to identify whether a population of stem cells has been induced from somatic tissue or is of embryonic origin. Methylation of cytosine residues is a major controlling factor of gene expression in mammalian systems and aberrant cytosine methylation is implicated in the development of tumours (Djuric and Ellis, 2010; Dolgin, 2011; Lister, *et al*., 2011; Perra, 2011). Although IPSCs potentially represent an unlimited source of cells for the study of NCCs at present work with these must continue in conjunction with ESCs to ensure epigenetic and genetic conformity.

### 1.2.2 Neural Crest Formation and Migration

In humans, the neural crest forms three to five weeks after conception on the borders of each side of the neural plate and the non-neural ectoderm in developing embryos prior to closure of the neural tube, which gives rise to the central nervous system (Bronner-Fraser, 1994; Amiel, *et al*., 2010). Upon neural tube closure, NCCs delaminate and migrate throughout the developing organism (Figure 1.2). Neural crest migration in mice, as well as in zebrafish, *Xenopus* and chick embryos begins rapidly after formation, typically within a few hours (Sandell and Trainor, 2006; Bae and Saint-Jeannet, 2014).

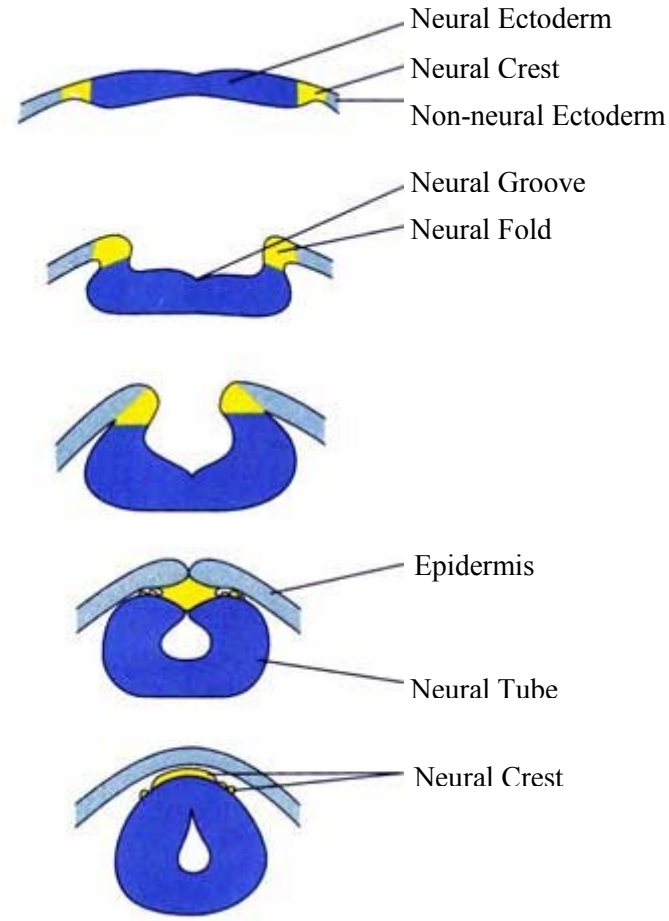


**Figure 1.2. Neural crest formation during neurulation**. The neural crest forms at the borders of the neural plate prior to the closure of the neural tube. Neural crest cells subsequently delaminate and migrate throughout the developing organism. (http://www.cornell.edu). Accessed 27-7-2014.

During the formation of the neural crest, signals from both the ectoderm and underlying mesoderm are required for proper differentiation (Basch and Bronner-Fraser, 2006). In addition activation of regulatory genes allowing survival in a variety of different tissue environments are necessary as the nascent NCCs undergo epithelial to mesenchymal transition along the rostro-caudal axis and migrate throughout the developing body (Trainor, 2010; Dupin, *et al*., 2006; Olaopa and Conway, 2012).

The process by which embryonic stem cells become terminally differentiated neural crest derived cells in multiple compartments of the body can be simplified and broken down into three distinct stages. The initial stage is induction, whereupon embryonic stem cells differentiate into neural crest stem cells in response to various cellular cues, most notably from BMPs, Wnts and FGFs (Basch and Bronner-Fraser, 2006). The next two stages, migration and differentiation are not clearly defined temporally, there being evidence that pre-migratory neural crest stem cells are lineage restricted *in vivo*. Nonetheless, neural crest stem cells have been shown to migrate to the appropriate tissue before final differentiation into somatic cell types (Etchevers *et al.,* 2006).

### 1.2.3 Migratory Patterning of Neural Crest Stem Cells

The fact that neural crest derived cells are found in a profusion of mammalian tissues is indicative of varying patterns of migration. For instance, the migrating cells that constitute the enteric nervous system must migrate along the whole length of the forming gut. Cells close the wavefront of the nascent enteric nervous system move preferentially along the rostro-caudal axis, while those behind show less directionality. This variability in migration direction leads to the colonisation of the

gut with populations of neural crest stem cells, which spread out and process neurites, leading to the innervation of the developing gut (Young, *et al*, 2014). Proliferation in migratory NCCs has been measured *in vivo* in the developing enteric nervous systems of mice. Experiments showed that in cells positive for the migratory neural crest marker Sox10 the percentage of cells remaining in the cell cycle did not vary significantly between E10.5 and E16.5, although cell cycle length increased by a factor of 50%. Gut innervation took place in the small intestine at E10.5 and in the colon at E12.5 respectively. Interestingly as migrating NCCs entered the gut a subsection began to express the neuronal marker Hu in comparison to Sox10 positive cells that ceased proliferation and exited the cell cycle (Gonsalvez *et al*, 2015). These data support the theory that proliferative, migratory neural crest stem populate the gut sequentially before terminal differentiation occurs.

Experiments have shown that vascularisation and innervation of many target tissues is concurrent and that endothelial cells secrete neurotrophins, while emerging neurons secrete vascular endothelial growth factor. These secretory agents conspire to guide the nascent vascular and nervous systems, suggesting roles for each in the migration of the other. However, in the emerging gut innervation is able to take place without vascularisation, indicating a supporting rather than a causative role (Delalande, *et al*, 2014).

Within a group of migrating cells, movement is directionally consistent across the population. Neural crest migration is distinct from that of other cell types in that migrating NCCs are more loosely associated, maintaining only transitory adhesion between neighbouring cells. Recent studies show that early migrating neural crest stem cells express different genes in comparison to their later migrating counterparts Uriu *et al,* 2014). It is hypothesised that in neural crest migration two distinct

subgroups arise. Leader cells follow a chemoatteractive signalling gradient to their final destination: Follower cells attach to and follow leader cells. The migration of the neural crest is both vast and tortuous in cellular terms requiring constant communication between cells, their neighbours and their environment (Wynn, *et al*, 2013).

The initial stage of neural crest migration is the epithelial to mesenchymal transition (EMT), which precedes delamination, although these terms are often used erroneously to describe a single process. The signalling cascades involved in the EMT are highly conserved between species, invariably proceeding through the BMP/Wnt pathways. Epithelial to mesenchymal transition promotes the expression of neural crest specifier genes, such as those of the *Sox* family of transcription factors. Delamination is precipitated via the alteration of cellular adhesion properties through the modification of *Cadherin* expression culminating in the degradation of *N-Cadherin* by the metalloprotease ADAM10. Before delamination, the expression of genes contributing to the process such as *Ets1* and *Snail,* is repressed by the p53 protein. Upon delamination p53 expression is reduced allowing delamination although the precise mechanisms involved are as yet unknown. A concurrent decrease in the expression of Noggin is suggestive of a role of BMP-4 in this process, as the former is known to be an antagonist of the latter (Theveneau and Mayer, 2012).

In the process of delamination, cells begin migration, extending lamellipods and filopods from the cytoplasm as well as bleb, marks associated with motility. In some cases emergence from the epithelium is followed by a phase in which cell remain immobile but undergo division cycles. During migration, three major factors conjoin to ensure appropriate directionality, chemoattractive signals from the target area,

repulsive signals from tissues that are not to be colonised and signal transduction between neighbouring cells (Clay and Halloran, 2010).

Signal transduction between cells can be mediated by direct contact or through the action of secretory signalling molecules such as the Wnt proteins, which are essential components for the migration of polarised cells such as those originating from the neural crest (Puroshothama and Kühl, 2010). Perhaps the most important cellular interaction controlling the cessation of neural rest migration is contact inhibition of locomotion (CIL). In this mechanism a cell, upon contact with a nearby cell withdraws the lamellipods and filopods that facilitate motility and alters its orientation and direction of movement. Contact inhibition of locomotion disrupts the unidirectional flow of cells or results in its cessation. Migrating NCCs form short-lived adhesion complexes during CIL, although little is known about the signal transduction that occurs if indeed any does during these interactions (Moore, *et al.*, 2013). Recent research in *Xenopus* has demonstrated that in the neural crest contact inhibition of locomotion requires temporary adhesion between both cells and developing placodes. This is modulated by cadherin molecules and involves transition of expression from Cadherin 1 in pre-migratory NCCs to Cadherin 2 in migratory (Scarpa *et al*, 2015).

Deficient migratory patterning of neural crest stem cells is responsible for numerous pathologies, for example being the leading cause of craniofacial deformation, accounting for approximately half of all human birth defects. Cranial NCCs originally migrate *en masse* before segregating into distinct populations, which subsequently populate the three branchial arches. The segregation and differentiation of populations of migrating neural crest stem cells both in the cranium and

throughout the developing embryo has been the subject of a wide body of research (Gong, 2014).

The peripheral nervous system (PNS) derives mainly from cells of the trunk neural crest with contributions such as sensory ganglia being generated from the cephalic. Just as in cranial neural crest, the fate of trunk NCCs is determined before the onset of delamination and migration and before the expression of somatic biomarkers can be observed. In the colonisation of the developing PNS with NCCs, specifying factors such as BMP-4 and pax3 continue to be expressed and sox10 is essential for the survival of migrating PNS precursors. Experiments with murine models show that termination of migration acts as a trigger for differentiation into somatic cell lines resulting into a ventral-to-dorsal pattern in the appearance of neural crest derived tissues. Neurogenesis in murine systems begins with the formation of large cell body neurons (Prendergast and Riable, 2014).

Fate determination plays an important role in the direction of migration of the forming neural crest. The rostro-caudal placement of NCCs along the nascent neural tube is a key determinant of cell fate (Olaopa and Conway, 2012), although some plasticity is observed in populations deriving from the trunk. In avian embryos initial migration of the trunk neural crest proceeds along the ventral axis, these cells go on to populate the peripheral nervous system and adrenal medulla. Later migrating cells from the same region move in a dorsolateral direction, eventually invading the epidermis to form melanocytes. Control of this variance in migration is thought to be mediated by Ephrin-B proteins, which prevent dorsolateral migration in early delaminating NCCs. Interestingly those cells delaminating at a later time point, express receptors enabling complexes to be formed with Ephrin-B. This facilitates dorsolateral migration by changing the interaction of cells with Ephrin-B from a

repulsive to attractive one (Santiago and Erickson, 2002). The pathways followed by migrating NCCs are replete with extracellular matrix factors conducive to the process in the case of peripheral nerve progenitors deriving from the trunk crest. F-spondin and versican are considered to act as repellents, guiding migrating cells away from non-target tissues whereas stromal cell-derived factor 1 (Sdf1) appears to act as a chemoattractant for sympathetic nervous system precursors (Theveneau and Mayer, 2014).

### 1.2.4 Cellular Interactions Governing Neural Crest Formation and Migration

A complex series of cellular interactions is required for proper patterning, migration and differentiation of neural crest stem cells into the wide variety of somatic cell types they will eventually form. Although the action of transcription factors responding to the influence of extracellular morphogens has been well characterised they do not act in isolation. Other types of interactions such as post-translational modifications of proteins play an important role. For example, ubiquitination is an enzyme-mediated process, which culminates in the addition of a small (8.5 kDa) polypeptide to target proteins. Primarily the addition of the ubiquitin peptide results in the recruitment of further ubiquitin molecules targeting the protein for degradation by the proteasome. Ubiquitination plays an implicit role in other cellular processes, it has been observed to adjust protein morphology, potentially affecting stability or molecular interactions. Ubiquitination can also positively regulate gene expression by targeting antagonist proteins for degradation (Mukhopadhyay and Riezman, 2007) and promote differentiation by lysis of pluripotent specific genes such as *c-myc* (Boix-Perales *et al*, 2007).

Within neural crest differentiation, protein kinase NEDD-4 mediated ubiquitination is required for cell survival and migration. *Nedd4* deficient mice show decreases in the expression of neural crest specifiers such as pax3 and sox10, these data may indicate that NEDD-4 is a positive regulator of these genes (Wiszniak, *et al*, 2013).

Interactions between cells and the extracellular matrix or other cells are mediated by the presence of adhesion molecules. The most common type of adhesion molecules are the integrins, transmembrane proteins consisting of alpha and beta subunits. The cell surface receptors of integrins chiefly bind ligands from the extracellular matrix although some are known to facilitate cell-cell signalling by coupling with receptors on adjacent cells. Integrins are important components of the mechanisms governing cell differentiation, migration and proliferation (Clark and Brugge, 1995). During neural crest delamination and migration, integrins are essential for cell survival and locomotion. Migrating neural crest stem cells present a wide array of integrins of differing functions, both relating to cell-cell and cell-ECM interactions. Functional studies of aberrant integrin expression have shown it to be a cause of anoikis where cells detach from the ECM and undergo programmed cell death. It has further been observed that the array of integrins expressed by post migratory NCCs changes with subsequent differentiation suggesting roles other than the facilitation of migration (Duband, 2006).

Although many forms of external receptors have been characterised, the intracellular mechanisms of integrin mediated signal transduction are less well understood. A number of prospective cytoplasmic targets have been proposed, including integrin linked kinase (ILK). Deletion of this gene, in murine neural crest specific tissues, causes altered migration patterns and cardiac malformations. These were coupled with a reduction in Akt protein, which has roles in cell proliferation and

differentiation and is commonly expressed in developing neural crest tissues (Nicholson and Anderson, 2002; Dai *et al.,* 2013).

### 1.2.5 Contribution of the Neural Crest to the Vertebrate Body

Due to the wide array of terminally differentiated progeny arising from neural crest stem cells, the neural crest has sometimes been termed the fourth germ layer (Hall, 2008). Initial migration of cells comprising the neural crest is known to be time dependant, for instance in chick embryos NCCs proximal to the rostrum delaminate almost a full day before the caudal-most population (Theveneau and Mayer, 2012).

The neural crest is a major contributing factor to the "new head" in which complex and specialised sensory structures combined with the formation of an articulated jaw allowed primitive vertebrates to develop from filter feeders into predators. Autonomic regulation of bodily functions by a sophisticated peripheral nervous system combined with additions to the cardiovascular system and the protection from DNA damage by ultraviolet light provided by melanocytes, confer upon vertebrates an ability to better adapt to the vicissitudes of their environment. The development of these anatomical structures has provided a boon for the evolution, spread and proliferation of the diverse vertebrate species extant today across a multitude of environments (Le Douarin, 2004; Durain and Dupin, 2014). The neural crest; prior to delamination can be divided into four main regions, each with distinctive patterning and positions of terminally differentiated cells (Table 1.1).

**Table 1.1. Tissues derived from neural crest.** Specific tissues differentiate from each region. The cephalic neural crest occupies the rostrum-most position and regions move caudally to the trunk (Avery *et al.,* 2014; Jasrapuria-Agrawal and Lwigale, 2014; Vincentz and Firulli, 2014).

| Tissue | Origin |
|---|---|
| Cranial bone | Cephalic |
| Cranio-facial cartilage | Cephalic |
| Inner ear bones | Cephalic |
| Ocular tissue | Cephalic |
| Dentine of teeth | Cephalic |
| Cardiac smooth muscle | Cardiac |
| Cardiac connective tissue | Cardiac |
| Enteric ganglia | Vagal |
| Glial cells | Trunk |
| Sensory neurons | Trunk |
| Autonomic neurons | Trunk |
| Motor neurons | Trunk |
| Melanocytes | Trunk |

## 1.2.6 Neural Crest Pathology (Neurocristopathy)

The importance of the neural crest is highlighted by the wide range of pathologies, associated with aberrant migration and development of neural crest stem cells in the vertebrate body. Although diverse in both symptomatic manifestation and severity, these pathologies are grouped together under the term neurocristopathy (Jenson, *et al*., 1992). A wide range of neurocristopathies have been described, including neuroendocrine tumours (Rosai, 2011) cardiac defects (Olapoa and Conway, 2012) and a range of congenital defects such as Apert Syndrome, CHARGE syndrome, Treacher-Collins syndrome and Hirchsprung's Disease (Wang, *et al*., 2005; Van De Putte, *et al*., 2003; Trainor, 2010; Henderson and Chaudhry, 2012).

Neuroblastoma accounts for approximately 1 in 10 incidences of cancer in children it frequently originates in the adrenal glands but can develop from any part of the sympathetic nervous system. Other cancers of neural crest origin include glioblastoma, Ewing's sarcoma and various melanomas (Powell *et al*, 2014). In addition to tumours arising because of aberrant prenatal gene expression, cells of neural crest origin in adult organisms can de-differentiate to obtain a cancerous phenotype. Malignant peripheral nerve sheath tumours (MPNST) arise from Schwann cells, typically in heavily enervated organs. Their aetiology is poorly understood but is linked to I neurofibromatosis, an inherited disease of the PNS indicating a potential connection between MPNST and neural crest development (Kaur *et al.,* 2015).

The aetiology of a number of neurocristopathies has been elucidated or inferred by a variety of studies. The majority of cases of Apert Syndrome for example show a point mutation where a tryptophan residue replaces the serine residue normally found at position 252 in the amino acid chain (S252W) of a receptor for FGF-2, a growth factor commonly associated with neural crest formation (Tanimoto, *et al*., 2004). Pax3 has been linked with numerous neural crest associated pathologies such as Hirchsprung's disease and Waardenburg syndrome, acting in accordance with sox10 to initialise the proper development of the cells comprising the enteric nervous system (Lang, *et al*., 2000). In addition to this NC related persistent trunk arteriosus, a common structural heart defect wherein the aorta and pulmonary artery fail to segregate have been linked to aberrant expression of pax3 (Olaopa and Conway, 2012). Cardiac defects arising from neural crest related tissues are not limited to the structural. In murine systems deficiencies in the cell signalling protein tyrosine phosphatase 2 lead to the incomplete innervation of the heart by NC derived

sympathetic neurons and irregularities in the heartbeat, specifically bradycardia (Lajiness *et al*, 2014).

CHARGE syndrome was only recently (2010) characterised as a neurocristopathy, although due to the nature of the symptoms it presents a connection to the neural crest was previously suspected. Sufferers manifest cranio-facial deformities, heart defects and deafness (Avery *et al*, 2014). Little is known of the precise aetiology of CHARGE syndrome but a connection to reduced expression of the CHD7 gene has been observed. In the murine model, the *Whirligig* mouse shows symptoms similar to CHARGE syndrome in heterozygous animals as a result of a mutation inserting a premature stop codon in CHD7; homozygous *Whirligig* mice display embryonic lethality (Schulz *et al*, 2014).

Although the precise aetiology of neuroblastoma remains unclear, genome-wide association studies have identified a number of single nucleotide polymorphisms (SNPs) in various genes that appear to be linked with susceptibility and clinical outcomes. For instance around 10% of neuroblastoma cases present a missense polymorphism in *Caspase8* (C > G) leading to the substitution of aspartic acid 302 with histidine. This polymorphism adjusts apoptotic behaviour in affected cells and is linked to metastatic tumour formation and poor clinical outcomes (Rihani *et al*, 2014). Other analyses have shown potential roles for polymorphisms in the *Interleukin-3*, *BARD1* and *CLF1* genes leading to aberrant developmental and apoptotic pathways (Lee *et al,* 2014).

Neuroblastomas are known to express the pluripotency-associated gene *Oct-4*, which co-operates with the *MYCN* oncogene to regulate expression of *NCYM*. Together these genes promote self-renewal and avoidance of apoptotic pathways in

oncogenesis. The expression of these genes in neuroblastoma cells is associated with poor clinical outcomes (Kaneko *et al*, 2015). Neuroblastoma cells expressing high levels of MYCN additionally express increased levels of the putative oncogenic protein Jarid1B. Jarid1B expressing neuroblastoma cells show a more stem cell like phenotype and exhibit increased invasive properties and chemoresistance than those with lower expression levels although whether this is linked to expression of *Oct-4* is unknown at present (Kuo *et al*, 2015).

Upregulation in *MYCN* expression is a common marker in neuroblastoma cases although it is not ubiquitous (Huang and Weiss, 2013). This gene is invariably expressed in the developing neural crest and continued transcription is noted during neurulation (Powell *et al*, 2014). In cases of neuroblastoma in which MYCN expression is not altered it has been demonstrated that the regulatory gene *Dicer1* is targeted and knocked down following the upregulation of the *miR-192* gene (Feinburg-Gorenshtein *et al*, 2013).

## 1.3 Factors Influencing Neural Crest Development

### 1.3.1 Growth Factors

A tightly controlled program of differentiation is required to recapitulate specific cell types, a stringent series of signal transduction pathways must be activated at the correct time with the appropriate application of cytokines and growth factors both *in vitro* and *in vivo*. The incorrect regulation of these processes is the causal factor for numerous birth defects and congenital diseases such as NC associated tumours and birth defects such as Waardenburg syndrome (Etchevers *et* al, 2006; Rao and Kühl, 2010).

Numerous signals, transcriptional activation, and repression events converge in the forming neural crest, both from the ectoderm and from the underlying mesoderm. Members of the fibroblast growth factor (FGF) especially FGF-2 are ubiquitously expressed in NC development *in vivo* (Basch and Bronner-Fraser, 2006; Marinez-Morales, *et al*., 2011).

FGF-2 is a small (approximately 18 kDa) protein, associated with the development of numerous organs and systems, including neural crest derived lineages. FGF-2 is a critical component of many morphogenetic and developmental pathways and has been shown to interact with four specific fibroblast growth factor receptors (FGFRs) numbered FGFR1-4 (Figure 1.3) in interactions mediated by the heperan sulphate proteoglycan (Lanner, *et al.,* 2010). All these receptors are positioned on the surface of the cell membrane and all share a transmembrane domain facilitating FGF-2s role in cell signalling (Bikfalvi *et al*, 1997; Plotnikov *et al,* 2000). The interaction of FGF-2 with its receptors ultimately results in signal transduction through activation

of tyrosine kinase receptors, linking FGF-2 strongly with mammalian organogenesis (De Moerlooze *et al.,* 2000)

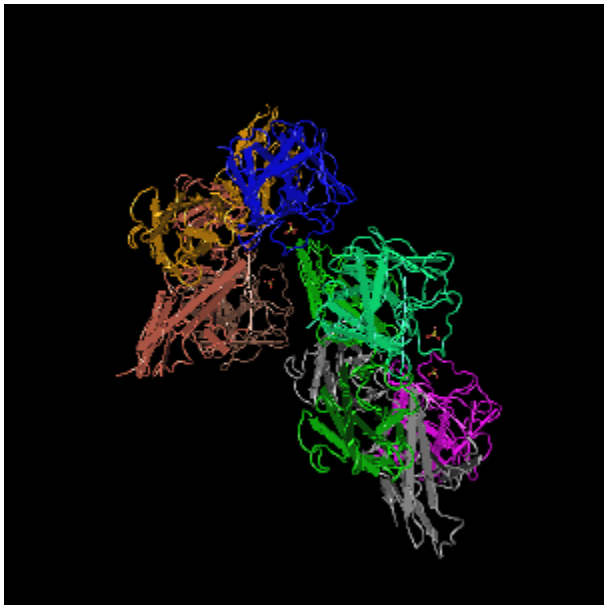

**Figure 1.3. Crystal structure of FGF-2**. Fibroblast growth factor (right) interacting with FGF-2 receptor (left) (http://www.ncbi.nlm.nih.gov accessed 24-9-12). Different colours denote different areas of tertiary structure that comprise the subunits of the protein.

FGF-2 has been proposed to play a role in the survival and proliferation of prospective NCCs, due to its ability to initiate mitosis with studies in quail and mouse models showing it to be indispensable in this regard (Sailer *et al.,* 2005). Although of fundamental importance to neural crest differentiation FGF-2 does not act alone. Other proteins are known to exert an influence on both neural crest specification and migration, most notably members of the bone morphogenetic protein family of morphogens (Basch and Bronner-Fraser, 2006).

### 1.3.2 Bone Morphogenetic Protein-4

Neural crest specification is further governed by the presence of factors promoting or inhibiting transcription, either directly or through convoluted pathways. Bone morphogenetic protein 4 (BMP-4) is known to be selectively antagonistic towards neurulation. Canonically, BMP-4 exerts its influence through the SMAD signalling pathway (Figure 1.4).

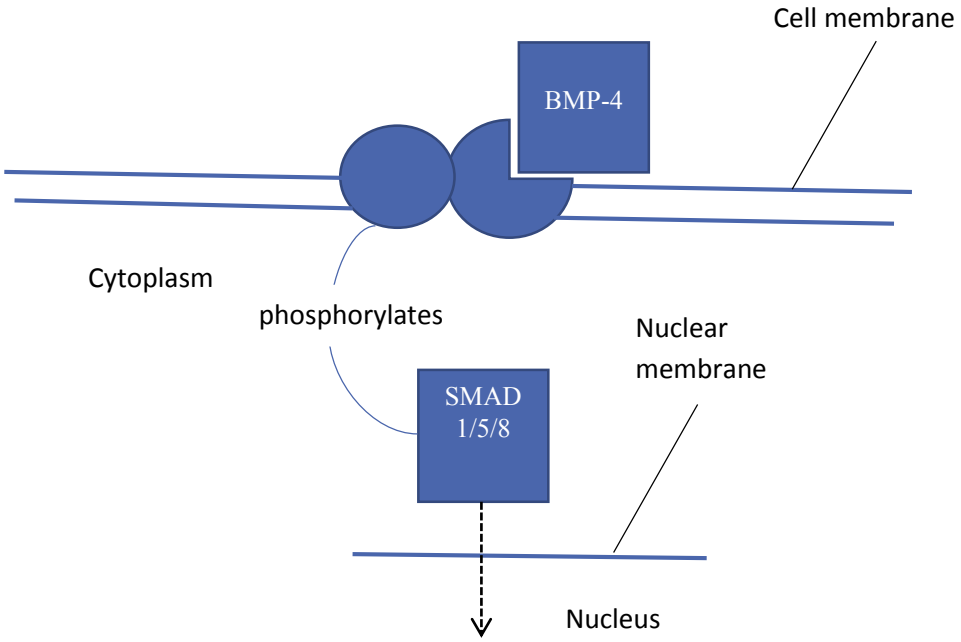


**Figure 1.4. Canonical BMP signalling**. BMP-4 forms a complex with a type I trans-membrane receptor (cut out circle) which phosphorylates a type II receptor (circle). The type II receptor phosphorylates cytoplasm bound SMAD proteins (1, 5 and 8) which form a complex, migrate to the nucleus and interact with DNA, affecting gene transcription (Xu, *et al*, 2008).

A BMP-4 concentration gradient is established across the developing ectoderm. The neural tube and subsequently the central nervous system are established from those areas of the ectoderm exposed to the least amount of BMP-4. Regions exposed to higher amounts, generate the non-neural ectoderm, while a median dose results in neural crest lineage specification. Exposure to BMP-4 across the ectoderm is difficult to accurately measure *in vivo,* but in *vitro* concentrations of 10 ng $ml^{-1}$ have been shown to be sufficient to prevent neurulation and promote neural crest lineage (Aihara *et al.,* 2010). The exact mechanisms controlling the establishment of this concentration gradient are unclear but the BMP-4 antagonist noggin may provide a role. (Marchant, *et al*., 1999; Barth, *et al*., 1999; Milet, *et al*., 2013). Known targets of BMP-4 include *Sonic Hedgehog* (*Shh*), a gene that acts in a mutually antagonistic manner to BMPs to establish dorso-ventral differentiation patterns. *Shh* expression in the emerging ectoderm is reciprocal to BMP-4 expression (Figure 1.5) (Leim, *et al*., 1995; Murgatroyd and Spengler, 2014).

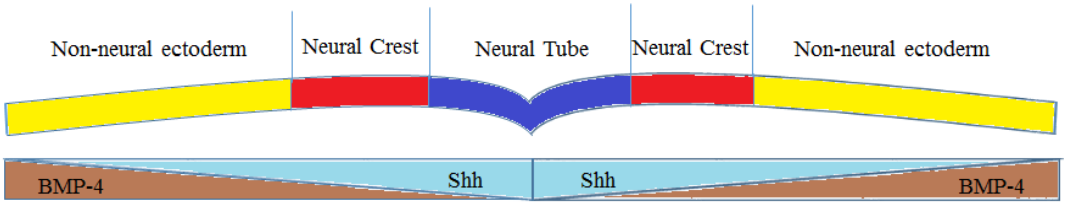


**Figure 1.5 Patterns of expression of pro and anti-neurulation genes across the developing ectoderm.** Sonic hedgehog and bone morphogenetic protein-4 are expressed in reciprocal concentration gradients over the developing ectoderm.

### 1.3.3 Neural Crest Specification Factors

In the formation of somatic tissues, a network of transcriptional activation and repression must converge. This is further complicated in the case of the neural crest by the array of somatic cell fates possible and the rigours of migration. Numerous transcriptional events are observed in initiation of differentiation, migration and final morphogenesis. The sex determining (*Sry*) high mobility group-box proteins (*Sox*) are a family of transcription factors expressed in a variety of vertebrate tissues. *Sox8*, *9, 10* and *11* are expressed at the neural fold during gastrulation although only *Sox9* and *10* are heralded as neural crest specifiers. *Sox9* plays multiple roles in the emergence of the neural crest. At gastrulation, its expression is observed to cause preferential differentiation of cells towards a neural crest rather than a neural phenotype. *Sox9* is also expressed in migratory NCCs and its post-migratory expression causes developmental bias towards glial and melanocyte lineages (Cheung and Briscoe, 2003; Gong, 2014). Deletion of *Sox10* results in severe defects in the PNS in murine models (Wegner and Stolt, 2005), expression of this gene being essential for the correct formation of myelinating Schwann cells (Glenn and Talbot, 2013). In the developing mouse embryo expression of *Sox* genes is observed 3 to 5 days after the induction of *FoxD3* (Hong and Saint-Jeannet, 2005).

FoxD3 is a member of the winged helix transcription factor family and has been shown to play a key role in the fate determination of nascent neural crest stem cells as well as in the regulation of their migration, through the developing organism. Recent research suggests that FoxD3 influences migration through the downregulation of Tetraspanin18, a protein regulating the expression of cadherins responsible for cell-cell adhesion (Fairchild, *et al*., 2014). FoxD3 is implicated in

numerous roles during neural crest formation; it promotes lineage selection in neural precursors, inducing a neural crest lineage and causes preferential differentiation of neural cell types at the expense of melanocytes. FoxD3 expression is anti-proliferative; cells showing high levels of expression exit the cell cycle and cease dividing. Aberrant downregulation of FoxD3 is associated with neuroblastoma and lung cancer (Wang *et al.,* 2015).

The Wnt protein family has a well-documented association with neural crest induction acting in concert with genes such as FTO and AWP1 in distinct signalling pathways involving the activation of β-catenin (canonical) and increased calcium ion output from the endoplasmic reticulum (non-canonical). Extracellular Wnt molecules complex with trans-membrane receptors and initiate a complex cascade of interactions, which occur in both the cytoplasm and nucleus. Loss of function in the non-canonical pathway has been shown to give rise to craniofacial deformities and downregulation of neural crest marker *Sox10* in zebrafish (Calisto, *et al*., 2005; Seo, *et al*., 2013; Osborn, *et al*., 2014). In both canonical and non-canonical pathways, Wnt interacts with the Frizzled transmembrane protein initiating a number of cellular cascade reactions. These cascades control diverse cellular processes, such as cytoskeleton rearrangement and inhibition and promotion of gene expression (Rao and Kühl, 2010). Wnt signalling is implicated in the adhesion of pre-migratory NCCs through activation of the frizzled-4 receptor, which subsequently binds to ADAM13, a metalloprotease that degrades cell-cell junction molecules reducing its ability to cleave these molecules and therefore acting in a refractory manner to migration (Abbruzzese *et al.*, 2015)

The complicated hierarchy of transcriptional activation and repression in the developing neural crest remains obscure. There is evidence to suggest that gene

regulation is highly conserved between species exhibiting the neural crest (Bronner and LeDouarin, 2011). Insights into the mechanisms governing the epithelial to mesenchymal transition of NCCs and their subsequent migration offer the prospect of greater understanding of vertebrate development. In addition, the invasive, proliferative nature of migrating NCCs infer potential value modelling the characteristics of metastatic tumours (Dupin and Sommer, 2012). The Wnt signalling pathway that is closely associated with neural crest development, has been observed to active in the propagation of some types of mammary cancer (Cleary, *et al.*, 2014). Tumour metastasis and the epithelial to mesenchymal transition undergone by neural crest stem cells are homologous events sharing many similarities in gene expression and cellular interactions. Activation of neural crest specifiers associated with the EMT is symptomatic of numerous cancers and cancer cells and NCCs show cadhedrin alteration and changes in polarity facilitating migration and invasion of disparate tissues (Powell, *et al.,* 2014).

The migration and survival of neural crest stem cells, through diverse tissue types in the developing organism is dependent on an exacting epigenetic program. Aberrations in this program are causative of neurocrisopathies such as Hirchsprung's disease in which increased methylation levels of the *MeCP2* gene has been hypothesised to perturb the proliferation of neural crest stem cells fated to form enteric ganglia in the intestine (Zhou, *et al*., 2013). The epithelial to mesenchymal transition (EMT) of NCCs is also underpinned by a delicately balanced series of regulatory cues and responses. *E-Cadherin* expression is repressed by the binding of *Snail2* to regulatory elements in its gene-coding region. *Snail2* is a known target of the canonical *Wnt* signalling pathway suggesting a link between *Wnt* and the EMT (Stemmer, *et al*., 2008; Schiffmacher, *et al*., 2014).

Experiments involving knockdown of *CMYB*, a transcription factor more commonly associated with the haematopoietic stem cell lineage have allowed some elucidation of neural crest differentiation and propagation. Disruption of *CMYB* expression has been shown to repress expression of neural crest associated genes such as *Slug*. However, expression of *Sox9* remains constant in the presence or absence of *CMYB* suggesting that it exerts its influence upstream of the *Slug* but downstream of *Sox9* (Betancour, *et al.*, 2014). Transcription factors such as *Pax3* and *Zic1* are known to be essential for specification of NCCs at the formation of the neural fold as well as migration and fate determination while other genes such as *AP2* are expressed only transiently during initial NC differentiation (Plouhinec, *et al*., 2014). Pax3 and Zic1 have been shown to act synergistically in specifying neural crest fate and treatment with these factors alone is sufficient to promote the expression of NC associated markers such as *Twist, Sox9* and *Snail2* as well as novel gene targets (Chang-Joon, *et al*., 2014). *Pax3* is a transcription factor containing both paired and homeobox domain DNA recognition sites, complexing with a TAATC motif on the non-coding DNA strand and is critical in the development of mammalian nervous systems acting in accordance with *Sox10* to initialise the proper development and migration of neural progenitors (Lang, *et al.,* 2000; Birrane *et al.,* 2009). The presence of Pax3 in tissues however is indicative, not definitive of a neural crest lineage. Pax3 and Zic1 interact with Gli2 in the formation of non-neural crest derived muscle (such as skeletal muscle) (Himada, *et al.*, 2013). Like Pax3 Zic1 acts as a transcription factor, it is a member of the zinc finger family of protein, which are characterised by the presence of a stabilising zinc molecule in the DNA binding domain. The expression of the *Zic1* gene is essential for proper neural development during organogenesis and plays an active role in the differentiation of neural crest stem cells, possibly

interacting with the Sonic Hedgehog signalling pathway (Aruga, 2004; Ali *et al.,* 2012). Although levels of *Shh* are expressed in lower levels in the neural crest than the central nervous system, it is nonetheless essential for correct formation of the enteric nervous system. Ablation of *Shh* in mice leads to abnormal patterning in the neurons colonising the small intestine and stomach (Liu and Ngan, 2014). Hedgehog signalling is thought to have an essential role in both the specification and proliferation of neurons along the developing gut.

### 1.3.4 Epigenetics of Neural Crest Formation

Underpinning the actions of various signalling pathways and genetic cues associated with the formation of the neural crest is a concomitant array of epigenetic modifications (Kim, *et al*., 2013). Epigenetics is defined as changes in gene expression without changes in the underlying genetic code with the most studied and ubiquitous form being DNA methylation. In this form of epigenetic modification, a methyl group ($CH_3$) binds to the 5-carbon position of the pyrimidine ring of a cytosine residue in a reaction mediated by methyltransferase enzymes (Wolffe, *et al*., 1999). These cytosine bases are commonly found to be adjacent to guanine residues in the promoter regions of genes forming CpG islands in which are found repeating CG residues (Herman, *et al*., 1996).

Methylation of CpG islands in the promoter regions of genes silences gene expression by acting as an antagonist to the acetylation of histone proteins – an epigenetic mark associated with the initiation of transcription. The exact mechanisms involved in gene silencing by methylation are largely unknown and methylation of CpG islands does not always result in transcriptional repression. Various mechanisms have been proposed including the occlusion of DNA binding sites from

the transcriptional machinery by methyl groups or the recruitment of methyl specific DNA binding proteins that obfuscate these sites (Curradi, *et al*., 2002). Little data is available pertaining to methylation patterns in the developing neural crest perhaps owing to its transient nature *in vivo* (Dupin and Sommer, 2012). Recent research has implicated DNA methyltransferase 3B (DNMT3B) as a key factor regulating migration of cranial neural crest in chick embryos through methylation of the promoter region of *Sox10*. Loss of function of DNMT3B caused excessive migration of neural crest and neural tube cells *in vivo* and subsequent craniofacial abnormalities. DNMT3B was therefore implied in the cessation of migration through repression of *Sox10*. Similar experiments in mice however showed less extreme effects suggesting either redundancy in the murine epigenetic program or simply differences in expression profiles between species (Hu *et al.,* 2014; Hu *et al.,* 2015).

The spatial arrangement of DNA within the cell is a further epigenetic mark that influences gene expression, the combined length of the complete DNA sequence contained within a nucleus of approximately 5μm diameter is almost 2 meters. It is logical therefore, that DNA is stored in a highly compacted manner, tightly bound to histone proteins in a structure termed chromatin. Chromatin exists in two distinct forms, euchromatin and heterochromatin. Euchromatin has a more open structure allowing access to the cellular machinery responsible for transcription while heterochromatin by comparison has a denser structure that prevents the access of transcription factors and impedes gene expression. Enzymatic processes can mediate chromatin structure. Histone acetyl transferases (HAT) catalyse the addition of an acetyl group to a lysine residue in the histone proteins while histone deacetylases (HDACs) reverse this reaction. Highly acetylated histone structures are associated with euchromatin and permissive gene expression while low levels of histone

acetylation are indicative of transcriptional silencing and a heterochromatin structure. The mechanisms by which histone acetylation regulates chromatin structure is the subject of some debate. Originally it was theorised that acetylation neutralised the positively charged lysine resulting in a change in the interactions with the negatively charged phosphate backbone of DNA. Recent research however, suggests acetylated histones recruit proteins involved with transcriptional activation. (Wu, 1997; Choudhary *et al,* 2009; Ho and Crabtree, 2010). Methylation of cytosine residues appears to act in opposition to the acetylation of histone proteins involved in chromatin assembly. Histones packed with artificially methylated DNA have been shown to be hypo-acetylated (Drendall, *et al*., 2010).

Stem cell chromatin is known to be loosely packed. This facilitates transcription at some level of most of the genes comprising the genome of a particular organism. Differentiation and cell fate restriction is accompanied by remodelling of the chromatin structure mediated by remodelling proteins (Gu *et al*, 2010). The Polycomb group (PcG) group proteins are associated with chromatin modelling in both embryonic stem cells and the neural crest. Polycomb repressive complex 2 (PRC2) consists of four proteins in the mouse, Suz12, Eed, Ezh2 and RbAp48. This protein complex is implicated in the methylation of histone proteins leading to repression of gene expression although in some cases it can interact with histones to promote expression. In *Xenopus* knockdown of the *Ezh2* or *Snail2* genes led to reduced numbers of cells expressing neural crest markers but did not entirely prevent neural crest specification. Interactions between *Snail2* and *Ezh2* have been observed in the promoter region of *E-cadherin* reducing expression during delamination although not in early specification (Tien *et al*, 2015). Interestingly p53 is known to downregulate *Snail* expression during epithelial to mesenchymal transition (section

1.23) and p53 ablation reduces migration of neural crest derivatives in mice (section 1.26). These data, taken together suggest a role in the modulation of *E-Cadherin* expression during EMT for all three genes through epigenetic interactions with the promoter region and one another. The *Snail* genes have further been shown to interact with the methyltransferase enzyme NSD-3 as have *FoxD3, Sox9,* and *Sox10.* With the exception of *Sox10* however, these interactions are more complex than simple methylation, leading to repression of expression and the mechanisms of interaction with the remaining genes are unclear. It was observed in chick embryos that inhibition of NSD-3 resulted in failure of migration in developed NCCs (Jacques-Fricke and Gammill, 2014).

Other important chromatin re-modelling proteins in the neural crest are chromodomain helicase DNA binding protein 7 (CHD7) and SWItch/Sucrose Non Fermentable B (SWI/SNF-B). Together these proteins act to influence both the expression of genes associated with neural crest specification, such as *p75,* and act synergistically with the BMP signalling pathway to maintain the multipotent state of neural crest stem cells (Fujita *et al*, 2014). *In vivo,* subjects lacking the *CHD7* gene show numerous defects in neural crest derived tissues manifesting as craniofacial deformities and abnormal cardiac muscle development. Studies in *Xenopus* show that in CHD7 knockout embryos neural crest tissue forms, as determined by the presence of specifier genes such as *Pax3* and *Zic1,* but fails to migrate (Bae *et al.*, 2014*)*. As mentioned above (section 1.2.6) CHD7 deficits are linked with the neurocristopathy CHARGE syndrome. Recent research has shown that the CHD7 protein binds to the promoter region of the tumour-suppressor gene *p53* ablating its expression. Dysfunction in the *CDH7* gene disrupted the formation of these complexes, causing overexpression of *p53* in mouse models. NCCs in affected

animals proliferated less and showed increased propensity to exit the cell cycle and undergo apoptosis. Mice heterozygous for *CHD7* knockdown expressed symptoms characteristic of CHARGE syndrome while double knockout was embryonic lethal. These data suggest that CHD7 may have a role in the proliferation and rapid expansion of the neural crest during development (Van Nostrand *et al*, 2015).

A multitude of post-translational histone modifications are involved in the specification and differentiation of the neural crest as well as in its subsequent delamination and migration, amongst them phosphorylation and ubiquitination. Although only the classical marks of acetylation and methylation have been studied in depth it is hypothesised that other post-translational alterations to histone structure act to recruit target proteins triggering the activation or silencing of specific genes (Strobl—Mazzulla and Bronner, 2013).

### 1.3.5 Neural Crest Plasticity

It has been a long held paradigm that neural crest stem cells undergo fate determination before their migration from the neural fold (Etchevers, 2006). However although differentiation is strictly and narrowly controlled according to position along the rostra-caudal axis some populations of neural crest derived somatic cells still retain plasticity. Neural crest derived cells from the skin, inner ear and dorsal root ganglia were isolated, those expressing NC marker Sox10 but not positive for CD117 were able to be differentiated into a variety of NC derived cell types while those positive for Sox10/CD117 were lineage restricted (Motohashi, *et al*., 2013). Schwann cell precursors have been shown to undergo partial dedifferentiation and give rise to melanocytes (Kaucka and Ademakyko, 2014). Further differentiation into somatic cell types has been shown to be dependent on

Notch signalling as well as the action of neuregulin1. These data, taken together suggest a complex array of signalling that is partly dependent on microenvironment of the cells as well as intrinsic genetic cues (Kipanyula, *et al.*, 2014). The neurotrophic factor NT-3 has been implicated in chemotaxis providing a concentration gradient up which cranio-facial NCCs migrate (Zanin, *et al*., 2013). Signalling molecules and transcription factors must combine to provide a complex network of appropriate cues both spatially and temporally not only to facilitate differentiation down the appropriate lineages but to allow survival and proliferation of migrating cells (Garcez, *et al*., 2014). Genes associated with the formation of the neural crest have, in recent years, been divided into two categories. Neural *crest* specifiers (such as *Slug, Snail* and the *Sox* family) are downstream targets of neural *plate* specifiers such as *Pax3* and *Zic1*, which are responsible for initiating the signal transduction pathways governing differentiation and migration of NCCs (Ono, *et al*., 2014).

## 1.4 Characterisation of Embryonic and Neural Crest Stem Cells

### 1.4.1 Embryonic Stem Cells

The characteristics of cells in any state of differentiation can be carried out by the detection of biomarkers associated with that state. In the case of embryonic stem cells, the presence of genes such as *Oct-4* (also termed *Pou5f1*) and *Nanog* in the transcriptome has been used to identify cells in a pluripotent state (Scheubert, *et al*., 2011). *Oct-4* and *Nanog* are both transcription factor expressed in the early stages of embryonic development and disruption of the expression of either one has been shown to result in differentiation of cultured cells suggesting that these factors work in tandem, playing a key role in the maintenance of pluripotency. *Oct-4* and *Nanog* are both able to bind to numerous sites in the mammalian genome, silencing or activating genes as necessary to maintain a pluripotent state (Okumura-Nakanshini, *et al*., 2004; Loh, *et al*., 2006; Takao*, et al*., 2007). In addition to *Oct-4* and *Nanog*, certain cell surface markers are uniquely expressed by embryonic stem cells. In murine systems these include stage-specific embryonic antigen 1 (SSEA-1) (Gu, *et al*., 2010), a carbohydrate closely associated with the facilitation of cellular adhesion (Yoshida-Noro, *et al*., 1999). SSEA-1 is commonly used as a marker of pluripotency, especially when co-expressed with proteomic indicators such as Oct-4 (Baharvnd, *et al*., 2007). The location of SSEA-1 on the cell surface has enabled the isolation of murine embryonic stem cells through techniques such as immunomagnetic separation. In this technique anti SSEA-1 antibodies are bound to magnetic microbeads, which conjugate to SSEA-1, presenting cells. The cell suspension is then passed through a column placed in a magnetic field. The beads are

retained by the column while unlabelled cells pass through, effectively isolating populations of SSEA-1 positive (pluripotent) cells (Ďurčová, *et al*., 1998).

The E14 murine embryonic stem cell line was established in the mid 1980's from the mouse strain 129/ola. The pluripotency of the cell line was established in experiments in which somatic cell nuclear transfer was used to transfer E14 nuclei into enucleated mouse oocytes. After implantation into a surrogate these transfected oocytes were able to produce viable offspring (Figure 1.6) indicating the ability of the cell line to form all tissues of the body (Wakayama, 1999).


**Figure 1.6. Hooper.** A representative mouse cloned from E14 nuclei implanted into enucleated murine oocytes (Wakayama, 1999). The generation of a viable animal from this stem cell line is indicative of a pluripotent nature.

## 1.4.2 Neural Crest Stem Cells

In a manner similar to cells maintained in an embryonic state a number of biomarkers are associated with neural crest stem cells. Initial differentiation into neuronal precursors can be verified by the presence of the intermediate filament protein Nestin (Pruszak *et al,* 2009). The low affinity nerve growth factor receptor p75 is a transmembrane protein closely associated with neurotrophin mediated signal transduction during cell differentiation (Stucky and Koltzenburg, 1997) and has been

used as a biomarker for neural crest stem cell in both murine and human models (Wong, *et al*., 2006). Intracellular molecular markers have also been described; zic1, musashi-1, sox9 and pax3 showing significant levels of upregulation in differentiating NCCs while other genes such as *Slug, Snail* and *Twist* are also quantifiably upregulated although to a lesser extent (Aihara *et al.,* 2010). Finally, the identity of neural crest stem cells can be confirmed by their directed differentiation into cells known to be of neural crest origin such as peripheral neurons, Schwann cells, neural glia and smooth muscle cells, the successful induction of these cell types being indicative of neural crest progenitors (Lee, *et al*., 2008).

Ret is a tyrosine kinase which is expressed in post - but not pre-migratory NCCs. It is exclusive to cells derived from the neural crest and has found use as a selective marker to isolate neuronal precursors and other cells. A network of regulatory and transcription factors associated with neural crest specification conjoin to induce the expression of *Ret* (Figure 1.7).

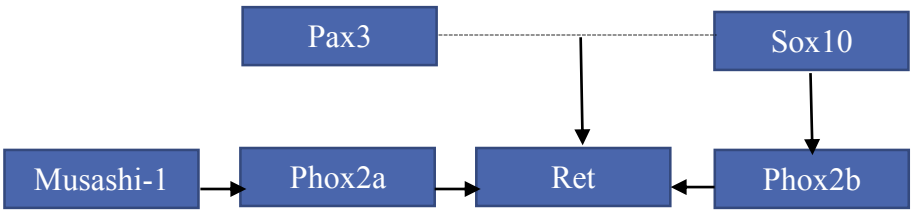


**Figure 1.7. Gene regulatory networks associated with the expression of Ret**. Dotted lines reresent interactions; arrows represet induction of expression.

*Ret* expression is considered essen tial for the innervation of tissues. For example neuralation is severly perturbed most markedly in the gut in *Ret* knockout mice and lethality ensues shortly after birth (Lo and Anderson, 1995; Anderson *et al*, 2006). Upon actiation by extracellular cues *Ret* stimulates the initiation of intracellular

signalling pathways such as the MAP kinase pathway which is required for the differentiation of neural crest derived cells (Goding, 2000; Ibáñez, 2013). Expression profiles of *Ret* through developing neural crest tissues may be dependent on the expression of the Homeobox (*Hox*) family of transcription factors consisting of a number (39 genes in four groups in mammals) of functionally redundant proteins controlling mammalian tissue patterning along the rostro-caudal axis. *Hox* genes have been identified as cofactors for BMP signaling and bind to and activate transcription of both *Sox9* and *Sox10*. The diverse *Hox* genes show overlapping patterns of expression across the vagal, trunk and sacral neural crest indicating that they may have a role in somatic fate determination which is dependent on placement along the anterior to posterior axis (Kam and Lui, 2015).

## 1.5 Characterisation of Somatic Cells Derived from the Neural Crest

### 1.5.1 Neural Progenitors

During differentiation and throughout the life of an organism a pool of neuronal progenitor cells emerges. Within the PNS, these progenitors are neural crest derived cells capable of forming sensory and autonomic neurons as well as glial cells. Neural progenitors are distinguished by the continued expression of pluripotency makers such as *Nanog* (Blake and Ziman, 2013) as well as certain exclusive proteins. Nestin is an intermediate filament protein expressed in neuronal precursors in both the central and peripheral nervous systems. Although there is little knowledge of its precise functions in part due to the short time period in which it is expressed it is commonly used as a biomarker for rapidly dividing migratory cells in both the PNS and CNS (Ramm, *et al.,* 2009; Aihara *et al.,* 2010).

### 1.5.2 Peripheral Neurons

The wide array of cell types of neural crest origin that make up the developing organism presents a challenge for their characterisation. In gross terms, the PNS can be divided into two distinct components. The somatic nervous system comprises neurons responsible for movement and sensory input while the autonomic nervous system regulates homeostasis and bodily response to stress (sympathetic) as well as controlling myogenic contractions such as those in the intestine (parasympathetic). (Swenson, 2006). All peripheral neurons function to transmit input from a sensor to an effector via the activation of action potentials. An action potential is generated when a neurons stimulus threshold is reached causing sodium ion ($Na^+$) channels to open in the cell membrane. This results in an influx of $Na^+$ into the cytosol changing

the polarity from negative to positive and allowing the conduction of the nerve impulse. Potassium ion ($K^+$) channels open less than one millisecond after the opening of the $Na^+$ channels restoring the cell to its original polarity. The passing nerve impulse activates the adjacent ion channels allowing the action potential to proceed along the axon. After the impulse has been propagated, the adenosine triphosphate ATP driven sodium potassium pump restores the ionic balance of the cytosol, transporting $K^+$ into the cell and $Na^+$ back into the extracellular fluid. Ion channels are found distributed along the axons of neurons either evenly in the case of unmyelinated neurons or at gaps in the myelin sheath (Nodes of Ranvier) in the case of myelinated neurons. This leads to two variants of impulse propagation, cable in which adjacent ion channels are opened sequentially and saltatory in which distal channels are activated causing the impulse to jump from node to node. Action potentials are initiated by a number of stimuli, for example the input from a specialised sensory organ or the endogenous signal generated by cells within myogenic structures such as the heart (Tortora and Derrickson, 2006; Purves *et al*, 2012).

Within the Somatic nervous system distinct subpopulations of neurons can be found, large body sensory neurons, responsible for proprioception differ morphologically and in gene expression profiles from small cell sensory neurons involved in nocioception (Table 1.2) (Raible and Ungos, 2006).

**Table 1.2. Differential gene expression in large and small cell body sensory neurons.**

| Gene | Large cell body sensory neuron | Small cell body sensory neuron |
|---|---|---|
| ***TrkA*** | | + |
| ***TrkC*** | + | |
| ***Brn3a**** | + | + |
| ***Runx1*** | | + |
| ***Runx3*** | + | |

The Trk family of tropomyosin-related kinases derive their name from the oncogene that facilitated the identification of the first discovered isoform TrkA. Subsequently isoforms TrkB and TrkC were isolated and characterised. Each isoform interacts preferentially with specific neurotrophin receptors although all are able to complex with p75 (Brahimi, *et al*., 2014). TrkA has been shown to form complexes with nerve growth factor (NGF) while TrkB and TrkC interact with brain-derived growth factor (*BDGF*) and neurotrophin-3 (*NT-3*) respectively. The neurotrophins, through ligand interactions with Trk receptors stimulate cellular processes such as dendrite growth and axon formation (Huang and Reichardt, 2003).

The *Runt* family of transcription factors are associated with specific sensory neuronal fates; *Runx1* has been shown to be expressed in nocioceptive neurons concurrently with *Ret*, a neurotrophin receptor presented in neural crest derived cells after the cessation of transiently expressed *TrkA* (Chen, *et al*., 2006). In embryogenesis, *Runx1* is indispensable in the proper innervation of outlying tissues, mice deficient for this gene show marked decreases in sensory neuronal presence in the hind paw (Yang, *et al*., 2013). Sensory neurons engaged in proprioception require the activity of *Runx3*, which is co-expressed with *TrKC*. Experiments with *Runx3* null mice have shown that they are characterised by limb ataxia, which is due

to disrupted connections between the spinal cord and motor neurons (Levanon, *et al*., 2002). *Brn3a* is a transcription factor expressed in the majority of cells in the sensory nervous system. The *Runx* factors are known downstream targets of this gene. *Brn3a* knockout mice express reduced axon growth and post-natal lethality inferring its role in neuronal development. Together, *Brn3a* and the *Runt* gene family repress the expression of *TrkB* facilitating proliferation of the *TrkA* and *C* responsive sensory neurons (Dykes *et al*, 2010).

Enteric neurons present a similar challenge in differentiation and characterisation to sensory neurons due to their diverse phenotypes. Different neurons in the enteric nervous target different cell types through a variety of neurotransmitters such as acetylcholine and noradrenaline. The successful recapitulation of specific peripheral neuron types from embryonic stem cells is dependent on their isolation from a pool of potentially homogenous cells (Anderson, 2006). Studies in which peripheral neurons were generated from embryonic stem cells commonly use the presence of the intermediate filament protein peripherin as a biomarker (Aihara*, et al.*, 2010; Kreitzer, *et al*., 2013). Peripherin localisation has been detected in both the cytoplasm and nuclei of neurons throughout the PNS as well as in selected regions of the central nervous system – most notably in those parts adjacent to the dorsal root ganglia. The presence of peripherin therefore whilst strongly indicative of peripheral neuron generation is not alone sufficient evidence and co-expression of biomarkers such as S-100 in ganglia is required for a more accurate classification (Eriksson, *et al*., 2008; Holland, *et al*., 2010). More robust characterisation would include functional analyses. Without evidence of the ability to transmit action potentials in putative differentiated neurons, for example it may be argued that differentiation protocols may differ from those observed *in vivo* and naturally, functionality must be

ensured if differentiation protocols are to eventually result in tissue replacement therapies.

### 1.5.3 Schwann Cells

Schwann cells are the glial cells of the PNS; they are found in close proximity with peripheral neurons and develop in several functional and morphological variants. Myelinating Schwann cells (MSCs) enshroud the axons of single neurons, providing an insulating sheath, which facilitates the conduction of saltatory action potentials. Myelinating Schwann cells can be identified by the presence of myelin protein zero, which contributes the major protein content of the myelin sheath (LeBlanc *et al*, 2006). Non-myelinating Schwann cells (NMSCs) in contrast to MSCs aid the conduction of action potentials via the cable method. They are associated with a group of clustered sensory neurons known as a Remak bundle. Perisynaptic Schwann cells (PSCs) are localised at the neuromuscular junction. PSCs detect and respond to synaptic activity and possess a greater number of neurotransmitter receptors than either MSCs or NMSCs inferring they play a less passive role in the conduction of action potentials than MSCs or NMSCs. Satellite cells (SCs) form a barrier around peripheral ganglia. They have supportive and maintenance roles, mediating the passage of nutrients and neuroactive chemicals to and from the ganglia (Auld and Robitaille, 2003; Corfas, *et al*., 2004; Hanami, 2005).

A number of factors modulate differentiation of the diverse types of Schwann cells from neural precursors. Neuregulin-1 (NGR-1) has been demonstrated to be important in directing NCCs to a glial fate and NGR-1 deficient mice have been shown to have reduced Schwann cell numbers and be susceptible to early lethality. However the exact role of NGR-1 in Schwann cell development remains unknown

(Chen, *et al*., 2006; Taveggla *et al.,* 2006). In murine adult nervous tissue a small subset of non-myelinating, Schwann cells express *Pax3* as well as *Sox2*. The presence of cells presenting these transcription factors and a pluripotency associated gene transcripts in adult tissues is indicative of a pool of potential glioblast cells with a potential role in repair and regeneration of damaged neurons (Blake and Ziman, 2013).

### 1.5.4 Cardiac Smooth Muscle

The neural crest contributes to a number of essential structures in the developing cardiovascular system. The pharyngeal arches, cardiac outflow tract and the great arteries (aorta and pulmonary) all feature smooth muscle cells derived from neural crest (Wiszniak and Schwartz, 2014). Colonisation of the emerging vascular system is dependent on signals originating from the underlying mesoderm and the endoderm. Wide varieties of signals converge on the NCCs both before and during migration. *Myocardin-related transcription factor B* (*MRTFB*) is necessary for both cardiac smooth muscle patterning and subsequent colonisation of outlying vessels. Mice lacking (*MRTFB*) present cardiac abnormalities similar to those described in Di George syndrome and a lack of smooth muscle actin positive cells in the aorta (Li *et al.,* 2005). Interestingly NCCs populating the outflow tract undergo programmed cell death upon completion of septation (Henderson and Chaudhry, 2012). As with the PNS, the mechanisms governing neural crest differentiation and population of the vascular system is poorly understood. It is clear however that a complex regimen of signalling is involved. The apoptosis of NCCs in the outflow tract is further evidence of their specialised function in the development of numerous mammalian tissues.

## 1.6 Summary

Development of the neural crest is a complex and involved process in vertebrate development. Although it is known that FGF-2 and BMP-4 are sufficient to derive a neural crest phenotype *in vitro* the precise mechanisms involved are at present poorly understood. Experiments have isolated numerous genes required for or assisting both patterning of neural crest, epithelial to mesenchymal transition and subsequent migration. Derivation and characterisation of neural crest tissues is further complicated by their transient nature and the lack of a single biomarker for identification. A number of genes are known to specify neural crest phenotype such as *Pax3*. However, this gene is expressed throughout the developing central nervous and the skeletal muscle systems and as such, expression of individual biomarkers cannot be taken as evidence of neural crest. Other neural crest markers such as *Sox9* are likewise expressed in diverse tissue types. Individual studies have identified numerous genes required for proper patterning and / or migration of neural crest stem cells but little is known about how these factors interact. Studies are further complicated by the use of serum or fibroblasts in some protocols, potentially perturbing analyses by the presence or excretion of bioactive factors into media. Culture in defined media may offer the scope for analyses of individual compounds in differentiation programs and global gene expression analysis may offer new insights on key factors and regulatory pathways underpinning neural crest development.

Perhaps the best identifier of neural crest stem cells is their multipotency. The ability to differentiate into a wide and diverse selection of tissues such as peripheral nerve and smooth muscle, taken together with the expression of neural crest associated

genes at key stages in differentiation can be indicative of neural crest lineage selection. Current methods to differentiate neural crest derived tissue focus on the expression of biomarkers such as peripherin for PNS neurons. Although this marker is indicative of a peripheral neuron phenotype, these analyses do not take into account functionality. Kreitzer *et al*. (2013) described functional neural crest stem cells by their ability to follow a chemotaxic gradient; however, no analyses beyond peripherin expression were carried out on terminally differentiated neurons. Verification of functionality would underpin transcriptional and translational analyses and aid in the validation of differentiation protocols.

The presented study aimed to investigate key factors in the specification and patterning of the neural crest through the development of serum-free, feeder free differentiation protocols. Differentiation into somatic cell lineages was focused on the peripheral neuron phenotype and analyses were underpinned by functional studies. Global gene expression analysis was used to determine the role of the key regulatory factor BMP-4 in the fate determination, proliferative and invasive characteristics and adhesion profile of the developing neural crest.

## 1.7 Aims and Objectives

- Generate neural crest derived peripheral neurons in serum-free, feeder-free culture conditions.
    - Initial assessment of neural crest phenotype by analysis of neural crest associated markers. Further confirmed by differentiation into somatic lineages of peripheral neuron and smooth muscle.
    - Peripheral neuron phenotype assessment by expression of peripherin, confirmed with functionality assays.
- Investigate potential novel key transcriptional factors in the differentiation of neural crest derived peripheral neurons.
    - Affymetrix® microarray analysis of differentiating peripheral neurons at key stages.
    - Computational analyses to identify potential regulatory elements and networks.
    - RT-qPCR, flow cytometry and Western blotting used to confirm microarray data.
- Investigate the role of BMP-4 on the development of the neural crest and derivative peripheral neurons.
    - Microarray, RT-qPCR and Western blotting analysis as above in cells treated with BMP-4 during differentiation and untreated cells.
    - Inhibition with BMP-4 antagonist Noggin to confirm affects and determine potential redundancy.

# Chapter 2: Materials and Methods

## 2.1 Preparation of E14 Complete Media

Foetal calf serum (FCS) (Lonza, UK) was inactivated by placing in a water bath held at 57°C for 30 minutes, inverting every 10 minutes. A 50ml aliquot was removed from a bottle of Knockout Dulbecco's Modified Eagles Medium (KO DMEM) (Gibco, UK) and 50 ml of inactivated FCS was added to the remainder. The medium was then supplemented with 5 ml 200 mM L-glutamine, 2.5 ml penicillin / streptomycin, 5 ml non-essential amino acids (NEAA) (100x) and 0.5 ml of 50 mM 2-mercaptoethanol (all Sigma, UK) as well as 0.5 ml of leukaemia inhibitory factor (LIF) (Millipore, UK).

## 2.2 Culture, Maintenance and Storage of E14 Murine Embryonic Stem Cells

0.1% (w/v) gelatin in deionised water (Sigma, UK) was sterilised by autoclaving at 121°C for 15 minutes. Between 2 and 5 ml was added to Nunclon$^{TM}$ surface flasks with filter caps (Thermo Fisher Scientific UK) for 25 $cm^2$ and 75 $cm^2$ flasks respectively. Initial seeding was carried out in 25 $cm^2$ flasks while established cultures were passaged into 75 $cm^2$ flasks. The gelatin-coated flasks were placed on a shaker at 100 rpm for 1 hour before excess gelatin was poured off and the flask rinsed with Dulbecco's Phosphate Buffered Saline (DPBS) (Oxoid, UK). For initial seeding 1 ml cryotubes frozen in liquid nitrogen were defrosted and the contents evenly distributed amongst three flasks. E14 complete media pre-warmed in a 37°C water bath was added before inoculated flasks were placed in an Autoflow IR direct heat $CO_2$ incubator (Nuaire, US) set to 37°C and 5% $CO_2$. After 24 hours medium

was changed by aspirating the original media before washing three times with DPBS, fresh media was added (both DPBS and media being pre-warmed at 37°C) and the flask was returned to the incubator. Medium was subsequently changed every two to three days depending on the rate of cell growth as determined by observation under an Axiovert 40 C phase contrast microscope (Zeiss, Germany) and noting the colour change from red to orange or yellow. Upon reaching approximately 70-80% confluence ascertained using a phase contrast microscope cells were either passaged into fresh flasks or frozen for storage.

Before passaging cells cultured in flasks were washed three times in DPBS before 0.5 ml or 1.5 ml (for 25cm$^2$ and 75 cm$^2$ flasks respectively) of 0.25% trypsin-EDTA (Sigma) was added. The flasks were then inoculated at 37°C and inspected under a phase contrast microscope. In order to break up any clumps of cells the bottom edge of the flask was gently tapped. The trypsinisation reaction was halted with the addition of serum containing medium (E14 complete) and the cells were evenly distributed into three new flasks before incubation as described above. For freezing of cells, 5 ml of dimethylsulphoxide (DMSO) (Sigma) was added to 45 ml of E14 complete medium. Cells were trypsinised and the reaction was halted as above. The cells and media were poured into a sterile universal tube, which was then centrifuged at 300g in a Sigma 1k10 centrifuge for 5 minutes before the medium was aspirated. A 3 ml volume of E14 medium containing DMSO was added and the pellet re-suspended by pipetting. A 1 ml volume of cell suspension was added to three sterile cryotubes, which were sealed and placed in a -20°C freezer for 1 hour. After this time the cryotubes were moved to a -80°C freezer, some cells were removed after 1 hour and placed in liquid nitrogen for long-term storage while the remainder were kept at -80°C.

## 2.3 Magnetic Activated Cell Sorting

Undifferentiated embryonic stem cells were isolated from spontaneously differentiated cells by magnetic activated cell sorting (MACS). Washing buffer was prepared by adding 0.5% (w/v) bovine serum albumin (BSA) and 2 mM EDTA to sterile DPBS and storing between 2-8°C. Flasks containing cells to be sorted were first washed twice in DPBS before 1.5 ml of 0.25% (w/v) trypsin EDTA was added. The reaction was allowed to proceed for 5 minutes at 37°C before being stopped by the addition of 8 ml of KO DMEM supplemented with 10% (v/v) FCS. A 10 ml serological pipette was used to generate a single cell suspension by repeated pipetting before transfer to a sterile universal tube. Cell counts were obtained using a Bio-Rad TC10 cell counter (Bio-Rad, US). An aliquot of cells was mixed with an equal volume of 0.4% (w/v) trypan blue. A 10 µl cell-trypan blue mixture was pipetted into the chamber of a counting slide (BioRad), which was inserted into the slot of the cell counter. The total cell count per ml and the percentage of live cells were recorded. The cell suspension was centrifuged at 300g for 10 minutes and the supernatant aspirated before the pellet was re-suspended in 80µl of washing buffer per $10^7$ total cells. Magnetic labelling was accomplished by adding 20 µl of anti SSEA-1 microbeads (Miltenyi Biotec, UK) per $10^7$ cells. Mixing was achieved by pipetting and the beads and cells were incubated for 15 minutes at 2-8°C. After this, cells were washed by the addition of 1 ml cold (2-8°C) washing buffer per $10^7$ cells before being centrifuged for 10 minutes at 300g. The supernatant was aspirated and the cells re-suspended in 500 µl of cold washing buffer. An LS MACS column, placed in the magnetic field of a MidiMACS separator (Miltenyi Biotec, UK) was prepared prior to use by the addition of 3 ml cold washing buffer. The 500 µl cell suspension was carefully added to the column ensuring the tip did not contact the

membrane. Unbound cells were removed from the column by the application of three washes of 3 ml of cold washing buffer. The flowthrough, containing unlabelled cells and any labelled cells not retained on the column was collected in a sterile universal tube. The column was subsequently removed from the magnetic field and held above a fresh sterile universal tube, 5 ml of cold buffer was added and a plunger used to force the cells from the column. Cell counts were obtained as described above.

## 2.4 Differentiation of E14 Murine Stem Cells into Neural Crest Cells in Defined Media

A modified version of Aihara *et al.*'s (2010) protocol was employed to derive neural crest stem cells from embryonic precursors. Plates of 24 wells (Thermo-Fisher Scientific) were coated with gelatin (Sigma) as previously described. Magnetically sorted SSEA-1 positive cells were seeded at a density of $5 \times 10^3$ cells per $cm^2$. Cells were grown in complete media for 2 days (Stage 0). Primary induction media (PIM) was produced by supplementing NMN basal media (Sciencell, UK) with 1x NEAA, 100μM L-glutamine, 10 μg $ml^{-1}$ insulin, 5 μg $ml^{-1}$ transferrin, 10 μM mercaptoethanol, 10 μM ethanolamine, 20 nM sodium selenite, 100 ng $ml^{-1}$ heperan sulphate and 10 ng $ml^{-1}$ FGF-2 (all from Sigma). Secondary induction media (SIM) was prepared by supplementing PIM with 8 ng $ml^{-1}$ BMP-4 (Sigma). Cells were treated with PIM for four days (Stage 1). Media was removed, the wells were rinsed three times with DPBS buffer and fresh media was added daily. A phase contrast microscope was used to obtain photomicrographs of the cells on each day. After 4 days culture in primary media cells were cultured in SIM for a further 10 days (Stage 2). Cells from the same isolated SSEA-1 positive fraction were seeded and cultured in complete media as a control.

## 2.5 Secondary Differentiation

After 10 days culture in SIM cells were cultured in PIM to induce differentiation into peripheral neuron lineages. To induce smooth muscle differentiation cells were cultured in KODMEM supplemented with 10% FCS, 20 μM L-glutamine, 1x NEAA and 50 μM mercaptoethanol (SM media). Analyses were carried out on cells at all stages of differentiation (Figure 2.1).

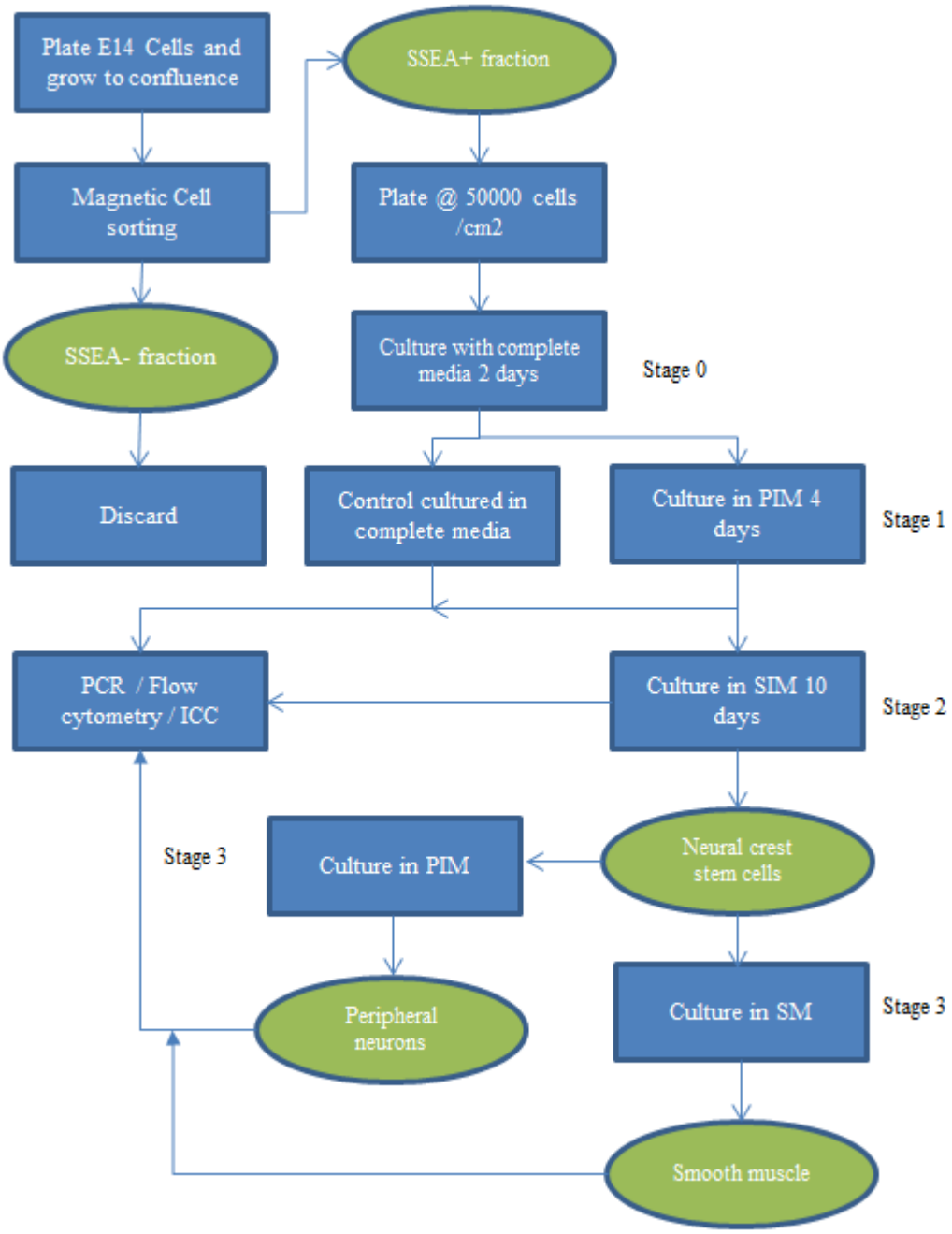


**Figure 2.1. Process flow of embryonic stem cell differentiation.** E14 mouse embryonic stem cells were differentiated in three stages into somatic cells. Green ovals represent cells at varying stages of differentiation; blue oblongs represent processes. All times are additive. Analyses were carried out after completion of each stage and at varying time-points throughout stage 2.

## 2.6 RNA extraction

RNA extraction was carried out using TriSure$^{TM}$ reagent (Bioline). Cells were cultured in 6 well plates until approximately 80% confluence was reached. Media was aspirated and 1 ml of TriSure$^{TM}$ was added. To ensure complete dissolution of the nucleoprotein complex cells were incubated for 15 minutes at room temperature. Cell lysates were pipetted into eppendorf tubes, 0.2 ml of chloroform was added, tubes were shaken for 15 seconds and left to stand at room temperature for 15 minutes. Phase separation was carried out by centrifuging for 15 minutes at 12000g at a temperature of 4°C. The RNA-containing aqueous phase was pipetted into fresh Eppendorf tubes taking care not to disturb the DNA containing interphase. RNA was precipitated by adding 0.5 ml of cold isopropanol before the tubes were stood for 10 minutes at room temperature. Tubes were centrifuged at 12000g for 10 minutes and the liquid phase was aspirated taking care not to disturb pelleted RNA. RNA pellets were dissolved in 30 µl of nuclease free water and stored at -80°C for up to 12 months. Cells were differentiated in three stages. During stage-2 of differentiation, cells were cultured in SIM to drive neural crest differentiation. Control cells were cultured in PIM. RNA was extracted at each stage and at the start (after 1 hour), middle (after 5 days) and end (after 10 days) of stage 2.

## 2.7 Quantification of Nucleic Acids

Quantification extracted RNA was carried out using a Nanodrop 2000 (Thermo-Fisher Scientific). The nucleic acid tab was selected and RNA chosen from the drop-down menu. A blank reading was obtained by placing 1 µl of nuclease free water on the pedestal and selecting blank. The pedestal was wiped with a lens tissue, 1 µl of each sample was added, and the measure button selected. The absorbance readings at

260 and 280 nm were recorded and the ratio (260:280) calculated. Concentration of RNA acids in ng $\mu l^{-1}$ were determined by multiplying absorbance at 260 nm by 40. RNA was diluted to a concentration of 200 ng $\mu l^{-1}$ for cDNA synthesis (section 2.8).

## 2.8 cDNA Synthesis

RNA reaction mixtures were prepared by adding 400 ng of RNA (at a concentration of 200 ng $\mu l^{-}1$) on ice to a microcentrifuge tube containing 1 µl of random hexamer primers (0.5 µg per reaction) (Promega). 2 µl of nuclease free water was added to each tube to bring volumes to 5 µl. In order to break down secondary structures and ensure complete denaturation this mixture was heated at 70°C in a Quanta Biotech Q-Cycler II thermocycler for 5 minutes then chilled on ice for a minimum of 5 minutes. Experimental reaction mixtures consisting of Improm-II Reaction buffer (5x), magnesium chloride, a deoxynucleotide mixture, Improm-II reverse transcriptase and recombinant RNasin® ribonuclease inhibitor (all Promega) were prepared on ice according to manufacturer's instructions (Table 2.1). Experimental reaction mixture (15 µl) was combined with each 5 µl target RNA reaction mixture before the reverse transcriptase reaction was carried out.

**Table 2.1 Experimental Reaction Mixtures for cDNA Synthesis.**

| Component | Concentration | Volume |
|---|---|---|
| **Reaction buffer** | 5x | 4.0 µl |
| **Magnesium Chloride** | 25 mM | 4.5 µl |
| **dNTP mix** | 10 mM | 1 µl |
| **Reverse transcriptase** | 50 units $\mu l^{-1}$ | 1 µl |
| **RNAse inhibitor** | 20 units $\mu l^{-1}$ | 0.5 µl |
| **Nuclease free water** | - | 4.0 µl |
| **Total** | - | 15 µl |

Tubes were placed in a thermocycler that was set for an initial annealing step of 25°C for 5 minutes followed by an extension step of 42°C for 1 hour before the reaction was halted by holding the tubes at 70°C for 15 minutes. The tubes were held at 4°C until removal from the thermocycler and stored at -20ºC.

## 2.9 Amplification of Target Gene Fragments by PCR

Reaction mixtures for PCR amplification of target gene fragments were prepared according to manufacturer's instructions (Table 2.2). 12.5 µl of 2x PCR mastermix (Promega) containing *Taq* polymerase, dNTPs, magnesium chloride and reaction buffer was added to a microcentrifuge tube on ice. Synthesised cDNA (section 2.8)

was diluted to 1:40. Primer solutions were diluted to a concentration of 10 pM $\mu l^{-1}$ and 1µl of forward and reverse primer was added primer sequences are presented in Appendix 2. Reaction mixtures were made up to 25 µl with nuclease free water and centrifuged for 30 seconds in a microcentrifuge.

**Table 2.2 Reaction mixes for PCR.**

| | **Reaction mix** | **Negative control** |
|---|---|---|
| **2 x PCR master mix** | 12.5 µl | 12.5 µl |
| **Forward primer** | 1 µl | 1 µl |
| **Reverse primer** | 1 µl | 1 µl |
| **cDNA** | 2 µl | - |
| **Nuclease free water** | 8.5 µl | 10.5 µl |
| **Total** | 25 µl | 25 µl |

The negative control reaction was carried out for each experiment to ensure all amplified bands were derived from cDNA and not from an external source. The reaction mixes were placed in a thermocycler. Initial denaturation was carried out at 95ºC for 5 minutes, denaturation at 95º C for 30 seconds was followed by annealing at 60-63º C for 15-30 seconds and extension was carried out at 72º C for 30-60s. Individual cycles may be found in Appendix 2. Upon completion of the PCR cycle, a 6 µl aliquot was removed from the tube and mixed with 2µl of loading dye (section 2.0). A 2% agarose gel was prepared by adding 0.6 g of agarose (Oxoid) to 30 ml of

1X TBE buffer and heating for 10 seconds at a time in a microwave oven on maximum power until the agarose was completely dissolved. This mixture was cooled to approximately 50°C and 30 µl of GelRed (Cambridge Bioscience, UK) was added. The preparation was poured into a mould, a comb was inserted and the gel allowed to set after which the comb was removed. The agarose gel was placed in a gel tank and immersed in 1X TBE buffer. The PCR product mixed with loading buffer was pipetted into the wells and 50V was applied. The current was stopped before the loading dye reached the bottom of the gel. The gel was removed and visualised using a G:Box transilluminator (Thermo-Fisher Scientific). Hyperladder I (Promega) was used as a size marker.

## 2.10 Real Time Quantitative PCR (RT-qPCR)

SSEA-1 positive E14 murine embryonic stem cells were isolated by magnetic cell sorting as previously described, seeded at a density of 50 000 cells $cm^{-3}$ and grown for two days in complete medium. Cells were treated with primary induction media for 4 days and secondary induction media for a further 10 days. Control cells were co-cultured in complete media. RNA was extracted using TriSureTM as previously described (section 2.6) from triplicate samples of treated and control cells. To establish baseline expression levels as a viable basis for comparison RNA was extracted from cells cultured in complete media for two days after cell sorting.

Extracted RNA was quantified by Nanodrop (section 2.7) and diluted to a concentration of 400 ng $\mu l^{-1}$ before cDNA synthesis (section 2.8). Synthesised cDNA was further diluted 1:40 prior to PCR. PCR mastermix was prepared on ice according to manufacturer's (Bioline UK) instructions in 96 well plates (Table 2.3).

**Table 2.3. Reaction mixture for RT-qPCR.**

| Component | Vol. per tube |
|---|---|
| **Sensi-fast lo-rox mastermix** | 10 µl |
| **Forward primer** | 0.8 µl |
| **Reverse primer** | 0.8 µl |
| **Nuclease free water** | 3.4 µl |

Volumes of 5 µl of diluted cDNA was added to each tube, each sample was added in duplicate negative control samples were prepared by adding 5 µl of nuclease free water to tubes containing reaction mixture before the plate was sealed and pulse spun to 500 rpm. PCR reactions were carried out in a Stratagene MX3000 (Agilent, US) with melt curve analysis ensuring amplification of single targets. Initial denaturation was carried out at 95°C for 2 minutes for all primer sets. Cycling conditions except annealing temperature/time and number of cycles were the same for all primer sets (Table 2.4). Primer sequences, annealing conditions and cycle number are shown in Appendix 2.

**Table 2.4. Cycling conditions for RT-qPCR.**

| | Temperature (°C) | Time (s) |
|---|---|---|
| **Initial denaturation** | 95 | 120 |
| **Denaturation** | 95 | 30 |
| **Annealing** | variable | variable |
| **Extension** | 72 | 30 |

Standard curves were developed by plotting the Ct of serial dilutions of cDNA against the log of the reciprocal of the dilution factor. The slope of the standard curves was used to determine primer efficiency, applying the equation efficiency = $10^{(-1/slope)}$. Reactions yielding efficiencies outside of the range 90-110 were subject to further optimisation. Relative quantification was calculated using the ΔΔCt method and all expression values were normalised to the average values of β-actin and 18s ribosomal RNA.

## 2.11 Immunocytochemistry

Glass coverslips were sterilised by autoclaving for 15 minutes at 121°C, placed in individual wells of a 24 well plate and treated with 0.1% (w/v) gelatin for 1 hour with gentle agitation. Cells counts were obtained using a Bio-Rad TC10 cell counter as previously described. Approximately 50 000 cells $cm^{-3}$ were seeded in each well and incubated at 37°C overnight. Media was aspirated and cells were fixed by the addition of 4% (w/v) paraformaldehyde. After 20 minutes, the paraformaldehyde was aspirated and cells were rinsed once with PBS. Permeabilisation of cells was carried out by 5 minutes incubation in 2% (w/v) BSA in PBS containing 0.1% (v/v)

Triton X-100, followed by blocking in 2% (w/v) BSA in PBS for 30 minutes with gentle agitation. Primary antibodies, diluted in 2% (w/v) BSA in PBS in varying concentrations (Table 2.5) were added to wells and incubated for 1 hour at room temperature. Cells were washed three times for 5 minutes in PBS. Before addition of secondary antibody

**Table 2.5. Primary antibodies used in ICC.**

| Antibody | Dilution | Supplier | Host |
|---|---|---|---|
| **p75** | 1:200 | AbCam | Rabbit |
| **p0** | 1:100 | AbCam | Rabbit |
| **Peripherin** | 1:500 | AbCam | Rabbit |
| **Sox10** | 1:200 | AbCam | Rabbit |
| **P-SMAD** | 1:300 | AbCam | Rabbit |
| **Neurexin3** | 1:250 | AbCam | Rabbit |
| **F-actin** | 1:1000 | Invitrogen | NA* |

*F-actin staining was carried out using phalloidin extracted from *Amanita phalloides* pre-conjugated with Texas-red.

Secondary antibody (Alexa-fluor 488, Life technologies, UK) was diluted to 1:800 in 2% BSA and added to wells, which were incubated in the dark for 1 hour at room temperature. Wells were washed 3 times for 5 minutes in PBS and the coverslips were removed and mounted on slides with DAPI Vectashield mounting media

(Vector Labs) secured with nail varnish and visualised using Axio vision software coupled to a Zeiss Axio Vison Z1 fluorescent microscope within two hours of staining.

## 2.12 Cell Cycle Analysis

Cells were cultured as described for RT-qPCR (2.10) before being trypsinised and counted. Cells were diluted to a concentration of 100 000 $ml^{-1}$ in PBS before being fixed by adding to 3 ml of ice-cold ethanol while vortexing. Cells were centrifuged for 10 minutes at 500xg and the ethanol was aspirated. Cells were washed by the addition of 2 ml PBS and centrifuged at 500xg for 10 minutes. A 500 µl volume of PBS was added to each sample followed by 25 µl of propidium iodide (PI) and 20 µl of RNAse A. Cells were incubated in the dark at 37°C for 30 minutes before centrifugation at 500xg for 10 minutes. Staining solution was aspirated, 1 ml of FACS flow buffer was added and cell cycle analysis was carried out using a BD FACS Calibur (BD Biosciences, US). Fluorescence of PI stained cells was measured on the FL-2 channel. Data was collected and analysed using CellQuest Pro (BD Biosystems) and Modfit LT (Verity Software House, US) respectively.

## 2.13 Protein extraction and quantification

Protein was extracted using radioimmunoprecipitation assay (RIPA) buffer which was prepared beforehand and stored in frozen aliquots. RIPA buffer consisted of 25mM Tris-HCl, 150mM NaCl, 0.5% sodium deoxycholate, 1mM EDTA 1mM EGTA, 1mM PMSF and 1% (v/v) Triton X-100 (all Sigma) in 100 ml $dH_2O$ pH adjusted to 7.5. Before use 10 µl per ml of protease inhibitor cocktail (Sigma) was added. Media was aspirated from cells in 6 well plates at 80% confluence and 300 µl of RIPA buffer was added. Wells were scraped using a cell scraper to aid detachment

and cell lysates were pipetted into Eppendorf tubes stored on ice. Protein was quantified using the Bradford assay. Duplicate stock solutions of bovine serum albumin were prepared in $dH_2O$ at 1 mg $ml^{-1}$. These were diluted into aliquots of 0.8, 0.6, 0.4 and 0.2 mg $ml^{-1}$. Bio-Rad assay buffer was diluted to 1 part in 5 in $dH_2O$ and 5 ml was pipetted into bijoux tubes. 100 µl of each BSA solution were added to diluted Bio-Rad buffer with $dH_2O$ used as a blank. Absorbance was measured for each dilution in duplicate and averages obtained. Standard curves were obtained by plotting absorbance against concentration. To quantify protein concentration 10 µl of cell lysate was added to 90 µl of $DH_2O$ this was added to 5 ml of diluted Bio-Rad buffer and absorbance was determined at 595 nm. The standard curve was used to determine protein concentration as a function of absorbance.

## 2.14 Sodium Dodecyl Sulphate-Polyacrylamide Gel Electrophoresis (SDS-PAGE)

Extracted protein was diluted to a concentration of 1 µg $ml^{-1}$ in Laemmli sample buffer (126 mM Tris-HCl, 20% (v/v) glycerol, 0.02% (w/v) bromophenol blue, pH adjusted to 6.8, 10 µl $ml^{-1}$ mercaptoethanol added prior to use) (all Sigma). Separating buffer was prepared by adding 45.5g Tris-base (Thermo-Fisher Scientific) and 1g of sodium dodecyl sulphate (SDS) (Sigma) to 200 ml of deionised water. The pH was adjusted to 8.8 with HCl before deionised water was added to a final volume of 250 ml. Separating gel was prepared by adding 4.2 ml of deionised water, 3.3 ml of cold 40% bis acrylamide (Bio-Rad), 100 µl 10% (w/v) of ammonium persulphate (APS) and 10 µl Tetramethylethylenediamine (TEMED) (both Sigma) to 2.5 ml of separating buffer in a universal tube. The tube was inverted 2-3 times and 4.5 ml of gel was pipetted into a gel caster (Bio-Rad).

Separating gel was left to polymerise at room temperature before the addition of stacking gel.

Stacking buffer was prepared by adding 15g of Tris-base and 1g of SDS to 200 ml of deionised water. The pH was adjusted to 6.8 with HCl and distilled water added to a final volume of 250 ml. Stacking gel was prepared by adding 6.1 ml of deionised water, 1.45 ml of cold 40% bis acrylamide (5% cross linker), 100 µl of 10% (w/v) APS and 10 µl TEMED to 2.5 ml of stacking buffer in a universal tube. The tube was inverted 2-3 times and stacking gel was pipetted into a gel caster on top of polymerised stacking gel to the top of the caster. A comb was added and the stacking gel allowed to polymerise at room temperature.

Two gel casters were placed in a gel tank, which was filled to the top between the casters and to the line outside with electrophoresis buffer (6.01g tris-base, 2.0g SDS, 28.84g glycine in 1 l deionised water). The combs were removed and 20 µg of protein was loaded in each well. 5µl of protein size ladder (Qiagen) was loaded in the outermost wells. The gel tank was connected to a power pack with voltage set to minimum and current to maximum. The pack was switched on and voltage adjusted to 60V initially and 200V when the dye front had migrated to the border of the stacking and resolving gel. Gels were run until clear separations of bands in the protein ladder were observed.

## 2.15 Western Blotting

Protein transfer was carried out by placing gels on a semi-dry blotter (Bio-Rad) on top of three sheets of blotting paper and a nitrocellulose membrane (Amersham Life Sciences). Paper and membranes were pre-soaked in Towbin buffer (1.51g Tris-base (Thermo-Fisher Scientific), 7.2g glycine, 0.167g SDS, 75 ml ethanol (all Sigma), in

deionised water, pH adjusted to 8.3 and filled to a final volume of 500 ml with deionised water). Three more sheets of pre-soaked blotting paper were added and the lid fixed in place. The apparatus was connected to the power supply adjusted to maximum voltage and minimum current, adjusted to 50 mA after power was applied; the transfer was carried out over 1 hour.

Membranes were inspected to ensure visible transfer of the protein ladder and blocked in 1% (w/v) BSA in TBS-Tween (1.211g tris-base, 8.18g NaCl (Sigma), 1 ml Tween-20 (Sigma) in deionised water, pH adjusted to 7.4, final volume adjusted to 1 litre). Membranes were incubated in blocking solution for 1 hour at room temperature with gentle agitation.

Primary antibodies were diluted in blocking solution according to manufacturer's specification and membranes were incubated at room temperature for one hour with gentle agitation. Membranes were given four 5 minute washes in TBS-Tween before incubation with secondary antibody, diluted in 5% (w/v) milk powder in TBS-Tween, according to manufacturer's specification. Membranes were incubated for 1 hour at room temperature and given four 5 minute washes in TBS-Tween. Developing solution was mixed equally with horseradish peroxidase solution (both Thermo-Fisher Scientific) and 1 ml of mixed solution was evenly spread over each membrane. After 1 minute excess solution was tipped off and the membranes were visualised using a Chemidoc touch transilluminator (Bio-Rad)

## 2.16 RNA Microarray Analysis

Total RNAs were extracted from cells cultured in induction media in the presence and absence of BMP-4 (Figure 2.2) during stage-2 according to section 2.6. RNA integrity was determined using an Agilent 2100 bioanalyzer (Agilent, US). Prior to

use gel-dye mix was prepared, 550 µl of RNA 6000 Nano gel matrix (Agilent) was pipetted into the top receptacle of a spin filter tube. The tube was placed in a microcentrifuge and spun at 1500g for 10 minutes. 65 µl aliquots of filtered gel were pipetted into microcentrifuge tubes and stored at 4°C. Gel-dye mix was prepared by adding 1 µl of RNA 6000 Nano dye concentrate (Agilent) to a 65 µl aliquot of filtered gel. The mix was vortexed thoroughly before being centrifuged at 13000g for 10 minutes. A fresh RNA Nano chip (Agilent) was placed on the chip priming station and 9 µl of gel dye mix was pipetted into the well marked G. The chip was closed; the plunger of the syringe was pressed down until held by the clip and released after 30 seconds. After a further 5 seconds, the plunger was pulled back to the 1 ml position. The chip priming station was opened and 9 µ of gel dye mix pipetted into the marked wells. An aliquot of RNA 6000 Nano marker (5 µl) (Agilent) was pipetted into the 12 sample wells and the ladder well. RNA was quantified as above and aliquots were diluted to 100 ng $\mu l^{-1}$. To minimise secondary structures samples were heat denatured at 70°C for 2 minutes before loading. Chips were loaded by adding 1 µl of sample into each sample well and 1 µl of nuclease free water into the ladder well. The chip was vortexed for 60 seconds at 2400 RPM before being placed in the bioanalyzer. Analysis was carried out by 2100 Expert Software (Agilent), returning ribosomal integrity numbers (RIN) for each sample. RNA aliquots of 200 ng $\mu l^{-1}$ were prepared and transported in dry ice to the University of Manchester Genomic Technologies Core Facility. Gene expression of stage-0 cells (embryonic stem cells) were compared to stage-1 cells cultured for 1 extra hour in PIM. Expression of these cells was compared to that of stage 2 cells (neural crest) which was in turn compared to stage 3 cells (peripheral neurons). To determine the effects of BMP-4 on differentiation during stage-2 gene expression

was compared between cells at the initial stage (1 hour) and final stage (10 days) to cells cultured during stage 2 in PIM cells cultured in SIM during stage 2 were termed treated, cells cultured in PIM were termed untreated (Figure 2.2).

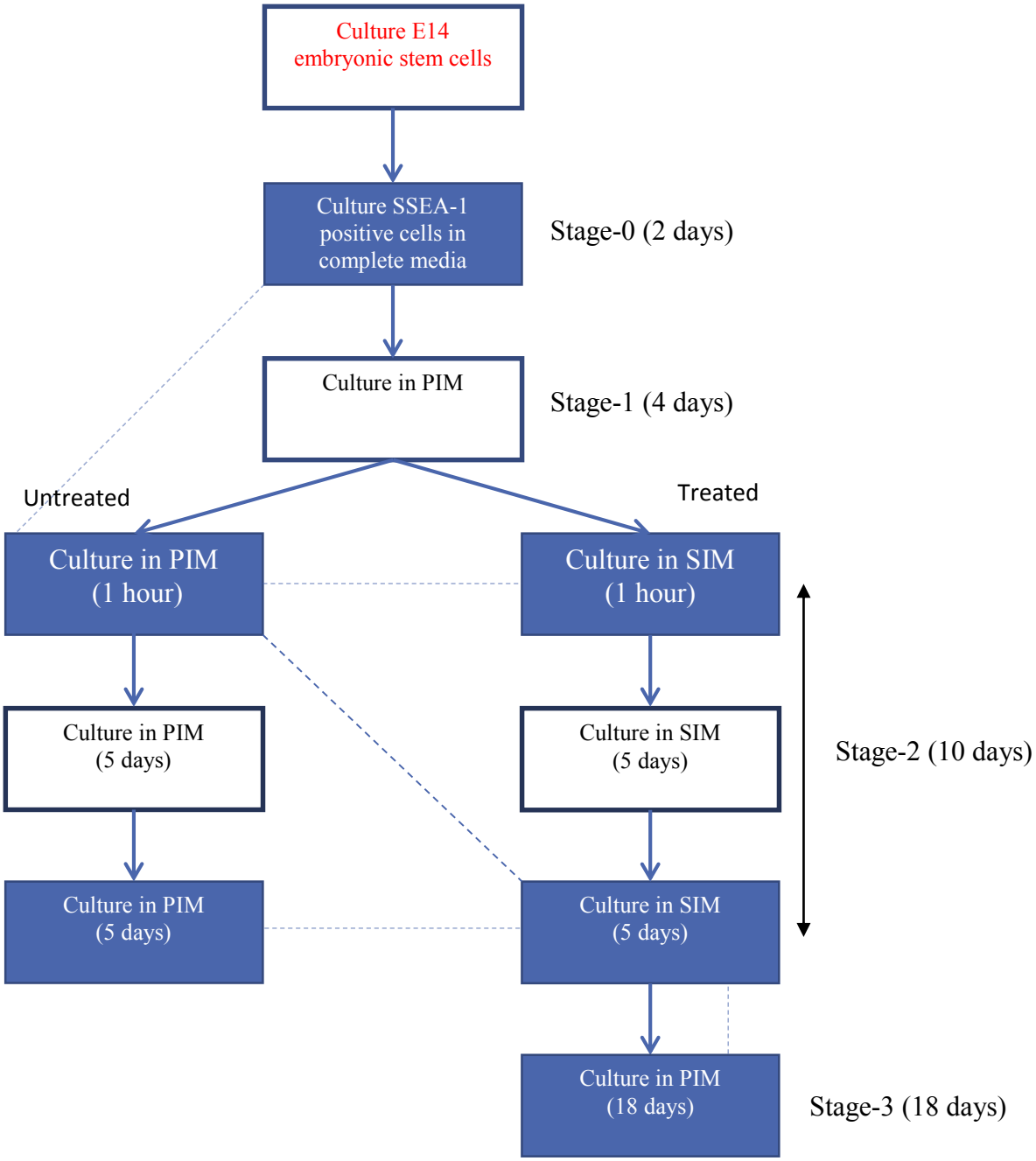


**Figure 2.2. Culture and selection of cells for microarray analysis.** White boxes denote culture processes, blue boxes denote samples sent for analysis dotted lines denote comparisons between samples. Stage 2 times were cumulative. Treated cells were cultured with SIM containing BMP-4 during stage 2 of differentiation; untreated cells were cultured in PIM.

Microarray analyses were carried out by Mr Michael Smiga using an Affymetrix 3 Prime IVT ID chip (Mouse genome 430 2 array). Data was transferred to the University of Manchester Bioinformatics Core Facility where principle component analysis and quality assurance was carried out by Dr Leo Zeef (University of Manchester). Median probe intensity before normalisation and percentage of outliers were recorded for each sample. Microarray data was presented in an Excel file detailing the sort function was used to identify the 500 most upregulated and downregulated genes in each comparison.

Pathway data was analysed using the DAVID functional annotation tool (National Library of Medicine). The 500 most upregulated or downregulated genes for each comparison were selected and pasted into the gene list. The relevant microarray (Affymetrix_3Prime_IVT_ID) was selected as the identifier from the drop down menu. Functional annotation clusters and charts with enrichment scores above 2 were analysed and KEGG analysis carried out where available.

## 2.17 Microelectrode Array Analysis

Cells were grown in primary induction media (Sections 2.4 and 2.5) for four days before either continued culture in PIM or culture with SIM for a further 10 days. Both sets of cells were grown in PIM and routinely cultured for 60 days, at this stage treated were shown to be peripherin positive (Figure 5.3). After this time cells were trypsinised, counted and approximately 100 000 were plated on MEA chips (Multi Channel Systems, Germany). Prior to use chips were washed with 70% IMS before being placed under UV light for 30 minutes. Chips were washed 3 times with PBS and coated with laminin according to manufacturer's instructions (Anon, 2015). Two hours before testing media was aspirated, chips were washed 3 times with PBS and fresh PIM was added. The chips were placed in the head stage of an MEA-2100

system, which had been pre-heated to 37°C. Cells were allowed to equilibrate for 5 minutes before readings were taken and all data were recorded using MC_Rack software (The MEA-2100 system and software were loaned from Multi Channel Systems). Cells were treated with N-methyl-D-aspartate (NMDA) (120 µl at a concentration of 1.7 µM) and gamma amino-butyric acid (GABA) (100 µl at a concentration of 1mM) to measure excitatory and inhibitory effects respectively. MC-Rack software allowed stimulation of specific or all electrodes. At all times when electrodes were stimulated, -120 µV was applied with 3 second pauses between pulses.

## 2.18 Biomarker Analysis by Flow Cytometry

Cells were fixed as in cell cycle analysis (2.12) before being re-suspended in 500 µl 0.1% Triton-x-100 in PBS. Cells were incubated in the dark at room temperature for 10 minutes before being centrifuged at 500G for 5 minutes before re-suspension in 500 µl PBS. Cell counts were taken as described in section 2.3 and cells were re-suspended at a concentration of approximately $10^6$ $ml^{-1}$ in 0.1% (v/v) Triton X-100 in PBS. Primary antibody (Rabbit anti-Peripherin (AbCam), 1:100, Rabbit anti-Oct-4 (Santa-Cruz), 1:100, Rabbit anti-Dppa5 (AbCam), 1:100, mouse anti-Nanog (Santa-Cruz), 1:50)) was added and cells were incubated in the dark for 1 hour before being centrifuged at 500g for 5 minutes and washed with PBS. Secondary antibody (Alexa-fluor 488 anti-rabbit or anti-mouse IgG conjugated with FITC) at a dilution of 1:800 was added in 500 µl Triton X-100 in PBS and cells were incubated in the dark for 1 hour. Cells were centrifuged at 500g for 5 minutes and washed with PBS before centrifugation was repeated and cells were re-suspended in FACS Flow. Cells were analysed on a BD FACS Calibur (BD systems) flow cytometer using Cell Quest Pro (BD systems).

## 2.19 Noggin Inhibition of BMP-4

Embryonic stem cells were magnetically isolated and cultured as in 2.3 and 2.4 (above) to induce neural crest differentiation (differentiation stages 1 and 2). During stage 2 Noggin (Sigma) was added at a concentration of 10 ng $ml^{-1}$. SIM supplemented with Noggin was termed inhibition media (IM). Culture in IM was carried out at the beginning of stage 2 and after culture in SIM for 5 days (Table 2.6). Cells were cultured for a total of ten days before RNA was harvested (section 2.6). The expression of pluripotency and neural crest biomarkers was measured using RT-qPCR (section 2.10). Expression levels were compared to cells cultured in SIM (expression value =1) and Student's T-tests were used to determine statistical significance. As a further point of comparison gene expression in cells cultured in PIM during stage 2 was also measured in order to gauge the efficacy of inhibition.

**Table 2.6 Noggin inhibition during stage 2 of differentiation**. The BMP-4 agonist Noggin was added to cultured cells at different time points during stage 2 of differentiation.

| Culture conditions | Media (days 1-5) | Media (days 5-10) |
|---|---|---|
| Treated | SIM | SIM |
| 10 days inhibition | IM | IM |
| 5 days inhibition | SIM | IM |
| Untreated | PIM | PIM |

## 2.20 Phylogenetic Analysis

The National Centre for Biotechnology Information (NCBI) database was used to obtain the amino acid sequence for proteins before these were entered into the Clustal W2 tool hosted by the European Bioinformatics Institute (EBI) (http://www.ebi.ac.uk/Tools/msa/clustalw2/) in order to generate a phylogenetic tree. Sequence comparison was carried out using the MUltple Sequence Comparison by Log Expectation (MUSCLE) tool (EBI) (http://www.ebi.ac.uk/Tools/msa/muscle/). The protein blast function (NCBI) was used to compare domain structures between proteins (http://www.ncbi.nlm.nih.gov/protein/).

# Chapter 3: Growth and Differentiation of E14 Mouse Embryonic Stem Cells.

## 3.1 Introduction

Cellular differentiation is the culmination of a complex network of cell regulatory mechanisms. Traditional culture techniques have relied on feeder layers of murine embryonic fibroblasts or the presence of FCS. The presence of FCS or feeder cells has limited the extent of investigation into the effects of individual growth factors due to the possible influence on differentiation from signals originating from either of these factors, both of which are known to introduce various inductive agents into media (Tamm, 2013). The use of defined factors in serum free media has allowed the elucidation of mechanisms of development without potential perturbation from exogenous sources (Keller, 2005). Culture in the absence of serum or feeder layers allows tighter control of growth parameters, enabling more accurate and reproducible experiments.

Although the development of the neural crest is both convoluted and intricate, it has been shown that just two extrinsic factors; FGF-2 and BMP-4 stimulate the differentiation of neural precursor cells into invasive, proliferative cells displaying markers found in neural crest stem cells. Differentiation of neural crest from ESCs is dependent on the establishment of a BMP-4 concentration gradient (Sailer *et al., 2005*, Milet *et al*., 2013). BMP-4 is one of the key regulators of differentiation acting in an inhibitory or inductive manner in various cellular processes (Xu, *et al.,* 2008; Fei, *et al.,* 2010). No single biomarker unique to the neural crest has been identified thus far; characterisation of neural crest stem cells is dependent on a number of

factors, commonly increased gene expression levels of *Pax3, Sox9, p75* and *Musashi-1* (Lo *et al.,* 1998; Cheung and Briscoe, 2003; Plouhinec, *et al*., 2014). Neural crest stem cells are able to differentiate into a wide range of somatic cells such as peripheral neurons, cranio-facial cartilage, melanocytes and smooth muscle. Populations of cells able to form these diverse tissues and expressing the above may be identified as neural crest (Dourain and Dupin, 2014).

### 3.2 Aims

- Differentiation of homogenous cultures of embryonic stem cells in defined media optimised to induce neural crest lineage.
- Further differentiation into somatic cell types – peripheral neurons and smooth muscle cells.
- Investigate the effects of BMP-4 on the growth characteristics and expression of neural crest biomarkers of embryonic stem cells in serum free culture.

### 3.3 Results

#### 3.3.1 Magnetic Activated Cell Sorting

After MACS isolation of SSEA-1 positive and negative fractions of E14 mouse embryonic stem cells RNA from SSEA-1 both fractions was extracted. RNA was reverse transcribed and PCR was used to test expression of *Oct-4* (a pluripotency marker), NCAM (a marker of early ectodermal differentiation and CD325 (associated with early endodermal and mesodermal differentiation) (Yaganisawa and Yu, 2007; Alimperti and Andreadis, 2015). *β-actin* was used as an internal control (sections 2.6-2.9). Transcription of *NCAM* and *CD325* was not detected in the SSEA-1 positive fraction although robust expression *Oct-4* was observed. All transcripts were detected in the SSEA-1 negative fraction, suggestive of spontaneously differentiated cells being selectively removed. The presence of *Oct-4*

transcripts in the negative fraction may be a function of low levels of expression in early differentiating cells or indicative that not all pluripotent cells were retained on the column. β-actin expression was shown to be consistent between samples (Figure 3.1).

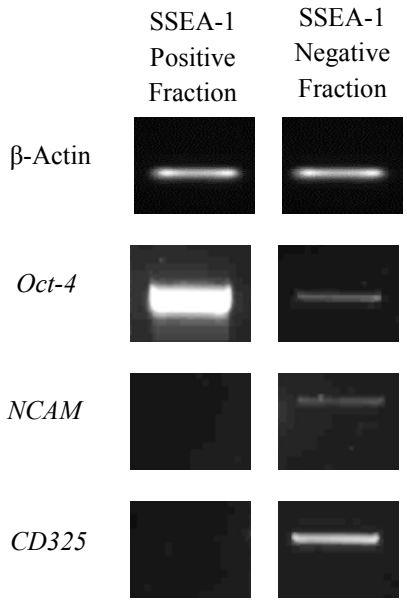


**Figure 3.1. Agarose gel electrophoresis of PCR amplified stem cell and early differentiation markers.** SSEA-1 positive and SSEA-1 negative fractions differentially expressed markers associated with pluripotency and germ layer formation. Representative bands following 2% agarose gel electrophoresis, n=3.

Efficacy of magnetic sorting was estimated by calculating yields and viability of both retentate and flow through, yields were calculated as a percentage of cells exposed to the column. Typical yields were 77% (SEM = 6.7), with 54% of cells (SEM = 8.6) being retained and 23% (SEM = 6.1) passing through the column (Figure 3.2).

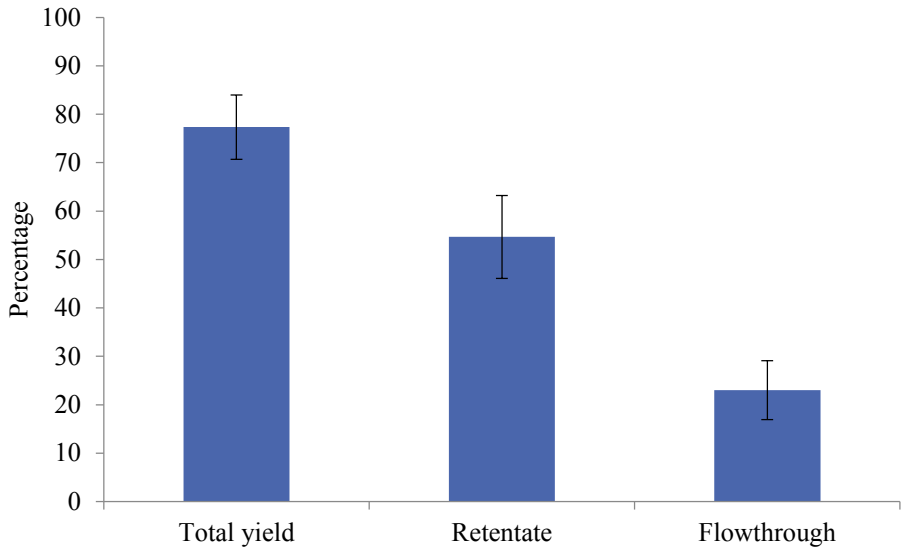


**Figure 3.2. Selection of SSEA-1 positive cells.** Magnetic sorting isolated populations of SSEA-1 positive cells (retentate) and SSEA-1 negative cells (flowthrough). Error bars = SEM, n=3.

Significant increases in viability were observed in the fraction of cells retained on the column compared to before sorting and cells passing through the column (p values 0.045 and 0.005 respectively (Figure 3.3). Variation in viability was similarly reduced in the retained fraction (SSEA-1 positive). To compare variation between fractions 95% confidence intervals were calculated for the means of each fraction, unsorted and flowthrough (SSEA-1 negative) fractions returned overlapping intervals with large spreads (23.4 and 19.6 respectively) while the interval of the retained fraction was 2.2, with no overlap with the others (Table 3.1).

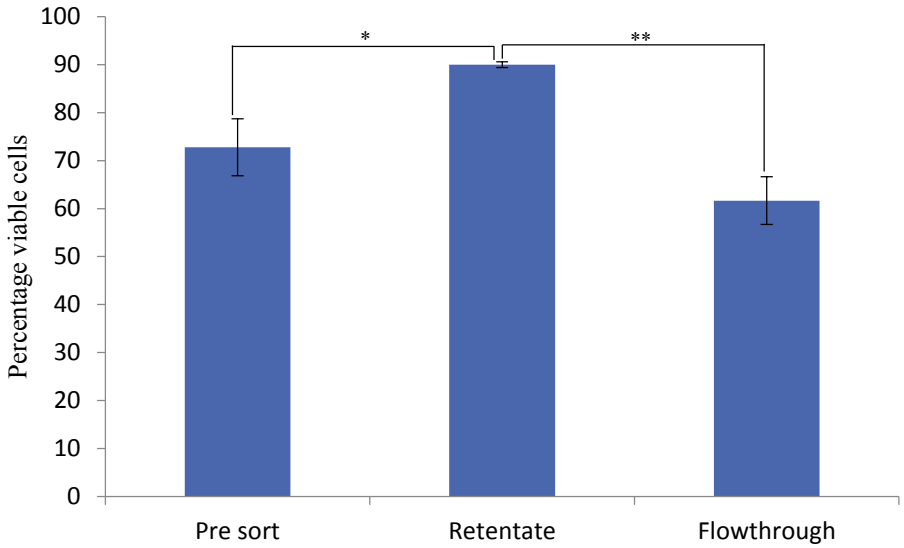


**Figure 3.3.Viable cell counts in magnetically separated fractions.** Magnetic sorting enriched the viability of populations of SSEA-1 positive cells (retentate). Error bars = SEM, n=3.

**Table 3.1. Magnetic cell sorting reduced variability in viability in SSEA-1 positive cells retained by the column.**

| | Mean Viability | 95% CI |
|---|---|---|
| Pre Sort | 72.8 | 61.1-84.5 |
| Retentate (SSEA-1 positive cells) | 90 | 88.9-91.1 |
| Flowthrough | 61.7 | 51.9-71.5 |

.

### 3.3.2 Differentiation of E14 Mouse Embryonic Stem Cells

To induce the differentiation of E14 cells into neural crest lineages SSEA-1 positive cells were cultured in primary induction media for four days before 10 days culture in secondary induction media (section 2.4). Cells cultured in complete media (CM) were grown alongside cells cultured in induction media to act as a control. Differentiation was divided into contiguous stages beginning at day -2 when SSEA-1 positive cells were cultured in complete media with induction commencing at day 0 (Table 3.2).

**Table 3.2 Differentiation stage times and presumptive cells types.**

| Stage | Culture Period | Media | Cell Type (End of stage) |
|---|---|---|---|
| 0 | Day -2 to day 0 | E14 complete | SSEA-1 positive mouse embryonic stem cells |
| 1 | Day 0 to day 4 | Primary induction media | Initially differentiated cells |
| 2 | Day 4 to day 14 | Secondary induction media | Neural crest stem cells |
| 3 | Day 14 onwards | Primary induction media | Terminally differentiated cells |

Morphological variation in cells cultured in complete and induction media was not discernible at the end of stage 1. In both cases, phase contrast microscopy showed cells growing in colonies with the morphology of individual cells difficult to determine. Culture for a further 5 days (the mid-point of stage 2) resulted in the disaggregation of colonies, with cells observed to round off and detach while growth characteristics of cells cultured in CM remained the same. Subsequent culture until the end of stage 2 resulted in the appearance of distinct morphologies in control and induced cells. Induction media treated cells began to take on a more elongated "arrowhead" shape and individual cells could be clearly demarked while micrographs of cells cultured in CM remained morphologically indistinct from earlier images (Figure 3.4). To better observe morphological variation, cells were stained with Texas Red conjugated phalloidin to determine cytoskeletal structures. Cells were fixed, stained and mounted as described previously (section 2.11). Phalloidin staining revealed induced and control cells to have differing cytoskeletal structures, control cells appeared more rounded although due to their close proximity individual structures were difficult to determine. Treated cells also grew in a

contiguous manner although with greater distance between nuclei. Control cells appeared to have a higher nuclear/cytoplasmic ratio than treated cells (Figure 3.5).

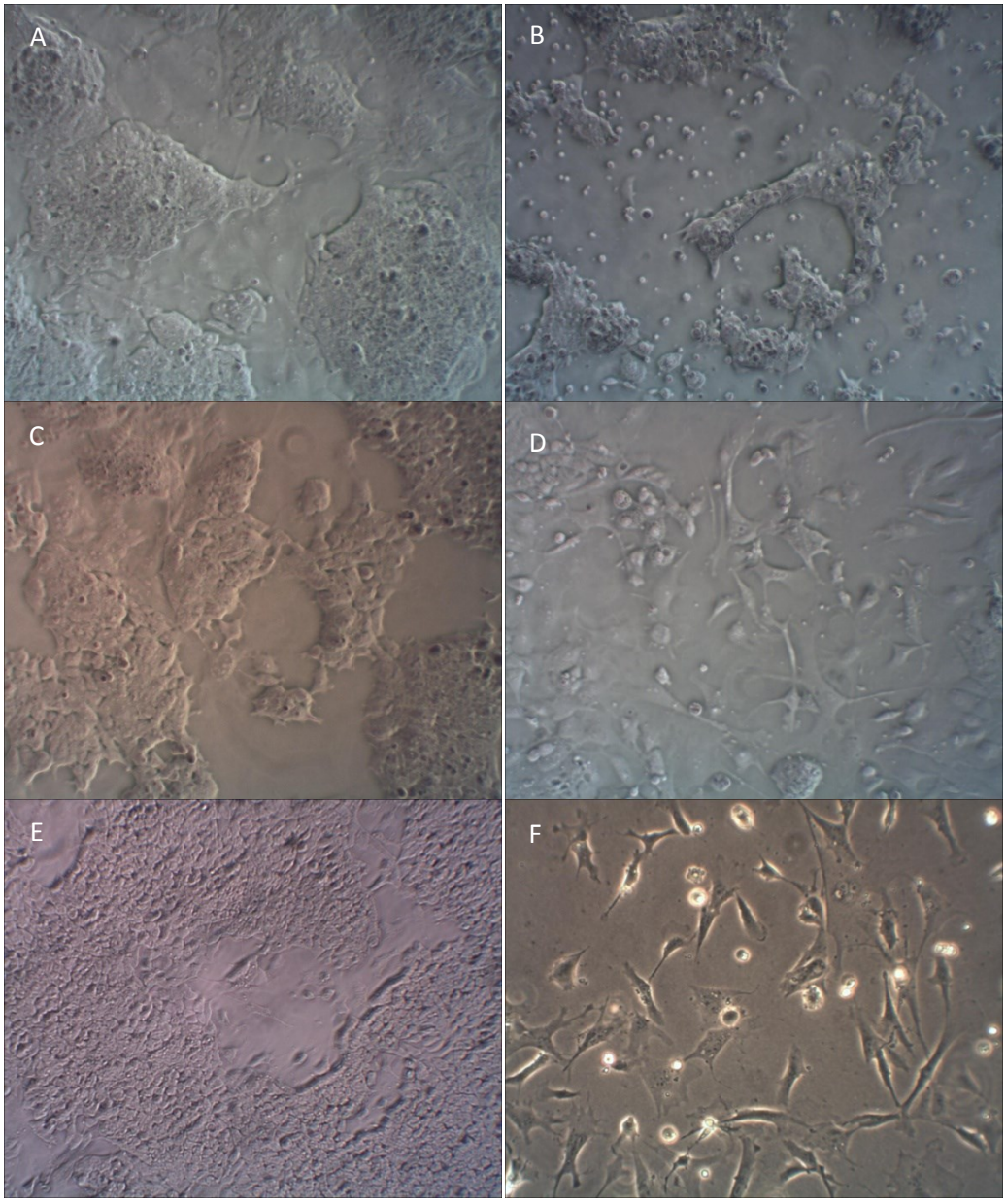


**Figure 3.4. Morphological variance in cultured cells.** Cells cultured in complete media for four days (A) showed little morphological difference to induced cells at the end of differentiation stage 1 (B). At the midpoint of stage 2 (9 days treatment) morphological differences were discernible between control (C) and induced (D) cells. More marked distinctions were observed at the end of stage 2 (14 days treatment):- cells in complete media (E) growing in colonies and cells in induction media (F) displaying a distinct elongated morphology. Magnification x120

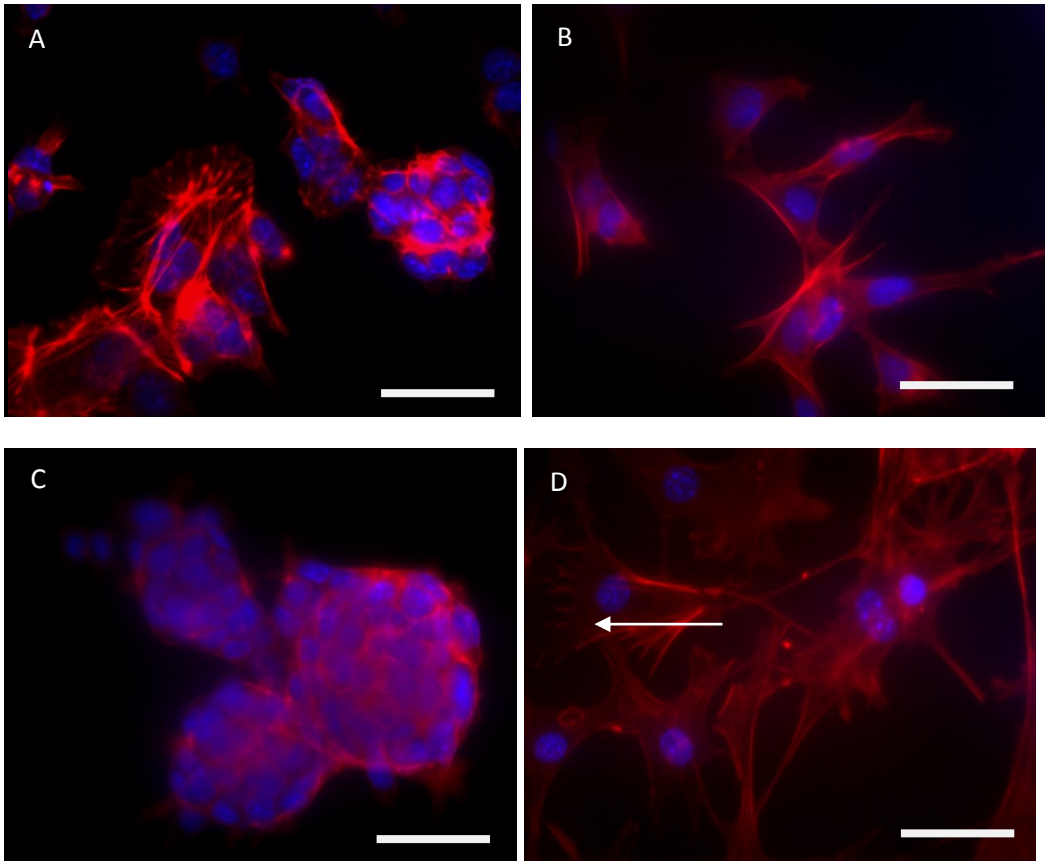


**Figure 3.5. Cytoskeletal variance in cultured cells.** F-actin filaments in the cytoplasm of cultured cells were stained with phalloidin (red). After 14 days, cells cultured in complete media (A) were morphologically distinct from cells cultured in induction media (B), which took on a distinctive arrowhead shape. Cells cultured in complete media did not change morphologically between 14 days and 24 days (A-C). After 24 days cells cultured in induction media (D) showed elongated cell bodies and dendrite like structures (white arrow). Nuclei were stained with DAPI (blue). Scale bars = 100 μm.

Staining for neural crest biomarkers *Sox10* and *p75* at the end of stage 2 showed strong expression in induced cells, while *Sox2*, indicative of a pluripotent state was present in cells cultured in CM but not in stage 2 induced cells (Figure 3.6).

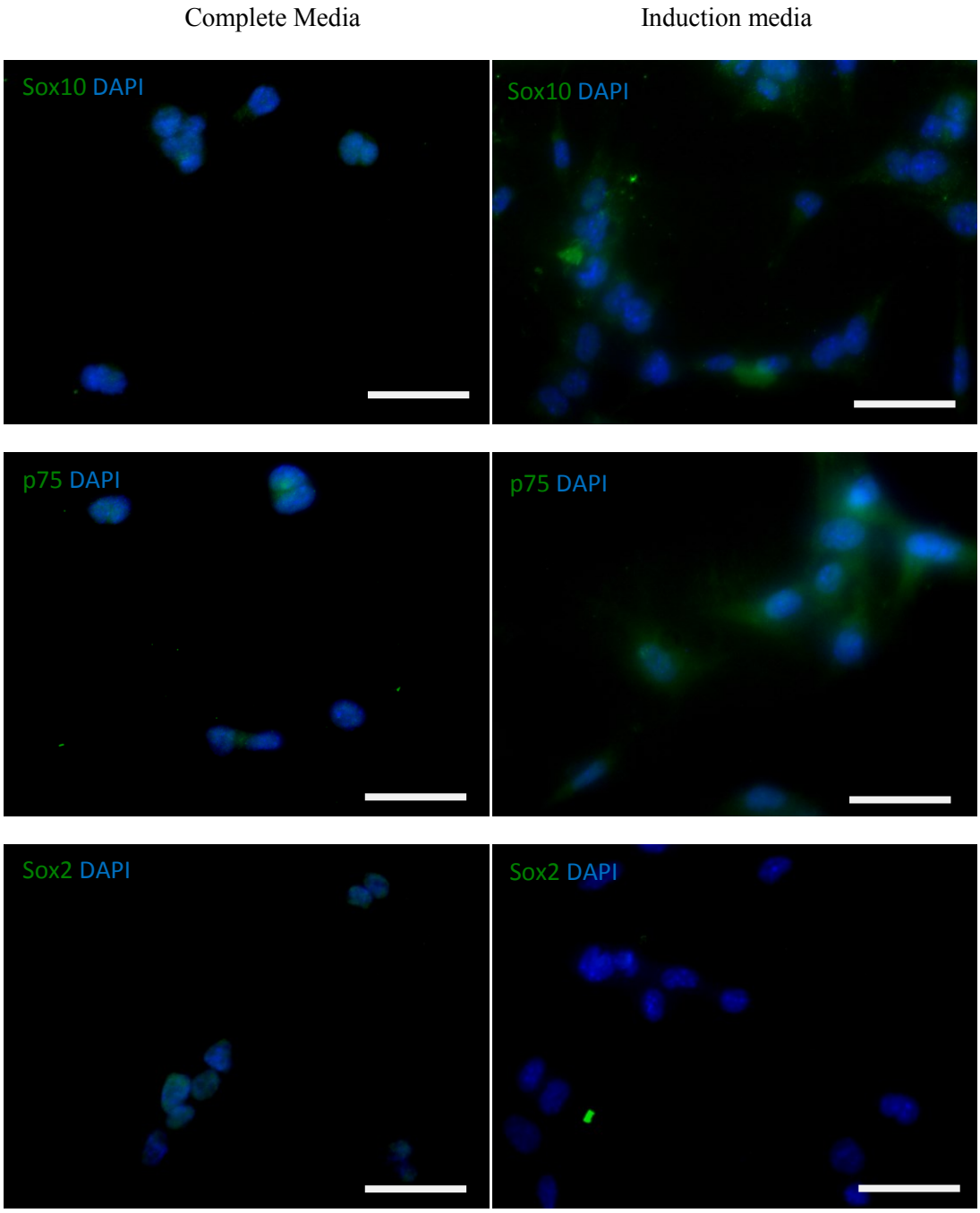


**Figure 3.6. Expression of neural crest and embryonic stem cell markers in E14 murine embryonic stem cells.** Staining for sox10, p75 and sox2 (all green) showed differential expression in cultured cells. Weak expression of both sox10 and p75 and nuclear localisation of sox2 was observed in cells cultured in complete media. In contrast, sox10 and p75 were more potently expressed in cells cultured in induction media and sox2 was not detected. Nuclei were stained with DAPI (blue). Scale bars 100 μm. Cells were fixed after stage 1 and stage 2 of differentiation (14 days total treatment).

Upon completion of stage 2 presumptive NCCs were cultured in PIM and KODMEM supplemented with 10% FCS (Smooth muscle media (SM)) (section 2.5). Distinct morphological variations were observed in both cultures over 5 days by phase contrast microscopy. Cells cultured in SM showed rapidly expanding cytoplasmic processes compared to those cultured in PIM (Figure 3.7).

Staining for smooth muscle actin showed expression in cells cultured in SM but not those cultured in induction media. Conversely, expression of the peripheral nervous system biomarker peripherin was observed in PIM cultured cells but not in cells grown in SM. Cells were counterstained with phalloidin to compare F-Actin arrangement in the cytoplasm and nuclei were stained with DAPI. Observation of cells after staining showed SM cultured cells had smaller nuclei in relation to cytoplasm and grew in closer proximity than PIM cultured cells (Figure 3.8). It was unclear at this stage whether morphological differences were as a result of differing signals from the media or from differing signals from cells which appeared to proliferate more rapidly in PIM (Figure 3.7). However, the ability of the cells to manifest variable phenotypes in differing culture conditions was indicative of a multipotent state.

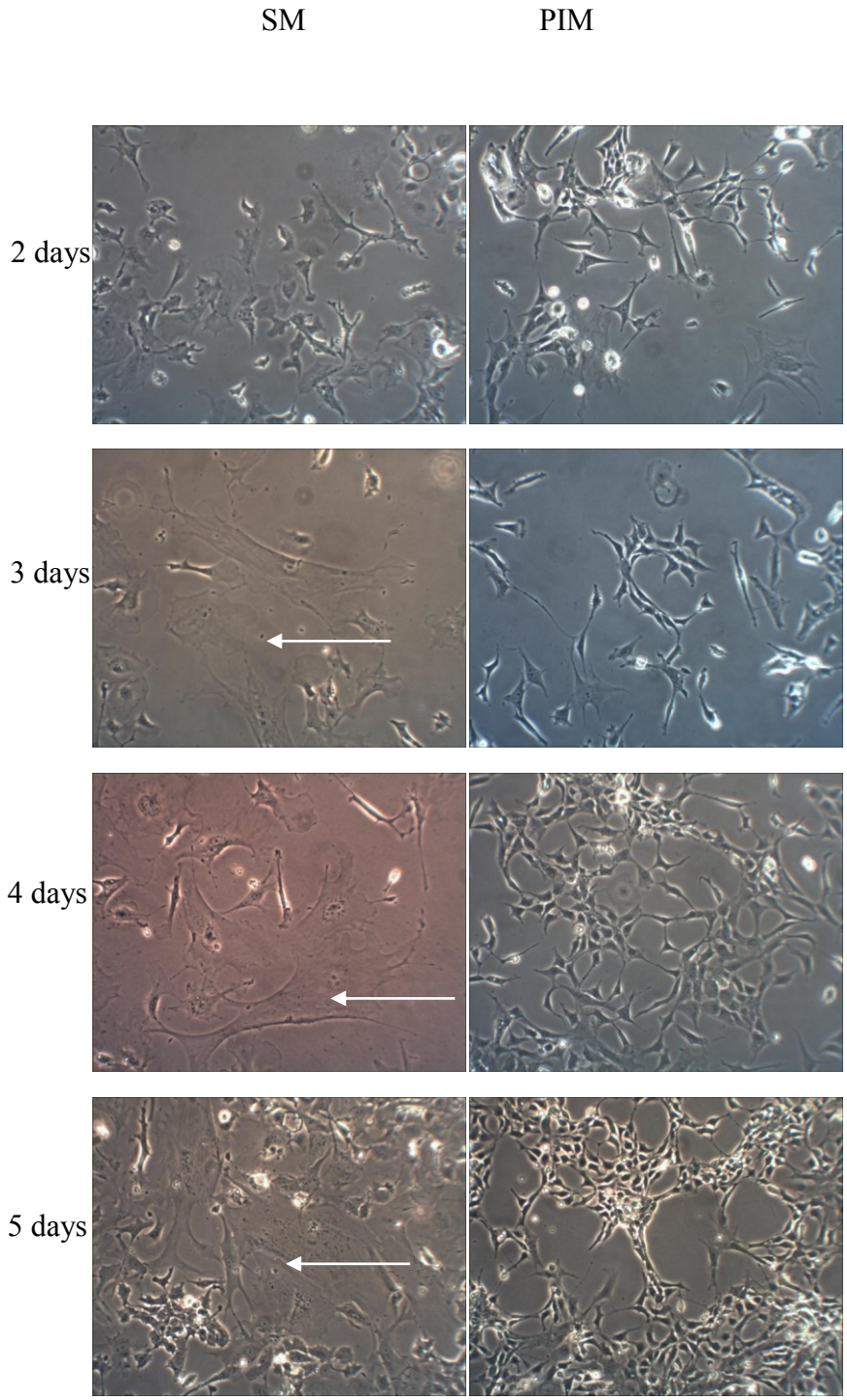


**Figure 3.7. Morphology of cultured cells after secondary differentiation.** Cells were cultured in either SM or PIM after stage 2 of differentiation (14 days total treatment). Cells cultured in SM media had a more heterogeneous morphology and large cells with visible striations were observed starting at 3 days (17 days total treatment - white arrows). Cells cultured in PIM appeared more homologous and grew in closer proximity with visible, linked colonies of cells observed starting at 4 days. Magnification 120x.

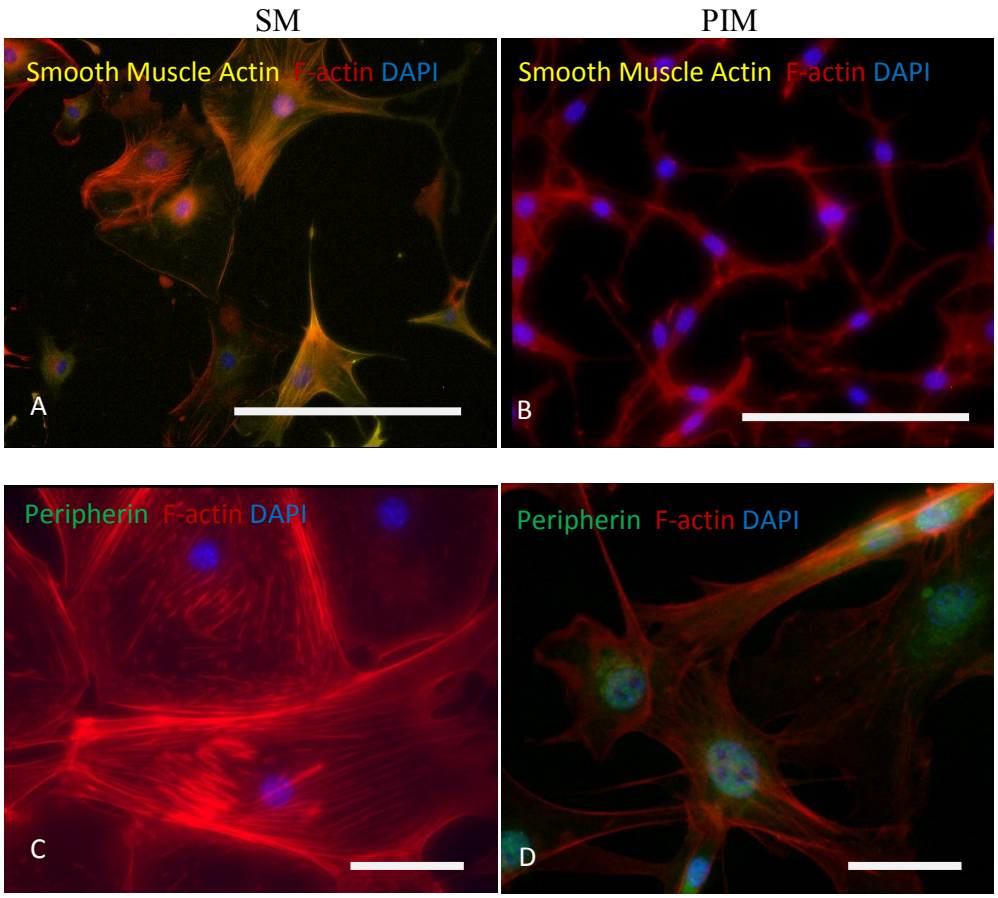


**Figure 3.8. Expression of biomarkers of smooth muscle and peripheral neuron in cultured cells.** Cells were cultured in SM (A and C) or PIM (B and D) after stage 2 of differentiation. Cells were stained for smooth muscle actin (yellow, A and B) and the peripheral neuron marker peripherin (green, C and D). SM cultured cells were positive for smooth muscle actin without peripherin expression, while PIM cultured cells did not express smooth muscle actin while expressing peripherin. All cells were counterstained with phalloidin, to observe F-actin filaments in the cytoplasm (red); nuclei were stained with DAPI (blue). Scale bars 100 μm.

### 3.3.3 Gene Expression Analysis in Differentiating E14 Murine Embryonic Stem Cells

Gene expression analysis was carried out by RT-qPCR (section 2.10) to characterise cells during the process of differentiation. RNA was isolated at 6 time points (Table 3.4). RNA was also extracted from isolated SSEA-1 positive cells cultured in CM for 2 days as a baseline control.

**Table 3.3 Time points and stages for RT-pPCR analysis.**

| Culture time (days) | Stage | Media |
|---|---|---|
| 4 days | 1 | PIM |
| 9 days | 2 (mid-point) | SIM |
| 14 days | 2 (end) | SIM |
| 21 days | 3 | PIM |
| 32 days | 3 | PIM |
| 48 days | 3 | PIM |

All expression values were normalised to β-actin and 18s ribosomal RNA. Two-tailed Student's T tests were used to determine significance with each sample compared to the previous time point. Differentiation resulted in significant downregulation of *Nanog* after stage 1 and for the first part of stage 2. A significant increase was observed between the middle and end of stage 2. *Nanog* expression remained constant in stage 3 cells up to 32 days and then was again observed to be downregulated at 48 days (Figure 3.9).

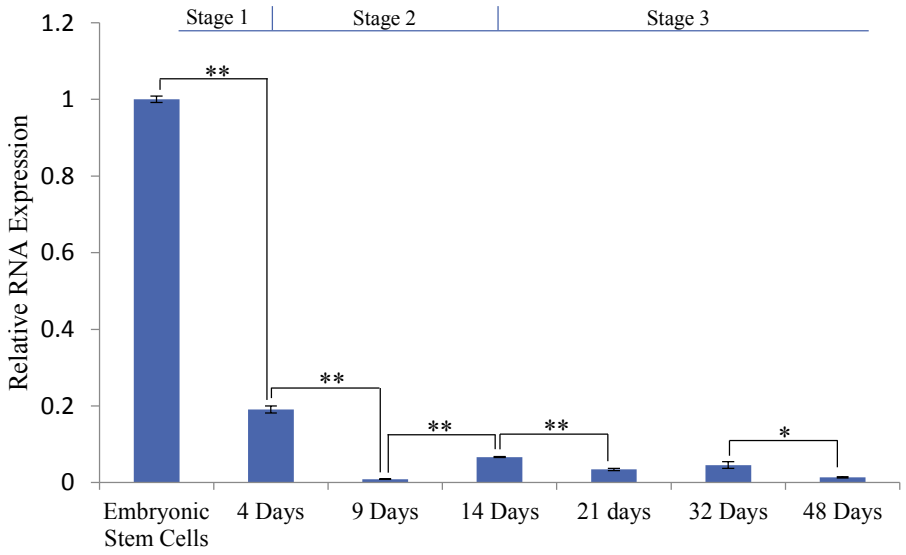


**Figure 3.9. Culture in induction media resulted in variable expression of *Nanog* compared to embryonic stem cells (value = 1).** E14 mouse embryonic stem cells were cultured in PIM at stage 1, SIM at stage 2 and PIM at stage 3. Expression fell rapidly on initiation of differentiation but increased after the mid-point of stage 2 Data is mean ± SEM, n=3. * Denotes p value <0.05, ** denotes p value <0.01.

Expression of *Nestin*, a marker associated with neural crest and neural differentiation was measured. Expression was constant between embryonic stem cells and the end of stage 1. Significant upregulation was observed throughout stage 2 and expression remained stable during the initial period of stage 3. As stage 3 progressed expression levels increased significantly before remaining stable (Figure 3.10).

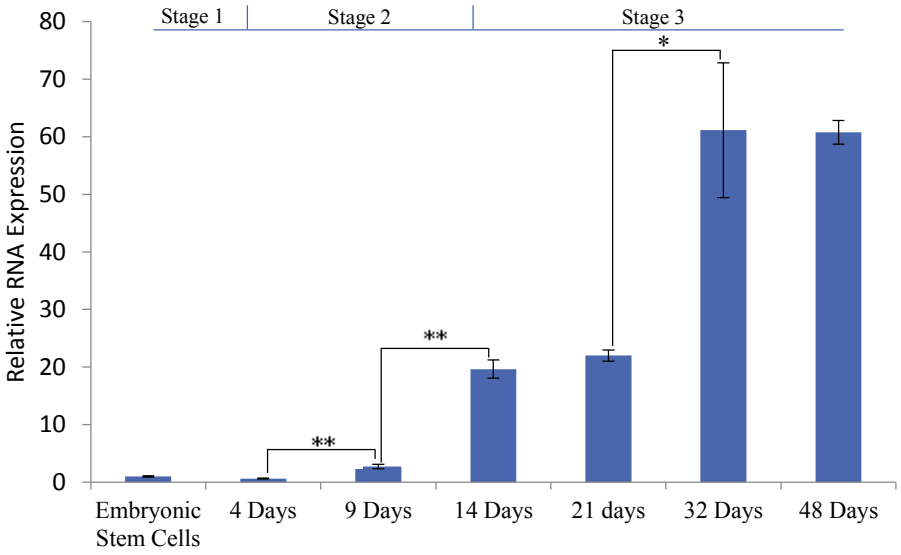


**Figure 3.10. Culture in induction media increased expression of *Nestin* compared to embryonic stem cells (value = 1).** E14 mouse embryonic stem cells were cultured in PIM during stage 1, SIM during stage 2 and PIM during stage 3. Peak expression was observed after 32 days and no change was observed between 32 and 48 days culture. Data is mean ± SEM, n=3. * Denotes p value <0.05, ** denotes p value <0.01.

The expression of three neural crest markers, *Pax3, Sox9,* and *Musashi-1* was assessed. Both *Pax3* and *Musashi-1* exhibited peaks in expression beginning during stage 2 and peaking during stage 3 before downregulation was observed, peak expression occurring at 21 days treatment in the case of *Pax3* and at 32 days for expression of *Musashi-1.* Peak upregulation of *Pax3* was markedly higher than that of *Musahi-1* with a 665-fold increase in expression observed compared to a 14-fold increase and *Musahsi-1* was also downregulated during stage 1 (Figures 3.11 and 3.12).

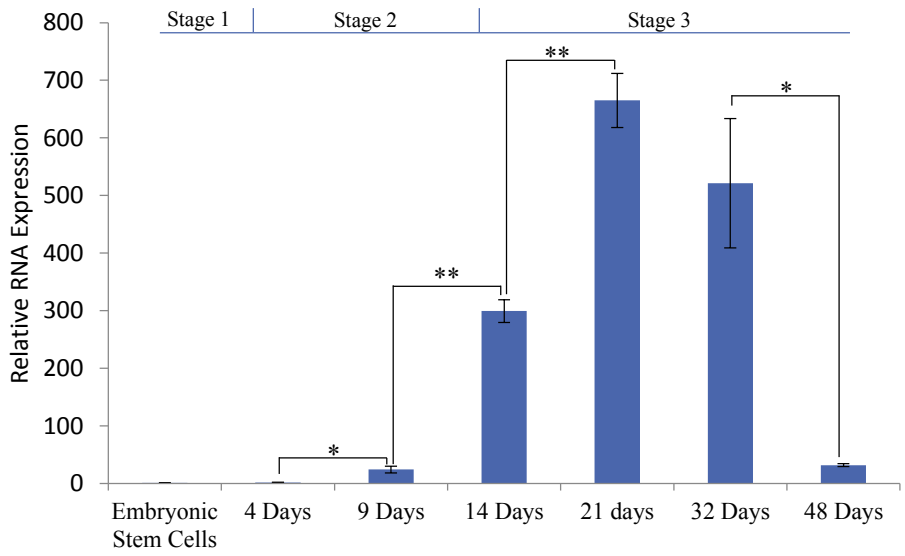


**Figure 3.11. Culture in induction media increased expression of *Pax3* in comparison to embryonic stem cells (value = 1).** E14 mouse embryonic stem cells were cultured in PIM during stage 1, SIM during stage 2 and PIM during stage 3. Peak upregulation was observed after 21 days, 7 days after removal of BMP-4 supplementation. Data is mean ± SEM, n=3. * Denotes p value <0.05, ** denotes p value <0.01.

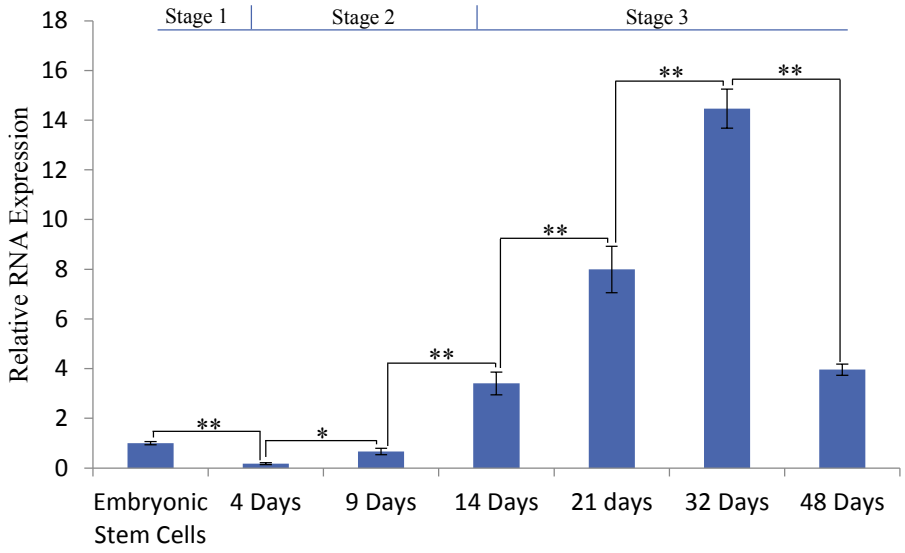


**Figure 3.12. Culture in induction media first decreased, then increased expression of *Musashi-1* in comparison to embryonic stem cells (value = 1).** E14 mouse embryonic stem cells were cultured in PIM during stage 1, SIM during stage 2 and PIM during stage 3. Peak upregulation was observed after 32 days, 18 days after removal of BMP-4 supplementation. Data is mean ± SEM, n=3. * Denotes p value <0.05, ** denotes p value <0.01.

Culture in PIM initially had no effect on the expression of *Sox9;* no significant differences in expression levels were detected between embryonic stem cells and stage 1 cells. A significant increase in expression occurred during stage 2 although no differences were observed between the mid and end-points. Stage 3 showed a small but significant increase (1.7-fold) at 21 days and more marked (5.75-fold) upregulation between 21 and 32 days, after which expression remained stable (Figure 3.13).

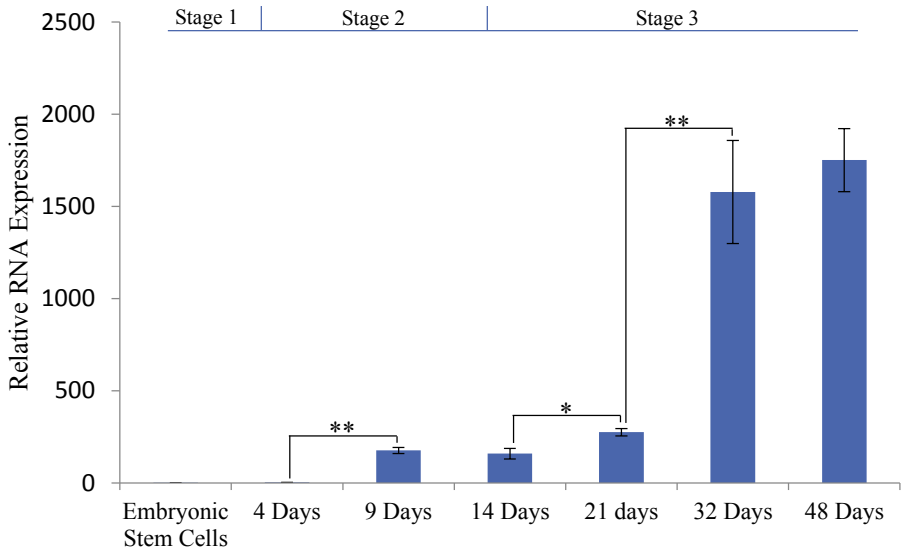


**Figure 3.13. Culture in induction media increased expression of *Sox9* in comparison to embryonic stem cells (value = 1).** E14 mouse embryonic stem cells were cultured in PIM during stage 1, SIM during stage 2 and PIM during stage 3. Peak upregulation was observed after 48 days, 34 days after removal of BMP-4 supplementation, high expression levels were detected after 32 days. Data is mean ± SEM, n=3. * Denotes p value <0.05, ** denotes p value <0.01.

### 3.3.4 The Effect of BMP-4 on Cell Proliferation and Viability in Differentiating E14 Mouse Embryonic Stem Cells

BMP-4 is known to be essential to neural crest differentiation and is a key regulator of abundant cellular processes (Varca and Wrana, 2005). In order to determine whether BMP-4 altered proliferation and viability during stage 2 of the differentiation process were plated at a density of 25 000 per well after completion of stage 1. Cells were co-cultured for a further ten days in SIM (treated cells) or PIM (untreated cells) during which cell counts and viabilities were measured after 1, 3, 6 and 10 days. Initially, untreated cells proliferated more rapidly but after 3, 6 and 10 days BMP-4 treatment was observed to increase proliferation, significantly at 6 and 10 days (Figure 3.14). In both cases, viabilities were initially low but increased as culture was continued; no significant differences were detected between treated and untreated cells (Figure 3.15). These data indicate a role for BMP-4 in the increased proliferation of treated cells. Similar viabilities indicate that BMP-4 was not simply aiding the survival of cultured cells.

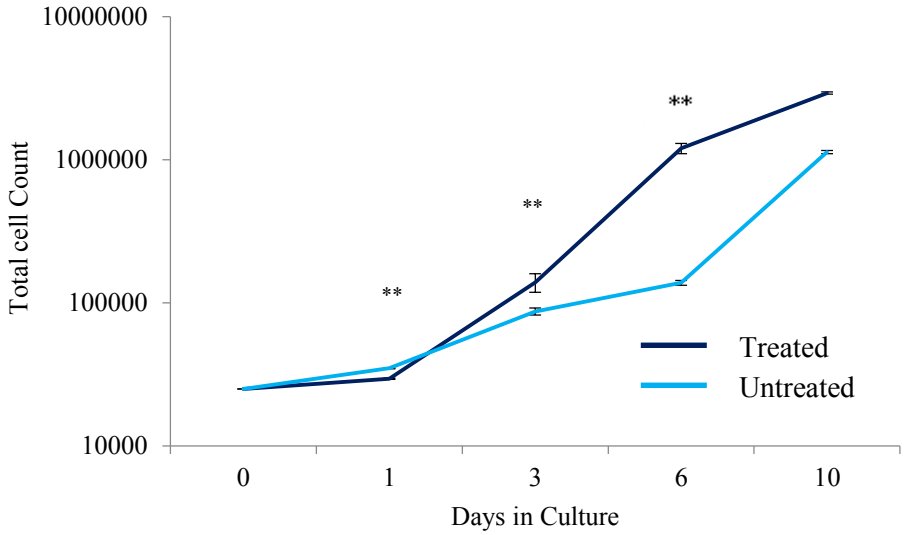


**Figure 3.14. BMP-4 supplementation affected proliferation of differentiating E14 embryonic stem cells.** Cells were cultured during stage 2 of differentiation with and without BMP-4 treatment. Proliferation was more rapid after one day in untreated cells, similar after 3 days and significantly increased in treated cells after 6 and 10 days. Data are mean ± SEM, n=3 ** denotes p value <0.01.

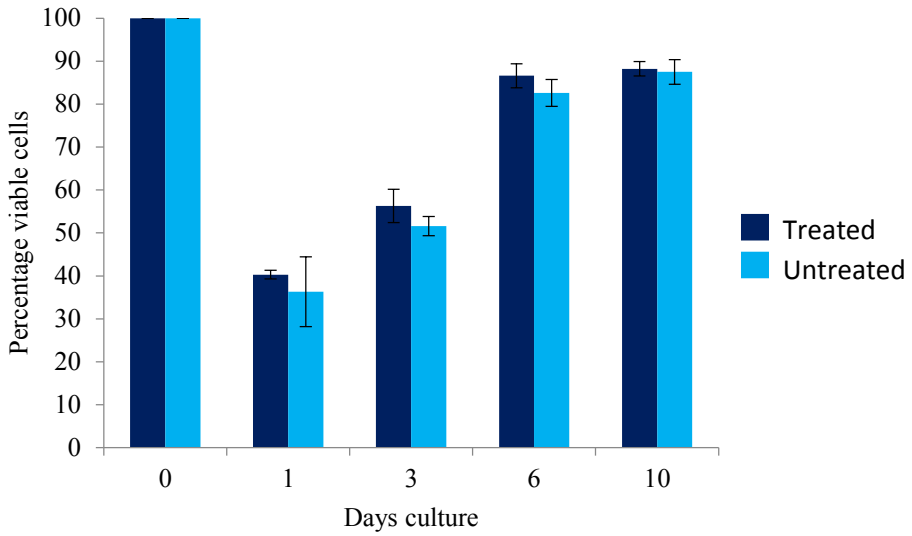


**Figure 3.15. BMP-4 supplementation did not affect viability of differentiating E14 embryonic stem cells**. Cells were cultured during stage 2 of differentiation with and without BMP-4 treatment. No significant differences were observed in viability between treated and untreated cells. Data are mean ± SEM, n=3.

### 3.3.5 Cell Cycle Analysis

Cell cycle parameters were examined by culturing stage 2 cells in PIM or SIM for 10 days before cells were fixed, stained with propidium iodide and subject to flow cytometry analysis (section 2.12). All cell cycle phases showed significant differences with the most conspicuous being G2 where more than a 10-fold increase was observed in treated cells compared to untreated. Cells cultured without BMP-4 had slightly higher percentages in G1 and S phases. Coefficient of variation did not significantly differ between samples (p-value 0.1) (Figure 3.16), indicating differences were not due to experimental variation.

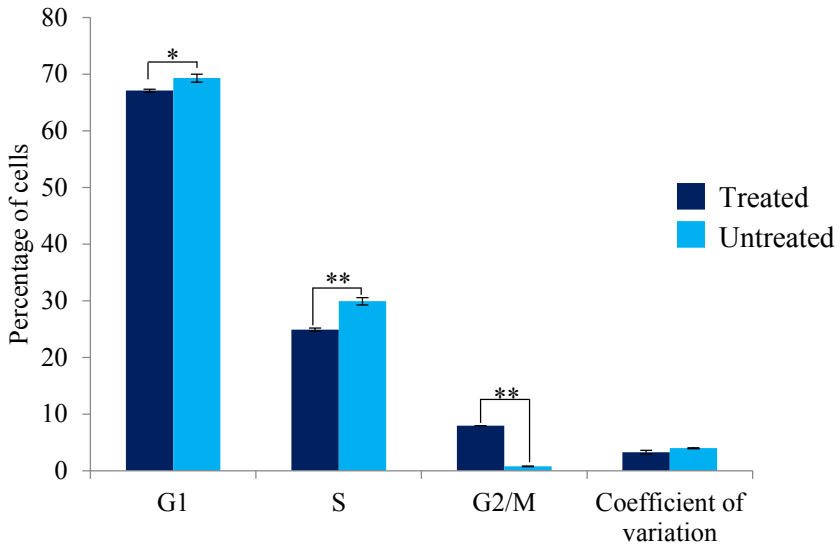


**Figure 3.16. BMP-4 supplementation altered cell cycle parameters of differentiating E14 mouse embryonic stem cells**. E14 mouse embryonic stem cells were cultured with and without BMP-4 treatment during stage 2 of differentiation. A lower percentage of treated cells were observed in the gap and synthesis phases with a concurrent increase in dividing cells. Data is mean ± SEM, n=3. * denotes p value < 0.05, ** denotes p value <0.01.

Duration of each cycle was calculated as in 3.3.2 (above) doubling times were determined to be 1.6 days for BMP-4 supplemented cells and 1.9 days for untreated cells (Figure 3.17). No significant differences were observed between time in G1 phase ($p = 0.06$) while BMP-4 supplementation decreased time in S-phase and increased time in G2 (p values 0.001 and $4.8 \times 10^{-8}$ respectively). Example histograms and doubling time calculations are presented in Appendix 3.

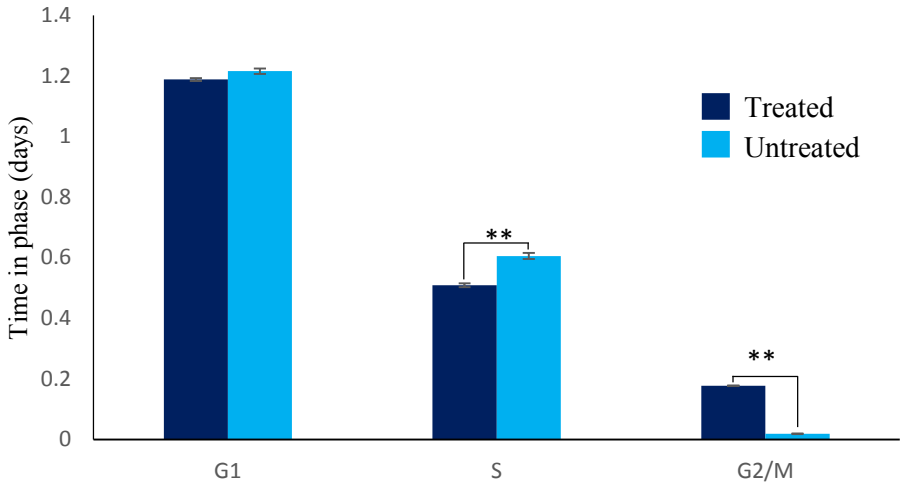


**Figure 3.17. BMP-4 supplementation did not alter time in gap phase (G1), but significantly altered time in S and G2 phases in differentiating E14 mouse embryonic stem cells**. E14 mouse embryonic stem cells were cultured with and without BMP-4 treatment during stage 2 of differentiation. Data is mean ± SEM, n=3. * denotes p value < 0.05, ** denotes p value <0.01.

### 3.3.6 The Effect of BMP-4 on Gene Expression in Differentiating E14 Mouse Embryonic Stem Cells

The influence of BMP-4 supplementation on the expression of embryonic, neural and neural crest markers mentioned above (3.3.3) was investigated. Cells were cultured until the end of stage 2 as above (*q.v.* Table 3.2) (treated). Control cells were cultured with PIM rather than SIM during the same period (untreated). RNA was harvested from each fraction at the beginning (1 hour), middle, (5 days) and end (10 days) of stage 2. RT qPCR was carried out as before (section 2.10). Expression levels were compared to those of untreated cells at the beginning of stage 2 (value = 1). All expression values were normalised to β-actin and 18s ribosomal RNA. Significance was determined by 2-tailed Student's T-test, comparing expression levels in the BMP-4 positive and negative fractions.

Downregulation of *Nanog* was stable in untreated cells, with the increase in expression at 10 days observed in culture with BMP-4 supplemented media not occurring. Expression of *Nanog* was seen to be significantly upregulated 6-fold at 10 days culture in treated cells compared to untreated. No significant differences in *Nanog* expression were observed after 1 hour and 5 days (Figure 3.18).

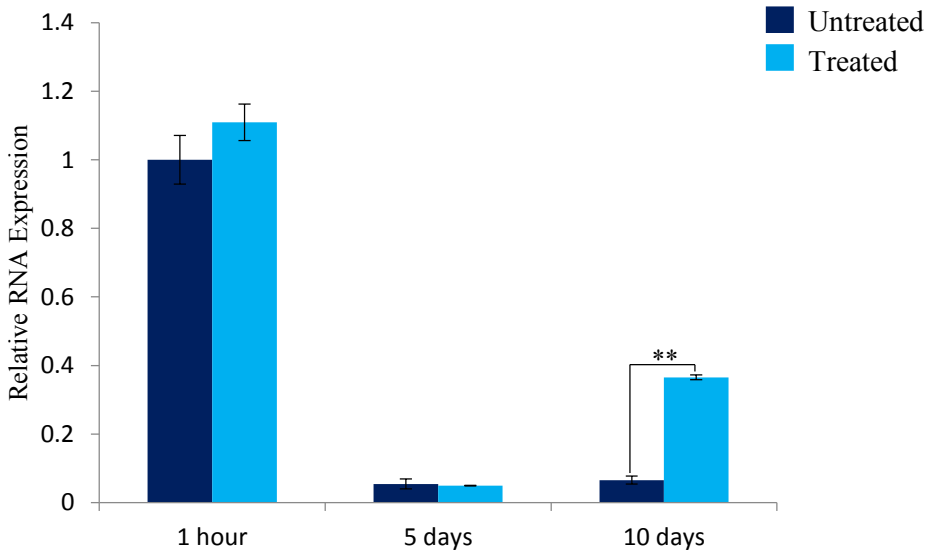


**Figure 3.18. BMP-4 supplementation upregulated *Nanog* expression after 10 days in stage 2 differentiating cells, but did not affect expression after 1 hour or 5 days.** E14 mouse embryonic stem cells were cultured with and without BMP-4 treatment during stage 2 of differentiation. Data is mean ± SEM, n=3. ** denotes p value <0.01.

*Nestin* expression increased over the culture period for cells cultured in both treated and untreated fractions. For both conditions, significant upregulation was observed between 1 hour and 5 days and 5 and 10 days. Significant upregulation was recorded in untreated cells after 5 and 10 days compared to cells cultured in induction media supplemented with BMP-4 (Figure 3.19).

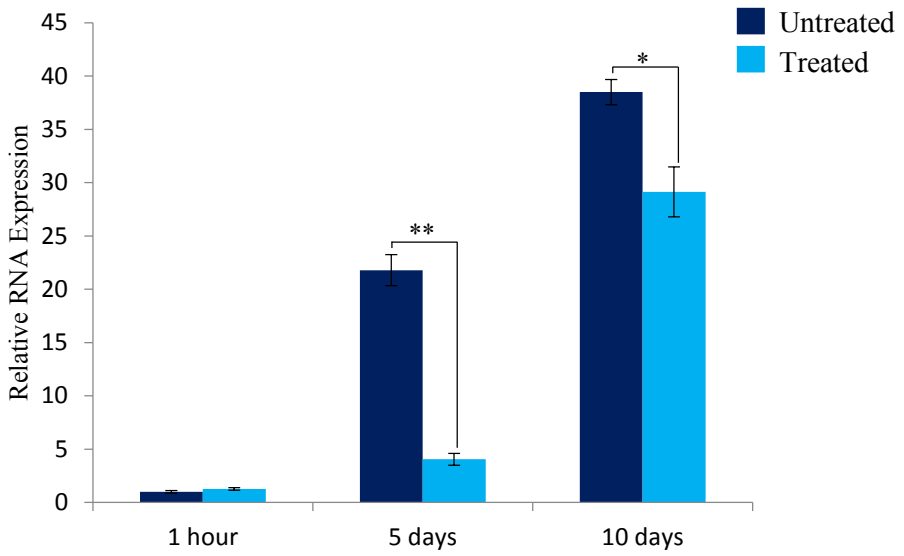


**Figure 3.19. BMP-4 supplementation reduced upregulation of *Nestin* after 5 and 10 days culture in stage 2 differentiating cells, but did not alter expression after 1 hour.** E14 mouse embryonic stem cells were cultured with and without BMP-4 treatment during stage 2 of differentiation. Data is mean ± SEM, n=3. * denotes p value < 0.05, ** denotes p value <0.01.

The untreated cell fraction showed transient high levels of *Pax3* expression, after 5 days 338-fold upregulation was observed, dropping to 53 fold after 10 days. BMP-4 treated cells expressed *Pax3* in a sequentially increasing manner. Comparison between supplemented and non-supplemented cultures revealed significant difference after 5 and 10 days. *Pax3* was downregulated 24 fold in BMP-4 supplemented cells at 5 days and upregulated 3 fold after 10 days compared to untreated cells. In both cases, changes in expression were statistically significant (Figure 3.20).

*Musashi-1* expression followed a similar pattern to *Pax3*, albeit with less profound changes. After 5 days, expression was reduced 8.7-fold in BMP-4 treated cells. Expression was increased 1.4-fold after 10 days although this was not statistically significant (p value = 0.11). Again, expression in untreated cells peaked after 5 days while treated cells showed increased expression over time (Figure 3.21).

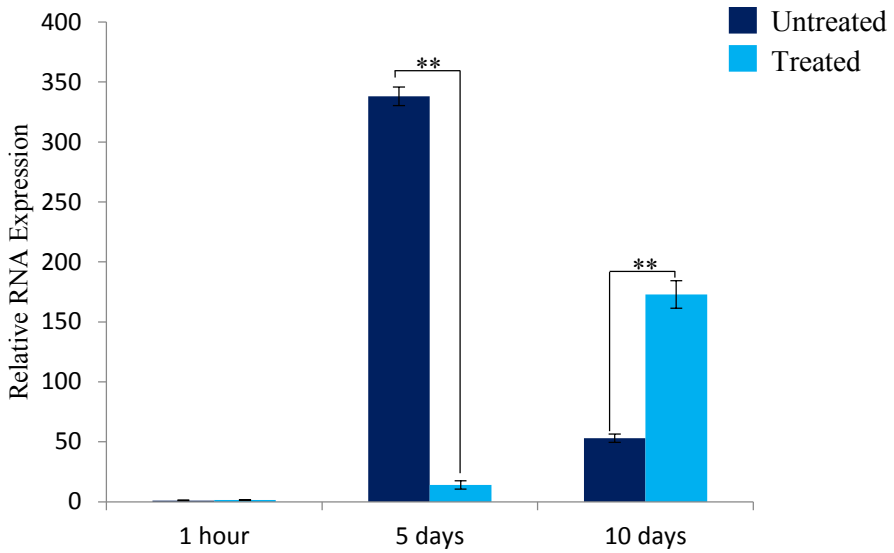


**Figure 3.20 BMP-4 supplementation altered expression of *Pax3* after 5 and 10 days in stage 2 differentiating cells, but did not alter expression after 1 hour.** E14 mouse embryonic stem cells were cultured with and without BMP-4 treatment during stage 2 of differentiation. Data is mean ± SEM, n=3. ** denotes p value <0.01.

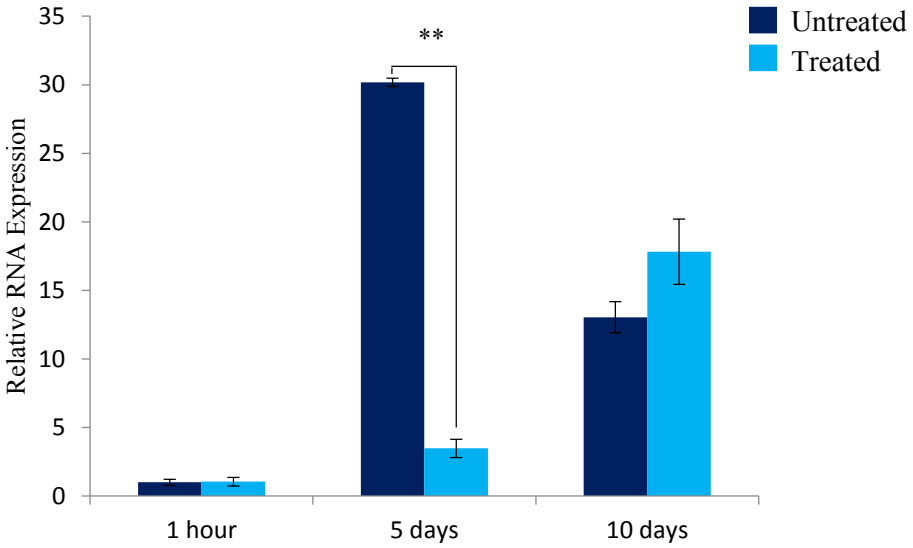


**Figure 3.21. BMP-4 supplementation affected expression of *Musashi-1* in stage 2 differentiating cells after 5 days culture, but did not affect expression after 1 hour or 10 days**. E14 mouse embryonic stem cells were cultured with and without BMP-4 treatment during stage 2 of differentiation. Data is mean ± SEM, n=3. ** denotes p value <0.01.

BMP-4 supplementation did not affect the expression of *Sox9* after 1 hour and 5 days. A small but significant (1.7 fold) decrease in expression was observed between supplemented (treated) and non-supplemented (untreated) cultures after 10 days. In both cases, expression of *Sox9* increased between 1 hour and 5 days and remained stable in supplemented culture conditions while continuing to increase in untreated cells (Figure 3.22).

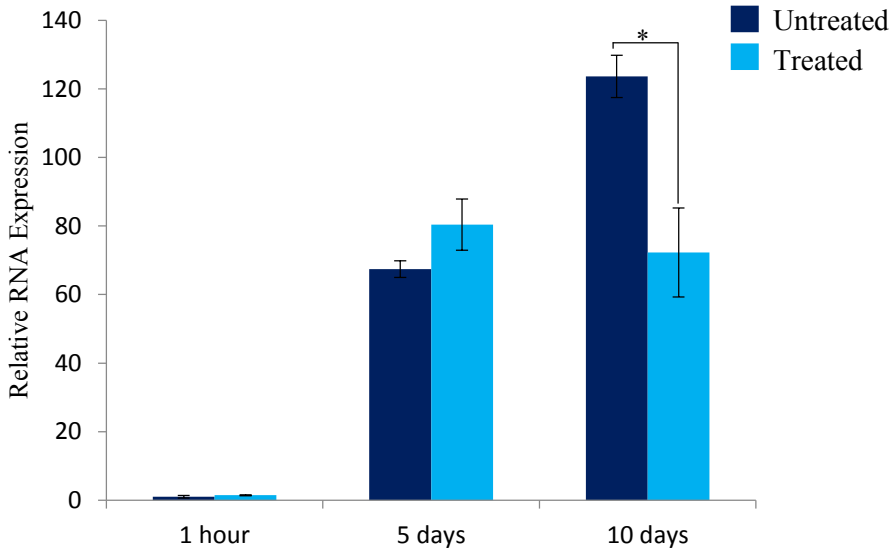


**Figure 3.22. BMP-4 supplementation affected *Sox9* expression after 10 days, but did not affect expression after 1 hour or 5 days.** E14 mouse embryonic stem cells were cultured with and without BMP-4 treatment during stage 2 of differentiation. Data is mean ± SEM, n=3. * denotes p value < 0.05.

### 3.4 Discussion

Treatment of E14 mouse embryonic stem cells in IM resulted in a 5.3-fold decrease in *Nanog* expression after four days (stage 1) and a further 21.1-fold decrease at the mid-point of stage 2 (from 4 to 9 days) corresponding to a net 112-fold downregulation between days 0 and 9. This decline in expression is consistent with a loss of pluripotent status in differentiating cells (Wang *et al,* 2012). However, at the end of stage 2 (14 days total treatment) *Nanog* was upregulated 7.8-fold, after which expression levels remained relatively stable into stage 3 up until 48 days at which point levels approximated those observed at 9 days (Figure 3.9). *Nanog* is known to be expressed in NCCs albeit at lower levels than in embryonic stem cells (Hagiwara *et al.,* 2014). Transcription of the gene encoding the intermediate neurofilament protein *Nestin* underwent alternating periods of stability and upregulation. Low expression in early stage (0, 1 and the midpoint of stage 2) cells was followed by an approximate 20 fold upregulation at the end of stage 2 (14 days). Expression remained stable at the beginning of stage 3 (21 days) before increasing 60 fold at 32 and 48 days relative to embryonic stem cells, a 3-fold upregulation from stage 2 (Figure 3.10). *Nestin* is associated with neuronal precursors and rapidly dividing neuronal cells in the immature murine nervous system (Ramm *et al*, 2009), taken with the expression of *Nanog* at these time points this may be indicative of cells of a neural crest lineage.

To aid confirmation of lineage the gene expression of three neural crest markers, *Pax3, Musashi-1* and *Sox9* was measured. Peak expression of *Pax3* was observed at 21 days (7 days of stage 3), exhibiting 665-fold upregulation compared to embryonic stem cells, although high levels of upregulation were also observed at 14 (stage 2) and 32 (18 days into stage 3) days. *Pax3* is expressed in NCCs before and after

delamination where it plays an essential role in cell survival and proliferation (Plouhinec, *et al*., 2014). *Musashi-1* and *Sox9* showed peak expression later than *Pax3,* during stage 3 at 32 and 48 days respectively (Figures 3.11-3.13). *Musashi-1* is known to be an inducer of neuronal fate in neural crest stem cells and *Sox9* is expressed in the migratory neural crest (Lo *et al.,* 1998; Cheung and Briscoe, 2003).

Immunocytochemistry was carried out after differentiation stage 2. Cells were positive for the neural crest markers p75 and Sox10, while expression of the embryonic stem cell marker Sox2 was reduced. Staining of the actin cytoskeletons with phalloidin showed morphologically distinct cells compared to those cultured in CM. Culture for an additional 32 days resulted in the generation of further morphologically distinct cell lineages displaying either markers of smooth muscle cells (smooth muscle actin) or peripheral neuron markers (peripherin) but not both Figures 3.7 and 3.8). Immunocytochemistry data, taken together with genetic analyses support the induction of neural crest stem cells capable of differentiating into divergent cell types while expressing associated biomarkers (Aihara *et al*, 2010).

The role of BMP-4 was investigated in various aspects of neural crest differentiation. BMP-4 has previously been associated with the regulation and proliferation of stem cells, and is a factor positively influencing the survival of neuronal progenitor cells during later differentiation. (Zhang and Li, 2005; Chalazontis and Kessler, 2012). BMP-4 accelerated cell proliferation after an initial fall with no effect in viability observed. In culture with treated and untreated media, both populations of cells decreased in viability then recovered over time (Figures 3.14 and 3.15). It is possible this can be attributed to adaptions to growth in serum free culture. Culture in serum free conditions has been shown to affect the survival of murine embryonic stem cells (Aihara *et al.,* 2010).

Cell cycle analysis after completion of stage 2 supported data gained from proliferation experiments. Upon completion of stage 1 cells were cultured for 10 days in either PIM or SIM (untreated and treated respectively). A slight but significant reduction in G1 and S phases in treated cells compared to untreated cells cultured for the same time period coupled with over a 10-fold increase in G2 phase in treated cells was indicative of more rapid cell division. Calculations of phase times reinforced these data with significant reductions in synthesis time recorded for the BMP-4 supplemented samples, indicative of more rapidly proliferating cells and concurrent with data from proliferation experiments (Pozarowski and Darynkiewicz, 2004).

Supplementation of BMP-4 had no effect on transcription of *Nanog, Nestin, Pax3, Musashi-1* or *Sox10* after 1 hour during differentiation stage 2. After 5 days of stage 2 expression of *Nanog* was similarly reduced in both treated and untreated cells (no significant difference between samples p-value 0.6). At 10 days *Nanog* expression in cells cultured without BMP-4 supplementation (untreated) remained stable, not exhibiting the increase observed in cells cultured in BMP-4 supplemented media (treated) (Figure 3.18). A 5.9-fold increase in expression in treated cells compared to untreated was observed (p-value 2 $x10^{-5}$). These data indicate that the increase in expression was mediated by BMP-4 but through a pathway potentially involving a number of downstream targets as indicated by the delay in upregulation following an initial fall in expression levels. BMP-4 has been implicated in the differentiation of (Wang *et al.,* 2012), as well as the maintenance of pluripotency of embryonic stem cells. BMP-4 in concert with leukaemia inhibitory factor is used to inhibit the differentiation of murine embryonic stem cells and induce self-renewal *in vitro* (Zhang *et al.,* 2013).

*Nestin* expression was upregulated for both treated and untreated cells. A relatively modest (4.1-fold) increase in expression was observed in treated cells and more potent expression (21.8-fold increase) in untreated cells after 5 days. 10 days culture yielded a smaller but still statistically significant difference (38.5-fold and 29.1-fold for treated and untreated cells respectively) (Figure 3.19). BMP-4 has been shown to be antagonistic towards neurulation in the ectoderm, giving rise to non-neural ectoderm in higher concentrations and neural crest at lower concentrations (Marchant *et al., 1998)*. These data suggest that low levels of BMP-4 may slow the expression of factors associated with neurulation rather than act in an inhibitory manner. This is in keeping with the paradigm that ectodermal patterning is dependent on a concentration gradient of BMP-4. Neural crest stem cells are known to express *Nestin* (Aihara, *et al.,* 2010) and be exposed to median levels of BMP-4 after gastrulation (Barth *et al*, 1999).

Pax3 is a commonly expressed biomarker of NCCs both at the neural plate border and during migration and colonisation of the developing embryo (Milet *et al.,* 2013). It is known to be expressed in cells in the nascent stages of central nervous system development (Maczkowiak *et al.,* 2010) although transcription is tightly regulated and restricted to the dorsal neural tube (Moore *et al.,* 2013). As with *Nestin*, treatment with BMP-4 acted to delay increasing gene expression of *Pax3* but prolonged period of expression. In untreated cells, *Pax3* expression was seen to swiftly peak and then decline as opposed to expression in treated cells, which increased more slowly but maintained increasing expression levels (Figure 3.20). Earlier experiments showed *Pax3* expression to peak after 1 week of stage 3 (21 days total treatment) in induction conditions (Figure 3.11). Pax3 is expressed transiently in a number of tissues in the developing organism, although expression is normally

curtailed before progenitor cells differentiate into somatic lineages. Prolonged expression of Pax3 has been described in neural crest derivatives such as peripheral neurons (Blake and Ziman, 2013) and it may act to maintain NCCs in a multipotent state before and during delamination and migration. (Wu *et al,* 2008). Neural crest differentiation is a multistep process and initial development can occur in the absence of *Pax3* although deficiencies in neural crest derived cell types, particularly melanocytes can be observed in addition to vestigial formation of skeletal muscle (Maczkowiak, *et al*, 2010). These data suggest that *Pax3* plays a key role in the migration but not the initial formation of the neural crest (Moore *et al.,* 2013). BMP-4 may play a role in these early stages by regulating *Pax3* expression prior to delamination.

*Musashi-1* is similarly associated with nervous system and neural crest development (Abreu *et al.,* 2009). The pattern of expression of *Musashi-1* followed similar trend to *Pax3* with delayed upregulation in BMP-4 treated cells. Expression in untreated cells did not significantly change between 5 and 10 days while increasing in treated cells over the same period (Figure 3.21). *Musashi-1* is part of the same regulatory network as *Pax3,* combining to stimulate the expression of *Ret, a* gene found in cells of neural crest lineage (Figure 1.10) indicating that co-expression of these genes is required for neural crest differentiation.

The role of BMP-4 on expression of *Sox9* during differentiation stage 2 was less clear. Cells cultured in BMP-4-supplemented (treated) and non-supplemented media (untreated) showed similar levels of upregulation (80-fold and 67-fold upregulation respectively) between the beginning and the mid-point (5 days) of stage 2. No significant difference was noted at this stage (p value = 0.34). *Sox9* expression in

treated cells remained relatively constant between the middle and end of stage 2 while expression in untreated cells almost doubled. The difference in expression levels was deemed significant (p value = 0.03) (Figure 3.22). These data indicate a regulatory role for BMP-4 in Sox9 expression; potentially maintaining a particular level of expression. Sox9 is inhibitory to neurulation and necessary for the delamination and migration of neural crest stem cells in its phosphorylated form. Transcriptional analysis was unable to determine the state of phosphorylation and whether or not this is affected by BMP-4 (Liu *et al*, 2013).

The expression of biomarkers, *Pax3, Musashi-1* and *Sox9* coupled with the ability of treated cells to differentiate into distinct lineages immunopositive for peripheral neuron and smooth muscle markers is indicative of a neural crest cell type for cells at stage 2 of differentiation. Transcriptional data requires verification through proteomic analysis such as Western blotting or immunocytochemistry (Chapter 6). The precise mechanisms of BMP-4 regulation on neural crest development remain unclear. Investigation of methylation status of affected genes such as *Nanog* may offer some insights into its transcriptional mechanisms. It is known that BMP-4 is sufficient together with the presence of LIF to maintain murine embryonic stem cells in an undifferentiated state, allowing for high levels of proliferation and self-renewal (Tamm *et al.*, 2013). Conversely, BMP-4 through the SMAD pathway, acts as a driver for early neural differentiation (Fei *et al.,* 2010) it is possible that BMP-4 plays more than one role in the onset of neural crest differentiation. Global genome analysis may be efficacious in identifying novel long and short-term targets. Finally, functional analysis of prospective neuronal cells is necessary for verification of targeted differentiation (Chapter 6). The development of functional neurons would

serve too act as validation of the culture process and perhaps a potential source of cells for future tissue replacement therapies.

# Chapter 4: Transcriptional Analysis of Neural Crest Derived Peripheral Neuron Differentiation from Mouse Embryonic Stem Cells.

## 4.1 Introduction

Global gene expression analysis has proven vastly beneficial in the analysis of stem cell differentiation. It enables the rapid characterisation and comparison of cells at different stages of differentiation. It also provides a method for the verification of differentiation protocols and potentially identifies key regulatory factors (Takahashi and Yamanaka, 2006). Previous studies in the field have measured the transcriptional changes inherent in the differentiation of NCCs from embryonic precursors (Kreitzer *et al*, 2013) but little information is available on the impact of specific factors such as BMP-4 that influence lineage selection.

Affymetrix Gene Chip microarrays are commonly used for the transcriptional analysis of multiple cell types, containing multiple probes representing thousands of genes across various species such as mouse, rat and human (Irizarry *et al.*, 2003). The large number of genes examined can prove challenging to analyse without deconvolution. However, software packages such as DAVID (http://david.abcc.ncifcrf.gov/tools.jsp) hosted by the National Institute of Health, which provide algorithms to sort and categorise microarray data are freely available (Huang *et al.,* 2007). These analyses quickly and efficiently provide candidate genes for verification by more sensitive techniques such as real time PCR (Rajeevan *et al.*, 2001).

## 4.2 Aims

- Carry out global transcription analysis of differentiating putative neural crest cells and peripheral neurons to elucidate transcriptional changes during differentiation and assess the role of BMP-4 in neural crest specification
- Use deconvolution software such as DAVID to assay possible regulatory factors
- Confirm expression profiles with RT-qPCR

## 4.3 Results

### 4.3.1 TriSure™ Extraction of RNA

Although Nanodrop analysis is ideal for determining the quantity and purity of nucleic acids it cannot differentiate between degraded and non-degraded samples. Accurate microarray analysis relies on high quality RNA (RNA integrity number (RIN) >7) and little variation between replicates (Thompson *et al.,* 2007). Electropherograms were produced for each sample earmarked for microarray analysis (Figure 4.1) and 2100 Expert Software (Agilent) was used to determine RINS. Non-degraded RNA shows characteristic peaks corresponding to 28s and 18s ribosomal RNA at 40 and 50 seconds respectively with no signal generated before, between or after the peaks. Degraded RNA shows the same ribosomal peaks but with other, lower peaks indicative of smaller fragments of RNA visible. A 25 bp marker added to the reaction mixtures was visualised as a peak at 25 seconds (Anon, 2013).

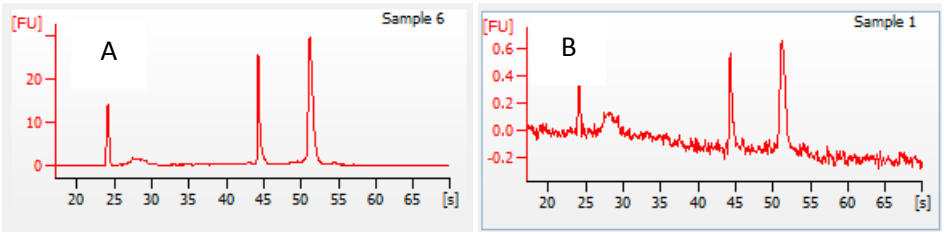


**Figure 4.1. Integrity of extracted RNA.** RNA was extracted with TriSure™ and analysed using Agilent 2100 software. (A) Representative electropherogram for non-degraded (RIN 10) RNA. (B) Representative electropherogram for degraded (RIN 2.6) RNA.

RNA from stage 0, 1, 2 and 3 cells was extracted and sent for analysis, each sample representing a discrete step in the differentiation process (Table 3.2). Stage 3 cells were harvested 20 days after withdrawal of BMP-4 supplementation (34 days total culture). To determine the immediate effects of BMP-4 on gene expression RNA was extracted from treated cells 1 hour into stage 2, this was compared to RNA from stage 1 cells. To ensure any differences were a result of BMP-4 supplementation fresh PIM was added to untreated cells at the same time and cells were incubated at 37°C for 1 hour. To assess the long-term effects of BMP-4 supplementation cells were cultured for the same time-period as stage 2 cells but media was not supplemented with BMP-4 after stage 1. These cells were termed stage 2 treated and untreated as previously described. Only RNA samples with RINS of 8 or higher were considered for microarray analysis. Bioanalyzer data showed that non-degraded RNA of consistent quality was produced by TriSure™ extraction (Table 4.1).

**Table 4.1. Extracted RNA for microarray experiments was of consistent, high integrity.** RNA was extracted in triplicate samples at each time point and analysed using an Agilent 2100 Bioanalyzer. All samples were above the threshold value and little variation in RIN was observed between samples.

| Differentiation stage | Culture period (cumulative) | Media | RIN (Sample 1) | RIN (Sample 2) | RIN (Sample 3) |
|---|---|---|---|---|---|
| Stage 0 | 0 days | E14 CM | 10 | 9.9 | 10 |
| Stage 1 | 4 days +1 hour (4 days +1 hour) | PIM | 10 | 9.7 | 9.9 |
| Stage 2 (1 hour) | 4 days +1 hour (4 days +1 hour) | SIM | 10 | 10 | 9.7 |
| Stage 2 (treated) | 10 days (14 days) | SIM | 10 | 10 | 9.9 |
| Stage 2 (untreated) | 10 days (14 days) | PIM | 10 | 9.9 | 10 |
| Stage 3 | 20 days (34 days) | PIM | 9.9 | 9.7 | 10 |

### 4.3.2 Affymetrix Microarray of Differentiating Mouse Embryonic Stem Cells

Microarray experiments were carried out by Mr Michael Smiga (University of Manchester Genomic Sciences Core Facility). Initial analyses were performed by Dr Leo Zeef at the University of Manchester Bioinformatics Core Facility. Quality control (QC) analysis showed little variance in median intensity before normalisation, a low percentage of outliers and no warnings triggered for any of the samples (Table 4.2).

**Table 4.2 Pre-normalisation intensities and outliers for Affymetrix Microarray experiments.** Median intensities for each sample were similar, no probes were called absent and low outlier percentages were noted.

| Array | Median Intensity (unnormalised) | P call % | % Array outlier | % Single outlier | Warning |
|---|---|---|---|---|---|
| Stage 0 | 144 | 0 | 0.058 | 0.021 | - |
| Stage 1 | 178 | 0 | 0 | 0.01 | - |
| Stage 2 (1 hour) | 156 | 0 | 0.002 | 0.007 | - |
| Stage 2 (end) | 187 | 0 | 0.193 | 0.032 | - |
| Stage 2 (BMP-4 negative) | 179 | 0 | 0.064 | 0.013 | - |
| Stage 3 | 151 | 0 | 1.055 | 0.169 | - |

Datasets were considered of sufficient quality for further analysis, following QC principal component analysis (PCA) was carried out to examine levels of variation between the samples. PCA analysis showed that principle components 1 and 2 accounted for 87.3 percent of variance across all samples with the majority of this (70.5%) due to principle component 1. Variations in both principle components were observed at each stage of the differentiation process. BMP-4 treatment manifested small changes after 1 hour and more discernible variance after 10 days treatment (Figure 4.2).

Data was converted into PUMA antilog format and reported as fold change in gene expression between variables, a threshold of 2.5-fold change in expression for upregulated genes and 2.5-fold for downregulated was selected. At each stage the majority of genes remained unchanged, however a number of genes were observed to be differentially expressed at each stage both positively and negatively (Table 4.3).

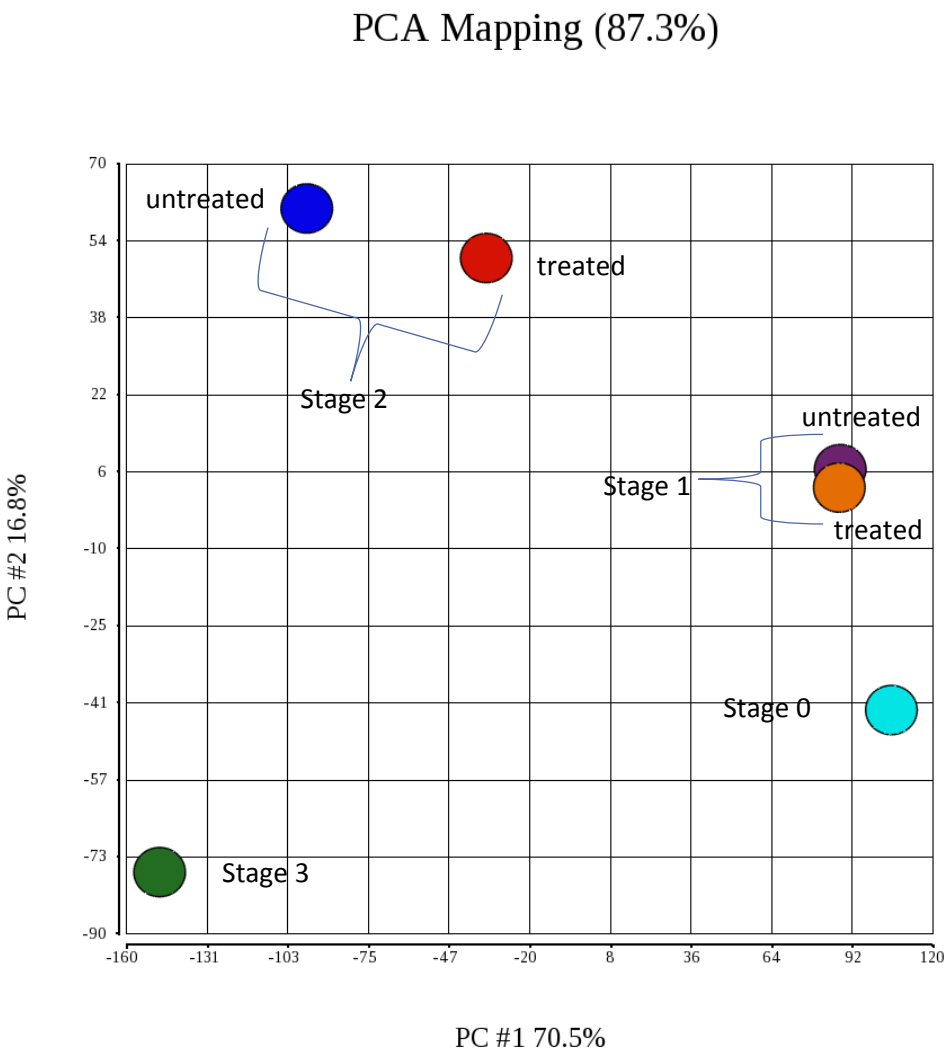


**Figure 4.2. Principle component analysis of global gene expression in differentiating E14 mouse embryonic stem cells.** Variation in gene expression was observed as stage 0 cells (cyan) were differentiated into stage 1 (tan), stage 2 (red) and stage 3 cells (green). After 1 hour of stage 2 small variations in gene expression were observed between treated and untreated cells (tan -purple). Greater variation was seen between treated (red) and untreated (blue) cells after stage 2.

**Table 4.3. Gene expression analysis of differentiating E14 mouse embryonic stem cells**. Cells were cultured as previously described (Table 3.2). Expression levels were compared between the later stage and earlier stage in each case.

| Differentiation stage | Upregulated | Downregulated | Unchanged |
|---|---|---|---|
| Stage 0 - Stage 1 | 3566 | 4910 | 36562 |
| Stage 1 - Stage 2 | 6086 | 5345 | 33607 |
| Stage 2 – Stage 3 | 7892 | 6220 | 30926 |

BMP-4 treatment was shown to exert an immediate effect with over 3000 genes upregulated and almost 1500 downregulated after 1 hour. After 10 days, slightly more genes (4355) were observed to be upregulated while over twice as many (3666) exhibited downregulation (Table 4.4). These early data may indicate a convoluted role for BMP-4 in neural crest development, involving the differential regulation of many genes.

**Table 4.4 BMP-4 treatment alters gene expression in differentiating stem cells.** RNA expression levels in stage 2 treated cells were compared to those in stage 2 untreated cells after 1 hour (immediate effects of BMP-4 treatment) and 10 days (long-term effects of BMP-4 treatment).

| Differentiation stage | Upregulated | Downregulated | Unchanged |
|---|---|---|---|
| Stage 2 - 1 hour | 3255 | 1486 | 40297 |
| Stage 2 - 10 days | 4355 | 3666 | 37017 |

It must be noted that the total number of *probes* (45038) does not correspond to the total number of *genes* analysed. Many genes in the microarray are represented by multiple probes. In order to identify possible regulatory factors computer analysis was used to deconvolute the data.

### 4.3.3 Putative Targets of BMP-4 in Differentiation of Mouse Embryonic Stem Cells

Microarray analyses revealed expression changes in thousands of genes for each point of comparison. The DAVID functional annotation tool was used to deconvolute data and assay potential pathways. Genes constituting parts of the cell adhesion molecule pathway were within the 500 most upregulated and downregulated genes in three of the five comparison points, with significant changes

in expression in differentiation stages 2 and 3 noted and potential BMP-4 mediated alterations during stage 2 (Table 4.5).

**Table 4.5 Cell adhesion molecules were differentially expressed during differentiation of E14 mouse embryonic stem cells.** DAVID analysis demonstrated significant changes in expression of adhesion molecules at each stage of differentiation.

| Stage | P-value |
|---|---|
| Stage 1-2 | 0.00059 |
| Stage 2-3 | 0.008 |
| Stage 2 treated / untreated comparison | 0.0001 |

In each case, the p-value was well below 0.05, suggesting a significant role for adhesion molecules in the differentiation process. Further analysis using the Kyoto Encyclopaedia of Genes and Genomes (KEGG) – supported by DAVID revealed two particular pathways – the neural system and tight junction formation pathways (Figure 4.3). KEGG analysis detailed known pathways with highly upregulated or downregulated genes marked by stars. Analysis of the genes in these pathways revealed that in particular the *Claudin* family, the *Cadherin* family of adhesion and the synaptic gene families coding for *Neurexins* and *Neuroligins* were important throughout the differentiation process and potential targets of BMP-4. Data from multiple probes was generated for *Cadherin* and *Claudin families* (summarised in Appendix 4), while *Neuroligin1*, *Neuroligin3* and their corresponding *Neurexin* genes were specifically noted as putative BMP-4 targets during neural crest differentiation.

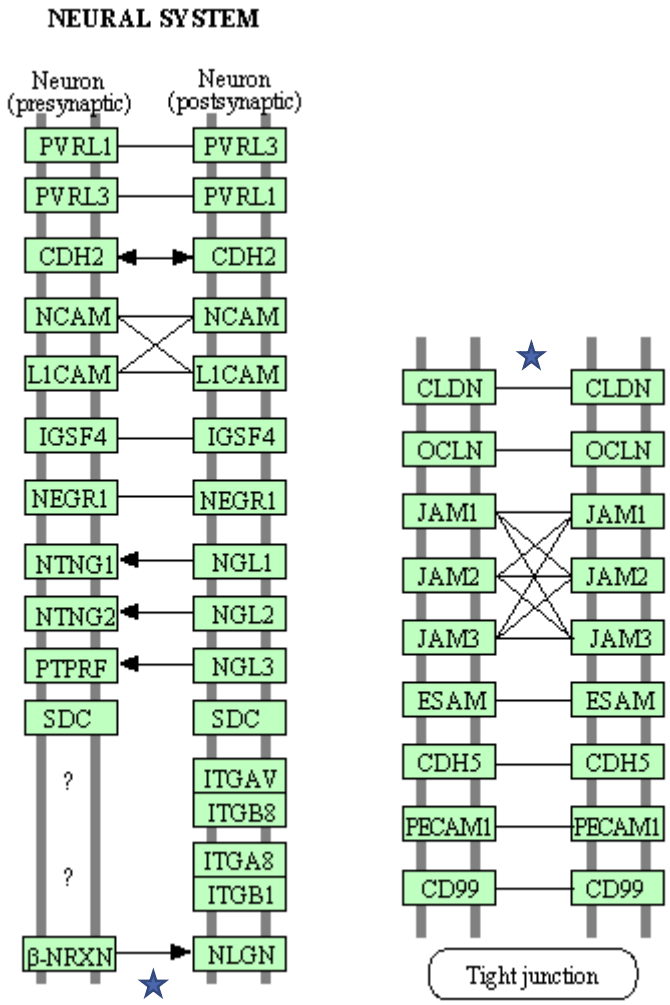


**Figure 4.3. KEGG analysis of microarray data.** The neural system and tight junction pathways are potentially important both in the formation of the neural crest and its derivative and as targets for BMP-4 signalling. KEGG analysis indicated the *Claudin* family of tight junction associated genes and the prosynaptogenesis genes of the *β-Neurexin* and *Neuroligin* families were differentially regulated by BMP-4 during differentiation into peripheral neurons, particularly *Claudin* and *Neurexin-Neuroligin* expression (marked by stars).

### 4.3.4 RT-qPCR of Candidate Genes Identified by Microarray Analysis

Analysis of microarray data indicated a number pluripotency associated genes were upregulated in the presence of BMP-4, specifically *Oct-4* and members of the developmental pluripotency family of genes. In order to confirm these data RT-qPCR was carried out using RNA from stages 0, 1, 2 and 3 corresponding to the time

points selected for microarray analyses. As previous data (Figure 3.12) showed that *Nanog* expression was at first downregulated and then upregulated during stage 2 RNA extracted at the midpoint of this stage was additionally extracted and analysed to determine whether this resurgence occurred in other genes (Table 4.6).

**Table 4.6 time points selected for RT-qPCR analysis after microarray experiments.** Cells were cultured in induction media with BMP-4 treatment during stage 2.

| Culture time (days) | Stage | Media |
|---|---|---|
| 0 days | 0 (SSEA-1 positive embryonic stem cells) | E14 CM |
| 4 days | 1 | PIM |
| 9 days | 2 (mid-point) | SIM |
| 14 days | 2 (end) | SIM |
| 34 days | 3 | PIM |

Five pluripotency associated genes were investigated, *Oct-4, Dppa2, Dppa3, Dppa4* and *Dppa5* as each was indicated as a putative BMP-4 target after microarray analyses. In each case a similar expression pattern was seen. Initially expression of these genes declined slightly or remained stable with between stages 0 and 1 followed by a sharp decline at the mid-point of stage 2. As with *Nanog* expression levels increased for all genes between the middle and end of stage 2. Except in the case of *Dppa2* and *Dppa3* expression levels decreased upon BMP-4 withdrawal. (Figures 4.4-4.8). All data was normalised to the housekeeping genes β-actin and 18s ribosomal RNA, both of which showed consistent levels of expression at each stage and significance was determined by students T-test comparing each time point sequentially.

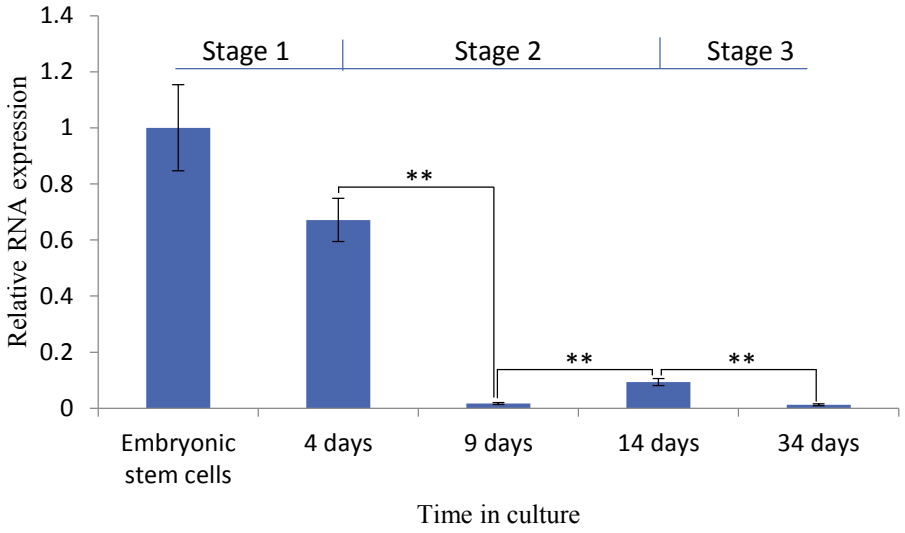


**Figure 4.4. Culture in induction media resulted in differential *Oct-4* expression relative to embryonic stem cells (value = 1).** E14 mouse embryonic stem cells were cultured in PIM during stage 1, SIM during stage 2 and PIM during stage 3. Rapid downregulation during stage 1 and the first half of stage 2 was reversed by the end of stage 2. Data is mean ± SEM, n=3. ** denotes p-value < 0.01. Denotes p-value < 0.01

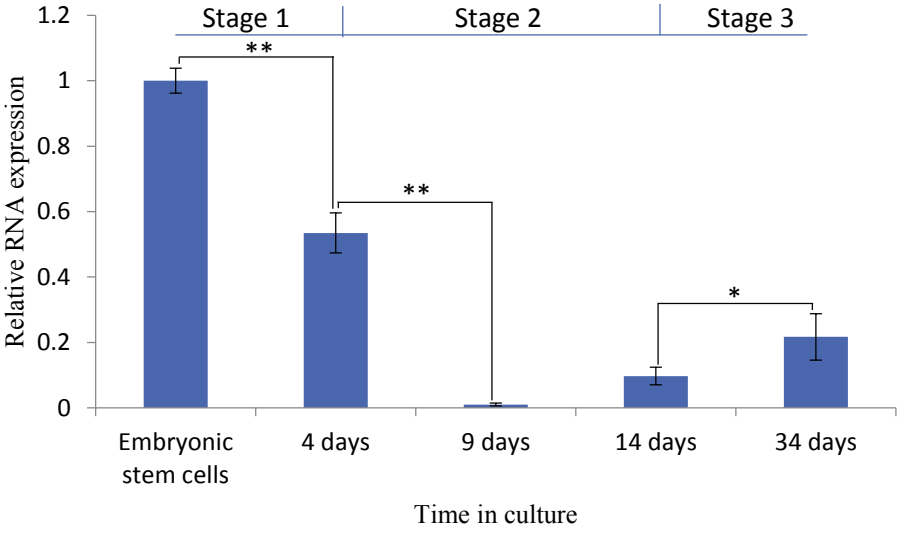


**Figure 4.5. Culture in induction media at first downregulated then upregulated *Dppa2* expression relative to embryonic stem cells (value = 1).** E14 mouse embryonic stem cells were cultured in PIM during stage 1, SIM during stage 2 and PIM during stage 3. Gene expression initially decreased and was upregulated following withdrawal of BMP-4 treatment after stage 2. Data is mean ± SEM, n=3. * Denotes p-value < 0.05. ** Denotes p-value < 0.01.

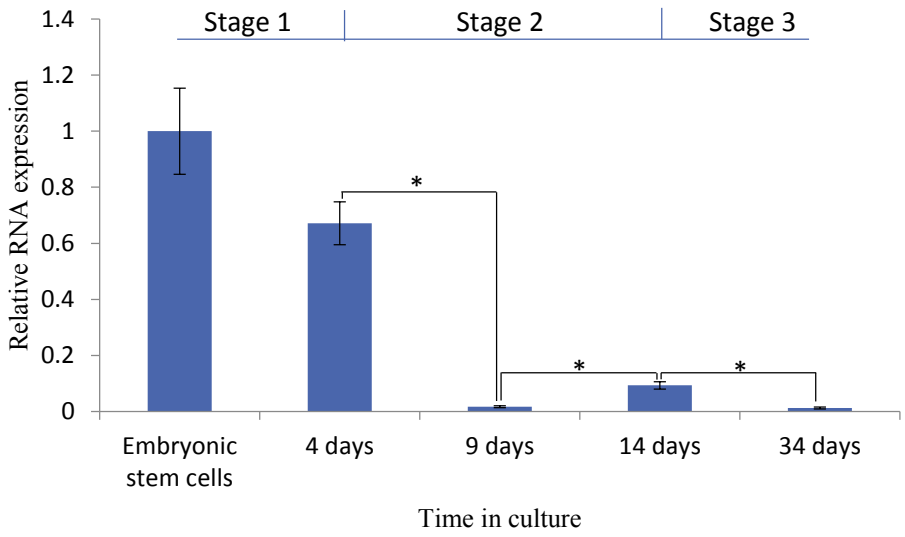


**Figure 4.6. Culture in induction media at first downregulated then upregulated expression of *Dppa3* compared to embryonic stem cells (value = 1).** E14 mouse embryonic stem cells were cultured in PIM during stage 1, SIM during stage 2 and PIM during stage 3. BMP-4 treatment increased expression after 10 days following an initial drop. Data is mean ± SEM, n=3. * Denotes p-value < 0.05.

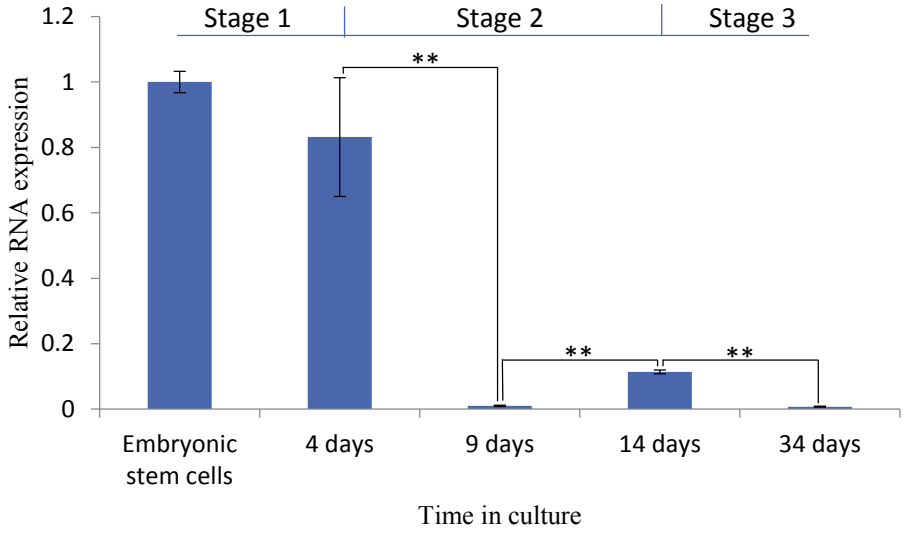


**Figure 4.7. Culture in induction media resulted in differential expression of *Dppa4* relative to embryonic stem cells (value = 1).** E14 mouse embryonic stem cells were cultured in PIM during stage 1, SIM during stage 2 and PIM during stage 3. BMP-4 supplementation significantly upregulated expression between the mid and end points of stage 2.Data is mean ± SEM, n=3 ** Denotes p-value < 0.01.

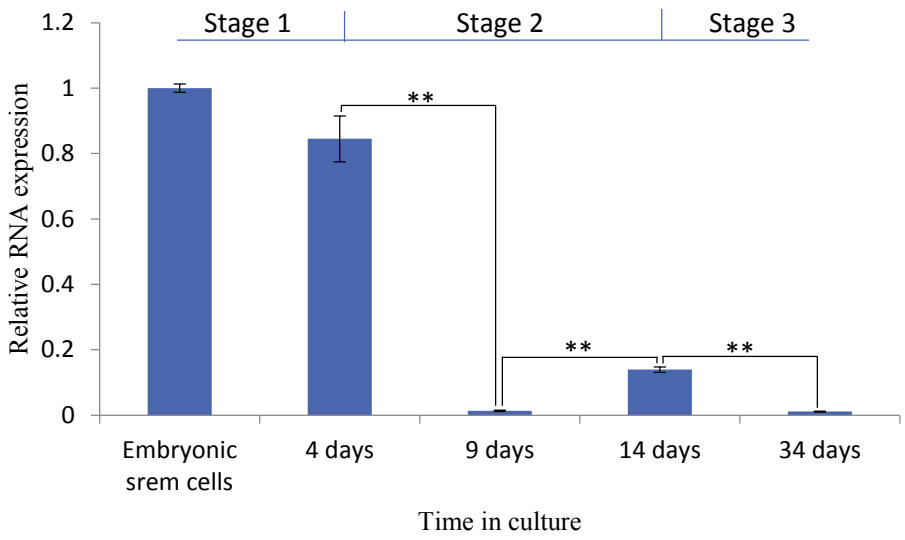


**Figure 4.8. Culture in induction media resulted in differential expression of *Dppa5* relative to embryonic stem cells (value = 1).** E14 mouse embryonic stem cells were cultured in PIM during stage 1, SIM during stage 2 and PIM during stage 3. BMP-4 supplementation significantly upregulated expression between the mid and end points of stage 2. Data is mean ± SEM, n=3. ** Denotes p-value < 0.01.

To assess the effects of BMP-4 on the above genes expression was tested as in section 3.3.6. No differences were observed after 1 hour and 5 days culture for four of the six genes examined. *Dppa2* and 3 showed increased expression levels of 4.4 and 6.9 fold respectively but high levels of variation in samples meant this was not significant. After 10 days in culture BMP-4 was shown to upregulate each gene, differences in expression levels were shown to be statistically significant except for *Dppa2* (p-value 0.09) (Figure 4.9). Expression values of treated cells were compared to those of untreated cells (value =1), data was normalised to the housekeeping genes β-actin and 18s ribosomal RNA. Students 2-tailed T-tests were used to determine significance.

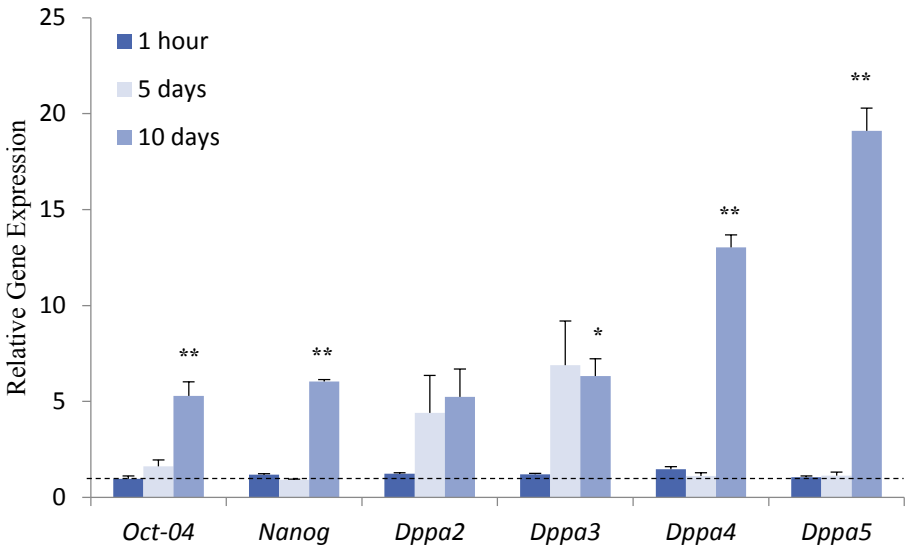


**Figure 4.9. BMP-4 increased expression of pluripotency associated genes after 10 days in culture**. Cells were cultured during stage 2 and gene expression was calculated relative to expression in untreated cells. Upregulation was observed in 5 out of 6 genes after 10 days. No significant difference in expression was noted after 1 hour and 5 days Data is mean ± SEM, n=3. * denotes p value < 0.05 ** denotes p value < 0.01. Expression levels in untreated cells are denoted by the dotted line (value = 1).

*Shh* expression is reported in the PNS, being essential for correct innervation of the gut (Jin *et al*, 2015) but is repressed by the secreted BMP-4 (Liem, *et al*, 1995). Microarray data showed two probes corresponding to *Shh* with differing values. RT-qPCR was used to determine whether or not transcriptional repression of Shh was taking place and whether this was mediated by BMP-4. Analysis over time showed a gradual increase in expression from stages 0-2 although these changes were not significant. Upon removal of BMP-4, significant upregulation (p-value 0.0007) was observed (Figure 4.10).

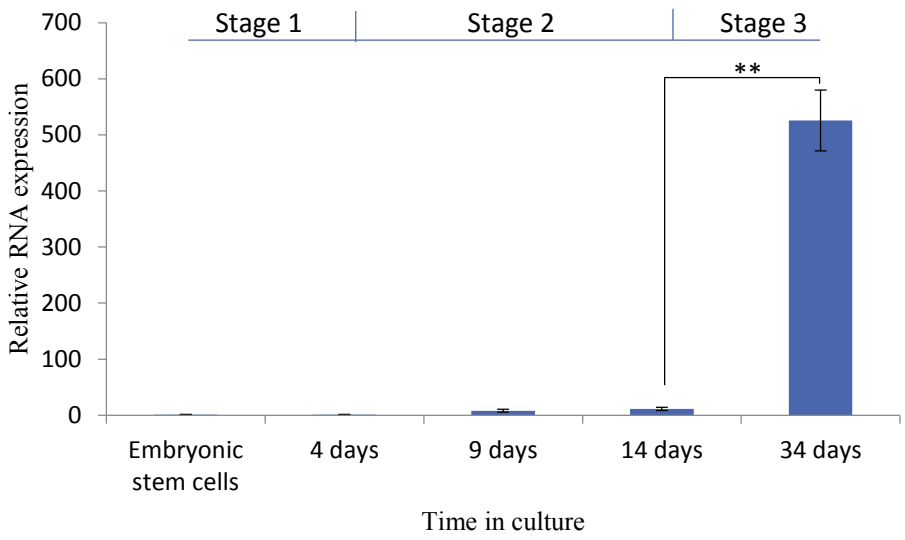


**Figure 4.10. Culture in induction media resulted in upregulation of *Sonic Hedgehog*, after removal of BMP-4.** E14 mouse embryonic stem cells were cultured in PIM during stage 1, SIM during stage 2 and PIM during stage 3. All values are compared to embryonic stem cells (value = 1). Data is mean ± SEM, n = 3. ** Denotes p-value < 0.01.

Pathway analysis was carried out using DAVID functional annotation tools (National Institute of Health) (section 4.4.3). A number of genes associated with cellular adhesion and migration were identified as putative targets of BMP-4 with a potential role in neural crest formation. Confirmation of microarray data was carried out by RT-qPCR as above. The tight junction proteins *Claudin1* and *Claudin23* were shown to be increasingly expressed over the period of differentiation. *Clauin23* expression remained unchanged after stage 2, while *Claudin1* was highly upregulated (Figure 4.11 and 4.12).

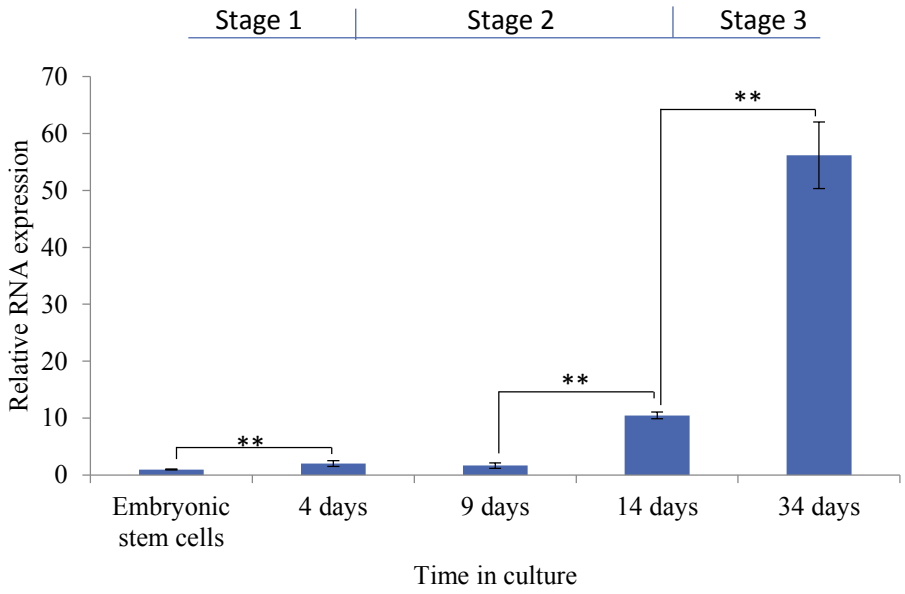


**Figure 4.11. *Claudin1* expression increased in comparison to embryonic stem cells (value = 1) in induction media.** E14 mouse embryonic stem cells were cultured in PIM during stage 1, SIM during stage 2 and PIM during stage 3. Data is mean ± SEM, n=3. ** Denotes p-value < 0.01.

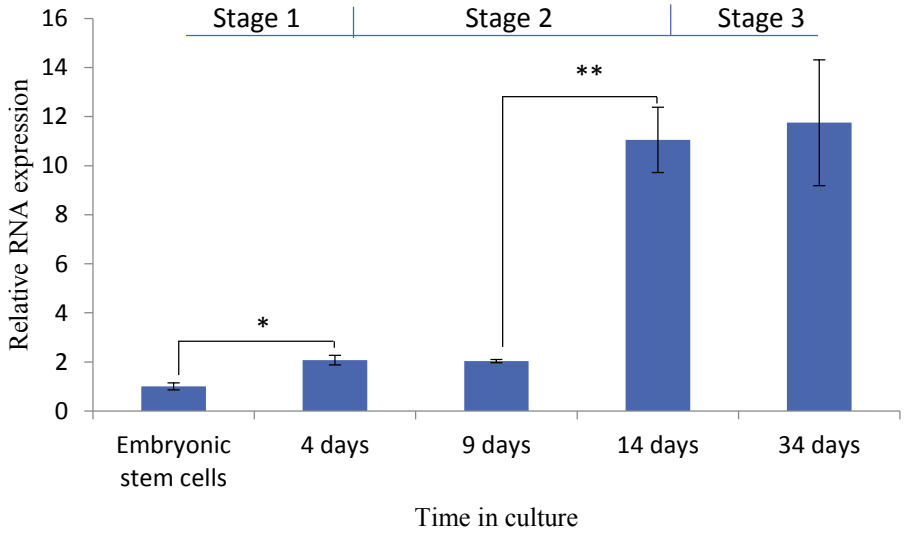


**Figure 4.12. *Claudin23* expression increased in comparison to embryonic stem cells (value = 1) in induction media.** E14 mouse embryonic stem cells were cultured in PIM during stage 1, SIM during stage 2 and PIM during stage 3. Data is mean ± SEM, n = 3. * Denotes p-value < 0.05. ** Denotes p-value < 0.01.

Expression of the synaptogenesis associated adhesion genes*Neuroligin1* and *Neuroligin3* were both upregulated during the differentiation process most notably in stage 3 after the withdrawal of BMP-4 supplementation. In the case of both, transcription was not detected in embryonic stem cells or stage 1 differentiated cells (4 days treatment). (Figures 4.13 and 4.14).

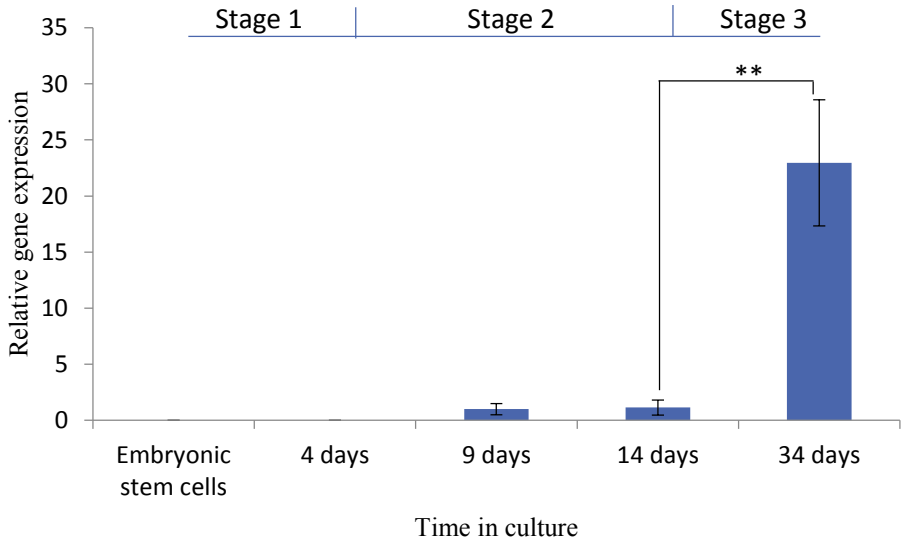


**Figure 4.13. *Neuroligin1* was weakly expressed in cells cultured in induction media supplemented with BMP-4.** E14 mouse embryonic stem cells were cultured in PIM during stage 1, SIM during stage 2 and PIM during stage 3. Expression was not detected before 9 days. Removal of BMP-4 resulted in significant upregulation. (Values compared to cells after 9 days culture = 1). Data is mean ± SEM, n = 3. ** Denotes p-value < 0.01.

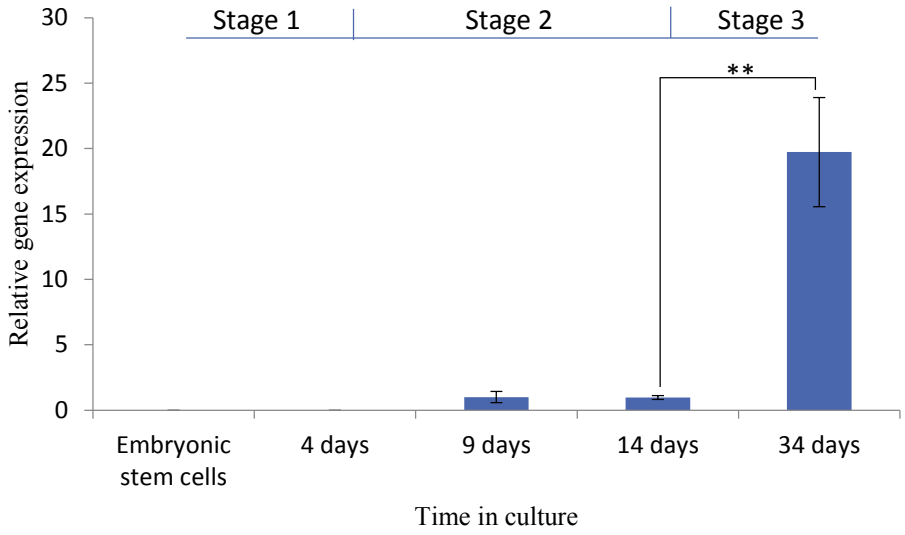


**Figure 4.14. *Neuroligin3* was weakly expressed in cells cultured in induction media supplemented with BMP-4.** E14 mouse embryonic stem cells were cultured in PIM during stage 1, SIM during stage 2 and PIM during stage 3. Expression was not detected before 9 days. Removal of BMP-4 resulted in significant upregulation. (Values compared to cells after 9 days culture = 1). Data is mean ± SEM, n = 3). ** Denotes p-value < 0.01

Expression levels of two adhesion and migration associated POU domain-containing genes (*Pou3f4* and *Pou4f2)* were interrogated after DAVID analysis revealed a potential role for both in the neurulation and adhesion of differentiating cells. Small changes in *Pou3f4* expression were observed between stage 0 and the mid-point of stage 2. However, between this point and the end of stage 2 an 11.9-fold upregulation was recorded. Removal of BMP-4 supplementation resulted in a further 10.8-fold increase (Figure 4.15). *Pou4f2* expression decreased in culture from stage 0 to stage 1 and was not detected at the midpoint of stage 2. Transcription was observed to resume by the end of stage 2 and was significantly upregulation during stage 3 (Figure 4.16).

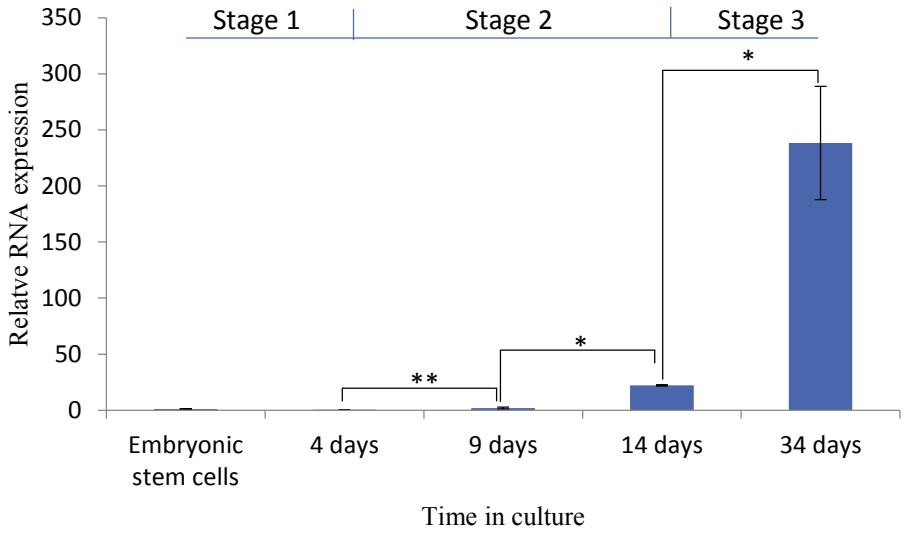


**Figure 4.15. *Pou3f4* was moderately expressed after 10 days culture with BMP-4, highly expressed after withdrawal of BMP-4 supplementation.** E14 mouse embryonic stem cells were cultured in PIM during stage 1, SIM during stage 2 and PIM during stage 3. Values compared to embryonic stem cells (= 1). Data is mean ± SEM, n = 3. * Denotes p-value < 0.05 ** Denotes p-value < 0.01.

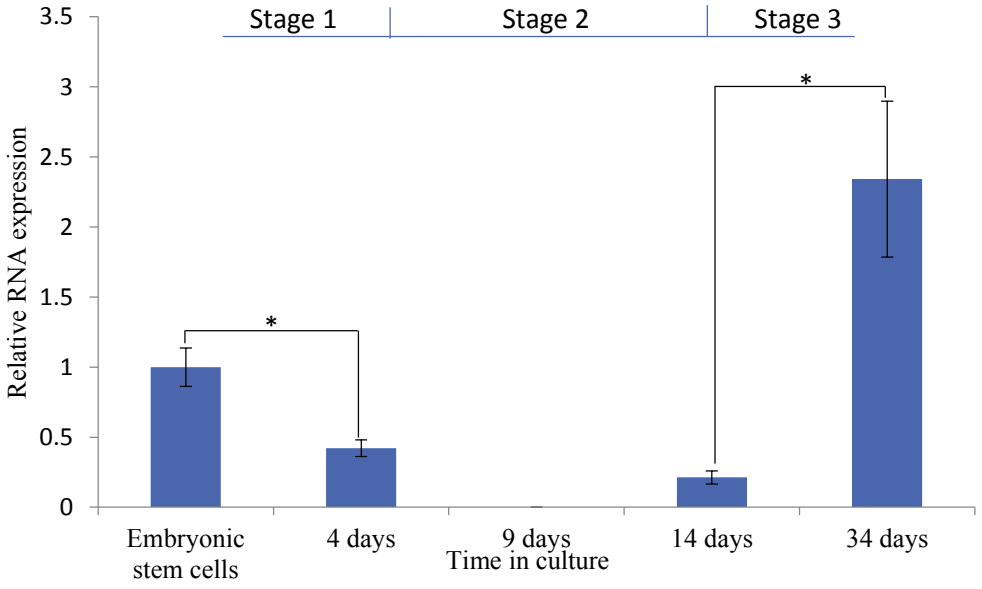


**Figure 4.16. Culture in induction media initially downregulated then upregulated *Pou4f2* expression compared to embryonic stem cells (Value = 1).** E14 mouse embryonic stem cells were cultured in PIM during stage 1, SIM during stage 2 and PIM during stage 3. Expression was not detected at 9 days. Data is mean ± SEM, n = 3. * Denotes p-value < 0.05.

Tudor Domain Containing Protein 12 (*Td12*) gene showed 97132-fold upregulation after 10 days culture in the presence of BMP-4 compared to culture without. No previous connections between neural crest development and expression were found. On the basis that such profound changes in expression levels may be indicative of a role in neural crest formation RT-qPCR was carried out as before. *Td12* expression remained stable between stage 0 and 1 days but declined during stage 2. The remainder of the treatment showed some fluctuation but changes were not significant varying between 2.6 and 6.3 fold downregulation compared to embryonic stem cells (Figure 4.17).

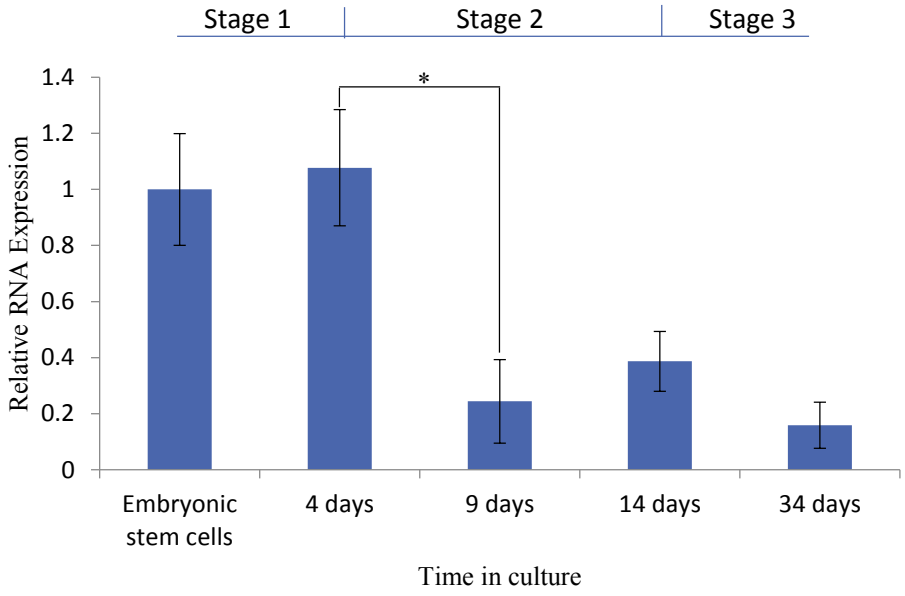


**Figure 4.17. Culture in induction media decreased expression of *Td12* after an initial period of stability. Expression levels did not vary thereafter.** E14 mouse embryonic stem cells were cultured in PIM during stage 1, SIM during stage 2 and PIM during stage 3. Expression levels were compared to embryonic stem cells =1. Data is mean ± SEM, n=3. * Denotes p-value < 0.05.

Expression of the above genes was measured after BMP-4 treatment for 1 hour, 5 days and 10 days as before, compared to untreated stage 2 cells (section 3.3.6). No significant changes were detected for any of the genes after 1 hour and neither *Neuroligin1* or *Neuroligin3* were not detected at this point. Culture for 5 days resulted in significant downregulation of *Shh* (4.3-fold), *Claudin1* (18.8-fold), *Neuroligin3* (2.2-fold) *Pou3f4* (88.2-fold) and *Pou4f2* (not detected in the treated sample) in treated cells compared to untreated. After 10 days *Shh (*6.4-fold), *Claudin1* (6.1-fold), *Pou3f4* (3.5-fold) and *Pou4f2* (4.4-fold) were all downregulated in cells cultured in BMP-4 supplemented media. *Neuroligin1* was downregulated significantly after 10 days (6.6-fold) while *Neuroligin3* expression was the same. In contrast to *Claudin1, Claudin23* expression was upregulated by BMP-4 showing a 3.5-fold increase after 10 days. *Td12* also exhibited an increase in transcriptional activity to a more modest extent then indicated by microarray data (10.1-fold), (Figure 4.18).

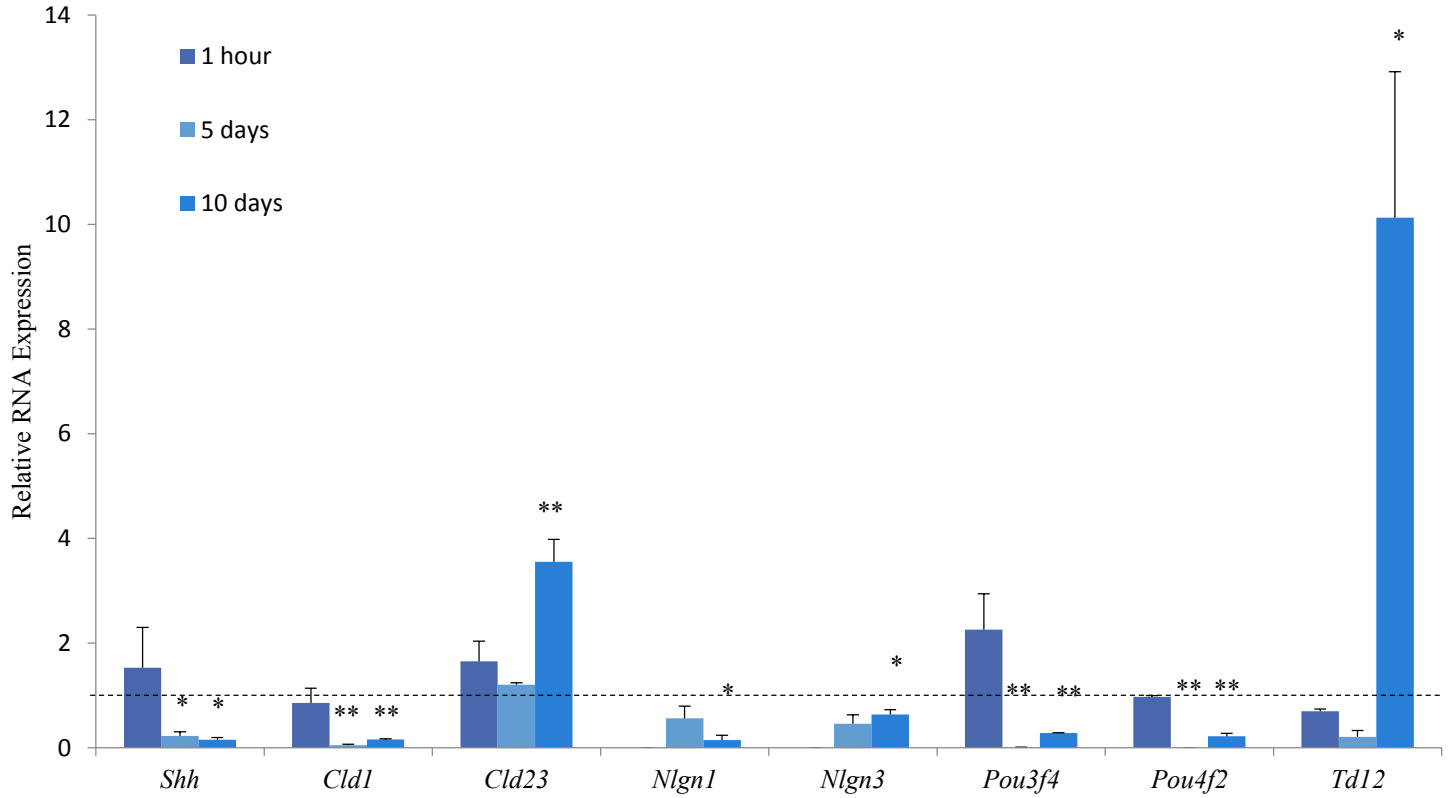


**Figure 4.18. BMP-4 supplementation altered expression of adhesion and neuronal associated genes.** Cells were cultured in primary induction media for four days (stage 1) before BMP-4 treatment for ten days (stage 2). Expression values were compared to stage 2 untreated cells (dotted line, value = 1). Data was normalised to β-actin and 18s ribosomal RNA. Data are mean ± SEM, n = 3. * denotes $p > 0.05$ ** denotes $p > 0.01$.

## 4.4 Discussion

Global gene expression analysis identified a number of putative genes that may play a regulatory role in BMP-4 mediated differentiation of murine embryonic stem cells. Confirmation by RT-qPCR confirmed expression changes in a quantifiable manner. BMP-4 was shown to have a positive regulatory effect on the expression of a number of genes associated with pluripotency. Initial downregulation was followed by upregulation after stage 2 in culture in all the genes surveyed. With the exception of *Dppa2* and *Dppa3,* withdrawal of BMP-4 resulted in these genes again being downregulated (Figures 4.4-4.8). The role of *Nanog* and *Oct-4* in the maintenance of pluripotency is well documented, (Loh, *et al*, 2006) the role of the *Dppa* genes is less well characterised although they are known as markers of pluripotency (Ruau *et al,* 2008). A role for these genes in the maintenance of pluripotency can be inferred as knockdown of *Dppa2* limited the self-renewal potential of murine embryonic stem cells and mediated differentiation. Knockdown of *Oct-4* resulted in reduced *Dppa2* expression suggesting a possibly regulatory role for the former (Du, *et al*, 2010). *Dppa2* and *Dppa4* have been recently identified as oncogenic and through the SAP signalling pathway increase cell proliferation, representing a possible model for their role in embryonic stem cells (Tung *et al*, 2013). *Dppa3* regulates gene expression by modification of the chromatin structure, facilitating the open heterochromatin rich structures of ESCs (Liu *et al*, 2012) while *Dppa5* is less well characterised but present in murine and human embryonic stem cells (Kim *et al.,* 2005).

The role of BMP-4 in stem cell biology is complex and diverse. Culture of murine embryonic stem cells with LIF and 10 ng $ml^{-1}$ BMP-4 acts antagonistically towards differentiation and stimulates self-renewal in the absence of serum. (Zhang, *et al*, 2013). Conversely, in human embryonic stem cells BMP-4, albeit at a higher

concentration (100 ng $ml^{-1}$) downregulates expression of the pluripotency factors *Nanog, Sox2* and *Oct-4* (Xu *et al*, 2008) acting to induce differentiation. BMP-4 plays an inhibitory role in the development of the murine nervous system and an inductive role in the development numerous cell lineages including hepatic, cardiac and osteoblast (van Bezooijen *et al*, 2005; Fei, *et al*, 2010). It is evident that BMP-4 signalling is a complex and dynamic process responding to variations in concentration and environment. The almost ubiquitous presence of BMP-4 signalling in the developing organism is indicative of the ability to respond to a number of extracellular and intracellular cues underlying its importance as a key regulator of gene expression (Varga and Wrana, 2005).

Microarray data, and subsequent RT-qPCR analyses revealed upregulation of pluripotency factors and downregulation of neurulation associated genes such as *Shh* (Figures 4.19 and 4.18). Differentiating cells were treated with similar levels of BMP-4 to those described by Zhang *et al* (2013) (8ng $ml^{-1}$) indicating a similar role for BMP-4 in proliferation and maintenance of multipotency in the developing neural crest. The positive regulation of several genes associated with ESCs, which are highly proliferative, is consistent with previous data. Proliferation and viability analyses showed BMP-4 treated cells to expand more rapidly in culture without concomitant alteration in viability (Figures 3.16 and 3.17). Altered cell cycle parameters (Figures 3.18 and 3.19) further supported the role of BMP-4 in regulating proliferation and multipotency through upregulation of ESC related genes.

The SMAD family of proteins are responsive elements in the transforming growth factor β (TGF-β) signalling pathway in which BMP-4 comprises an essential role. The interaction of BMP with transmembrane receptors results in phosphorylation and nuclear localisation of SMAD complexes, which exert an effect on the

expression of a number of genes, influencing cellular development and proliferation responses. SMADs can act in both an inhibitory and stimulatory manner (Heldin *et al*, 1997; Wrighton *et al,* 2009). Microarray data revealed modest upregulation of *SMAD1* during neural crest differentiation (approximately 1.5-fold) and by BMP-4 exposure (Approximately 1.2-fold); however, pplr values were 0.75 and 0.86 respectively necessitating further analyses.

DAVID analysis indicated that cell adhesion related genes might be of importance during the differentiation of the neural crest. The role of adhesion molecules in neural crest induction is poorly understood but recent studies have indicated that they are essential for epithelial to mesenchymal transition, migration and contact inhibition of locomotion during migration prior to somatic differentiation (Moore *et al,* 2013; Alimperti and Andreadis, 2015). Expression levels of a number of adhesion molecules was assessed by RT-qPCR.

Neuroligins are associated with the formation of synaptic junctions; they associate with neurons and modulate cell adhesion in the developing nervous system. Adhesion between adjoining neurons offers an effective method of transmitting signals between cells, enabling the transmission of nerve impulses (Dean and Dresbach, 2006; Fabrinchy *et al.,* 2007). In induction culture conditions expression of neither *Neuroligin1* nor *3* was detected until midway through stage 2 and removal of BMP-4 supplementation prior to stage 3 resulted in significant upregulation of both. BMP-4 supplementation resulted in downregulation of *Neuroligin1* after 5 and 10 days although this was not statistically significant at 5 days and transient downregulation of *Neuroligin3* (Figures 4.13, 4.14, 4.18). These data are conversant with the role of BMP-4 as an inhibitor of neurulation, backing up earlier data

showing BMP-4 mediated repression of *Nestin* expression and concurrent with the downregulation of the neuronal specifier *Shh.*

The *Claudin* family of genes is associated with the formation of tight junctions, they help to regulate the structure of tissues by maintain cellular positions; in the neural crest repression of *Claudin1* is necessary to maintain a migrating population of cells. In adult tissue, loss of function of *Claudin1* is associated with the initiation of mammary tumours (Fishwick, *et al*, 2012; Di Cello *et al*, 2013). *Claudin23* is known to be differentially expressed in invasive and non-invasive pancreatic cancer cells (Wang *et al*, 2010). Downregulation of this gene is observed in more invasive cells, suggesting a role in the maintenance of cellular adhesion. Treatment in induction media resulted in gradual increases in gene expression and more marked increases upon removal of BMP-4 supplementation. BMP-4 was shown to repress expression of *Claudin1* but not *Claudin23*; in the case of the former, this may be indicative of a role for BMP-4 in the modulation of cellular adhesion and migration (Figures 4.11, 4.12, 4.18)

*POU4f2* expression was not altered during initial differentiation. Withdrawal of BMP-4 resulted in significant upregulation but this was only 2.34-fold above transcription levels expressed in embryonic stem cells. The repression of expression demonstrated by culture in BMP-4 supplemented media may be indicative of its anti-neurulation properties. *POU4f2* is associated with the development of neuron structures in the eye, the low levels of transcription may be indicative that cells were not differentiating into this lineage (Mao *et al*, 2008). *POU3f4* is similarly associated with sensory neuronal development, specifically in the inner ear where perturbations in expression result in sensorineural hearing loss (Lee *et al*., 2009). Significant and profound upregulation was observed after withdrawal of BMP-4 supplementation

with a 238-fold increase in expression recorded compared to embryonic stem cells. Expression in culture conditions with BMP-4 treatment was decreased compared to conditions without, in untreated cells expression peaked after 9 days in culture (5 days after initiation of differentiation) (Figures 4.15, 4.16, 4.18). The high levels of expression in of this gene may be indicative of a sensory neuronal lineage. The *Td12* gene has no reported links to neural crest differentiation, being associated with repression of transposons in germline development in the murine gonads. This role functions to prevent mutations during spermatogenesis (Pandey *et al.,* 2013). Other than this little is known about its function. The pronounced decrease in expression levels after four days differentiation may be indicative of a function during early stages of development. It is possible that culture with BMP-4 mitigates this downregulation; however, microarray data showed extremely low expression in the untreated sample – intensity was 0.002 compared to a mean of 768.49 for all probes. This may have affected the accuracy of the analyses, falsely amplifying any differences. RT-qPCR data confirmed upregulation with BMP-4 treatment but low levels of expression combined with inherent inaccuracies in microarray analyses exaggerated the extent (Figures 4.17 and 4.18). It is unlikely that *Td12* plays a role in neural crest development being repressed in opposition to the upregulation of neural crest markers such as Pax3 and Sox10.

# Chapter 5: Characterisation of Neural Crest Derived Peripheral Neurons Differentiated from Mouse Embryonic Stem Cells

## 5.1 Introduction

Differentiation of cells comprising the PNS has proven challenging. Early studies on ESCs plated on PA6 stromal demonstrated that the stromal cells induced differentiation into central nervous system lineages. Treatment with BMP-4 was shown to retard this lineage selection and give rise to neural crest derived tissues such as peripheral neurons and smooth muscle (Mizuseki *et al*, 2003). The use of feeder cells results in exposure of ESCs to a variety of secreted factors, any or all of which may contribute to cell fate determination. More recently, culture in serum-free conditions has been shown to generate neural crest derived cell types *in vitro*, however little information on the specific effects of important transcription factors in this process such as BMP-4 are currently available (Aihara *et al,* 2010). Functionality studies *in vivo* have focused on the successful grafting of induced tissue into rodent brain, however this process is delicate and time consuming in addition to being unavailable to some research groups (Zhang *et al*, 2013; Lavasani *et al*, 2014). *In vitro* analysis of the ability of cultured neurons to relay action potentials may be able to provide insights into mechanisms of differentiation and allow rapid and easily repeatable experiments into the effects of compounds such as neurotoxins or neurotransmitters. MEA chips have been used to determine the response of cultured rat cortical tissue to toxins by observing the change in electrophysiological activity. Computer software converts this activity into characteristic spikes that can be altered by the administration of various compounds (Scelfo *et al*, 2012). At present there is little information regarding the

electrophysical properties of differentiated neurons and their response to various chemical stimuli. Development of protocols for this may allow for rapid turnaround of experiments and support neuronal differentiation procedures as well as facilitating characterisation.

In the previous study protocols to induce terminally differentiated progeny from E14 mouse embryonic stem cells were developed. Differentiation was carried out in three distinct stages based on a modified version of the protocol developed by Aihara and co-workers (2010) (Sections 2.4, 2.5, Figure 2.1)

**5.2 Aims**

- Characterise differentiated cells as peripheral neurons by examining expression of neuronal marker genes
- Assess functionality of differentiated cells through MEA analysis
- Assess Efficacy of differentiation protocols using flow cytometry

## 5.3 Results

### 5.3.1 Expression of Neuronal Marker Genes was Different in Cells Cultured With and Without BMP-4 Treatment during Stage 2 of Differentiation

PCR analysis of cells cultured for 60 days in differentiation conditions revealed the expression of a number of neuronal associated markers. Cells cultured with and without BMP-4 treatment during stage two both expressed *Neuroligin1, Neuroligin3* and *Neurexin3*. These proteins are essential for the formation of functional synapses in maturing organisms and facilitate the formation of pre-synaptic and post-synaptic signalling complexes. (Krueger *et al*, 2012). Transcription of *Neuexin1* was not detected. Similar expression profiles for *TrkC* were observed in treated and untreated culture conditions while faint levels of *TrkA* were detected in the supplemented cells. *Runx1* and *Runx3* expression was not observed in non-supplemented cells and recorded in one of three populations of supplemented cells tested (Figure 5.1).

Cells were cultured and fixed as described in 2.11. Staining with phalloidin revealed different cytoskeletal structures (Figure 5.2). Peripherin was detected in the treated fraction with some evidence of distribution as a filamentous structure that was more readily observable under high power (400x magnification) (Figures 5.3 and 5.4). The untreated fraction showed sporadic, weak expression of *Peripherin* while both fractions were highly positive for *Neurexin3* (Figure 5.3). These data suggest that different fate selections occurred in cells cultured with and without BMP-4 treatment.

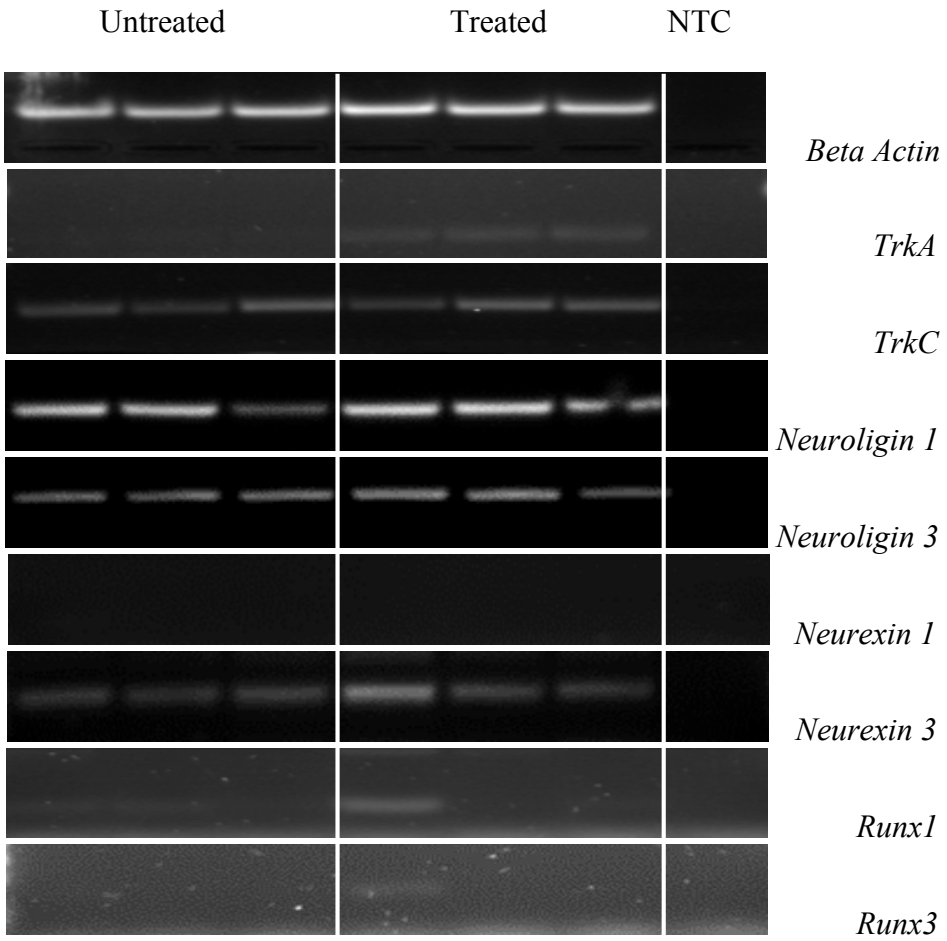


**Figure 5.1. Expression of neuronal biomarkers.** RNA from cells cultured for 60 days in induction media was extracted, reverse transcribed and analysed by PCR, compared to cells cultured in induction media without BMP-4 treatment during stage 2. Expression of synaptic genes *Neuroligin1, Neuroligin3* and *Neurexin3* was observed in all samples while *Neurexin1* was not detected. Altered expression of neurotrophin receptors (*TrkA* and *TrkC*) was observed. Expression of the transcription factors *Runx1* and *Runx3* was observed in one population of treated cells. cDNA was normalised to β-actin, which showed consistent expression. NTC = no template control.

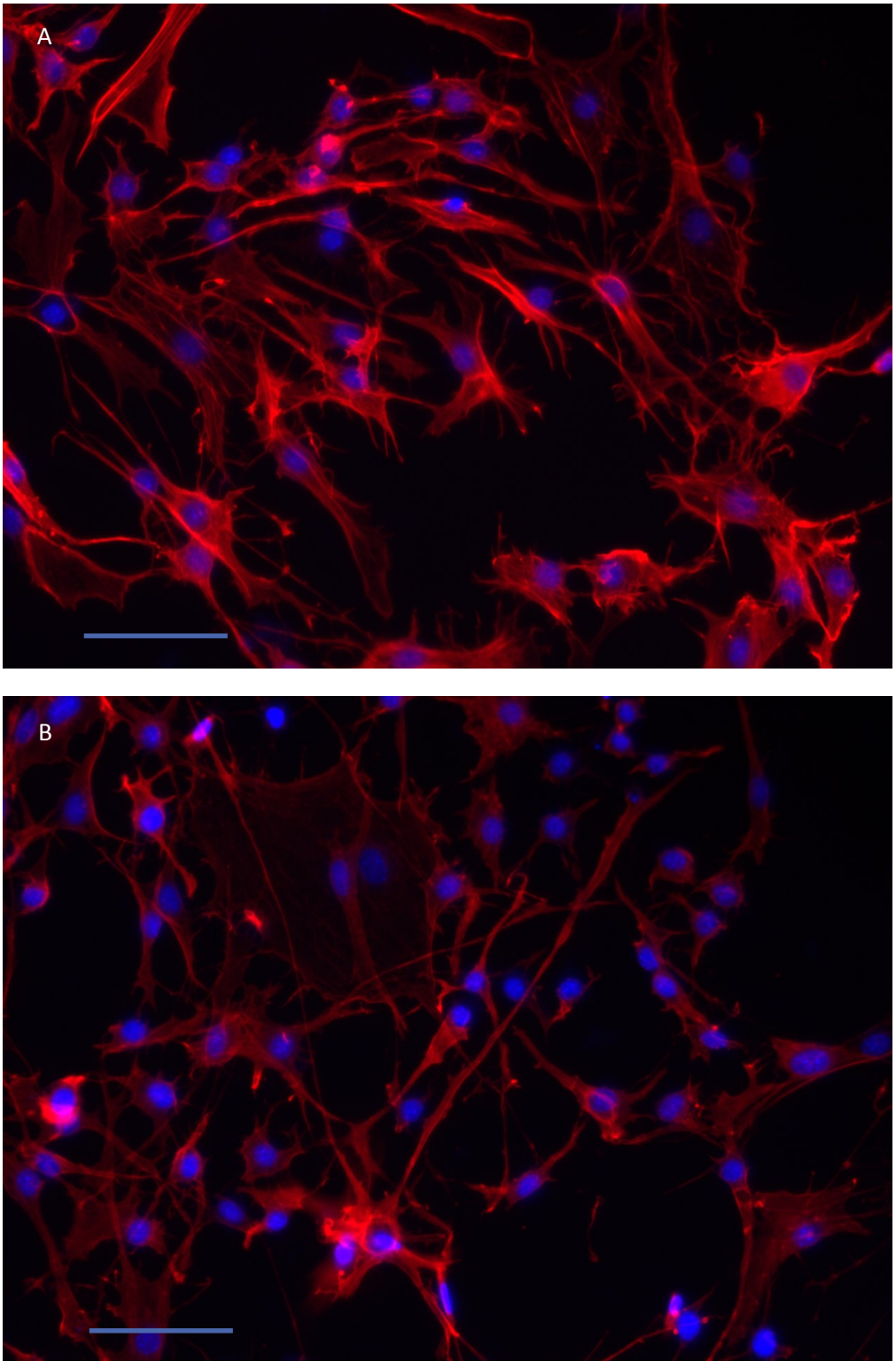


**Figure 5.2. Cytoskeletal structures of cells cultured for 60 days in differentiation conditions.** (A) BMP-4 treated (B) Untreated fraction. Phalloidin staining (red) was used to visualise F-actin filaments in the cytoplasm, nuclei were stained with DAPI (Blue). Scale bars = 100 µm.

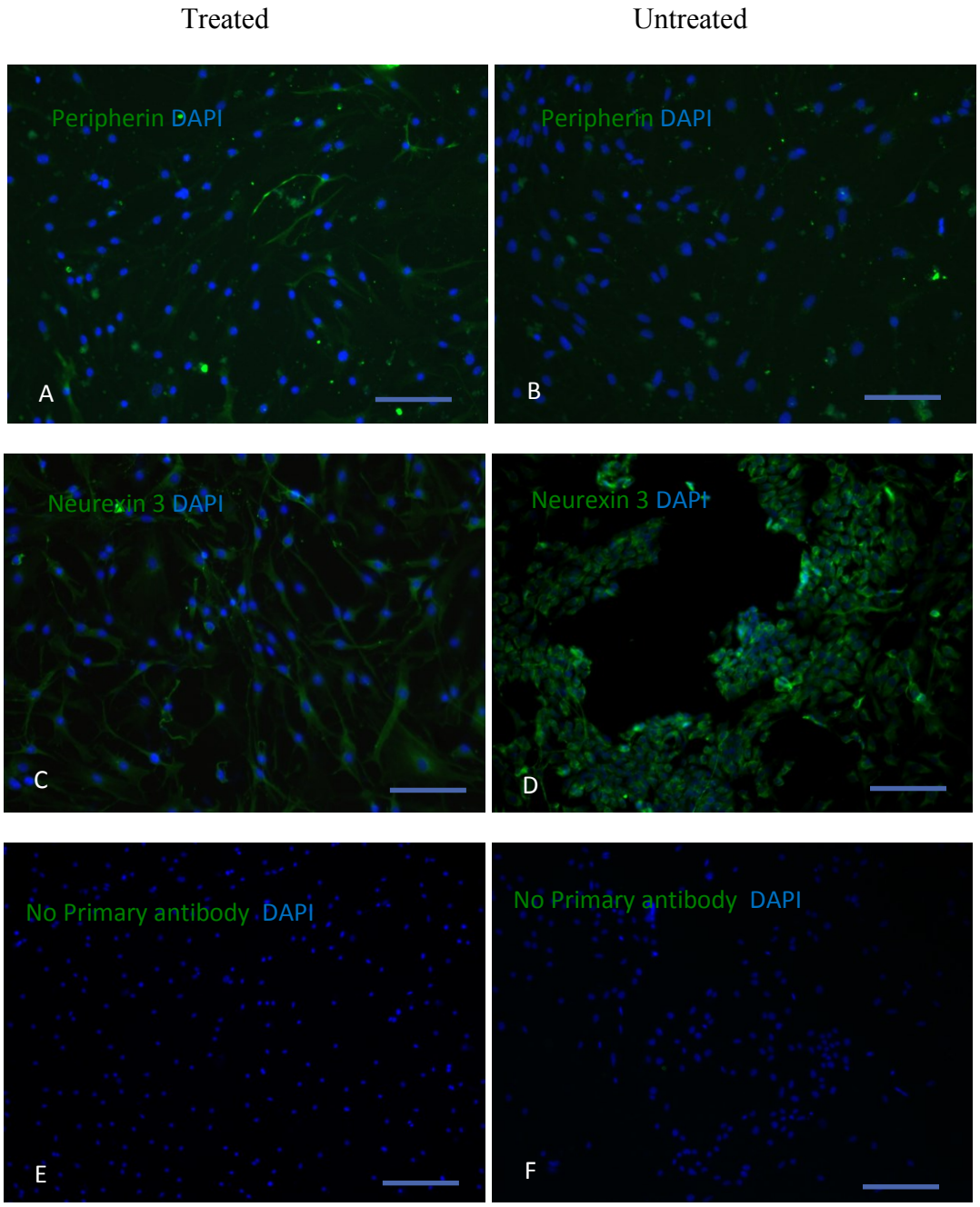


**Figure 5.3. Expression of neuronal markers in cultured cells.** Stage 3 cells were cultured for a total of 60 days. During stage 2 cells were cultured in either SIM (BMP-4 treated) or PIM (untreated). Both treated and untreated fractions expressed the peripheral neuronal marker peripherin (A and B - green) although staining in untreated cells was weak. Robust expression of the synaptic protein Neurexin 3 was detected in both samples (C and D - green). No primary antibody controls are shown in E and F. Nuclei in all samples were stained with DAPI (blue). Scale bars = 100 µm.

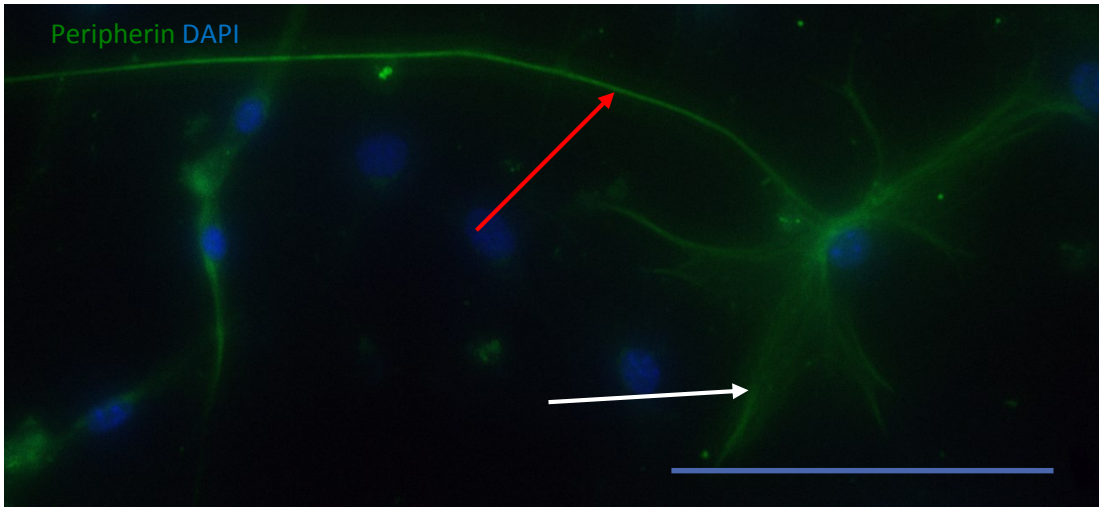


**Figure 5.4. Peripherin expression in differentiated cells**. Cells were cultured in induction media for 60 days with BMP-4 treatment during stage 2. Cells were immunopositive for peripherin (green) and displayed axonal (red arrow) and dendrite (white arrow) like structures**.** Nuclei were stained with DAPI (blue). Scale bar = 100 µm.

### 5.3.2 Peripherin Expression in BMP-4 Treated and Untreated Fractions

In order to determine gating for flow cytometry experiments the human neuroblastoma cell line sy-5y was used as a positive control. This cell line is known to express (Pederson *et al*, 1993). Unstained sy-5y cells were used as a negative control and the fluorescence threshold for *Peripherin* positive cells was set so that no more than 2% of unstained cells were in the right hand (positive) quadrant. Unstained and stained controls were measured as 1.36% positive (SEM 0.16) and 83.74% positive (SEM 0.83 respectively). BMP-4 positive and BMP-4 negative cells were analysed; higher intensity of staining was observed in the BMP-4 positive fraction (Figure 5.5 and 5.6). Cell Quest Pro was used to determine the percentage of *Peripherin* expressing cells. Significant variation was detected between the two samples with over 88% of BMP-4 treated cells presenting *Peripherin* epitopes compared to 52.2% in the untreated fraction (p-value o.oo5) (Figure 5.7).

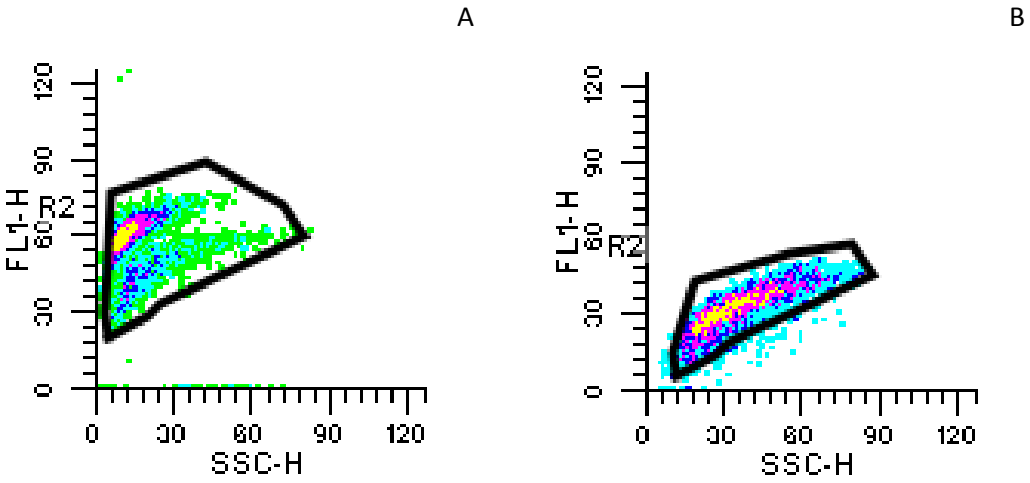


**Figure 5.5. BMP-4 supplementation increased peripherin expression.** Expression was measured by intensity of staining in the FITC channel (FL1-H). SSC-H measured granularity of cells, which was similar between samples. Cells were cultured with and without BMP-4 exposure during differentiation stage 2 before further culture for a total of 60 days. Treated cells (A) showed higher levels of expression than untreated cells (B).

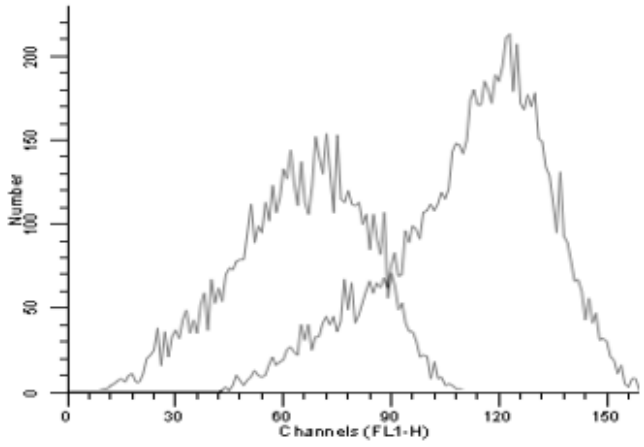


**Figure 5.6. Representative comparative histograms of *Peripherin* expression levels in cultured cells.** The treated fraction (right) showed higher intensity of staining than the untreated fraction (left).

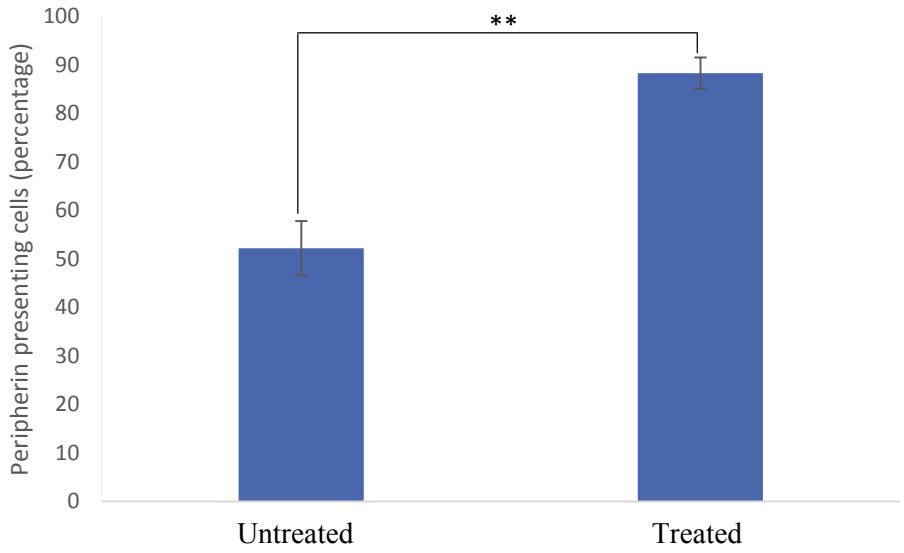


**Figure 5.7. *Peripherin* expression was significantly altered in culture with BMP-4 supplemented medium during differentiation of E14 mouse embryonic stem cells.** Cells were cultured for 60 days in induction media and the number of peripherin expressing cells compared. Cells cultured in BMP-4 supplemented media during stage 2 (treated) were compared to cells cultured in non-supplemented media (untreated). Data is mean ± SEM, n=3. ** denotes p-value less than 0.01.

### 5.3.3 Microelectrode Array Analysis of Cultured Cells

Cells after 60 days culture were observed to grow on MEA chips and form connections between electrodes (Figure 5.8). Preliminary data indicated that electrophysiological activity was occurring in cells cultured under both conditions. Both fractions displayed characteristic spikes with similar frequency but higher amplitude in untreated cells (Figure 5.9).

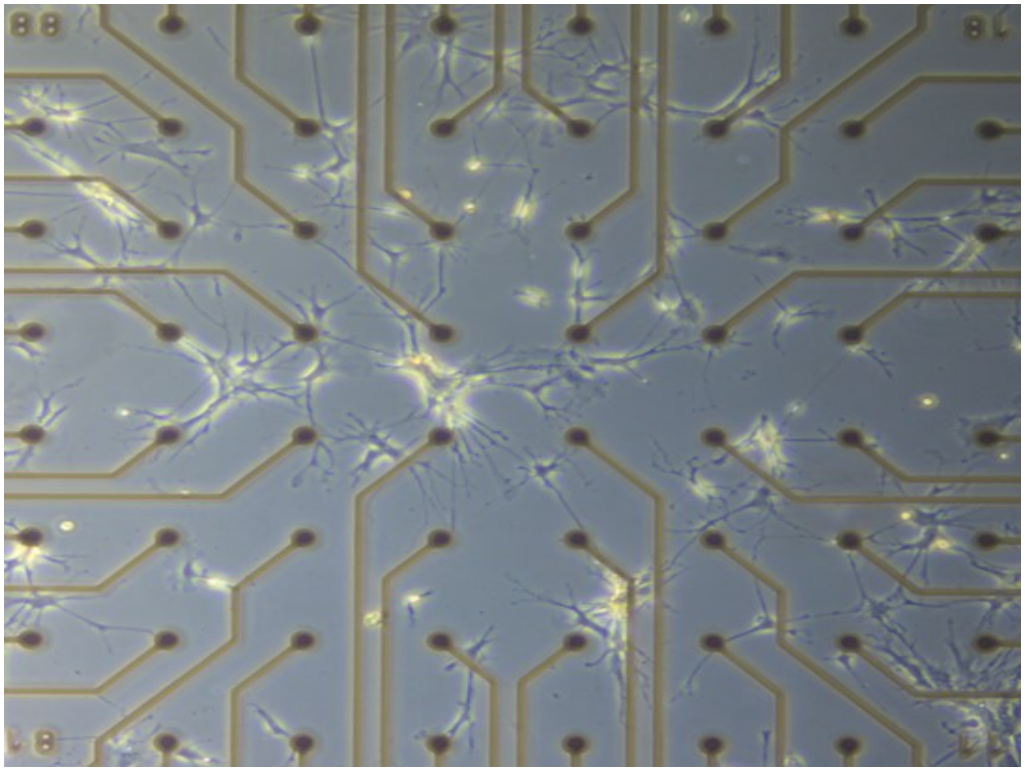

**Figure 5.8. Cultured cells on an MEA chip.** Differentiated cells were able to adhere and grow on MEA chips. Cells formed connections between electrodes in single and multiple cell relays. Magnification x120.

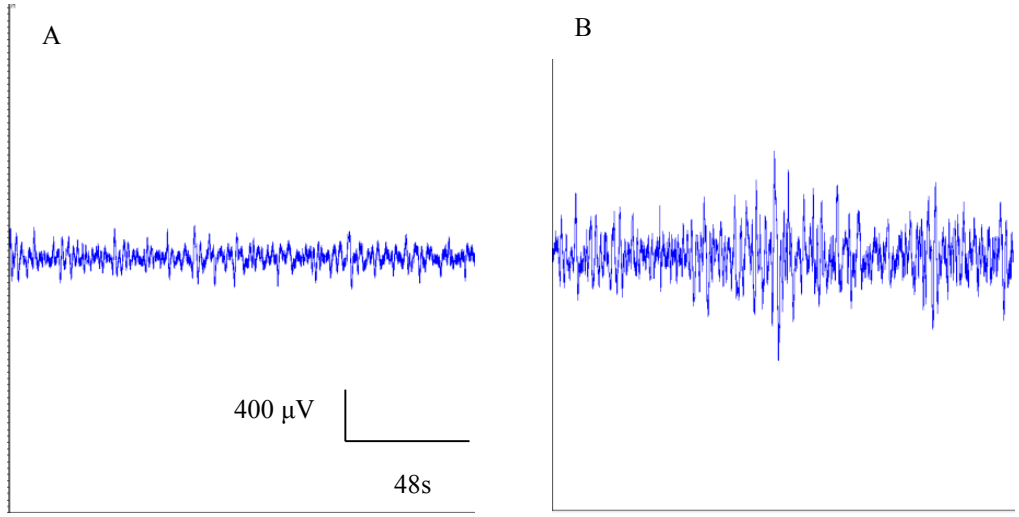


**Figure 5.9. Electrophysiological activity in cultured cells.** BMP-4 positive (A) and Negative (B) fractions displayed spontaneous electrophysiological activity with characteristic peaks. Both fractions were able to produce activity in the abence of stimulation.

### 5.3.4 The effects of NMDA and GABA on the Electrophysiological Activity of Cultured Cells

Treatment of cells with NMDA produced variable results. Addition of 20 µl 1.7 µM NMDA solution facilitated after a delay of approximately 1 minute in the BMP-4 treated fraction when added to cells previously not displaying spontaneous electrical activity. Cessation of these bursts occured immediately after the addition of GABA (Figure 5.10). Addition of the same volume to untreated cells resulted in no reaction in unresponsive cells (data not shown) and rapid decreases in both frequency and amplitude of traces after a delay of approximately 1 minute (Figure 5.10). No response to GABA was recorded in any of the untreated cells tested. Increasing the dosage of GABA to 400 µl at 1 mM also failed to ilicit a response (data not shown).

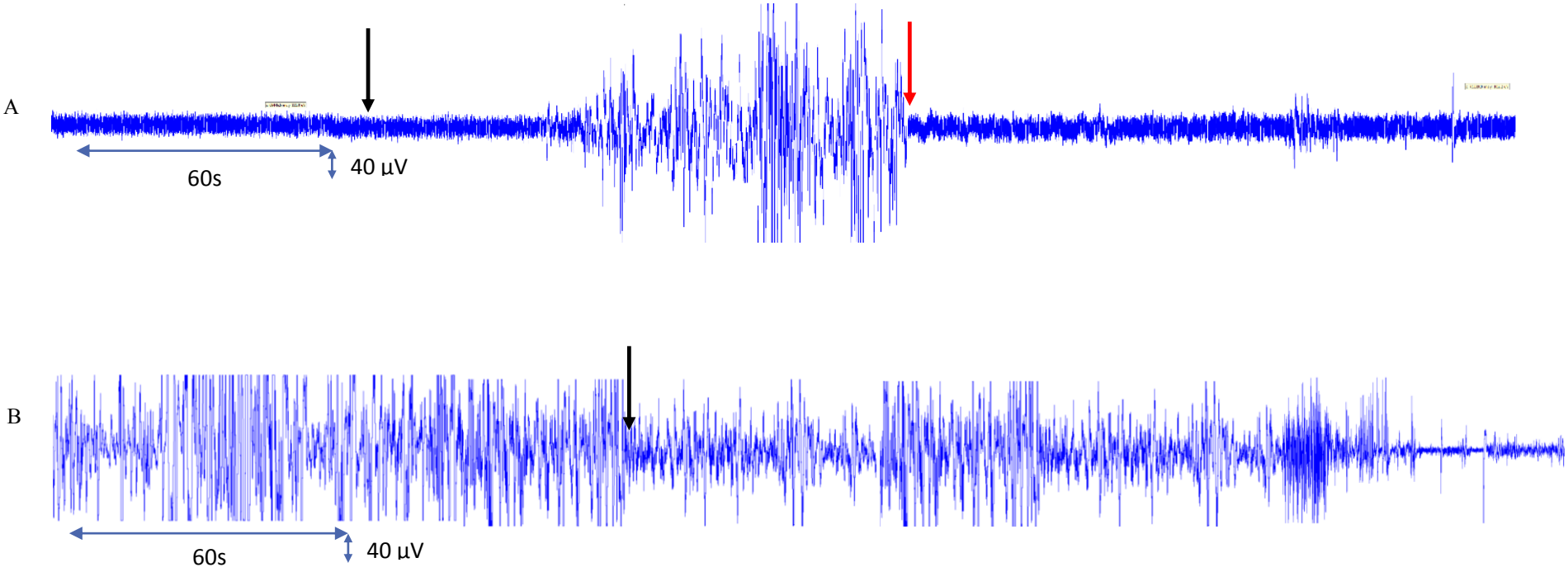


**Figure 5.10. Response of cultured cells to neuroactive compounds.** Treated cells (A) were responsive to NMDA and GABA. Non-responsive cells were stimulated with NMDA (black arrow) after approximately 1 minute electrophysiological activity was observed. The addition of GABA (red arrow) resulted in immediate reduction of spike frequency and amplitude. Untreated cells (B) showed reduction in amplitude and frequency of traces approximately 1 minute after the addition of NMDA.

## 5.4 Discussion

Neurexins and neuroligins interact across the synaptic cleft and enable the recruitment of structural molecules and receptors that are essential for the correct functioning of the nervous system. Neurexins and neuroligins form GABA and glutamatergic synapses *in vivo.* Both neuroligins 1 and 3 and neurexin3 were expressed in cells cultured with and without BMP-4 treatment during differentiation stage 2 but transcription of Neuexin1 was not detected in either (Figure 5.1). However, a large number of splice variants (more than 2000) have been identified deriving from these genes, which may obstruct accurate measurement, by PCR (Craig and Kang, 2007). Expression of *Neurexin3* was confirmed by immunocytochemistry with the majority of cells in both fractions positive for this protein (Figure 5.3). Transcription of these molecules and translation of *Neurexin3* may be suggestive of functional synapse formation for both culture conditions.

BMP-4 supplementation appeared to be necessary for the transcription of *TrkA* but not *TrkC* Figure 5.1). The presence of both transcripts in BMP-4 treated cultured cells is indicative of heterologous populations. These genes are expressed in large body and small body sensory neurons respectively within the PNS (Raible and Ungos, 2006). Testing for transcription of *TrkB* may further characterise neuronal types as this receptor is for the most part confined to CNS neurons whilst TrkA and C are found in both peripheral and central tissues (Nikoletopoulu *et al.,* 2010). All three *Trk* genes contribute to the numerous roles of neurons in both the central and peripheral nervous system during development and within mature animals. Each receptor has an extracellular domain, which forms complexes with specific ligands to initiate signalling cascades (Stoleru *et al.,* 2013). These ligands – the neurotrophins are secreted proteins, which promote neuronal survival as well as facilitating

synaptogenesis, axonal and dendritic expansion and the formation of ion channels although the exact mechanisms of their functions remain unclear (Huang and Reichardt, 2003; Scaper, 2012).

Expression of the Runt family of transcription factors was observed only in one population of cells cultured with BMP-4. Both *Runx1* and *Runx3* were expressed by this population (Figure 5.1). The runt-related family of transcription factors act to delineate proprioceptive and nociceptive peripheral neurons *in vivo*. *Runx1* is coupled with the expression of *TrkA* in large body sensory neurons while *Runx3* is associated with *TrkC* and small body sensory neurons. *Runx1 and 3* control the characteristics of the ion channel necessary for proprioception and nociception respectively. Expression patterns of both *Runx1* and *Runx3* is chiefly confined to post mitotic neurons, in the central and peripheral nervous systems in the case of the former and solely in the peripheral for the latter (Inoue *et al*, 2008; Bhatt *et al*, 2013). Cells at 60 days were able to proliferate on MEA chips indicating that mitotic populations were still extant.

Immunocytochemistry and flow cytometry data suggest that BMP-4 supplementation enhances expression of *Peripherin* in cultured cells. Cells not treated with BMP-4 were also shown to express peripherin albeit with weaker staining and fewer cells presenting the epitope (Figures 5.3 A and D, 5.5, 5.6 and 5.7). Functional redundancy of BMP molecules has been observed in skeletal development (Bandyopadhyay *et al*, 2006) and *Peripherin* is not solely confined to the PNS (Ko *et al*, 2005). Nonetheless, the high levels of cells presenting *Peripherin* alongside transcripts of *Neurexin3, Neuroligins1 and 3* and *TrkA* and *C* is indicative of a peripheral neuron lineage in the BMP-4 treated fraction. *Peripherin* filaments in

these cells were further observed to form axon and dendrite-like structures (Figures 5.1-5.4).

Cells were capable of spontaneous generation of electrophysiological activity pointing towards the generation of functional neurons. Preliminary experiments showed that differentiated cells were sensitive to NMDA albeit with different responses; stimulatory in the BMP-4 treated fraction and inhibitory in the untreated fraction (Figures 5.10 and 5.11). NMDA has been shown to be deleterious to neurons through the mechanism of excitotoxicity. Overexposure to NMDA can severely limit cell function and ultimately induce cell death (Li *et al*, 2012). It is likely that the BMP-4 negative cells, which saw cessation of electrophysiological activity after the application of NMDA, were damaged through this mechanism rather than by NMDA acting in an outright inhibitory manner (Section 5.3.4). NMDA receptors function by opening ion channels within the neuron, stimulating the passage of action potentials. NMDA receptors are more numerous in the central nervous system than the peripheral, suggesting untreated cells may be of a central phenotype whilst BMP-4 treated cells may be of a peripheral (Blanke and VanDongen, 2009). GABA is one of the most well known synaptic inhibitors, affecting a wide variety of neurons. GABA receptors are known to complex with Neurexins, as are NMDA receptors (Magnaghi *et al*, 2006; Zhang, *et al*, 2010). The presence of Neurexins as well as responses to both NMDA and GABA in BMP-4 treated cells coupled with the high number of *Peripherin* presenting cells strongly suggests that differentiation resulted in populations of peripheral neurons. The presence of proprioceptive and nociceptive markers may indicate heterologous populations but individual cell types may be able to be isolated through mechanisms such as magnetic activated cell sorting or fluorescence activated cell sorting.

Peripheral neuron differentiation through the neural crest is induced by activation of the SMAD pathway (Kreitzer *et al*, 2013). BMP-4 is known to activate SMAD1 although BMP-2 and BMP-7 can also exert a similar effect. The TGF-β signalling pathway through which BMP activation of SMAD1 results in phosphorylation of several serine residues on the protein and causes nuclear localisation (Heldin *et al*, 1997; Fei *et al*, 2010). Transcriptional analysis, Western blotting and immunocytochemistry targeting phosphorylated SMAD residues may offer greater insights into whether or not BMP-4 is required for SMAD-mediated neurulaution.

# Chapter 6: Proteomic Analyses and Noggin Inhibition of BMP-4 in the Differentiation of E14 Mouse Embryonic Stem Cells

## 6.1 Introduction

### 6.1.1 Proteomic Analysis of Target Gene Expression

Microarray and RT-qPCR analysis indicated that expression levels of number of pluripotency-associated genes were comparable in cells cultured in SIM or PIM after 1 hour and 5 days of differentiation stage 2. However after 10 days of stage 2 (14 days total culture) differential expression was observed with all genes being significantly upregulated in cells cultured in SIM compared to those cultured in PIM (Figure 3.20, Figure 4.9 ). Initial declines in expression of these genes in differentiating cells was reversed between days 5 and 10 in cells cultured in SIM (Figure 3.11, Figures 4.4-4.8). These data indicate a potential role for BMP-4 in regulating expression of pluripotency-associated genes during neural crest development. Selected factors identified previously were subject to proteomic analysis via Western blot (Sections 2.13-2.15) and flow cytometry (Section 2.19) to determine whether transcriptional regulation was reflected in the translational landscape.

BMP-4 is known to contribute through the maintenance of pluripotency of embryonic stem cells in concert with LIF through activation of *Cochlin* expression (Zhang *et al*., 2013). Immunocytochemistry, flow cytometry and MEA experiments demonstrated that BMP-4 treatment altered lineage outcome of differentiating cells.

BMP signalling through SMAD is an intrinsic factor to a wide variety of cellular functions (Retting *et al*, 2009; Fei *et al*, 2010; Feng *et al*, 2014). Within the nervous system SMAD signalling is involved in the development in both peripheral and central nervous system neurons and is essential for the formation of the neural crest (Hegarty *et al*, 2013). Induced cells of neural crest lineage are derived through activation of the SMAD pathway in the human system (Kreitzer *et al*, 2013).

In order to determine whether BMP-4 signalling was upregulating pluripotency associated markers through induction of Cochlin Western blotting was used to compare Cochlin protein expression after stage 2 in cells that had been treated in treated and untreated cells. Expression of SMAD1, a factor in the transforming growth factor β pathway mediated by BMP-4 was investigated through Rt-qPCR and Western blotting.

### 6.1.2 Noggin Inhibition of BMP-4

BMP signalling is indispensable in the correct formation of ectoderm-derived tissues. Correct patterning of the neural crest as well as the neural and non-neural ectoderm is dependent on BMP-4 exposure in varying amounts. The selective antagonism of BMP-4 by Noggin is one mechanism of control exercised in developing vertebrates. Noggin binds to BMP-4 and prevents complex formation with its receptors (McMahon, *et al.*, 1998). During early organogenesis a balance between Noggin and BMP-4 expression is vital; ablation of Noggin is embryonic lethal in murine systems and phenotypically manifest in the form of axial skeletal deformation (Wijgerde *et al*, 2005). Patterning of the nascent neural tube is dependent on Noggin-mediated inhibition of BMP signalling. Exposure of the neural plate of murine embryos *to Noggin* induced the formation of dorsolateral hinge

points, which facilitate the closure of the neural tube *in vitro*. These morphological effects were concurrent with a reduction in phospho-*SMAD1/5/8*, expression. The SMAD proteins are downstream targets of the BMP mediated transforming growth factor signalling pathway, abrogation of their expression is indicative of the inhibitory role of Noggin (Ybot-Gonzalez, 2007). Exposure to Noggin to promotes expression of *Shh* and other genes associated with central nervous system development in the generation of seratogenic neurons *in vitro* (Shimada *et al*, 2012). Previous experiments (Sections 5.3.1 and 5.3.2) determined that culture with BMP-4 induced lineage selection to peripheral neurons and that pluripotency-associated factors and neural crest markers were upregulated between the middle and end of stage 2 of differentiation and this upregulation was mediated by BMP-4 (Figures 3.12-3.15, Figures 3.21-3.24, Figure 4.4-4.9). In order to further elucidate the effect of BMP-4 on these factors cells were incubated in the presence of Noggin (Section 2.18).

## 6.2. Aims

- Carry out flow cytometry analysis to ascertain whether transcriptional upregulation of pluripotency factors observed between days 5 and 10 of differentiation stage 2 results in increased levels of protein expression.
- Confirm of the role of BMP-4 in mediating expression levels of pluripotency and adhesion molecules by examining protein expression through Western blot analysis.
- Examination of mRNA expression levels of pluripotency and neural crest biomarkers by RT-qPCR following Noggin inhibition of BMP-4 signalling during stage 2 of differentiation.

## 6.3 Results

### Expression of Pluripotency Factors during Stage 2 of Differentiation

Flow cytometry was performed as in section (2.19) for the pluripotency markers Oct-4, Nanog and Dppa5. Embryonic stem cells were used to define gates, which were assigned so that fewer than 2% of ESCs that were incubated with secondary antibody without exposure to primary were counted positive. Gene expression was measured at 2, 5 and 10 days during stage 2 of differentiation. Oct-4 expression was low during the earlier stages but was shown to increase at 10 days as marked by increasing intensity of signal in the FITC channel. In contrast, Dppa5 expression remained more stable throughout stage 2 although lower intensity of FITC staining was observed after 5 days, suggesting fewer Dppa-5 expressing cells. Expression of Nanog remained stable with a small decrease between days 2 and 5, which was reversed between days 5 and 10 (Figures 6.1-6.3).

Numbers of cells presenting the above markers were calculated relative to cells at 2 days of stage 2. The number of Oct-4 expressing cells increased sequentially with a 1.8-fold increase (p value 0.16) between days 2 and 5 and a 15.8-fold increase between days 5 and 10 (p-value 0.02). Dppa5 expression at first declined (3.3-fold decrease, p-value $7 \times 10^{-5}$) and then increased (1.84-fold compared to 2 days, 6.1-fold compared to 5) significantly (p-value $2 \times 10^{-5}$ compared to 2 days) at 10 days. Nanog presenting cell numbers did not significantly alter during stage 2. A 2.1-fold reduction (p-value 0.06) between 2 and 5 days was followed by a 1.9-fold rise in the number of cells positive for Nanog expression (p-value 0.7) (Figs 6.1-6.3).

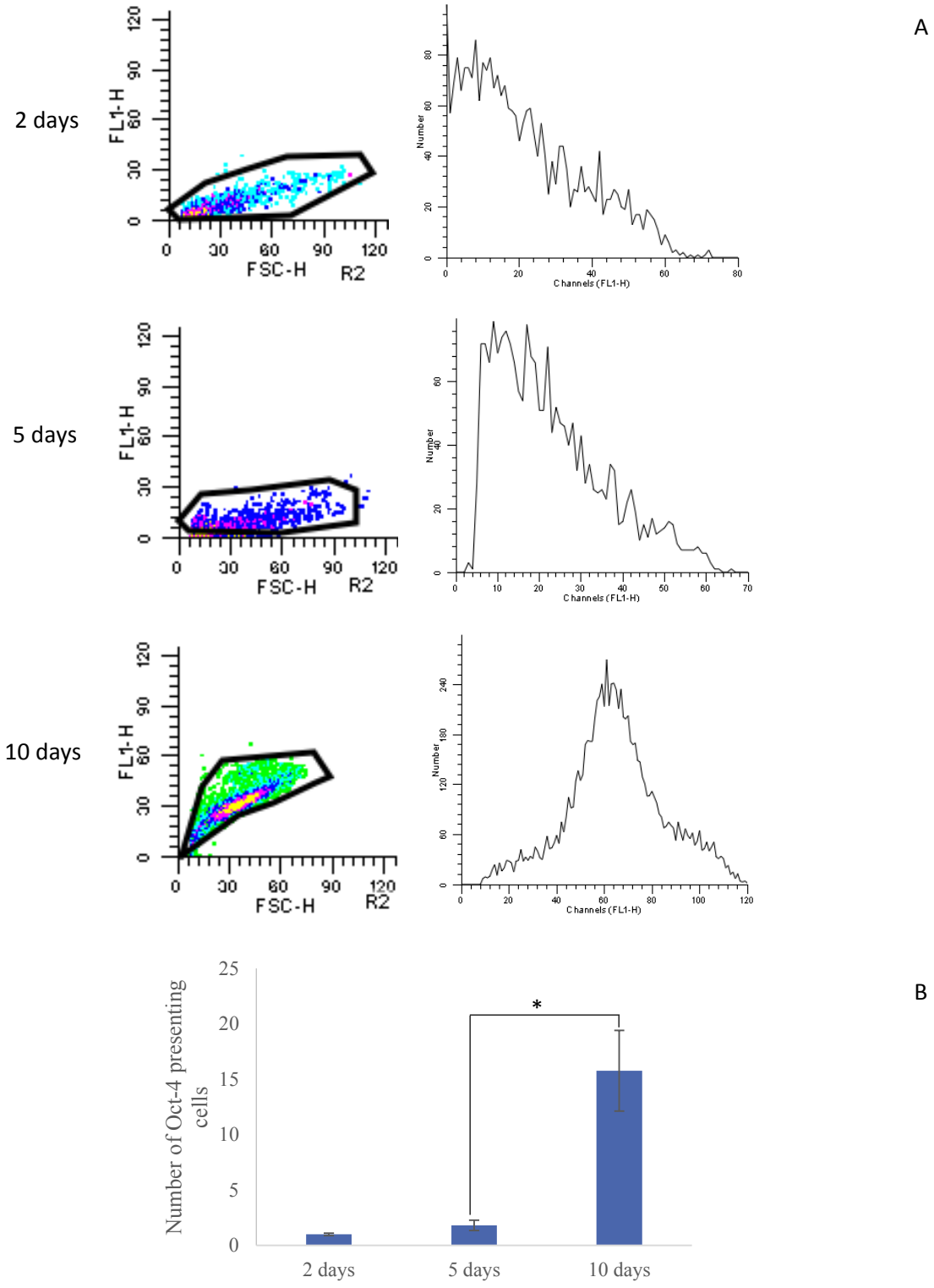


**Figure 6.1. Oct-4 expression increased during stage 2 of differentiation of mouse embryonic stem cells.** (A) Expression was measured by intensity of FITC staining in the FL-1channel, FSC-H measured size of cells. Relative number of Oct-4 presenting cells compared to 2 days (=1). Data are mean ± SEM, n =3. * denotes p value < 0.05.

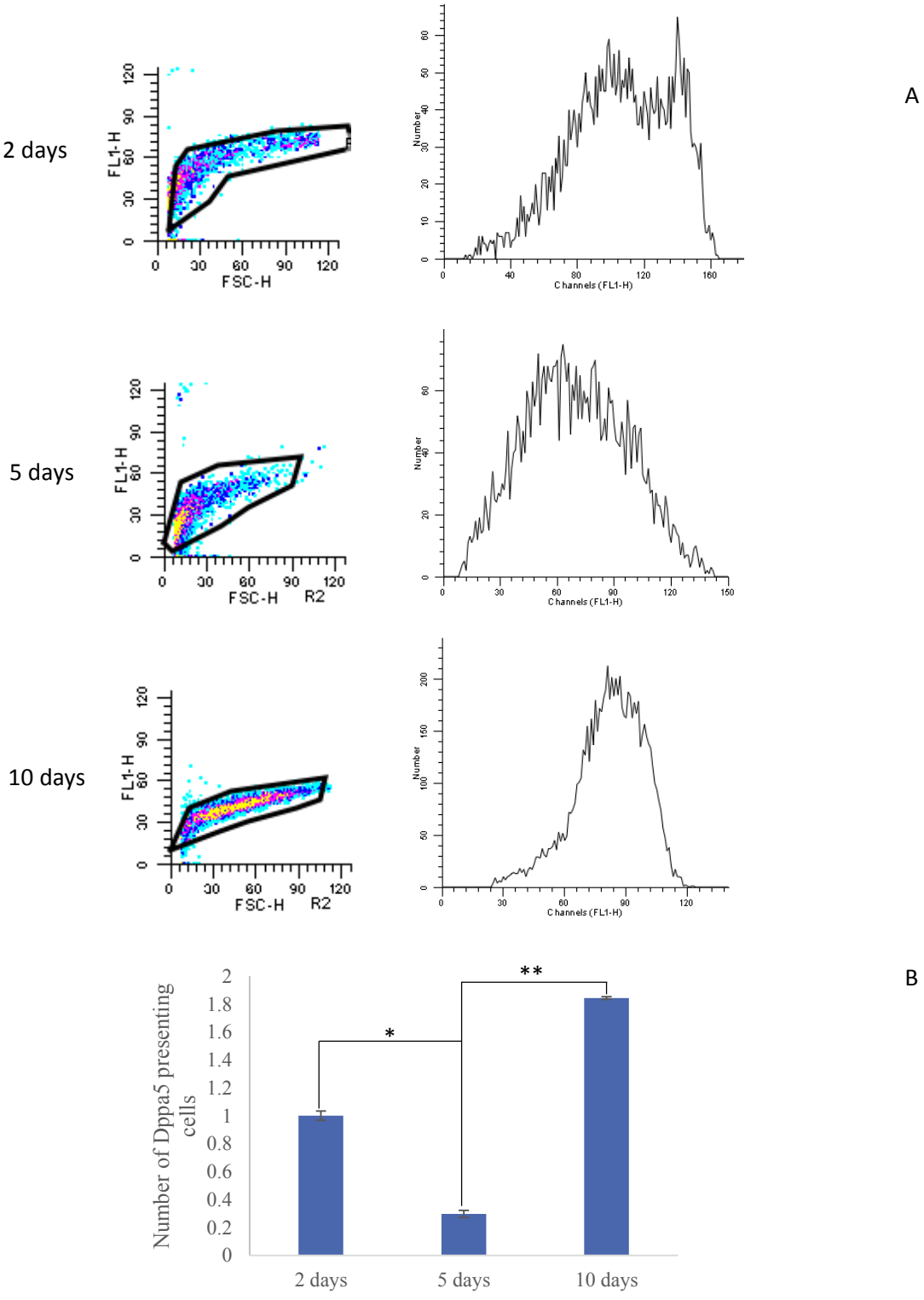


**Figure 6.2. Dppa5 expression during stage 2 of differentiation of mouse embryonic stem cells.** (A) Expression decreased between 2 and 5 days increased between 5 and 10 days as measured by intensity of FITC staining in the FL-1 channel. FSC-H measured size of cells. (B) Number of cells expressing Dppa5 relative to 2 days (=1). Data are mean ± SEM, n =3. ** denotes p value < 0.01.

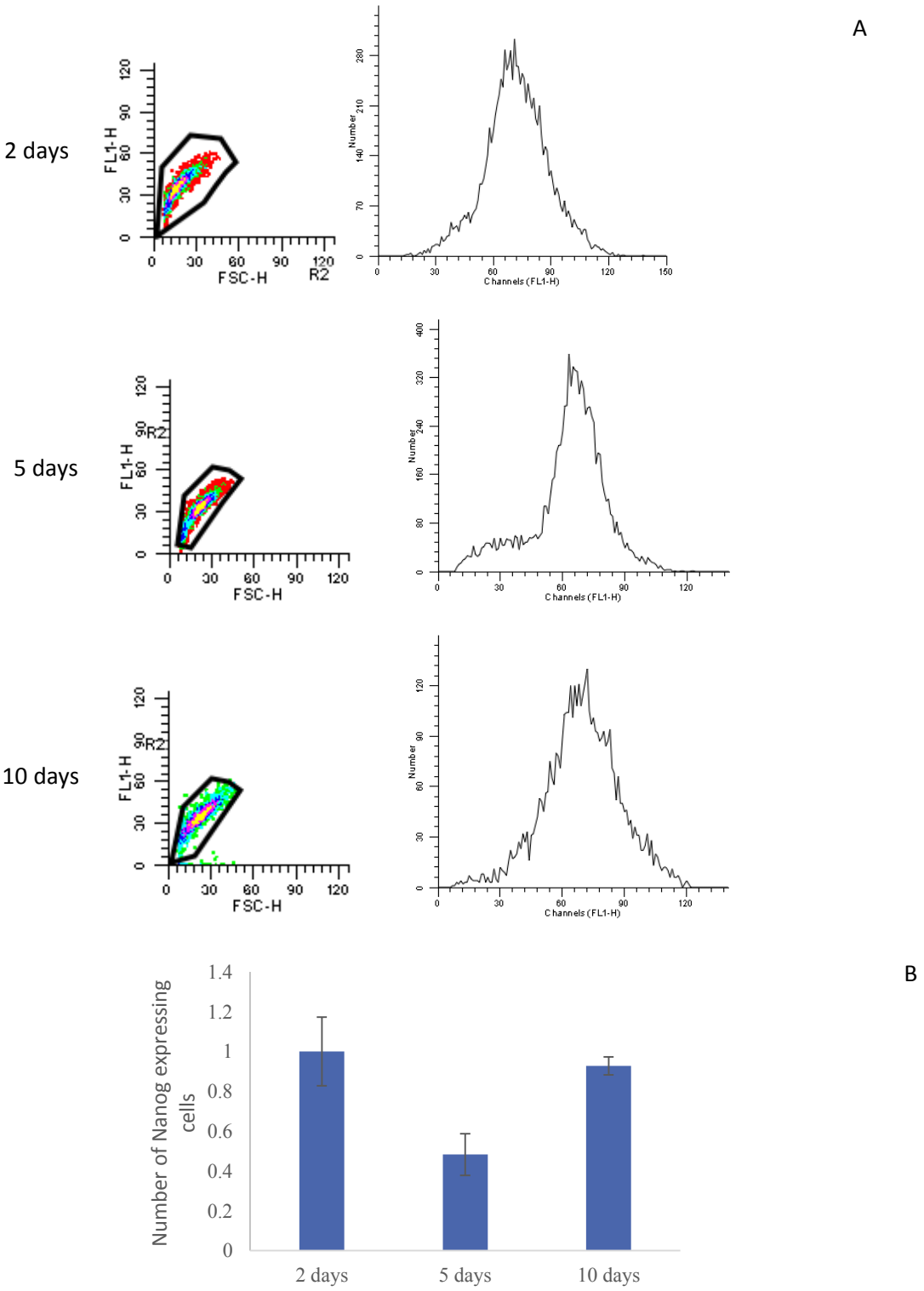


**Figure 6.3. Nanog expression during stage 2 of differentiation of mouse embryonic stem cells.** (A) Little change was observed over the period of differentiation as observed by consistent signals in the FL1-H channel. Cell size was measured by FSC-H. (B) Number of cells expressing Nanog relative to 2 days (=1). Data are mean ± SEM, n =3.

### 6.3.2 The effects of BMP-4 Supplementation on Transcription of SMAD-1

Expression levels were measured to determine whether BMP-4 mediated SMAD signalling was occurring during differentiation into peripheral neurons. RT-qPCR was carried out as in section 4.3.4 (Table 4.6). No significant difference was observed in expression between stage 0 and 1 cells (p-value 0.7). A 3.02-fold increase was noted between stage 1 and mid stage 2 cells. Between the mid-point and end of stage to expression declined slightly (1.25-fold reduction p-value 0.2) and another slight decrease (1.16-fold reduction, p-value = 0.6) was observed between stages 2 and 3 (Figure 6.4).

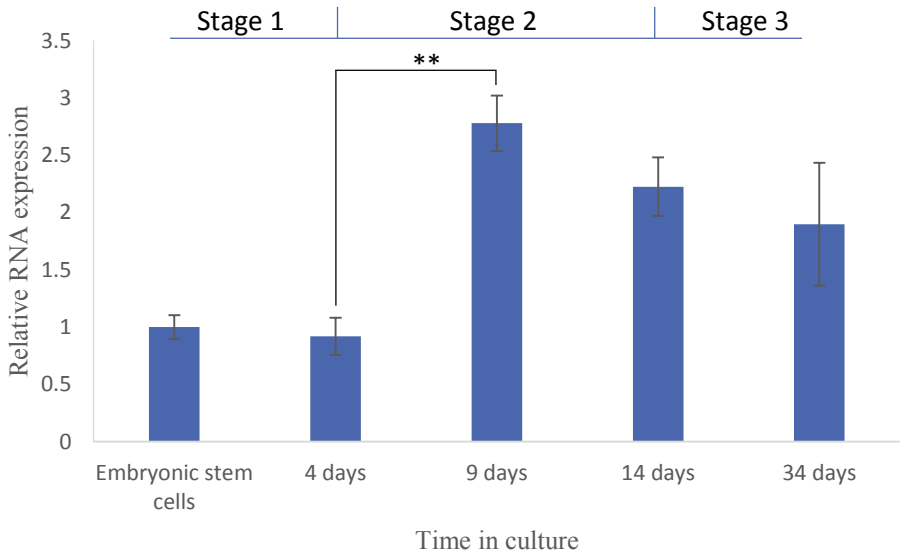


**Figure 6.4. SMAD-1 expression in differentiating E14 mouse embryonic stem cells.** Cells were cultured in PIM during stage 1, SIM during stage 2 and PIM during stage 3. Culture of Embryonic stem cells in PIM for four days did not alter expression of SMAD-1. The addition of BMP-4 at four days resulted in upregulation after a further 5 days culture (9 days total) after which expression remained elevated. Data is mean ± SEM, n = 3. All values were compared to embryonic stem cells (value = 1) and normalised to β-actin and 18s ribosomal RNA. ** denotes p value < 0.01.

As expression remained unchanged during stage 1 and increased at stage 2, it was hypothesised that BMP-4 signalling was mediating SMAD-1 expression during differentiation RT-qPCR was carried out as in section 3.3.6 on stage 2 differentiating cells. No significant difference in expression was observed after 1 hour, 5 days or 10 days (p-values 0.4, 0.4 and 0.3 respectively). Expression profiles in both samples remained similar with peak expression at 5 days (Figure 6.5).

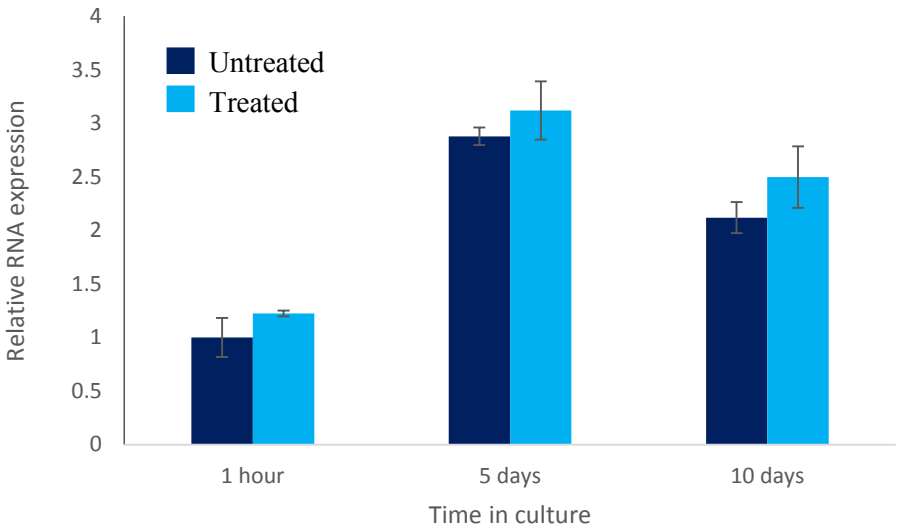


**Figure 6.5. BMP-4 supplementation did not alter expression of SMAD-1 during stage 2 of differentiation.** Data is mean ± SEM, n = 3. All values were compared to the 1 hour untreated sample (value = 1) and normalised to β-actin and 18s ribosomal RNA.

BMP-4 signalling causes phosphorylation of *SMAD1* at specific serine residues (187, 195, 206 and 214). As PCR is unable to distinguish differentially phosphorylated proteins an antibody specific to SMAD1 phosphorylated at S187 was used for Western blotting.

### 6.3.3 Western Blot Analysis of Pluripotency and Adhesion Molecules during Differentiation Stage 2

In all extracted protein samples, observed Oct-4 expression was higher in cells cultured with BMP-4 supplementation during stage 2. Dppa5 expression was also increased albeit to a lesser extent these data were concurrent with data from RT-qPCR analyses. No differences could be determined in Neurexin expression between BMP-4 treated and untreated samples. Similarly, expression of SMAD1 phosphorylated at S187 was detected in both cases although blots were faint in both samples. Expression levels of the housekeeping genes α-tubulin and β-actin was consistent between samples (Figure 6.6). Expression of Cochlin and Nanog were not detected by Western blot in either sample (data not shown).

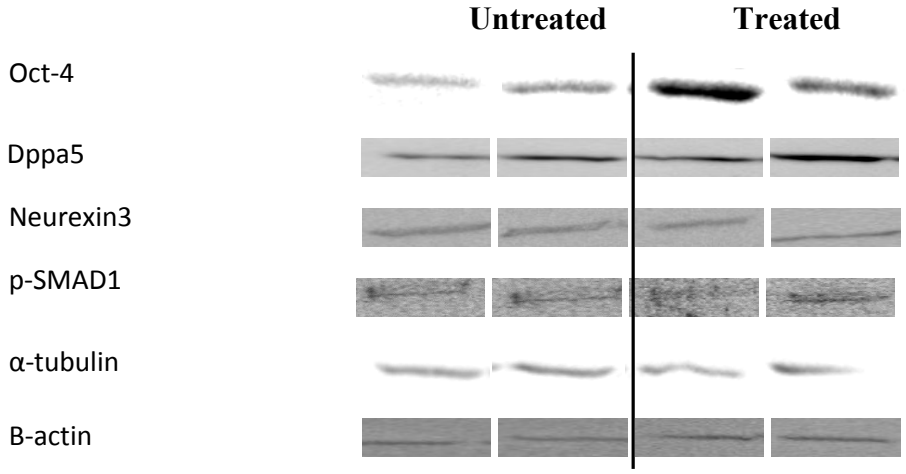


**Figure 6.6. Representative Western blots of putative BMP-4 targets during stage 2 of differentiation.** BMP-4 supplementation upregulated Oct-4 and Dppa5 but did not alter expression of Neurexin3 or p-SMAD1 (serine 187). Representative blots for cells cultured in PIM (untreated) and SIM (treated) during differentiation stage 2.

### 6.3.4 Inhibition of BMP-4 Signalling by Noggin

The effect of Noggin supplementation of SIM on expression of pluripotency and neural crest markers in treated cells was measured as in section 2.18. After culture with inhibition for 10 days three of the six pluripotency genes tested (*Oct-4*, *Dppa2* and *Dppa4*) showed increases in expression compared to cells cultured in SIM. These changes were not statistically significant (p values 0.80, 0.62 and 0.13 respectively). Changes in expression levels were slight, with the highest being a 1.15-fold increase in the case of *Dppa4*. *Dppa5* expression decreased 1.09-fold (p-value 0.6) while significant reduction in expression was observed for *Nanog* (1.29-fold, p-value 0.008) and *Dppa3* (2.3-fold, p-value 0.03). IM cultured cells showed increased expression of the pluripotency factors *Oct-4, Nanog, Dppa2, Dppa4 and* Dppa5 but not *Dppa3* when compared to cells cultured in PIM (untreated cells) during stage 2. Expression of *Dppa3* in 10 day inhibited cells was increased 1.4-fold (p-value 0.5). Fold change in expression levels varied from 310-fold upregulation (*Dppa5,* p-value 0.002) to 3.4-fold upregulation (*Nanog* p-value 0.001) for the other tested genes. Significant changes in expression levels were seen after inhibition for all three tested neural crest marker genes. *Pax3* was downregulated (3.13-fold, p-value 0.0001) in inhibited cells compared to non-inhibited (treated) cells. Expression was consistent with that in untreated cells (1.22-fold increase in expression, p-value 0.26). In comparison with treated cells *Sox9* and *Nestin* expression was downregulated to a similar degree (1.84-fold, p-value 001 and 1.86-fold, p-value 0.007 respectively) compared to inhibited cells. However, expression levels were not consistent with those in untreated cells. *Sox-9* expression was reduced 3.1-fold (p-value, 0.02) while *Nestin* was downregulated 3.2-fold (p-value $7 \times 10^{-5}$).

Culture in inhibition conditions after 5 days culture in treated cells during stage 2 produced similar results for *Dppa2, Dppa3* and *Dppa5*. Expression of *Dppa2* after 5 days inhibition was increased compared to 10 days (1.33-fold upregulation compared to treated cells as opposed to 1.04) but this increase was not statistically significant (p-value 0.2). Expression was significantly higher than in untreated cells (5.54-fold upregulation, p value 0.004). Inhibition at 5 days of stage 2 did not alter *Dppa3* expression compared to inhibition for the full 10 days – a 2.2-fold reduction was observed, this was deemed statistically significant (p-value 0.02). Compared to untreated cells expression levels were similar, a 1.5-fold increase was observed but this was not significant (p-value 0.4). Expression profiles of *Dppa5* were similar after inhibition for the full 10 days or between days 5 and 10 of stage 2. No significant difference was detected between cells cultured in IM between days 5 and 10 and treated cells (1.22-fold reduction in expression, p-value 0.1). Compared to untreated cells *Dppa5* expression was profoundly upregulated (273-fold, p-value 0.0002) in 5 day inhibited cells, similar values to those obtained after inhibition for 10 days. In contrast, *Dppa4* expression was significantly upregulated in cells treated with Noggin after 5 days. Expression was 3.58-fold that of uninhibited cells and 32.50-fold higher than in non-supplemented cells (p-values were 0.08 and 0.03 respectively). Expression of *Oct-4* and *Nanog* was increased by Noggin inhibition after 5 days. *Nanog* expression was 2.77-fold (p-value 0.01) that of non-inhibited cells and 12-fold (p-value 0.004) that of non-supplemented cells. *Oct-4* expression was upregulated 7.55-fold compared to non-inhibited cells and 27.96-fold compared to non-supplemented cells (p-values were 0.0009 and 0.0006 respectively).

Neural crest marker transcription was differentially affected by inhibition at the mid-point of stage 2. *Pax3* expression was reduced significantly with an 18.87-fold (p-

value 4 x $10^{-6}$) and a 4.91-fold (p value 0.0004) decrease observed compared with non-inhibited and non-supplemented cells respectively. *Sox9* expression was similarly reduced – 6.66-fold (p-value 0.0001) when compared to non-inhibited cells and 11.07-fold (p-value0.007) compared to non-supplemented cells. Inhibition after 5 days had less effect on the expression of *Nestin.* Reductions were observed compared to both non-inhibited and non-supplemented cells but these changes were 1.47-fold (p-value 0.04) and 2.5-fold (p-value 0.0004) respectively, in both cases less profound than after 10 days inhibition (Figures 6.7 and 6.8).

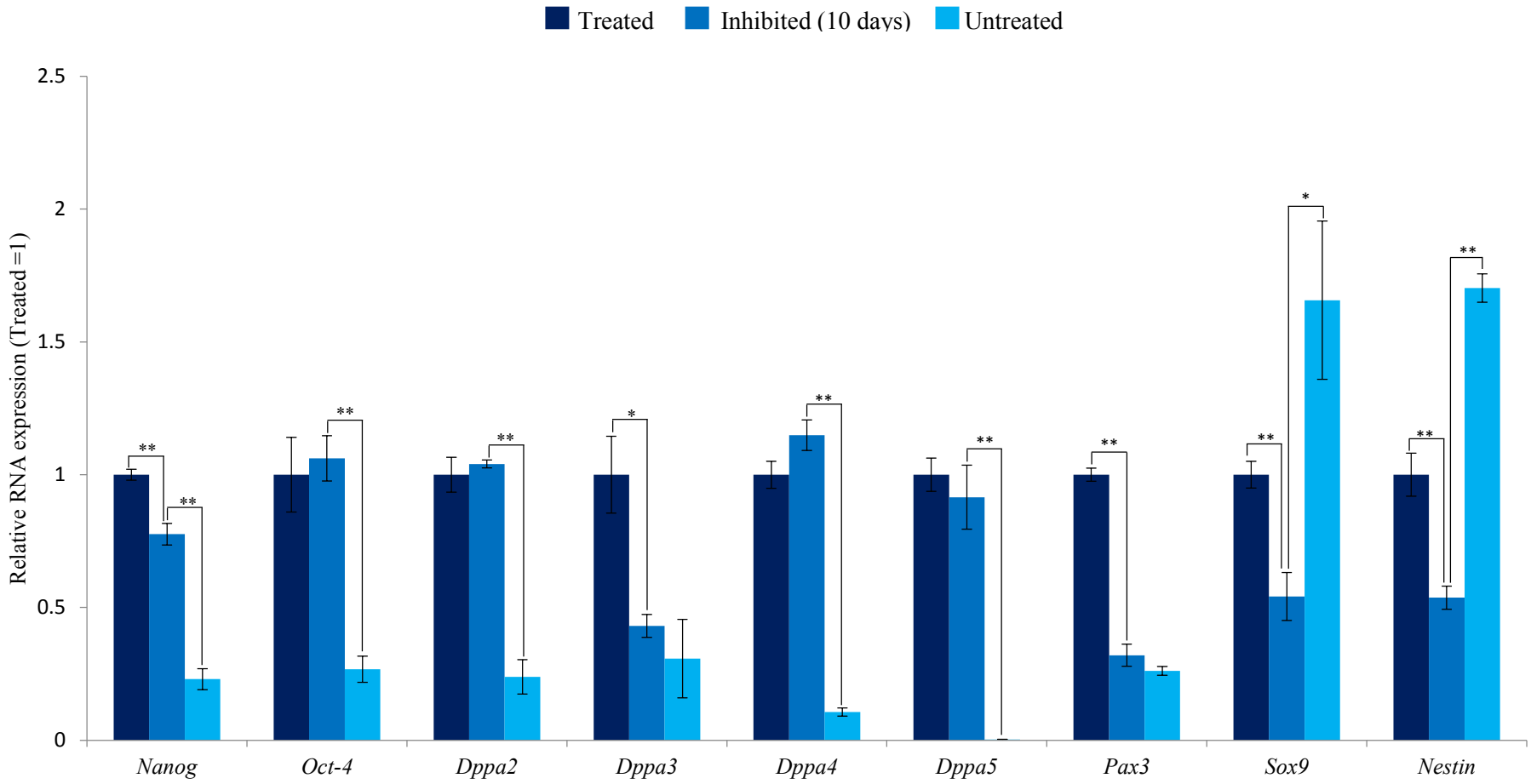


**Figure 6.7. The expression of pluripotency and NC marker genes following the inhibition of BMP-4 by Noggin for 10 days**. Gene expression was measured in cells cultured in IM during stage 2 of differentiation (Inhibited (10 days)). Relative expression was compared to cells cultured in SIM (treated) and PIM (untreated). *denotes p-value <0.05, ** denotes p-value <0.01. Data are mean ± SEM, n=3.

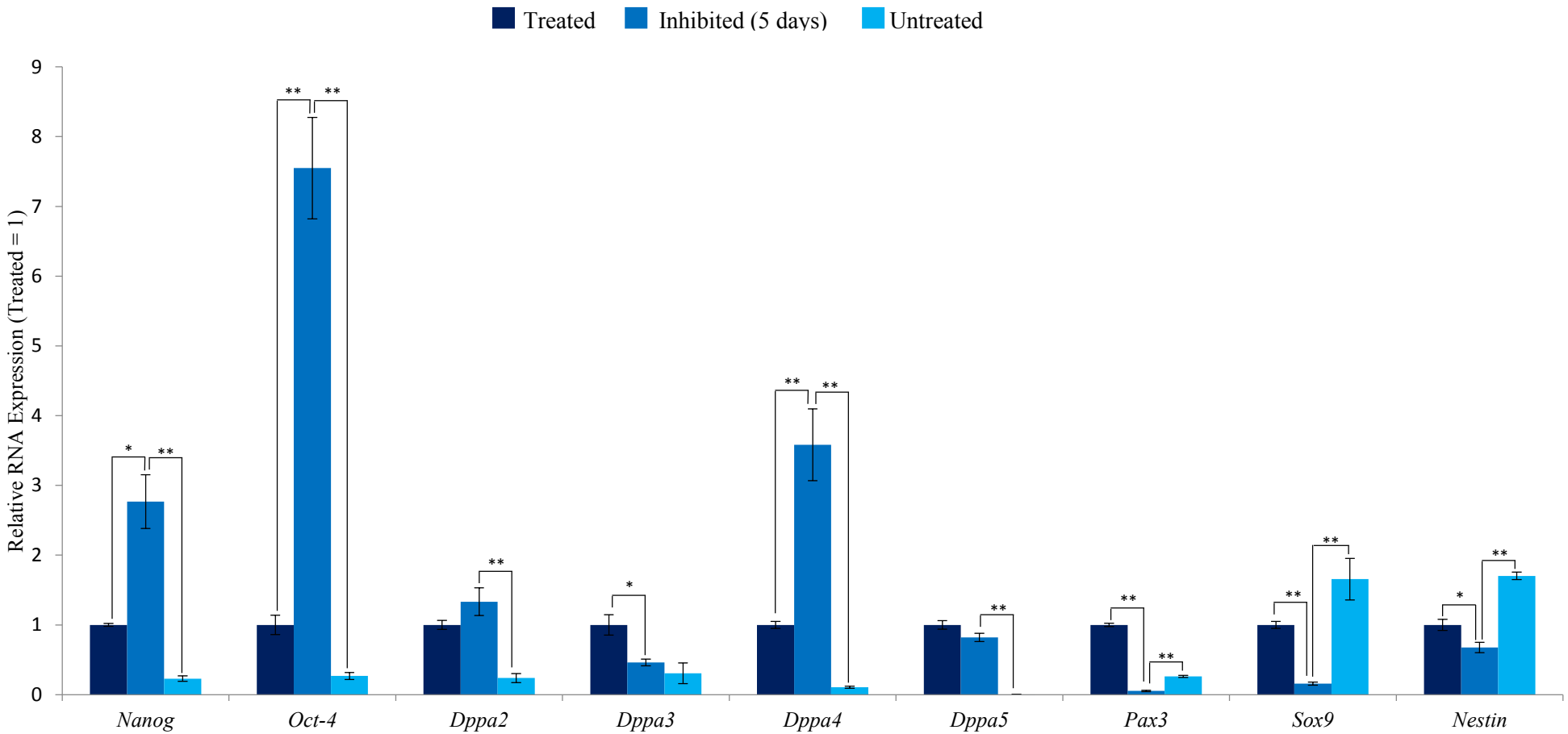


**Figure 6.8. The expression of pluripotency and NC marker genes following the inhibition of BMP-4 by Noggin for 5 days.** Gene expression was measured in cells cultured in IM for 5 days after 5 days culture in SIM during stage 2 of differentiation. Relative expression was compared to cells cultured in SIM (no inhibition) and PIM (no supplementation). *denotes p-value <0.05, ** denotes p-value <0.01. Data are mean ± SEM, n=3.

Efficacy of Noggin inhibition was determined by comparison of expression profiles of *Shh;* which is known to be downregulated by BMP-4 and *E-cadherin*; which is known to be upregulated. Previous experiments demonstrated downregulation of *Shh* in culture with BMP-4 supplemented medium (Figure 4.18). *E-cadherin* was shown to be upregulated in treated cells compared to untreated after 5 days and 10 days of stage 2 with increased upregulation observed after 10 days (8-fold upregulation opposed to 2.5-fold, p values were 0.008 and 0.0006 respectively). No significant variation was noted after 1 hour (Figure 6.9).

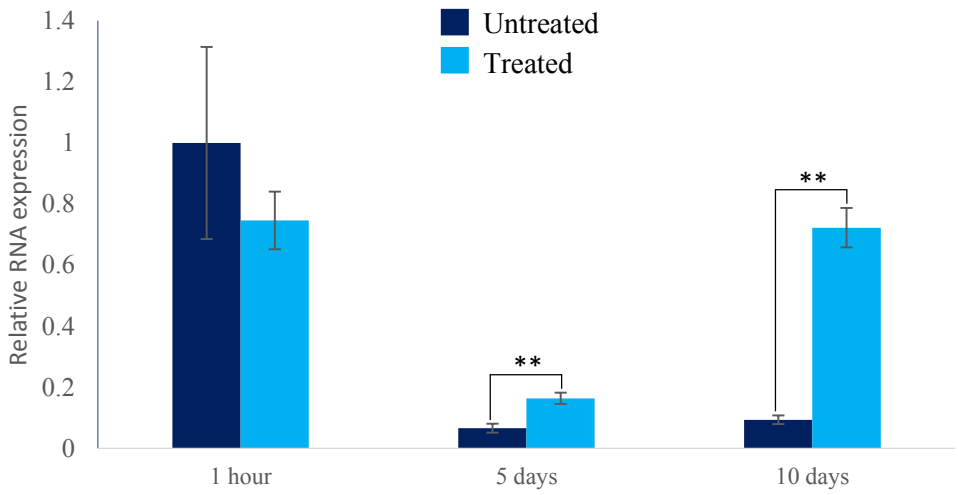


**Figure 6.9. BMP-4 Upregulates E-cadherin expression in stage 2 differentiating mouse embryonic stem cells.** Data is mean ± SEM, n = 3. All values were compared to the 1 hour BMP-4- sample (value = 1) and normalised to β-actin and 18s ribosomal RNA. ** denotes p-value <0.01.

Expression of *Shh* and *E-cadherin* was tested after Noggin inhibition as before. All values were compared to treated cells (value = 1) and Student's T-tests were used to determine significance. Inhibition for the full 10 days of stage 2 showed that *Shh* was upregulated (3.79-fold, p-value 0.004) compared to treated cells but downregulated (2.68-fold, p-value 0.04) compared to untreated cells. *E-Cadherin* expression was likewise intermediate between treated and untreated cells with a 3.1-fold

downregulation (p-value 0.03) and a 1.88-fold upregulation (p-value 0.004) compared to non-supplemented cells (Figure 6.10). These data indicate that Noggin treatment was partially but not wholly effective at reducing BMP-4 signalling.

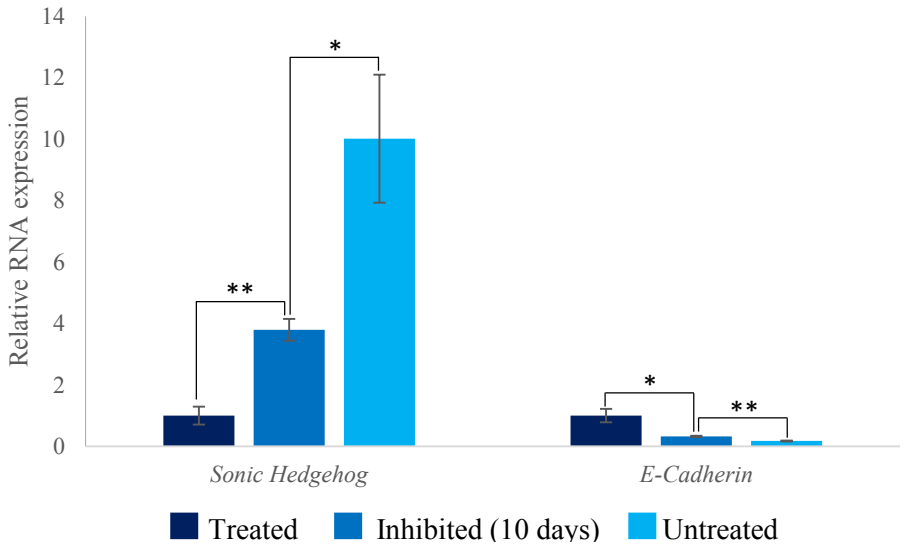


**Figure 6.10 Noggin inhibition partially ablated BMP-4 activity in differentiating cells.** Cells were cultured during stage 2 of differentiation in SIM (treated), IM (Inhibited (10 days) or PIM (untreated). Data is mean ± SEM, n=3. * denotes p-value <0.05, ** denotes p-value < 0.01.Statistical analyses compared inhibited cells to both non-inhibited and non-supplemented cells.

When Noggin inhibition was applied five days into stage 2, the reverse effect was observed. *Shh* was downregulated (4.34-fold) compared to untreated cells and *E-cadherin* was upregulated (2.89-fold). In both cases, statistical significance was observed with p-values of 0.04 for *Shh* and 0.01 for *E-cadherin* (Fig 6.11).

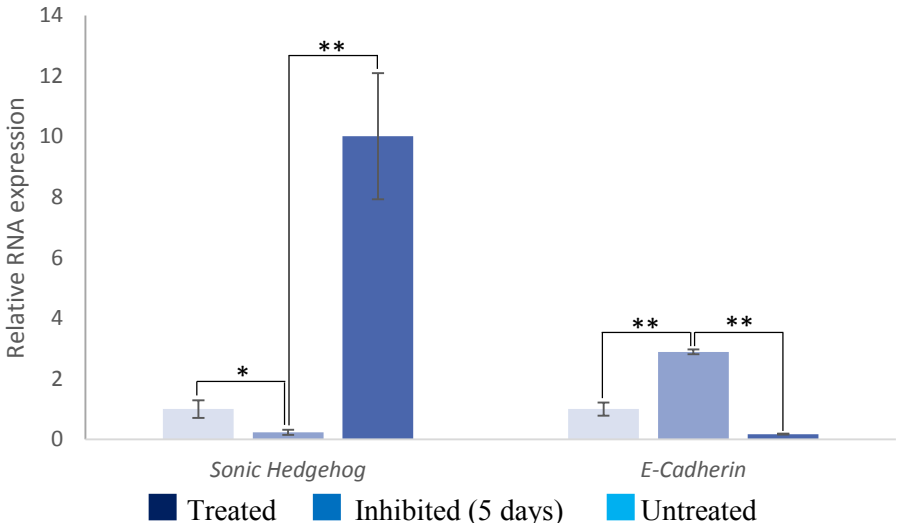


**Figure 6.11. Noggin inhibition of BMP-4 midway through stage 2 differentially altered BMP-4 mediated gene expression compared to inhibition at the start.** Cells were cultured during stage 2 of differentiation in SIM (treated), IM after 5 days culture in SIM (Inhibited 5 days) or PIM (Untreated). Data is mean ± SEM, n=3. * denotes p-value <0.05, ** denotes p-value < 0.01.Statistical analyses compared inhibited cells to both non-inhibited and non-supplemented cells.

### 6.3.5 Phlyogenetic Comparisons of Pluripotency Factors Mediated by BMP-4 during Neural Crest Differentiation

Phylogenetic analysis of pluripotency factors revealed that *Oct-4* and *Dppa3* were closely related (Figure 6.12) and Multiple Sequence Comparison by Log-Expectation (MUSCLE) revealed areas of conservation in sequences between the two (Figure 6.13) (Section 2.19). Conserved domain analysis of the two revealed a lack of common domain architecture suggesting that these proteins do not have a similar function or any similarities are due to the action of as yet undescribed domains. In contrast, *Dppa2* and *Dppa4* share the *Dppa2-4* conserved domain and between them display no other domain architecture. Other domains in these pluripotency factors were unique to individual proteins.

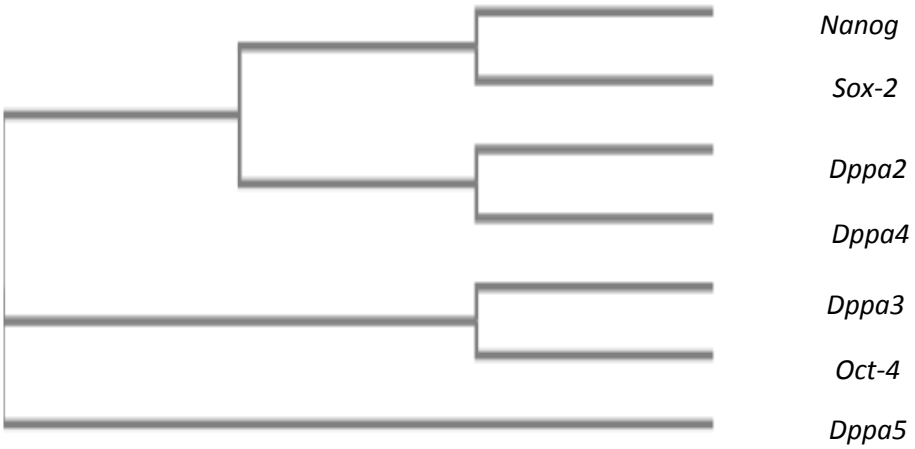


**Figure 6.12. Phylogenetic tree of putative BMP-4-mediated pluripotency factors.** More closely related proteins occupy adjacent branches on the tree.

```
MAGHLASDFAFSPPPGGGDGSAGLEPGWVDPRTWLSFQGPPGGPGIGPGSEVLGISPCPP
---------------------------MEEPSEKVDPMKDPETPQKKDEEDALD------
                             :*  .:.    *  *     .:.*.

AYEFCGGMAYCGPQVGLGLVPQVGVETLQPEGQAGARVESNSEGTSSEPCADRPNAVKLE
----------------------DTDVLQP------------------------------
                      ..:.***

KVEPTPEESQDMKALQKELEQFAKLLKQKRITLGYTQADVGLTLGVLFGKVFSQTTICRF
-------------------ETLVKVMKKLTLNPGVKRS---------------------
                   * :.*::*:  :. * ..:

EALQLSLKNMCKLRPLLEKWVEEADNNENLQEICKSETLVQARKRKRTSIENRVRWSLET
-ARRRSLRNRIAAVPV-----------ENKSEKIRREVQSAFPKRRVRTLLS--------
 * . **.*     *:           ** .*  . *.     **.  :: .

MFLKCPKPSLQQITHIANQLGLEKDVVRVWFCNRRQKGKRSSIEYSQREEYEATGTPFPG
-VLKDPIAKMRRLVRIEQR-------------QKRLEG----------NEFERDSEPFR-
 .** * ..:..:..* :.             :.* :*          :*:*  . **

GAVSFPLPPGPHFGTPGYGSPHFTTLYSVPFPEGEAFPSVPVTALGSPMHSN
-------------------------CLCTFCHYQRWDPSENAKIG----KN
                         .*   : : .   : :*    .*
```

**Figure 6.13. MUSCLE alignment of Oct-4 (top) and Dppa3 (bottom) amino acid sequences**.
* represents identical amino acids
: denotes non-identical but structurally similar amino acid residues.

### 6.3.6 Microarray Analysis of *Cochlin* Expression in Differentiating E14 Mouse Embryonic Stem Cells

BMP-4 supplementation during differentiation stage 2 appeared to have no effects on the expression of the synapse adhesion molecule Neurexin3 or p-SMAD1. Investigation of the effects of BMP-4 on Cochlin expression were inconclusive, as it remained undetected by Western blot in either sample. Examination of microarray data showed evidence of differential transcription during differentiation and possible regulation by BMP-4 (Figures 6.14 and 6.15). However, significance could not be determined as microarray samples were confined to a single experiment for each time point.

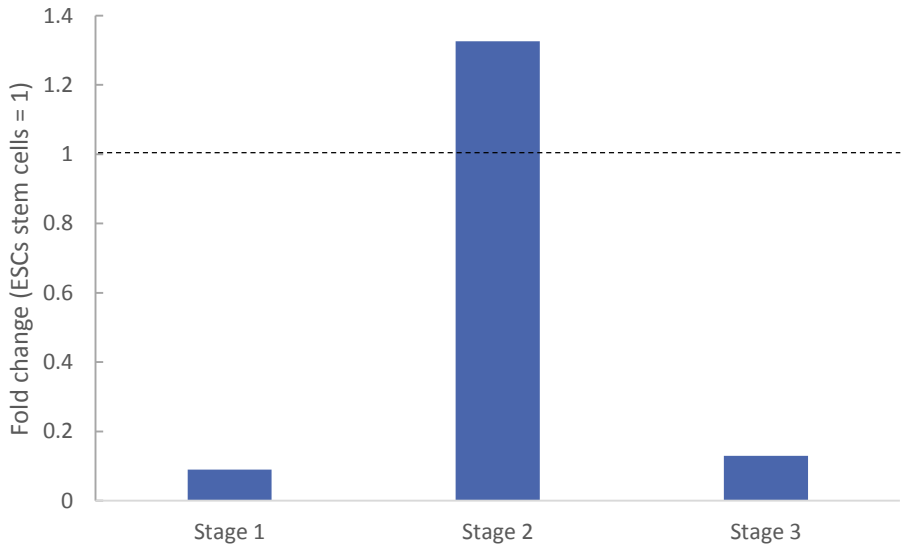


**Figure 6.14. Cochlin expression during peripheral neuron development.** Cells were cultured in PIM for stage 1, SIM for stage 2 and PIM for stage 3. Expression of *Cochlin* first decreased at stage 1, then increased at stage 2 with BMP-4 supplementation Withdrawal of BMP-4 treatment during stage 3 resulted in a decrease in expression. Values were compared to embryonic stem cells (value 1, denoted by the dotted line).

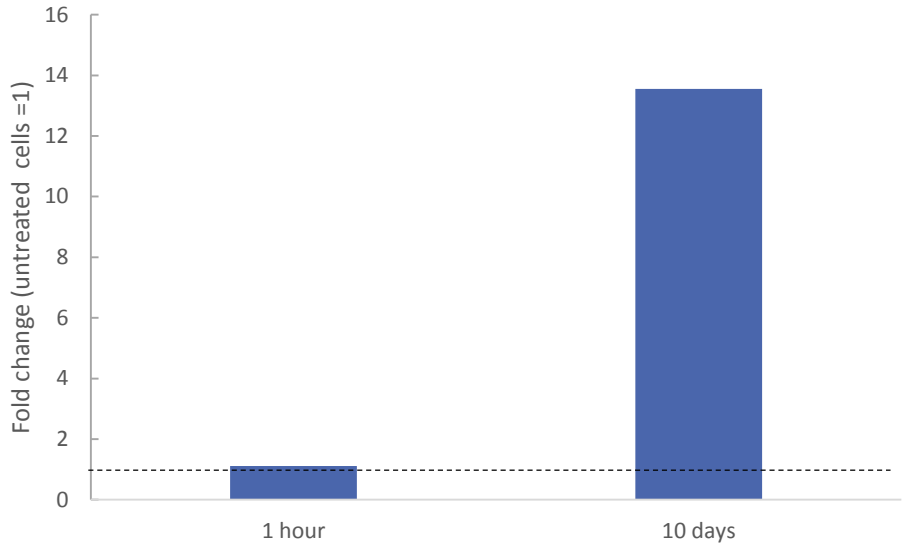


**Figure 6.15. BMP-4 affects Cochlin expression during stage 2 of differentiation.** *Cochlin* expression was measured in stage 2 cells after 1 hour and 10 days of BMP-4 treatment. Values were compared to untreated cells cultured for the same time (value = 1, denoted by the dotted line). Cochlin expression was upregulated by BMP-4 after 10 days of stage 2 differentiation but unchanged after 1 hour.

## 6.4 Discussion

Flow cytometry experiments demonstrated that Oct-4 expression increased during stage 2 of differentiation (Figure 6.1). Western blotting determined that expression levels of *Oct-4* were higher in cells cultured in SIM during stage 2 than those cultured in PIM (Figure 6.6). These findings correlate with microarray and Rt-qPCR data from the previous study (Figures 4.4 and 4.9).Taken together these data point to BMP-4 as a key regulator of the pluripotency factor *Oct-4* during the induction of neural crest stem cells.

*Oct-4* is one of the major pluripotency associated genes characterising embryonic stem cells. Canonically it is held to be the most important of the triumvirate (*Oct-4, Sox2* and *Nanog*) governing multipotency and self-renewal ability in murine stem cells and conferring resistance to differentiation into somatic cell types or dedifferentiation into trophoectoderm (Niwa *et al.*, 2000). *Oct-4* is known to work in concert with *Sox-2*; binding of the promoter region of *Nanog* by the translated proteins of these genes is thought to be necessary for the continuation, although not the initiation, of *Nanog* expression in developing organisms (Rodda *et al.*, 2005). *In vivo Oct-4* and *Sox-2* form a complex that facilitates interaction with the enhancer regions of genes associated with self-renewal (Ng *et al*, 2012). It is known to be expressed in neural crest stem cells but the mechanisms of its continued expression are unclear as it is rapidly downregulated in differentiating stem cells (Pesce *et al., 1998)*.

*Noggin* inhibition of BMP-4 during stage two was partially effective at altering transcriptional control of pluripotency factors (Figure 6.7). Expression of *Nanog* and *Dppa3* was significantly reduced although *Nanog* was not downregulated to a level

conversant with that in untreated cells unlike *Dppa3*. Expression of *Oct-4, Dppa2, Dppa4* and *Dppa5* remained unchanged compared to treated cells. *In vivo* a concentration gradient of BMP-4 governs fate determination post-gastrulation in the ectoderm (Milet *et al,* 2013). However, the borders between neural ectoderm, neural crest and non-neural ectoderm are not clearly delineated (Sargent, 2006). That *Noggin* inhibition was sufficient to influence expression of only two of five genes tested may be indicative of differential sensitivity. Expression of *Dppa3* and to a lesser extent *Nanog* may require higher levels of exogenous BMP-4. Effectiveness of inhibition was determined by measurement of expression levels of known BMP-4 targets, *E-cadherin* and *Shh* (Scott *et al*, 2010; Bond *et al*, 2012; Theveneau and Mayer, 2012) were respectively down and upregulated by following inhibition for the 10 days of stage 2. However, expression levels were between treated cells and untreated cells indicating that complete ablation of BMP-4 activity did not take place. Higher concentrations of Noggin may have given a greater inhibitory effect.

The increase in expression levels of *Nanog, Oct-4* and *Dppa4* following inhibition at 5 days of stage 2 (Figure 6.8) is indicative of a complex role of BMP-4 in the control of gene expression. In murine ESCs BMP-4 has been used as a serum replacement in culture with LIF to promote self-renewal and the maintenance of pluripotency (Zhang *et al*, 2013). *Nanog* is also a target of SMAD signalling which is activated by transforming growth factor β signalling, a pathway in which BMP-4 is a major component (Xu *et al*., 2008). Conversely in the absence of LIF BMP-4 plays an integral role in the differentiation of ESCs into trophoblast (Hayashi *et al*., 2010), chondrocytes (Kramer *et al*., 2000) and lung cell lineages (Lee *et al*, 2014). Previous experiments on expression of pluripotency factors showed a positive correlation between BMP-4 supplementation and gene expression (Figure 4.8). Flow cytometry

analysis and Western blot of *Oct-4* support this hypothesis on a translational as well as transcriptional level. The upregulation of factors such as *Oct-4* and *Nanog* after stage 2 in 5 day-inhibited cells demonstrate that BMP-4 may act in a negative regulatory fashion.

Phylogenetic analysis revealed that Oct-4 and Dppa3 closely related compared to other pluripotency factors and share regions of similar amino acid sequence (Figures 6.12 and 6.13). Similarity in amino acid sequence may indicate similarity in function, however although both Dppa3 and Oct-4 are crucial for self-renewal and pluripotency Oct-4 exerts its influence as a transcription factor as described above whilst *Dppa3* acts to prevent demethylation of imprinted and maternal genes that induce differentiation (Niwa *et al.,* 2000; Liu *et al.,* 2012*;* Xu *et al.,* 2013).

Noggin inhibition for the full 10 days of differentiation stage 2 reduced *Pax3* expression compared to treated cells. Expression levels were similar to untreated cells. Further downregulation was observed in cells inhibited for 5 days; with levels significantly lower than in untreated cells (Figures 6.7 and 6.8). Similar expression levels between inhibited and non-supplemented cells when BMP-4 was inhibited for the entire stage point to a role for BMP-4 in the regulation of *Pax3* expression. However, previous experiments suggest that this role is also diverse. Peak expression of *Pax3* in differentiating cells occurred after withdrawal of BMP-4 (Figure 3.13). BMP-4 supplementation initially decreased, then increased expression during stage 2 compared to non-supplemented (untreated) cells (Figure 3.22). It is possible that BMP-4 mediates the temporal expression of *Pax3;* a gene known to influence migration of numerous cell types during development. Treatment with exogenous BMP-4 can induce invasive characteristics and increased migration in non-invasive

rat neural stem cells (Sailer *et al*., 2013). Interestingly Pax3 can itself inhibit BMP-4 signalling pathways through regulation of the expression of *Sostdc1* potentially conferring resistance to differentiation in neural crest stem cells (Wu *et al*., 2008). Both BMP-4 and Pax3 are crucial for neural crest development (Varga and Wrana, 2005) although little is known about their interactions.

*Sox9* expression is not necessary for neural crest specification but is essential for epithelial to mesenchymal transition and subsequent migration (Liu *et al*, 2013). Treatment with BMP-4 during stage 2 did not prevent expression of *Sox9*; expression levels were similar at the mid-point for treated and untreated cells but downregulated at the end of stage 2 in treated populations (Figure 3.25). *Shh* signalling initiates *Sox9* transcription therefore BMP-4 supplementation can be expected to exert an inhibitory effect as the two are mutual antagonists *in vivo* (Scott *et al*, 2010; Bond *et al*, 2012). Early experiments corroborated this as *Sox9* expression increased markedly (more than 10-fold over 34 days) after withdrawal of BMP-4 supplementation from differentiating cells (Figure 3.16). Inhibition of BMP-4 signalling by *Noggin* however did not increase *Sox9* expression. Transcription levels were significantly lower than untreated cells whether inhibition was initiated at the beginning or mid-point of stage 2 (Figures 6.7 and 6.8). These data indicate that while BMP-4 is a regulator of *Sox9* expression it acts neither in a straightforward inhibitory or stimulatory manner.

Inhibition of BMP-4 signalling had similar effects on *Nestin* expression as on *Sox9*. Significant reductions in expression were observed compared to treated cells at both time-points (Figure 6.7 and 6.8). This was not conversant with earlier experiments in which BMP-4 treatment reduced expression compared to untreated cells. BMP-4 can

act in an inhibitory manner to neurulation (Li *et al*., 2011) or promote neuronal specification (Chalazontis and Kessler, 2011). These data support this paradigm showing increased downregulation when BMP-4 signalling was abrogated by *Noggin* supplementation and suggesting dual modes of action based on concentration.

Although microarray data suggested BMP-4 upregulated expression of *Cochlin*, potentially inferring a pathway through which pluripotency genes are positively regulated this data should not be taken in isolation. Further investigation would be required before it can be definitively stated that BMP-4 exerts it influence on differentiating neural crest stem cells through activation of *Cochlin* expression. Immunocytochemical staining or flow cytometry may offer insights furthering the elucidation of BMP-4 mediated pathways during neural crest differentiation.

# Chapter 7: Discussion, Conclusions and Future work

This study initially described a method to differentiate peripherin positive cells of a neuronal phenotype from mouse ESCs in serum-free culture *in vitro.* The differentiation protocol was based on the methods described by Aihara *et al* (2010) and may be seen as a replacement, given that the media used in this preceding study is no longer commercially available. This method has several advantages over traditional methods of neuronal generation using stromal derived inducing activity (SDIA) (Shimada *et al*, 2012) or serum for all or part of the differentiation process (Kreitzer *et al*, 2012), in that the defined medium allowed the influence of a single growth factor (BMP-4) to be analysed. Electrophysical analysis after plating cultured cells on MEA chips showed that differentiated cells were capable of transmitting action potentials and were responsive to GABA and NMDA (Figure 5.10). Functionality assays are important, as the recapitulation of non-functional neurons may not give an accurate portrayal of the genetic landscape during differentiation. To the author's knowledge this is the first study to combine functionality assays with global gene expression analysis evaluating not only genes dictating lineage selection but the influence of BMP-4 on neural crest derivation in serum-free, feeder layer free conditions.

## 7.1 BMP-4 Treatment Increased Expression of the Key Pluripotency Factor *Oct-4* and the RNA Binding Pluripotency Associated Factor *Dppa5*

Microarray and RT-qPCR analysis indicated that several key factors pertaining to the maintenance of self-renewal potential and inhibitory to differentiation were

upregulated by BMP-4 treatment during stage 2 of differentiation. Several factors were further investigated by Western Blot and flow cytometry analyses. Expression of *Dppa5* was observed to decline then increase during stage 2 and protein expression was observed to be higher in cells treated with BMP-4 compared to untreated cells (Figures 6.2 and 6.7). Little is known about the role of *Dppa5* in neural crest development and to our knowledge a link between expression and BMP-4 has not previously been established. The function of *Dppa5* in another multipotent cell lineage has recently been discerned. *Dppa5* acts to reduce apoptosis and facilitate cell division by the reduction of endoplasmic reticulum stress. The exact role of *Dppa5* remains currently unclear although it is known to regulate gene expression through RNA binding (Miharada *et al*, 2014).

Similarly, to *Dppa5* Oct-4 expression decreased between the start and mid-point of stage 2 before increasing in BMP-4 treated cells. Flow cytometry analysis supported microarray and RT-qPCR data showing an initial reduction then an increase in Oct-4 presenting cells as stage 2 progressed. The initial decrease is consistent with current knowledge of Oct-4 expression, which is silenced, early in the developmental process (Jerabek *et al*, 2014). NCCs however are known to express Oct-4, which contributes to the epithelial to mesenchymal transition (Simões-Costa and Bronner, 2013). Western blot analysis confirmed the upregulation of Oct-4 on a proteomic as well as transcriptional level. Taken together these data point to a key role of BMP-4 in the reassertion of Oct-4 expression during neural crest development. BMP-4 is known to mediate the expression of Oct-4 in ESCs but its role in expression in neural crest was previously unrecognised.

### 7.2 BMP-4 Treatment Caused Differential Expression of Neurulaution Associated Genes and of Neural Crest Associated Factors.

BMP-4 treatment caused downregulation of *Nestin* during stage 2 of differentiation compared to cells grown in similar media without supplementation as well as delayed expression of the neuronal associated adhesion genes *Neuroligin1, Neuroligin3, Pou3f4* and *Pou4f2* (Figures 3.21 and 4.17). This delay in expression is conversant with the role of BMP-4 as an inhibitor of neurulaution (Ying *et al*, 2003). In the developing murine embryo, BMP-4 acts antagonistically to the pro-neurulation transcription factor *Shh* (Bastida *et al*, 2009). RT-qPCR data demonstrated downregulation of *Shh* in BMP-4 treated cells although expression was not ablated (Figure 4.17). These data suggest that BMP-4 and *Shh* may work synergistically in neural crest formation, with *Shh* specifying a neural lineage while BMP-4 delays differentiation. Higher levels of BMP-4 are observed in the non-neural ectoderm indicating a higher level of antagonism towards *Shh* expression.

Although increases in expression were seen in both BMP-4 supplemented and untreated stage 2 cells for the neural crest markers *Pax3* and *Musashi-1* both genes were upregulated earlier in the untreated fraction before expression fell (Figures 3.22 and 3.23). These data further indicate a complex role for BMP-4 in neurulation and neural crest formation. Musashi-1 is linked to asymmetric cell division in stem cells (Okano *et al*, 2005). Expression of *Pax3* is required for proper migration of the neural crest (Milet *et al*, 2013) Initial BMP-4-mediated downregulation of these genes after the first five days of stage 2 may act to maintain a stem cell like state, allowing for the symmetric division and rapid proliferation of neural crest stem cells while limiting migration. These data are supported in that BMP-4 withdrawal after

stage 2 caused upregulation of both genes before expression levels once again fell (Figures 3.14 and 3.15).

### 7.3 Noggin Inhibition Altered BMP-4 Mediated Expression of Pluripotency and Neural Crest Related Genes

Efficacy of *Noggin* inhibition was determined by measuring expression of *Shh* and *Cadherin* in inhibited cells. Cells inhibited at day 0 of stage 2 showed increased expression of *Shh* after 10 days although expression was less than in untreated cells with 3.8-fold upregulation in inhibited cells compared to treated and a further 2.6-fold between inhibited and untreated. E-*Cadherin* expression in inhibited cells was lower than that of treated and higher than untreated cultures with 3.13-fold downregulation and 1.88-fold upregulation observed respectively (Figure 6.7). These data are indicative that culture of BMP-4 treated samples with Noggin supplementation partially inhibited BMP-4 activity. Culture with Noggin at the mid-point of stage 2 (5 days, 9 days total differentiation), however resulted in differing changes in expression. E-*Cadherin* expression, rather than being reduced compared to treated cells was increased significantly (2.89-fold, p-value 0.001) and *Shh* expression was reduced (4.35-fold reduction compared to treated cells, p-value 0.009). Inhibition at 5 days served to enhance rather than decrease the effects of BMP-4 on these genes (Figure 6.8). These data indicate that BMP-4 may modulate its own expression in the developing neural crest, although whether directly or through downstream targets is unclear. In order to ascertain whether these data corresponded to similar changes in gene expression in pluripotency factors and

neural crest specifiers genes investigated previously were subject to RT-qPCR analysis after inhibition.

*Noggin* treatment at the beginning of stage two reduced *Pax3* expression to similar levels expressed in cells cultured in the absence of supplementation. These data support previous microarray and RT-qPCR data that *Pax3* expression after stage 2 was influenced by BMP-4 supplementation. Research has shown that BMP-4 is inhibitory to *Pax3* mediated myogenesis but promotes transcription in the central nervous system while *Shh* is known to be antagonistic towards its expression (Kennedy *et al*, 2009; Moore *et al*, 2013). A decrease in expression in this case may be the effect of transcriptional regulation by *Shh*, which could exert a greater influence due to reduced antagonism brought about by inhibition of BMP-4 signalling. Interestingly *Pax3* itself has shown to act on transcription factors that inhibit the BMP-4 signal cascade, specifically *Sclerostin Domain Containing 1* (*SostdC1)* (Wu *et al*, 2008). Microarray analysis showed that this gene was upregulated 22.62-fold during stage 2 of differentiation and a further 86.43-fold during stage3. *Follistatin*, a second BMP-4 inhibitory compound was also upregulated during stage 2 although to a lesser extent (9.49-fold) and downregulated during stage 3 (1.74-fold). A third antagonist, *Chordin* did not show greater than 1.5-fold upregulation in any sample tested. Potentially BMP-4 and *Pax3* may form a feedback loop in which BMP-4 slows but does not prevent early expression of *Pax3* during neural crest formation (Figure 3.20) before an accumulation of Pax3 protein activates suppressors of BMP-4.

Inhibition of *Dpap3* and *Nanog* expression was observed following Noggin inhibition during stage 2. Both were significantly downregulated by inhibition although this was less profound in the case of *Nanog* in which 1.28-fold

downregulation was observed as opposed to the 2.43-fold decrease in expression of *Dppa3*. These data support previous RT-qPCR analyses suggesting BMP-4 plays a role in mediating their expression during neural crest differentiation.

*Sox9* and *Nestin* expression were further downregulated by Noggin inhibition. BMP-4 is a known regulator of *Sox9* expression (Theveneu and Mayor, 2012) in culture during stage 2 expression increased between the start and mid-point (0-5 days) before remaining stable for the remainder (5-10 days). The lower expression levels observed after Noggin treatment may simply be indicative of direct inhibition of *Sox9* transcription by Noggin. Increased *Sox9* expression in the absence of BMP-4 during stage 2 is indicative of multiple factors influencing the expression of differentiation-associated genes. The downregulation of *Nestin* expression by inhibition was unexpected, BMP-4 is known to restrict neurulaution therefore inhibition of signalling (Bastida *et al*, 2009) may be expected to increase the expression of a neural precursor gene. However, BMP-4 in presence with other factors has been shown to promote *Nestin* expression in differentiating cells (Torres *et al*, 2012). Potentially BMP-4 could act synergistically with other factors present in both PIM and SIM media (transferrin or insulin) to promote modest upregulation of *Nestin* compared to culture in untreated cells; inhibition of this interaction could lead to reduced expression.

Expression of *Oct-4, Dppa2, Dppa4* and *Dppa5* was not significantly altered by inhibition, suggesting either redundancy leading to their expression through alternative signalling or increased sensitivity to BMP-4. A reduction in *Shh* expression to a level between non-inhibited and non-supplemented cells demonstrated that that inhibition did not ablate BMP-4 signalling (Figure 6.7). Where inhibition was recorded, it was observed to lead to expression levels

intermediate to non-inhibited and non-supplemented cells. Additional experiments with increasing concentrations of Noggin would be required to further elucidate the effect of BMP-4 inhibition on expression of these genes. Additional time-points (e.g. mid-point of stage 2) would also allow greater insights into the process.

Inhibition by Noggin after 5 days of stage 2 resulted in highly variable expression of pluripotency and neural crest specification factors. *Dppa3* was downregulated to an extent comparable to inhibition for the entirety of stage 2 with no significant difference observed between expression in the inhibited cells and untreated cells. Similarly, *Dppa2* and *Dppa*5 expression was consistent in cells inhibited at 0 and 5 days of stage 2, no significant difference was observed between these cells and treated cells. In contrast, *Oct-4*, *Nanog* and *Dppa4* were all upregulated after inhibition and *Pax3, Sox9* and *Nestin* were downregulated, all differences were significant with p-values ranging from 0.04 to $4 \times 10^{-6}$. Initially no patterns could be discerned but when expression values of uninhibited cells and cells inhibited at 5 days of stage 2 were compared to untreated cells (value = 1) variations in expression were seen to be enhanced or remain unaltered in 7 out of 9 genes examined (Table 7.1). *Dppa3* was upregulated but to a lesser extent in the inhibited sample and the expression change in *Pax3* was reversed. *Dppa2* and *Dppa5* expression remained constant.

**Table 7.1 Noggin inhibition after 5 days of stage 2 altered the effects of BMP-4 on pluripotency and neural crest biomarker expression.**

| Gene | Relative RNA expression (Treated) | Relative RNA expression (noggin inhibition at day 5) |
|---|---|---|
| *Oct-4* | 5.03 | 12.04 |
| *Nanog* | 5.29 | 27.93 |
| *Dppa2* | 5.24 | 5.54 |
| *Dppa3* | 6.33 | 1.49 |
| *Dppa4* | 13.03 | 32.55 |
| *Dppa5* | 19.1 | 15.56 |
| *Pax3* | 3.25 | 0.2 |
| *Sox9* | 0.71 | 0.1 |
| *Nestin* | 0.76 | 0.4 |

These data may support a regulatory relationship between BMP-4 and Pax3 with inhibition at 5 days disrupting regulation. In differentiating cells, *Pax3* upregulation was observed across stage 2 (Figure 3.11) during the later section of stage 2, BMP-4 supplementation was shown to increase *Pax3* expression compared to untreated cells (Figure 3.20). Inhibition of BMP-4 signalling by noggin for the entirety of stage 2 reduced expression to levels similar to that of untreated cells. Inhibition after 5 days of stage 2 reduced the expression of *Pax3* significantly, with a 5-fold reduction from levels in untreated cells observed (Fig. 7.1). If as previously hypothesised increasing *Pax3* expression causes reduction in BMP-4 signalling an increase in expression of putative BMP-4 targets is a logical expectation. As above additional investigation is required in order to confirm changes, additional time-points during stage 2 may give a greater insight into the transcriptional landscape altered by BMP-4 and pax3 interactions.

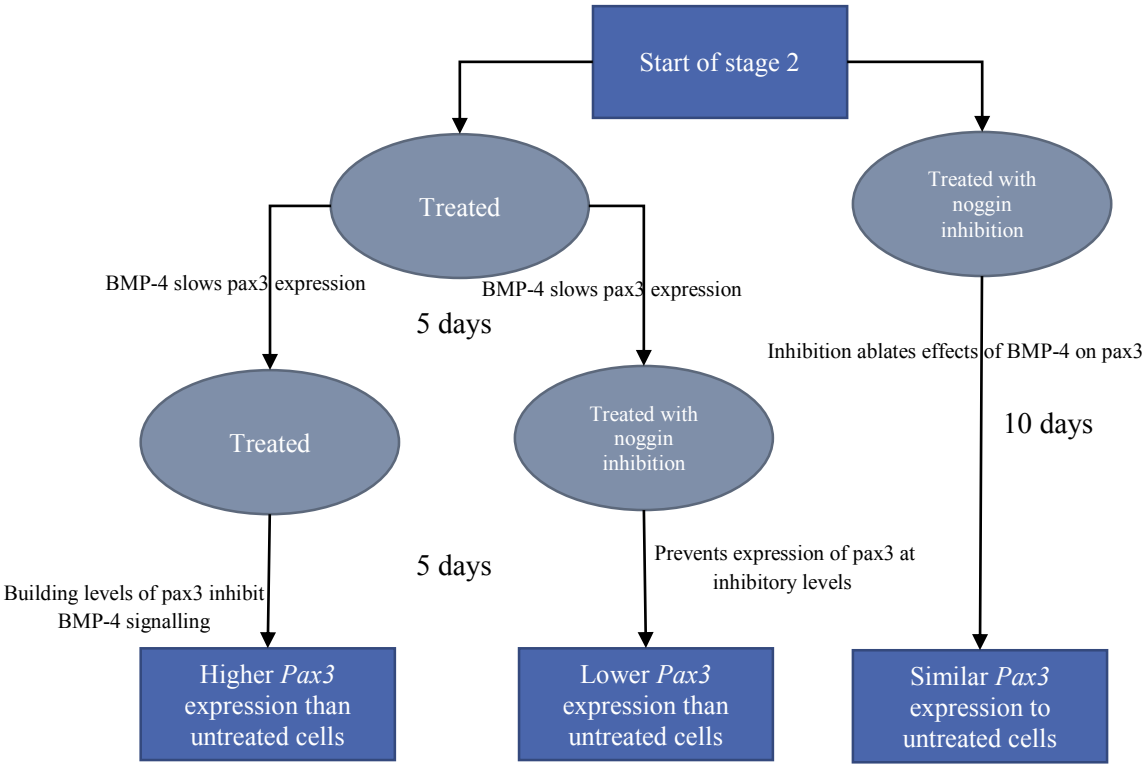


**Figure 7.1. Noggin inhibition revealed potential interactions between BMP-4 and pax3 in neural crest specification.** Theoretical interactions between BMP-4 and pax3After 10 days treatment inhibited cells expressed *Pax3* at levels similar to untreated cells – levels were reduced 3.2-fold from treated cells (Figure 6.7) indicating a regulatory relationship between BMP-4 and pax3. In contrast, inhibition at 5 days almost completely abrogated expression – levels were 5-fold reduced compared to untreated cells (Figure 6.8). The expression of neural crest markers was also downregulated and expression of pluripotency associated genes *Oct-4, Nanog* and *Dppa4* was increased (Table 7.1). BMP-4 treatment was previously shown to delay expression of *Pax3* and upregulate expression of pluripotency associated genes (Figures 3.18, 3.20 and 4.9). Pax3 is known to inhibit BMP-4 signalling (*c.f.* section 6.4), potentially these data point to an interaction of these two factors in neural crest patterning, with BMP-4 delaying expression of pax3 but not abrogating it, contributing to maintenance of pluripotency before pax3 interrupts BMP-4 signalling for somatic fate selection prior to migration.

## 7.4 BMP-4 Treated Cells Presented Differential Expression of Adhesion Molecules

During differentiation patterns of expression of the tight junction molecules *Claudin1* and *Claudin23* exhibited differences. Both were sequentially upregulated during stages 1 and 2 but *Claudin1* continued to be more strongly expressed during stage3 whilst *Claudin23* expression remained constant (Figures 4.10 and 4.11).

BMP-4 response in these genes was in contrast, *Claudin1* expression was significantly downregulated by BMP-4 after 5 and 10 days of stage 2 whereas *Claudin23* expression was increased (although not significantly) after 1 hour and 5 days and significantly after 10 days culture (Figure 4.17). *Cadherin1* expression was observed to decline over each stage of differentiation though this was mitigated significantly by BMP-4 during stage 2. Cells cultured during stage 2 without BMP-4 supplementation demonstrated increased *Cadherin1* downregulation compared to supplemented cells (Figure 4.17). Microarray analysis showed variance in expression of both *Cadherins* and *Claudins* (Appendix 4). Of the 19 *Cadherins* probed 10 were upregulated after stage 1, 11 after stage 2 and 13 after stage 3 with 5, 7 and 4 downregulated at the equivalent stages. The 22 *Claudin* probes plus the closely related *Occludin* probe indicated 13 genes upregulated during stage1, 10 during stage 2 and 8 during stage 3 with 7, 9 and 12 being downregulated at the same time points. BMP-4 treatment for 1 hour during stage 2 increased expression in 6 *Cadherin* genes and 10 *Claudins* whilst downregulating 8 and 5 respectively. After 10 days of stage 2 culture with BMP-4 6 *Cadherins* were upregulated and 11 downregulated, 15 *Claudins* showed increased gene expression and 7 decreased. BMP-4 is known to play a role in the expression of adhesion molecules during neural crest specification and delamination (Theveneneau and Mayor, 2012). However, its scale of influence is

not yet known. Further research on the effects of BMP-4 on expression of Claudins and Occludins, particularly those that are known to be tissue specific may elucidate the role of this molecule in mediating adhesion complexes in differentiating and terminally derived cells. BMP-4 has been shown to affect the expression of cell adhesion molecules such as cadherins and Claudins (Figure 4.14, Appendix 4). Inhibition of signalling may be a trigger for adhesion changes in pre-migratory committed NCCs. The high levels of expression of *Sox9* which is required for EMT and migration after withdrawal of BMP-4 supplementation somewhat support this although investigation in detail would be required to confirm this hypothesis (Liu *et al*, 2013).

### 7.5 BMP-4 Signalling May Mediate Regulation of Pluripotency Genes through the Cochlin Pathway

Culture with BMP-4 in conjunction with LIF has been shown to retard the differentiation of ESCs *in vitro* in addition to promoting the expression of pluripotency factors, such as *Oct-4.* Experiments have shown that the LIF-Stat pathway, which canonically promotes self-renewal in the presence of serum or a feeder layer, is not involved in this process (Ying *et al*, 2003). Later studies indicated that BMP-4 mediated pluripotency in ESCs through the expression of *Cochlin* (Zhang *et al*, 2013). The current study assessed whether this mechanism was also active in promoting the expression of embryonic stem cell associated genes in NCCs, elucidating a key role for BMP-4 in NC selection, differentiation and expansion. Microarray data supported this theory with *Cochlin* expression being upregulated in cells cultured in SIM during stage 2 of differentiation. *Cochlin* expression decreased during stage 3 after withdrawal of BMP-4 supplementation. These data infer a role for BMP-4 in mediating *Cochlin* expression which in turn may promote expression

of pluripotency factors, facilitating the proliferation, multipotency and self-renewal potential of neural crest stem cells. Proteomic analysis however, did not support transcriptional data, neither Western blotting nor immunocytochemistry detected expression in any samples tested. Further analysis should focus on alternate methods of measuring protein expression such as flow cytometry or the efficiency and sensitivity of the antibody could be examined through the use of a positive loading control for Western blotting, facilitating optimisation of reaction conditions.

### 7.6 Differentiated Cells were Positive for Neural Associated Genes Arising from the Trunk Neural Crest after Stage 3.

Differentiation using stripped media containing FGF-2 and BMP-4 resulted in cell types expressing genes associated with neural crest upon which removal of BMP-4 supplementation yielded cells positive for peripheral neuron biomarkers. Microarray analysis revealed several thousand genes were differentially regulated at each differentiation stage and a similar number were altered by culture with and without BMP-4 during stage 2 (Tables 4.3 and 4.4). Confirmation of microarray results by RT-qPCR confirmed alternate expression patterns in numerous genes associated with pluripotency and cell adhesion, which was further confirmed with Western blotting, and flow cytometry analysis. Complete analysis of transcriptional changes however was not possible due to the quantity of genes alternately expressed at each stage and with and without BMP-4 supplementation. Microarray data was used to further categorise differentiated cells and elucidate the effects of BMP-4 on gene expression during neural crest and peripheral neuron differentiation.

Craniofacial cartilage derives exclusively from cranial neural crest. During specification osteochondrogenesis is supressed by Hox genes; inactivation of the

gene Ezh2 reduces Hox methylation and prevents cartilage formation in cranial NC cells, ablation of Ezh2 expression did not affect differentiation into sensory and autonomic neurons. Knockout of Ezh2 reduced expression of Runx2, osterix and Alkaline phosphatase as well as reducing all the Hox genes (Schwarz, *et al,* 2014). Microarray analysis showed little change in *Hox* gene expression over the differentiation period as was the case with expression of *runx2* and *alkaline phosphatase*. Data for expression of *Osterix* was not given by microarray analysis. These expression patterns are not characteristic of patterns expected in osteochondrogenesis, indicating that treatment with FGF-2 and BMP-4 does not activate Ezh2 in vitro and other signals are required for cranio-facial cartilage development. Experiments on chondrocyte development have revealed a role of Hox2a in the blocking of *Sox9* after neural crest specification to divert cells from a neuronal fate (Bhatt *et al*, 2013). Research undertaken over the past century or more has determined that craniofacial neural crest specification is initiated after the epithelial to mesenchymal transition and is dependent on signalling from the developing somites as migratory NCCs pass amongst them (Schilling and Le Plabec, 2014)

The adrenal medulla is distinct both physiologically and functionally from the adrenal cortex. It serves to modulate the Fight-or-flight response by releasing quantities of adrenaline or noradrenaline in response to stress (Fung *et al*, 2008). Differentiation of adrenal medulla cells from neural crest is dependent on the transient expression of *Sox8* and *Sox10.* Sox 10 null mice lack the adrenal medulla in its entirety but this phenotype can be rescued with overexpression of *Sox8*. Early expression of *Sox9* is required for initial delamination and migration but this gene is not expressed in the developing medulla (Reiprich *et al*, 2008). RT-qPCR data

showed expression of *Sox9* into stage 3 while immunocytochemistry confirmed expression of *Sox10* after stage 2. Microarray analysis however showed that *Sox8* expression changed little during differentiation. The continued expression of *Sox9* is indicative that differentiating cells are not selected for an adrenal medulla phenotype.

Melan-A and mitf are differentiation factors expressed both during lineage selection to melanocytes from NCCs and in certain melanomas (Weinstein *et al*., 2013). Microarray data showed little changes in expression of these markers from ESCs through all stages of differentiation, indicative of a lack of response to BMP-4 signalling.

Vimentin and glial fibrillary acid protein (GFAP) are commonly used biomarkers of neuroglial lineage. Early during differentiation, vimentin is expressed preferentially but this is replaced by GFAP later during gestation (Bramanti *et al*., 2010). Potentially differentiation of E14 murine stem cells resulted in the formation of heterogeneous populations containing neuroglia as well as other peripheral neuron types as evidenced by the expression of GFAP during stage 3 following an increase in vimentin expression during stage 2.

In murine systems developing Schwann cells are characterised by the expression of numerous genes at early stages. Nascent Schwann cells deriving from the neural crest express myelin protein 0 (p0), Gap43 and F-spondin. Between neural crest delamination and birth myelin p0 expression decreases with a concomitant increase in S100β expression (Corfas *et al*, 2004). During differentiation, microarray data revealed an increase in expression of *p0*; however, pplr values were approximately 0.5 at all stages, indicating low significance for these changes. *S100β* expression significantly increased during differentiation, increasing 4.5 fold during stage 2 and a

further 13.8 fold during stage 3. *GAP43* similarly increased in stage 2 and 3, 21.1-fold and a further 7.8-fold respectively with similar patterns of expression of *F-spondin* observed during the same periods.

Cardiac NCCs require expression of numerous genes for premigratory lineage selection and subsequent colonisation. In murine systems, the genes *lbx1* and *Pdgfrα* are required for cardiac smooth muscle specification. Correct migration patterns and ultimate spatial patterning necessitate expression of *Et-1, Et-A* and *Vegfr2* (Olaopa and Conway, 2012). *Lbx1* expression was found to increase during stage 3 of differentiation but little change was exhibited previously. *ET-1* and *ET-A* were downregulated at the same stage. Microarray data for expression of *Pdgfra* and *Vegfr2* was unavailable. Data for gene expression is summarised in Appendix 5.

Taken together with immunocytochemistry, transcriptional analyses and functionality tests these data indicate that differentiation produced peripheral neurons of trunk neural crest lineages. Microarray data revealed genes linked to differentiation into cranio-facial and cardiovascular derivatives were not upregulated. A variety of neural associated genes were downregulated compared to untreated controls during stage 2 of differentiation and subsequently upregulated after withdrawal of BMP-4 at stage 3. Synaptogenesis was not impaired by culture with BMP-4, as both treated and untreated cells were able to transmit electrochemical signals when cultured on MEA chips. However, transcriptional production of the synaptic junction protein family *Neuroligin* was delayed by culture with BMP-4. For the first time global gene expression analysis was carried out on functional neural crest derived neurons, investigating the role of BMP-4 in neural crest specification data indicated that a number of pluripotency and adhesion factors were altered.

## 7.7 Future Work

Oct-4 expression was shown to be mediated transcriptionally and translationally by BMP-4 treatment. Initially expression declined before recovering to a point approximately 10% of that of ESCs. Decline and decrease in expression were confirmed by flow cytometry and protein expression was confirmed by Western blot. Analysis of methylation patterns at various time points during stage 2 of differentiation would add depth to these findings and potentially offer new insights into mechanisms of control of pluripotency factors in the developing neural crest. Western blotting and immunocytochemistry were used to interrogate Cochlin and Phospho-SMAD1 expression in differentiating cells. No difference was noted in P-SMAD expression and data from Cochlin experiments was inconclusive. Flow cytometry may offer additional insights into expression of these proteins during the differentiation process.

Further confirmation of microarray data may be possible on a higher scale by the use of 2D differential gel electrophoresis (DIGE). This method involves pooled samples labelled with different fluorophores on the same gel, negating the differences in loading and transfer that can be experienced with older methods such as Western blotting (Lilley and Freidman, 2005). DIGE has seen use in proteomic analysis investigating differential expression in cells comprising the hematopoietic system (Mihrada *et al*, 2014).

Chromatin immunoprecipitation experiments may highlight the potential interaction between Pax3 and BMP-4. Identifying genes bound by *Pax3* during stage 2, particularly the BMP-4 inhibitory factors *Follistatin* and *SostdC1*. RT-qPCR experiments would confirm microarray data for these genes indicating the presence

of BMP-4 inhibitors at a transcriptional level at this stage. Proteomic analysis of Pax3 at various time points, with, and without Noggin inhibition could provide important insights into the role of this protein in could be combined with analysis of its putative targets in neural crest induction. These experiments could be run in parallel with migration experiments to elucidate the role of *Pax3* in EMT and migration.

Culture of ESCs before cell sorting in media containing LIF and BMP-4 may have resulted in higher viability and allowed analyses at a greater number of time-points, particularly stage 2. Cell viability during stage 2 initially dropped to approximately 40% after 1 day before climbing steadily over the stage (Figure 3.15). Adaption to growth in serum free culture earlier may have resulted in increased yields of cells, particularly during the mid-point of stage 2 at which point low viabilities made the extraction of sufficient quantities of RNA for analysis difficult.

Murine ESCs were used in the experiment; findings should be confirmed in human ESCs and human induced pluripotent cells. If successful differentiation through this protocol is possible a potential source of neural tissue for investigation of neurochristopathies such as neuroblastoma and Hirchsprung's disease. Tissue replacement therapies may be possible in the long term; however, data suggests that heterologous populations of neurons were derived. Methods such as fluorescence activated cell sorting should be employed to isolate homologous strains before this can be considered.

# Chapter 8: References


Xu, R-H., Sampsell-Barron, T., Gu, F., Root, S., Peck, R., Pan, G., Yu, J., Antosiewicz-Bourget, J., Tian, S., Stewart, R. and Thomson, J. (2008). NANOG is a direct target of TGFβ/Activin-mediated SMAD signalling in human ESCs. *Cell Stem Cell*, **3**, 196-206.

Abbruzzese, G., Gorny, A-K., Kaufmann, L., Cousin, H., Kleino, L., Steinbeisser, H. and Alfandari, D. (2015). The Wnt receptor Frizzled-4 modulates ADAM13 metalloprotease activity. *Journal of Cell Science*, **128**, 1139-1149.

Abreu, R., Sanchez-Diaz, P., Vogel, C., Burns, S., Ko, D., Burton, T., Vo, D., Chennasamudaram, S., Lee, S-Y., Shapiro, B. and Penalava, L. (2009). *Journal of Biological Chemistry*, **284**(18), 12125-12135.

Aihara, Y., Hayashi, Y., Hirata, N., Ariki, N., Shibata, S., Nagoshi, N., Nakinashi, M., Ohnuma, K., Warashina, M., Michiue, T., Uchiyama, H., Okano, H., Asashima, M. and Furue, M. (2010). Induction of neural crest cells from mouse embryonic stem cells in a serum free culture. *Int. J. Dev. Biol.*, **54**, 1287-1294.

Ali, R., Bellchambers, H. and Arkell, R. (2012). Zinc fingers of the cerebellum: Transcription factors and co-factors. *The International Journal of Biochemistry and Cell Biology*, 44, 2065-2068.

Alimperti, S. and Andreadis, S. (2015). CDH2 and CDH11 act as regulators of stem cell fate decisions. *Stem Cell Research*, **14**, 270-282.

Amiel, J., Benko, S., Gordon, C. and Lyonnet, S., 2010. Disruption of long-distance highly conserved noncoding events in neurocristopathies. *Annals of the New York Academy of Sciences,* **1214**, 34-46.

Anderson, R., Newgreen, D. and Young, H. (2006). Neural crest and the development of the enteric nervous system. *Neural Crest Induction and Differentiation*. *Advances in Experimental Medicine and Biology Vol. 589.* Edited by Saint-Jeannett, J-P. Springer Science and Business Media LLC, New York, USA. pp181-197.

Anon. (2013). Agilent RNA 6000 Nano Kit Guide. Agilent Technologies. Germany

Anon. (2015). Microelectrode Array Manual. Multichannel Systems. Germany.

Aruga, J. (2004). The role of Zic genes in neural development. *Molecular and Cellular Neuroscience*, 26, 205-221.

Auld, D. and Robitaille, R. (2003). Perisynaptic Schwann cells at the neuromuscular junction: Nerve and activity-dependant contributions to synaptic efficacy, plasticity and reinnervation. *The Neuroscientist*, 9(2), 144-157.

Avery, J., Menendez, L., Cunningham, M., Lovvorn III, H. and Dalton, S. Using induced pluripotent stem cells as a tool to understand nreurocristopathies. *Neural Crest Cells. Evolution Development and Disease.* Edited by Trainor, P. Elsevier, London, UK. pp 441-455.

Bae, C-J., Park, B., Lee, Y., Tobias, J., Hong, C. and Saint-Jeannet, J-P. (2014). Identification of Pax3 and Zic1 targets in the developing neural crest. *Developmental Biology,* **386**(2), 473-483.

Baharvnd, H. Fathi A., Gourabi, H., Mollamohammedi, S. and Salekdeh, G. (2007). Identification of mouse embryonic stem cell associated proteins. *Journal of Proteome Research*, **7**, 412-423.

Bandyopadhyay, A., Tsuji, K., Cox, K., Harfe, B. and Tabin, C. (2006). Genetic analysis of the roles of BMP2, BMP4 and BMP7 in limb patterning and skeletogenesis. *PloS One Genetics*, **2**(12), e216.

Barth, K., Kishimoto, Y., Rohr, K., Seydler, C., Schulte-Merker, S. and Wilson, S. (1999). Bmp activity establishes a gradient of positional information throughout the entire neural plate. *Development,* **126**, 497-4987.

Basch, M. and Bronner-Fraser, M. (2006). Neural crest inducing signals. *Neural Crest Induction and Differentiation*. *Advances in Experimental Medicine and Biology Vol. 589.* Edited by Saint-Jeannett, J-P. Springer Science and Business Media LLC, New York, USA. pp24-31.

Bastida, M., Sheth, R. and Ros, M. (2009). A BMP-*Shh* negative-feedback loop restricts *Shh* expression during limb development. *Development*, **136**, 3779-37789.

Betancour, P., Simoes-Costa, M., Sauker-Spengler, T. and Bronner-Fraser, M. (2014). Expression and function of transcription factor cMYB during cranial neural crest development. *Mechanisms of Development,* **132**, 38-43.

Bhatt, S., Diaz, R. and Trainor, P. (2013) Signals and switches in mammalian neural crest differentiation. *Cold Spring Harbour Perspectives in Biology*, **5**(2), a008326

Biehl, J. and Russel, B. (2009). Introduction to stem cell therapy. *Journal of Cardiovascular Nursing*, **24**(2), 98-103.

Bikfalvi, A., Klein, S., Pintucci, G. and Rifkin, D. (1997). Biological roles of fibroblast growth factor – 2. *Endocrine Reviews,* 18(1), 26-45.

Birrane, G., Soni, A., and Ladias, J. (2009). Structural basis for DNA recognition by the *Pax3* Homeodomain. *Biochemistry*, 48, 1148-1155.

Blake, J., and Ziman, M. (2013) The characterisation of Pax3 expressant cells in adult peripheral nerve *PLOS One*, **8**(3), e59184.

Blanke, M. and VanDongen, A. (2009). Activation mechanisms of the NMDA receptor. *Biology of the NMDA Receptor: Frontiers in Neuroscience.* Edited by Van Dongen. CRC Press, Bota Racon, USA. pp283-312.

Boix-Perales, H., Horan, I., Wise, H., Lin, H-R., Chuang, L-C., Yew, P. and Philpott, A. (2007). The E3 ubiquitin ligase skp2 regulates neural differentiation independent from the cell cycle. *Neural Development*, **2**(27), 1-16.

Bond, A., Bhalala, O. and Kessler, J. (2012).The dynamic role of bone morphogenetic proteins in neural stem cell fate and maturation, *Developmental Neurobiology, 72(7), 1068-1084.*

Brahimi, F., Ko, E., Malakhov, A., Burgess, K., and Saragovi, H. (2014). Combinatorial assembly of small molecules into bivalent antagonists of TrkA or TrkC receptors. *PLOS One , 9* (3), 1-12.

Bramanti, V., Tomassoni, D., Avitabile, M., Amenta, F. and Avola, R. (2010). Biomarkers of glial cell proliferation and differentiation in culture. *Frontiers in Bioscience*, **1**(2), 558-570.

Bronner, M. and LeDouarin, N. (2011). Development and evolutoin of the Neural Crest: An overview. *Developmental Biology,* **366(**1), 2-9.

Bronner-Fraser, M. (1994). Neural crest formation and migration in the developing embryo. *FASEB J.,***8**, 699-706.

Calisto, J., Araya, C., Marchant, L., Chaudhary, R. and Mayor, R. (2005). Essential role of non-canonical Wnt signalling pathway in neural crest migration. *Development,* **132**, 2587-2597.

Caspi, O., Lesman, A., Basevitch, Y., Gepstein, A., Arbel, G., Habib, I., Gepstein, L., and Levenberg, S. (2007). Tissue Engineering of Vascularized Cardiac Muscle From Human Embryonic Stem Cells. *Circulation Research,* **100**(2), 255-262.

Chai, Y., Jiang, X., Ito, Y., Bringas, P., Han, J., Rowitch, D., Soriano, P., McMahon, A and Sucov, H. (2000). Fate of the mammalian neural crest during tooth and mandibular morphogenesis. *Development,***127**, 1671-1679.

Chalazontis, A. and Kessler, J. (2012). Pleiotropic effects of the bone morphogenetic proteins on the development of the enteric nervous system. *Developmental Neurobiology*, **72**(6), 843-856.

Chen, S., Velardez, M., Warot, X., Miller, S., Cross, D. and Corfas, G. (2006). Neuregulin 1-erbB signalling is necessary for normal myelination and sensory function. *The Journal of Neuroscience*, **26**(12), 3079-3086.

Cheung, M. and Briscoe, J. (2003). Neural rest development is regulated by the transcription factor Sox9. *Evelopment*, **130**, 681-5693.

Choudhary, C., Kumar, C., Gnad, F., Nielson, M., Rehman, M., Walthers, T., Olsen, J. and Mann, M. Lyseine acetylation targets protein complexes and co-regulates major cellular functions. *Science*, **325**(5942), 834-840.

Corfas, G., Velardez, M., Ko, K-P., Ratner, N. and Peles, E. (2004). Mechanisms and roles of axon-Schwann cell interactions. *The Journal of Neuroscience*, **24**(42), 9250-9260.

Clay, M., and Halloran, M. (2010). Control of neural crest behaviour and migration. *Cell Adhesion and Migration*, **4**(4), 586-594.

Clark, E., and Brugge, J. (1995). Integrins and signal transduction pathways: The road taken. *Science,* **268**(5208), 233-241.

Cleary, A., Leonard, T., Gesti, S. and Gunther, E. (2014). Tumour cell hetrogeneity maintained by cooperating subclones in Wnt-driven mammary cancers. *Nature,* **508**(7494), 113-117.

Corfas, G., Velardez, M., Ko, K-P., Ratner, N. and Peles, E. (2004). Mechanisms and roles of axon-Schwann cell interactions. *The Journal of Neuroscience*, 24(42), 9250-9260.

Craig, A. and Kang, Y. (2007). neurexin-neuroligin signalling in synapse development. *Current Opinion in Neurobiology*, (**17**), 1, 1-16.

Curradi, M., Izzo, A., Badaracco, G. and Landsberger, N. (2002). Molecular models of gene silencing mediated by DNA methylation. *Molecular and Cellular Biology,* **22**(9),3167-3173.

Dai, X., Jiang, W., Zhang, Q., Xu, L., Geng, P., Zhuang, S., Petrich, B., Jiang, C., Peng, L., Bhattacharya, S., Evans, S., Sun, Y., Chen, J. and Liang, X. (2013). Requirement for integrin linked kinase in neural crest migration and differentiation and outflow tract morphogenesis. *BMC Biology*, **11**, 107-122.

De Moerlooze, L., Spencer-Dene, B., Revest, J-M., Hajihosseini, M., Roswell, I. and Dickson, C. (2000). An important role for the IIIb form of fibroblast growth factor receptor 2 (FGFR2) in mesenchymal-epithelial signalling during mouse organogenesis. *Development,* 127, 483-492.

Dean, C. and Dresbach, T. (2006). Neuroligins and Neurexins: Linking cell adhesion, synapse formation and cognitive function. *Trends in Neuroscience*, **29**,(1), 21-29.

Delalande, J-M., Natarajan, D. Vernay, B., Finlay, M., Ruhrbrg C., Thaar, N. ad Burns, A. (2014). Vascularisation is not necessary for gut colonisation by tri curls. *Developmental Biology*, **385**, 220-229.

Di Cello, F., Cope, L., Li, H., Jeschke, J., Wang, W., Baylin, S. and Zahnow, C. (2013). Methylation of the *Claudin 1* promoter is associated with loss of expression in estrogen receptor positive breast cancer. *PLOS One*, **8**(7), E68630.

Djuric, U. and Ellis, J. (2010). Epigenetics of induced pluripotency, the seven headed dragon. *Stem cell research and therapy,* **3**(1), 1-6.

Dolgin, E. (2011). Flaw in induced stem cell model. *Nature,* **470**(7332),13.

Dourain, N. and Dupin, E., (2014). The neural crest, a fourth germ layer of the vertebrate embryo: Significance in evolution. *Neural Crest Stem Cells. Evolution Development and Disease*. Edited by Trainor, P. Elsevier, MA, USA. pp4-22.

Du, J., Chen, T., Zou, X., Xiong, B. and Lu, G. (2010). *Dppa2* knockdown-induced differentiation and repressed proliferation of mouse embryonic stem cells. *The Journal of Biochemistry*, **147**(2), 265-271.

Duband, J-L. (2006) Neural crest delamination and migration: Integrating regulations of cell interactions, locomotion, survival and fate. *Neural Crest Induction and Differentiation*. Edited by Saint-Jeannet, J-P. Springer Science and Business Media LLC. New York, US. pp 45-78.

Dupin, E., Creuzet, S. and Douarin, N. (2006). The contribution of the neural crest to the vertebrate body. *Neural Crest Induction and Differentiation*. *Advances in Experimental Medicine and Biology Vol. 589.* Edited by Saint-Jeannett, J-P. Springer Science and Business Media LLC, New York, USA, pp 97-119.

Dupin, E. and Sommer, L. (2012). Neural crest progenitors and stem cells: From early development to adulthood. *Developmental Biology,* **366**(1), 83-95.

Ďurčová, G., Yamaguchi, M., Takahashi, S. and Imai, H.(1998). Immunomagnetic isolation of mouse embryonic stem cells from heterogeneous cell population. *Journal of Reproduction and Development,* **44**(1), 85-89.

Dykes, I., Lanier, J., Eng, S and Turner, E. (2010). Brn3a regulates neuronal subtype specification in the trigeminal ganglion by promoting Runx expression during sensory differentiation. *Neural Development*, **5**(3), 1-18.

Eriksson, K., Zhang, S., Lin, L., Lariviére, R. Julien, J-P. and Mignot, E. (2008). The type III neurofilament peripherin is expressed in the tuberomammillary neurons of the mouse. *BMC Neuroscience,* **9**(26), 1-9.

Etchevers, H., Amiel, J. and Lyonnet, S. (2006). Molecular basis of human neurocristopathies. *Neural Crest Induction and Differentiation*. *Advances in Experimental Medicine and Biology Vol. 589.* Edited by Saint-Jeannett, J-P. Springer Science and Business Media LLC, New York, USA, pp213-234.

Fabrinchy, I., Leone, P., Sulzenbacher, G., Comoletti, D., Miller, M., Taylor, P., Bourne, Y. and Marchot, P. (2007). Structural analysis of the synaptic protein neuroligin and its β-neurexin complex: determinants for folding and cell adhesion. *Neuron,* **56**(6), 979-991.

Fairchild, C., Conway, J., Schiffmacher, A., Tanevhill, L. and Gammil, S. (2014). FoxD3 regulates cranial neural crest EMT via downregulation of tetraspanin 18 independant of its functions during neural crest formation.. *Mechanisms of Development,* **132**,1-12.

Fei, T., Xia, K., Li, Z., Zhou, B., Chen, H., Zhang, J., Chen, Z., Xiao, H., Han, J-D. and Chen, Y-G. (2010). Genome-wide mapping of SMAD target genes reveals the role of BMP signalling in embryonic stem cell fate determination. *Genome Research*, **20**, 36-44.

Feinburg-Gorenshtein, G., Guedj, A. Shichrur, K., Jeison, M., Luria, D., Kodman, Y., Ash, S., Feinmesser, M., Edry, L., Shomrom, N., Weizma, A., Yaniv, I. and Avigad, S. (2013). miR-192 directly binds and regulates Dicer1 exression in neuroblastoma. *PLoS One*, **8**(11), 78313-78322.

Feng, J., Gao, J., Li, Y., Yang, Y., Dang, L., Ye, Y., Deng, J. and Li, A. (2014). BMP4 enhances foam cell formation by BMPR-2/SMAD1/5/8 signalling. *International Journal of Molecular Science*. **15**, 5536-5552.

Fisher, M., Ferrari, D.,Li., Y., Shepard, J., Patterson, S., Anderson, N. and Dealy, C. (2012). The potential of human embryonic stem cells for articular cartilage repair and osteoarthritis treatment. *Rheumatology: Current Research,* **3**(4), 1-10.

Fishwick, K., Neiderer, T., Jhinghory, S., Bronner, M. and Taneyhill, L. (2012). The tight junction protein claudin-1 influences cranial neural crest cell emigration. *Mechanisms of Development*, **129**, 275-283.

Fujita, K., Ogawa, R., Kawawaki, S. and Ito, K. (2014). Roles of chromatin remodelers in maintenance mechanisms of multipotency in mouse trunk neural crest cells in the formation of neural crest-derived cells. *Mechanisms of Development*, **133**, 126-135.

Fung, M., Viveros, O. and O'Connor, D. (2008). Diseases of the adrenal medulla. *Acta Physiologica*, **192**(2), 325-335.

Garcez, R., Douarin, N. and Creuzet, S. (2014). Combinatorial activity of Six1-2-4 genesin cephalic neural crest cells control craniofacial and brain development. *Cellular and Molecular Life Sciences,* **71**(1), 2149-2164.

Glenn, T. and Talbot, W. (2013). Signals regulating myelination in peripheral nerves and the Schwann cell response to injury. *Current Opinion in Neurobiology,* **23**(6), 1041-1048.

Goding, C. (2000). Mitf from neural crest to melanoma: signal transduction and transcription in the melanocyte lineage. *Genes Development*, **14**, 1712-1728.

Goldman, S. and Windrem, M. (2006). Cell replacement therapy in neurological disease. *Philosophical Transactions of the Royal Society,* **361**, 1463-1475.

Gong, S-G. (2014). Cranial neural crest: Migratory cell behavior and regulatory networks. *Experimental Cell Research*, **325**, 90-95.

Gonsalvez, D., Li-Yuen-Fong, M., Cane, K., Stamp, L., Young, H. and Anderson, C. (2015). Different neural crest populations exhibit diverse proliferative behaviours. *Developmental Neurobiology*, **75**(3), 287-301.

Graf, U., Casanova, E. and Cinelli, P. (2011). The role of the leukemia inhibitory factor (LIF) — pathway in derivation and maintenance of murine pluripotent stem cells. *Gene,* **2**, 280-297.

Gu, B., Zhang, J., Wang, W., Mo, L., Chen, L., Liu, Y. and Zhang, M. (2010). Global expression of cell surface proteins in embryonic stem cells. *PLoS One,* **5**(12), e15795.

Hagiwara, K., Obayashi, T., Sakayori, N., Yamanishi, E., Hayashi, R. Osumi, N., Nakazawa, T. and Nishida, K. (2014). Molecular and cellular features of murine craniofacial and trunk neural crest cells as stem cell-like cells. *PLOS One*, **9**, 1, 84072-84085

Hall, B.( 2008). The neural crest and neural crest cells: Discovery and significance for theories of embryonic organisation. *J. Biosci.,* **33**(5), 781-793

Hanani, M. (2005). Satellite glial cells in sensory ganglia: From form to function. *Brain Research Reviews*, 48, 457-476.

Heldin , C-H. Miyazono, K. and Dijke, P. (1997). TGF-β signalling from cell membrane to nucleus through SMAD proteins. *Nature*, **390**, 465-471.

Hegarty, S., O'Keeffe, G. and Sullivan, A. (2013). BMP-SMAD 1/5/8 signalling in the development of the nervous system. *Progress in Neurobiology*, **109**, 28-41.

Henderson, D and Chaudhry, B. (2012) The new heart for the new head. *Neural Crest Stem Cells. Breakthroughs and Applications*. Edited by Sieber-Blum, M. World Scientific, New Jersey, USA. pp3-34.

Heo, J., Lee, J., Takahama, Y. and Thorgeirsson, S. (2005). Spontaneous differentiation of mouse embryonic stem cells. *Biochemical and Biophysical Research Communications,* **332**, 1061-1069.

Herman, J., Graff, J., Myöhänen, S., Nelkin, B. and Baylin, S.(1996). Methylation specific PCR: A novel PCR assay for methylation status of CpG islands. *PNAS,* Volume **93**(18), 9821-9826.

Himada, C., Barro, M. and Emerson, C. (2013). Pax3 synergizes with Gli2 and Zic1 in transactivating the Myf5 epaxial somite enhancer. *Developmental Biology,* Volume **383**, 7-14.

His, W. (1868). Studies of the first system of the vertebrate body: The first development of the chick in the bird egg. FCW, Leipzig, Germany p237.

Ho, L. and Crabtree G. (2010). Chromatin remodelling during development. Nature, 436(7041), 474-485.

Holland, S., Hessler, R., Reis-Nicholson, M., Ramalingam, P. and Lee, J. (2010). Utilization of peripherin and S-100 immunohistochemistry in the diagnosis of Hirchsprung disease. *Modern Pathology,* **23**, 1173-1179.

Hong, C. and Saint-Jeannet, J.-P. (2005). Sox proteins and neural crest development. *Seminars in cell and developmental biology,* **16**(6), 694-703.

Hu, N., Strobl-Mazzulla, P. and bronner, M. (2014). Epigenetic regulation in neural crest development. *Developmental Biology*, **396**, 159-168.

Hu, N. Strobl-Mazzulla, P., Simoes-Costa, M., Sánchez-Vásquez, E. and Bronner, M. (2015). DNA methyltransferase 3B regulates duration of neural crest production via repression of *Sox10*. *PNAS*, **111**(50), 17911-17916.

Huang, E., and Reichardt, L. (2003). Trk receptors: Roles in neural signal transduction. *Annual Review of Biochemistry, 72*, 609-642.

Huang, X. and Siant-Jeannet, J.-P. (2004). Induction of the neural crest and opportunitied for life on the edge. *Developmental Biology,* **275**, 1-11.

Huang, D, Sherman, B., Tan, Q., Collins, J., Alvord, W., Roayaei, J., Stephens, R., Baseler, M., Lane, H. and Lempicki, R. (2007). The DAVID functional classification tool: A novel biological module-centric algorithm to functionally analyze large gene lists. *Genome Biology,* (**8**), 9, R183-R183.16Ibáñez, C. (2013). Structure and physiology of the RET receptor tyrosie kinase. *Cold Spring Harbour Perspectives In Biology*, **5**, 9134-9144.

Huang, M. and Weiss, W. (2013). Neuroblastoma and MYCN. *Cold Spring Harbour Perspectives in Medicine*, **3**, a014415.

Inoue, K-I, Shiga, T and Ito, Y. (2008). Runx transcrition factors in neuronal development. *Neural Development*, **3**(20), 1-7.

Irizarry, R., Bolstad, B., Collin, F., Cope, L., Hobbs, B. and Speed, T. (2003). Summaries of Affymetrix gene chip probe level data. *Nucleic Acids Research*, **31**(4), e15.

Jenson, N., Garvey, J., Miller, C. and Hood, L.(1993). Transgenic mouse model for neurocristopathies: Schwannomas and facial bone tumors. *PNAS,* Volume **90**, 3192-3196.

Jerabek, S., Merino, F., Schöler, H. and Cojucaru, V. (2014). Oct4: Dynamic DNA binding pioineers stem cell pluripotency. *Biochimica et Biophysica Acta*, **1839**, 138-154.

Jiang, X., Gwye, Y., McKeown, S., Bronner-Fraser, M., Lutzko, C. and Lawlor, E. (2009). Isolation and characterization of neural crest stem cells from *in vitro*-differentiated human embryonic stem cells. *Stem Cells and development*, **18** (7), 1059-1070.

Jin, S., Martinelli, D., Zheng, X., Tessier-Lavigne, M. and Fan, C-H. (2015). Gas1 is a receptor for sonic hedgehog to repel enteric axons. *PNAS*, **112**(1), 73-83.

Kam, M., and Lui, V. (2015). Roles of Hoxb5 in the development of vagal and trunk neural crest cells. *development, Growth and Differentiatio*n, **57**, 158-168.

Kaneko, Y., Suenaga, Y., Islam, S., Matsumoto, D., Nakamura, Y., Ohira, M., Yokoi, S. and Nakagawara, A. (2015). Functional interplay between MYCN, NYCM and OCT4 promotes aggressiveness of human neuroblastomas. *Cancer Science*, **106**(7), 840-847.

Kaucka, M. and Ademakyko, I. (2014). Non-canonical functions of the peripheral nerve. *Experimental Cell Research,* **321**(1), 17-24.

Kaur, J., Madan, R., Sharma, D., Julka, P., Rath, G. and Roy, S. (2015). Malignant peripheral nerve sheath tumour of penis. *Andrologia*, **47**, 333-335.

Keller, G., (2005). Embryonic stem cell differentiation: Emergence of a new era in biology and medicine. *Genes and Development*, **19**, 1129-1125.

Kennedy, K., Porter, T., Mehta, V., Ryan, S., Price, F., Peshdary, V., Karamboulas, C., Savage, J., Drysdale, T., Li, S-C., Bennet, S. and Skerjanc, I. (2009). Retinoic acid enhances skeletal muscle progenitor formation and bypasses inhibition by bone morphogenetic protein 4 but not dominant negative β-catenin. *BMC Biology*, **7**(67). 1-21.

Kim, S-K., Suh, M., Yoon, H., Lee, J., Oh, S., Moon, S., Moon, S-H., Lee, J-Y., Hwang, J., Cho, W. and Kim, K-S.(2005). Identification of developmental pluripotency associated 5 expression in human pluripotent stem cells. *Stem Cells*, **23**, 458-462.

Kim, H., Kang, T. and Kim, J. (2013). Environmental effects on the epigenetics of neural crest development. *OA Molecular and Cell Biology,* **1**(1), 1-4.

Kipanyula, M., Kimaro, W., Yepnjio, F., Aldebasi, Y., Farahna, M., Kamdje, A., Abdel-Magied, E. and Etet, S. (2014). Signalling pathways bridging fate

determination of neural crest cells to glial lineages in the developing peripheral nervous system.. *Cellular Signalling,* **26**(4), 673-682.

Ko, T-L., Chien, C-L. and Lu, K-S. (2005). The expression of α-interexin and peripherin in the mouse pineal gland. *Journal of Biomedical Science*, **12**, 777-789.

Kramer, J., Hegert., C., Guan, K., Wobus, A., Müller, P. and Rohwedel, J. (2000). Embryonic stem cell-derived chondrogenic differentiation *in vitro*: Activation by BMP-2 and BMP-4. *Mechanisms of Development*, **92**, 193-205.

Kreitzer, F., Salamonis, M., Sheehan, A., Huang, M., Park, J., Spindler, M., Lizarraga, P., Weiss, W., So., P-L. and Conklin, B. (2013). A robust method to derive functional neural crest cells from human pluripotent stem cells. *American Journal of Stem Cells,* **2**(2), 119-131.

Krueger, D., Tuffy, L., Papadopoulos, T. and Brose, N. (2012). The role of neurexins and neuroligins in the formation, maturation and function of vertebrate synapses. *Current Opinion in Neurobiology*, (**22**), 3, 412-422.

Kuo, Y-T., Liu, Y-L., Adebayo, B., Shih, P-H., Lee, W-H., Wang, L-S., Liao, Y-F., Hsu, W-M., Yeh, C-T., Lin, C-M. (2015). JARID1B expression plays a critical role in chemoresistance and stem cell-like phenotype of neuroblastoma cells. *PLoS One,* **10**(5), e0125343.

Lajiness, J., Snider, P., Wang, J., Feng, G-S., Krenz, M. and Conway, S. (2014). SHP-2 deletion in postmigratory neural crest cells results in impaired cardiac innervation. *PNAS,* **111**(14), E1374-1382.

Lang, D., Chen, F., Milewski, R., Li, J., Lu, M. and Epstein, J. (2000). Pax3 is required for enteric ganglia formation and functions with Sox10 to modulkate expression of C-ret. *Journal of Clinical Investigation,* **106**, 963-971.

Lanner, F., Lee, K., Sohl, M., Holmborn, K., Yang, H., Wilbertz, J., Poellinger, L., Rossant, J. and Farnebo, F. (2010). Heparan sulfation–dependent fibroblast growth factor signalling maintains embryonic stem cells primed for differentiation in a heterogeneous state. *Stem Cells,* **28**, 191-200.

Lavasani, M., Thompson, S., Pollet, J., Usas, A., Lu, A., Stolz, D., Clark, K., Sun, B., Péault, B. and Huard, J. (2014). Human muscle-derived stem/progenitor cells promote functional murine peripheral nerve regeneration. *The Journal of Clinical Investigation*, **124**(4), 1745-1756.

LeBlanc, S., Jang, S-W., Ward, R., Wrabetz, L. and Svaren, J. (2006). Direct regulation of myelin protein zero expression by the egr2 transactivator. *The Journal of Biological Chemistry*, **281**(9), 5453-5460.

Le Douarin, M. (2004). The avian embryo as a model to study the neural crest: A long and still ongoing story. *Mechanisms of Development*, **121**, 1089-1102.

Le Dourain, N. and Dupin, E. (2014). The neural crest, a fourth germ layer of the vertebrate embryo: Significance in evolution. *Neural Crest Cells. Evolution Development and Disease.* Edited by Trainor, P. Elsevier, London, UK. pp 4-22.

Lee, G., Kim, H., Elkabetz, Y., Shamy, G., Panagiotakos, G., Barberi, T., Taber, V. and Studer, L. (2008). Isolation and directed differentiation of neural crest stem cells derived from human embryonic stem cells. *Nature Biotechnology,* **25**(12), 1486-1475.

Lee, H-K., Lee, S-H., Lee, K-Y., Lim, E-J., Choi, S-Y., Park, R-K., Kim, U-K. (2009). Novel *POU3f4* mutations and clinical features of DFN3 patients with cochlear implants. *Clinical Genetics,* **75**, 572-575.

Lee, J-H., Bhang, D., Beede, A., Huang, T., Stripp, B., Bloch, K., Wagers, A., Tseng, Y-H., Ryeom, S. and Kim, C. (2014). Lung stem cell differentiation in mice directed by endothelial cells via a BMP4-NFATc1-Thrombospondin-1 axis. *Cell*, **156**(3), 440-455.

Lee, Y., Kim, K-H. and Song, G. (2014). Genome wide pathway analysis in neuroblastoma. *Tumour Biology*, **35**, 3471-3485.

Leim, K., Tremi, G., Roelink, H. and Jessel, T. (1995). Dorsal differentiation of neural plate cells induced by BMP-mediated signals from epidermal ectoderm. *Cell,* **82**, 969-979.

Levanon, D., Bettoun, D., Harris-Cerruti, C., Woolf, E., Negreanu, V., Eliam, R., *et al*. (2002). The runx3 transcription factor regulates development and survival of TrkC dorsal root ganglia neurons. *The EMBO Journal , 21* (13), 3454-3463.

Lister, R. Pelizzola, M., Kida, Y., Hawkins, D., Nery, J., Hon, G., Antosiewicz-Bourget, J., O'Malley, R., Castanon., R., Klugman, S., Downes, M., Yu, R., Stewart, R., Ren, B., Thomson, J., Evans, R. and Ecker, J. (2011). Hotspots of aberrant epigenetic reprogramming in human induced pluripotent stem cells. *Nature*, **471**, 68-73.

Li, H., Huang, J., Du, W., Jia, C., Yao, H. and Wang, Y. (2012). TRPC6 inhibited NMDA receptor activities and prevented neurons from ischemic excitotoxicity. *Journal of Neurochemistry*, **123**, 1010-1018.

Li., Z. Zhu, X., Chen, M., Cheng, L., Zhou, D., Lu, M., Du, K., Epstein, J. and Parmacek, M. (2005), Myocardin-related transcription factor B is required in cardiac neural crest for smooth muscle differentiation and cardiovascular development. *PNAS*, **102**(25), 8916-8921.

Li, Z., Fei, T., Zhang, J., Zhu, G., Wang, L., Lu, D., Chi, X., Teng, Y., Hou, N., Yang, Y., Zhang, H., Han, J-D. and Chen, Y-G. (2011). BMP4 signaling acts via dual-specificity phosphatase 9 to control ERK activity in mouse embryonic stem cells. *Cell Stem Cell*, **10,** 171-182.

Lilley, K. and Freidman, D. (2005). All about DIGE: quantification technology for differential-display 2D-gel proteomics. *Expert Review of proteomics*, **4**, 401-409.

Liu, J. and Ngan, E. (2014). Hedgehog and notch signaling in enteric nervous system development. *Neurosignals*, **22**, 1-13.

Liu, J., Wu, M-H., Yan, C., Chau, B., So, H., Ng, A., Chan, A., Cheah, K., Briscoe, J. and Cheung, M. (2013). Phosphorylation of Sox9 is required for neural crest delamination and is regulated downstream of BMP and canonical Wnt signalling. *PNAS*, **110**(8), 2882-2887.

Liu, Y-J., Nakamura, T. and Nakamo, T. (2012). Essential role of *Dppa3* for chromatin condensation in mouse oocytogenesis. *Biology of Reproduction*, **86**(2), 1-8.

Lo, L. and Anderson, D. (1995). Postmigratory neural crest cells expressing c-Ret dislay restricted developmental and proliferative capabilities. *Neuron*, **15**, 527-539.

Lo, L., Tiveron, C. and Anderson, D. (1998). MASH1 activates expression of the paired homeodomain transcription factor Phox2a, and couples pan-neuronal and subtype-specific components of autonomic neuronal identity. *Development*, **125**, 609-620.

Loh, Y-H., Wu, Q., Chew, J-L., Vega, V., Zhang, W., Chen, X., Borque, G., George, J., Leong, B., Liu, J., Wong, K-Y., Sung, K., Lee, C., Zhao, X-D., Chiu, K-P., Lipovich, L., Kuznetzov, V., Robson, P., Stanton, L., Wei, C-L., Ruan, Y., Lim, B. and Ng, H-H. (2006). The Oct4 and Nanog transcription network regulates pluripotency in mouse embryonic stem cells. *Nature Genetics*, **38**(4), 431-440.

Lunyak, V. and Rosenfield, M. (2008). Global epiproteomic signatures distinguish embryonic stem cells from differentiated cells. *Stem Cells,* **17**(1), 28-36.

Maczkowiak, F., Matéos, S., Wang, E., Roche, D., Harland, R. and Monsoro-Burq, A. (2010). The Pax3 and Pax7 paralogs cooperate in neural and neural crest patterning using distinct molecular mechanisms, in *Xenopus laevis* embryos. *Developmental Biology*, **340**(2), 381-396.

Magnaghi, V., Consoli, B., lambert, J., Roglio, I. and Melcanngi, R. (2006). GABA receptor-mediated effects in the peripheral nervous system: A cross-interaction with neuroactive steroids. *Journal of Molecular Neuroscience*, **28**(1), 89-102.

Mao, C-A., Kiyama, T., Pan, P., Furuta, Y., Hadjantonakis, A-K. and Klein, W. (2008). Eomesodermin, a target of Pou4f2, is required for retinal ganglion cell and optic nerve development in the mouse. *Development*, **135**, 271-280.

Marchant, L., Linker, C., Ruiz, P and Mayor, R. (1999). The inductive properties of mesoderm suggest that the neural crest cells are specified by a BMP gradient. (1999). *Developmental Biology*, **198**, 319-329.

Martin, G. (1981). Isolation of a pluripotent cell line from mouse embryos cultured in medium conditioned by teratocarcinoma stem cells. *PNAS,* **78**(12), 7638-7648.

Martinez-Morales, P., del Corral, R., Olivera-Martinez, I., Quironga, I., Das, R., Barbas, J., Storey, K. and Morales, A. (2011). FGF and retinoic activity gradients control the timing of neural crest emigration in the trunk. *Journal of Cell Biology*, **194**(3), 489-503.

McMahon, J., Takada, S., Zimmerman, L., Harland, R. and McMahon, A. (1998). Noggin-mediated antagonism of BMP signalling is required for growth and patterning of the neural tube and somite. *Genes Development* **12**(10), 1438-1452.

Miharada, K., Sigurdsson, V. and Karlsson, S. (2014). Dppa5 improves hematopoietic stem cell activity by reducing endoplasmic reticulum stress. *Cell Reports*, **7**, 1381-1392.

Milet, C., Maczkowiak, F., Roche, D., and Mosoro-Burq, H. (2013). Pax3 and Zic1 drive induction and differentiation of multipotent, migratory and functional neural crest in Xenopus embryos. *PNAS , **110**(14)*, 5228-5233.

Mizuseki, K., Sakamoto, T., Watanabe, K., Muguruma, K., Ikeya, M., Nishiyama, A., Arakawa, A., Suemori, H., Nakatsuji, N., Kawasaki, H., Murakami, F. and Sasai, Y. (2003). Generation of neural crest derived peripheral neurons and floor plate cells from mouse and primate embryonic stem cells. *PNAS*, **100**(10), 5828-5833.

Moore, R., Theveneau, E., Pozzi, S., Alexandre, P., Richardson, J., Merks, A., Parsons, M., Kashef, J., Linker, C. and Mayor, R. (2013). Par3 controls neural crest migration by promoting microtubule catastrophe during contact inhibition of locomotion. *Development*, **140**, 4763-4775.

Moore, S., Ribes, V., Terriente, J., Wilkinson, D., Relaix., F. and Briscoe., J. (2013). Distinct regulatory mechanisms act to establish and maintain *Pax3* expression in the neural tube. *PLoS One*, **9**(10) e1003811.

Motohashi, T., Kitagawa, D., Wanatabe, N. and Kunisada, T. (2013). Neural-crest derived cells sustain their multipotency after entry into their target tissues. *Developmental Dynamics,* **243**, 368-380.

Mukhopadhyay, D. and Riezman, H. (2007). Proteasome-independent functions of ubiquitin in endocytosis and signalling. *Science*, **315**(5809), 201-205.

Murgatroyd, C. and Spengler, D. (2014). Polycomb Binding Precedes Early-Life Stress Responsive DNA Methylation at the Avp Enhancer. *PLoS One,* **9**(3), e90277.

Narazaki, G., Uosaki., H., Teranishi, M., Okita, K., Kim, B., Matsuoka, S., Yamanaka, S. and Yamashita, J. (2008). Directed and systematic differentiation of cardiovascular cells from mouse pluripotent stem cells. *Circulation,* **118**, 498-506.

Ng, C., Li, N., Chee, S., prabhakar, S., Kolatkar, P. and Jauch, R. (2012). Deciphering the Sox-Oct partner code by quantitative cooperativity measurements. *Nucleic Acids Research*, **40**(11), 4933-4941.

Nicholson, K. and Anderson, N. (2002). The protein kinase B/Akt signalling pathway in human malignancy. *Cellular Signalling*, **14**, 381-395.

Niclis, J., Trounson, A., Dottori, M., Ellisdon, A., Bottomly, S., Verlinsky, Y. and Cram, D. (2009). Human embryonic stem cell models of Huntington disease. *Reproductive Biomedicine Online,* **19**(1), 106-113.

Nikoletopoulu, V., Licert, H., Frade, J., Rencurel, C., Giallonardo, P., Zhang, L., Bebel, M. and Barde, Y-A. (2010). Neurotrophin receptors TrkA and TrkC cause neuronal death whereas TrkB does not. *Nature,* **467**(7311), 59-63.

Niwa, H., Miyazaki, J-I. and Smith, A. Quantitative expression of Oct3/4 defines differentiation, dedifferentiation or self-renewal of ES cells. *Nature Genetics*, **24**, 372-376.

Ohtsuka, Y., Matsumoto, J., Katsuyama, Y. and Okamura, Y. (2014). Nodal signalling regulates specification of ascidian peripheral neurons through control of the BMP signal. *Development*, **141**, 3889-3899.

Okano, H., Kawahara, H., Toriya, M., Nakao, K., Shibata, S. and Imai, T. (2005). Function of RNA-binding protein Masashi-1 in stem cells. *Experimental Cell Research*, **306**, 349-356.

Okumura-Nakanshini, S., Saito, M., Niwa, H. and Ishikawa, F. (2004). Oct-3/4 and Sox2 regulate Oct-3/4 gene in embryonic stem cells. *The Journal of Biological Chemistry,* **280**(7), 5307-5317.

Olapoa, M. and Conway, S. (2012) Dual but converging roles: A tale of two crests. *Neural Crest Stem Cells. Breakthroughs and Applications*. Edited by Sieber-Blum, M. World Scientific, New Jersey, USA, pp35-75.

Ono, H., Kozmik, Z., Yu, J.-K. and Wada, H. (2014). A novel N-terminal motif is responsible for the evolution of neural crest-specific gene-regulatory activity in vertebrate Fox3D. *Developmental Biology,* **385**, 396-404.

Osborn, D., Roccasecca, R., McMurray, F., Hernandez-Hernandez, V., Muckherjee, S., Barosso, I., Stemple, D., Cox, R., Beales, P. and Christou-Savina, S. (2014). Loss of FTO antagonises Wnt signallingand leads to developmental defects associated with ciliopathies. *PLOS One,* **9**(2), e87662.

Osei-Bempong, C., Ali, H. and Ahmad, S. (2012). The cornea, neural crest and stem cells. *Neural Crest Stem Cells. Breakthroughs and Applications*. edited by Sieber-Blum, M. World Scientific, New Jersey, USA, pp 75-83.

Pederson, W., Becker, L. and Yeger, H. (1993). Expression and distribution of peripherin protein in human neuroblastoma cell lines. *International Journal of Cancer*, (**53**), 3 463-470.

Perra, M. (2011). The dark side of induced pluripotency. *Nature,* **471**(7336), 46-47.

Pesce, M., Wang, X., Wolgemuth, D. and Scöler, H. (1998). Differential expression of the Oct-4 transcription factor during mouse germ cell differentiation. *Mechanisms of Development*, **71**(1-2), 89-98.

Plotnikov, A., Hubbard, S., Schlessinger, J. and Mohammedi, M. (2000). Crystal structures of two FGF-FGFR complexes reveal the determinants of ligand-receptor specificity. *Cell*, **101**, 413-424.

Plouhinec, J., Roche, D., Pegoraro, C., Figureueirido, A., Maczowiak, F., Milet, C., Vert, J., Pollet, N., Harland, R. and Monsoro-Burg, A. (2014). Pax3 and Zic1 trigger the early neural crest gene regulatory network by the direct activation of multiple key neural crest specifiers. *Developmental Biology , **386***, 361-472.

Powekk, D., O'Brien, J., Ford, H. and Arttinger, J. (2014). Neural crest cells and cancer: Insights into tumor progression. *Neural Crest Cells. Evolution Development and Disease.* Edited by Trainor, P. Elsevier, London, UK. pp 335-349.

Prendergast, A. and Raible, D. (2014). Neural crest cells and peripheral nervous system development. *Neural Crest Cells. Evolution Development and Disease.* Edited by Trainor, P. Elsevier, London, UK. pp256-276.

Pruszak, J., Ludwig, W., Blak, A., Alavian, K. and Isacson, O. (2009). CD15, CD24, and CD29 define a surface biomarker code for neural lineage differentiation of stem cells. *Stem Cells,* **27(**12)*,* 2928-2940.

Purves, D., Augustine, G., Fitzpatrick, D., Hall, W., LaMantia, A-S. and White, L. (Editors). (2012). *Neuroscience 5$^{th}$ Edition*, Sinaeur Associates, Inc. Sunderland, USA.

Raible, D. and Ungos, J. (2006). Specification of sensory neuron cell fate from the neural crest. *Neural Crest Induction and Differentiation*. *Advances in Experimental Medicine and Biology Vol. 589.* Edited by Saint-Jeannett, J-P. Springer Science and Business Media LLC, New York, USA, pp 170-180.

Rajeevan, M., Ranamukhaarachchi, D., Vernon, S. and Unger, E. (2001). Use of real-time quantitative PCR to validate the results of cDNA array and differential display PCR technologies. *Methods*, **25**, 443-451.

Ramm, P., Couillard-Despres, S., Plötz, S., Rivera, F., Krampert, M., Lehner, B., Kremer, W., Bogdahn, U., Kalbitzer, H. and Aigner, L. (2009). A nuclear magnetic

resonance biomarker for neural progenitor cells: Is it all neurogenesis? *Stem Cells*, **27**, 420-423.

Rao, T. and Kühl, M. (2010). An updated overview on Wnt signaling pathways. A prelude for more. *Circulation Research,* **106**, 1798-1806.

Raible, D., and Ungos, J. (2006). Specification of sensory neuron cell fate from the neural crest. *Neural Crest Induction and Differentiation. Advances in Experimental Medicine and Biology Vol. 589.* Edited by Saint Jeunett, J-P. Springer Science and Business Media LLC. New York. USA. pp170-180.

Rajeevan, M., Vernon, S., Taysavang, N and Unger, E. (2001). Validation of array based gene expression profiles by real-time (kinetic ) PCR. *Journal of Molecular Diagnostics*, **3**(1), 26-31.

Reiprich, S., Stolt, C., Schreiner, S., Parlato, R. and Wenger, M. (2008). SoxE proteins are differentially required in mouse adrenal gland development. *Molecular Biology of The Cell*, **19**, 1575-1586.

Retting, K., Song, B., Yoon, B. and Lyons, K. (2009). BMP canonical SMAD signaling through SMAD1 and SMAD5 is required for endochronal bone formation. *Development*, **136**, 1093-1104.

Rihani, A., De Wilde, B., Zeka, F., Laureys, G., Francotte, N., Tonini, G., Coco, S., Versteeg, R., Noguera, R., Schulte, J., Eggert, A., Stallings, R., Speleman, F., Vandesompele, J., Van Maerken, T. (2014) *CASP8* SNP D302H (rs1045485) is associated with worse survival in *MYCN*-amplified neuroblastoma patients. *PLoS One*, **9**(12), e114696.

Rosai, J. (2011). The origin of neuroendocrine tumours and the neural crest saga. *Modern Pathology,* **24**, 53-57.

Ruau, D., Ensat-Waser, R., Dinger, T., Vallabhapurapu, D., Rolletschek, A., Hacker, C., Hieronymous, T., Wobus, A., Müller, A. and Zenke, M. (2008). Pluripotency associated genes are reactivated by chromatin-modifying agents in neurosphere cells. *Stem Cells*, **26**, 920-926.

Sailer, M., Hazel, T., Panchison, D., Hoeppner, D., Schwabb, M. and McKay, R. (2005). BMP2 and FGF2 cooperate to induce neural crest like fates from foetal and adult CNS stem cells. *Journal of Cell Science*, **118**, 5849-5860.

Sailer, M., Gerber, A., Tostado, C., Hutter, G., Cordier, D., Mariani, L. and Ritz, M-F., (2013). Non-invasive neural stem cells become invasive *in vitro* by combined FGF2 and BMP4 signaling. *Journal of Cell Science*, **126**(16), 3533-3540.

Sandell, L. and Trainor, P. (2006). Neural crest plasticity: Size matters. *Neural Crest Induction and Differentiation*. *Advances in Experimental Medicine and Biology Vol.*

*589.* Edited by Saint-Jeannett, J-P. Springer Science and Business Media LLC, New York, USA, pp 78-95.

Santiago, A. and Erickson, C. (2002). Ephrin-B ligands play a dual role in the control of neural crest cell migration. *Development*, **129**, 3621-3632.

Sargent, T. (2006), Transcriptional regulation at the neural plate border. *Neural Crest Induction and Differentiation*. *Advances in Experimental Medicine and Biology Vol. 589.* Edited by Saint-Jeannett, J-P. Springer Science and Business Media LLC, New York, USA, pp33-44.

Saxena, S., Wahl., J., Huber-Lang, M., Stadel, D., Braubach, P., Debatin, K-M . and Beltinger, C. (2103). Generation of murine sympathoadrenergic progenitor-like cells from embryonic stem cells and postnatal adrenal glands. *PloS One*, **8**(5), e64454.

Scaper, S., (2013). The neurotrophin family of neurotrophic receptors: An overview. *Neurotrophic Factors: Methods and Protocols. Methods in Molecular Biology 846.* Edited by Scaper, S. Humana Press. New York. USA. pp1-12.

Scarpa, E., Szabó, A., Bibonne, A., Theveneau, E., Parsons, M. and Mayor, R. (2015). Cadherin switch during EMT in neural crest cells leads to contact inhibition of locomotion via repolarisation of forces. *Developmental Cell*, **34**, 421-434.

Scelfo. B., Politi, M., Reniero, F., Palosaari, T., Whelan, M. and Zalvídar, J-M. (2012). Application of multielectrode array (MEA) chips for the evaluation of mixtures neurotoxicology. *Toxicology*, **299**, 172-183.

Scheubert, L., Schmidt, R., Repsilber, D., Luštrek, M. and Fuellen, G. (2011). Learning biomarkers of pluripotent stem cells in mouse. *DNA Research*, **18**, 233-251.

Schiffmacher, A., Padmanabhan, R., Jhingory, S. and Taneyhill, L. (2014). Cadherin-6B is proteolytically processed during epithelial-to-mesenchymal transitions of the cranial neural crest. *Molecular Biology of the Cell,* **25**, 41-54.

Schilling, T. and Le Pabic, P. (2014) Neural crest cells in craniofacial skeletal development. *Neural Crest Stem Cells. Evolution, Development and* Disease, Trainor, P (Ed), Elsevier, USA. pp 89-100.

Schwartz, D., Varum, S., Zemke, M., Schöler, A., Baggiolini, A., Draganova., K., Koseki, H., Scübeler, D. and Sommer, L. (2014). Ezh2 is required for neural crest-derived cartilage and bone formation. *Development*, **141**(4), 867-877.

Scott, C., Wynn., S., Sesay, A., Cruz, C., Cheung, M., Gaviro, MV., Booth, S., Gao, B., Cheah, C., Lovel-Badges, R. and Briscoe, J. (2010). SOX9 induces and maintains neural stem cells. *Nature Neuroscience*, **13**, 1181-1189.

Seo, J., Park, D., Hong, M. and Choi, S. (2013). Essential role of AWP1 in neural cret specification in Xenopus. *International Journal of Developmental Biology,* **57**(11), 829-836.

Shimada, T., Takai, Y., Shinohara, K., Yamasaki, A., Tominaga-Yoshino, K., Ogura, A., Toi, A., Asano, K., Shintani, N., Hiyata-Takano, A., Baba, A and Hashimoto, H. (2012). A simplified method to generate seratonergic neurons from mouse embryonic stem cells and induced pluripotent stem cells. *Journal of Neurochemistry*, **122**, 81-93.

Shulz, Y., Wehner, P., Optiz, L., Salinas-Riester, G., Bongers, E., van Ravenswaaij, C., Wincent, J., Schoumanns, J., Kohlhase, J., Borchers, A. and Paulie, S. (2014). Chd7, the gene mutated in CHARGE syndrome, regulates genes involved in neural crest cell guidance. *Human Genetics,* **133**, 997-1009.

Simões-Costa, M. and Bronner. (2013). Insights into neural crest development and evolution from genomic analysis. *Genome Research, **23**,* 1069-1080.

Stemmer, V., de Craene, B., Berx, G. and Behrens, G. (2008). Snail promotes Wnt target gene expression and interacts with Beta-catenin. *Oncogene,* **27**, 5075-5080.

Stoleru, B., Popescu, A., Tache, D., Neamtu, O., Emami, G., Tataranu, L., Buteica, A., Dricu, A. and Purcaru, S. (2013). Tropomyosin-receptor-kinases signalling in the nervous system. *Maedica – a Journal of Clinical Medicine*, **8**(1), 43-48.

Strobl—Mazzulla, P. and Bronner, M. (2014). Epigenetic regulation of neural crest stem cells. *Neural Crest Cells. Evolution Development and Disease.* Edited by Trainor, P. Elsevier, London, UK. pp 89-97.

Stucky, C. and Koltzenburg, M. (1997). The low-affinity neurotrophin receptor p75 regulates the function but not the selective survival of specific subpopulations of sensory neurons. *The Journal of Neuroscience,* **17**(11), 4398-4405.

Swenson, R. (2006). *Review of Clinical and Functional Neuroscience - Swenson.* Hanover: Dartmouth Medical School, New Hampshire,USA.

Takahashi, K. and Yamanaka, S. (2006). Induction of pluripotent stem cells from mouse embryonic and adult fibroblast cultures by defined factors. *Cell*, **126**, 663-676.

Takahashi, K., Tanabe, K., Ohnuki, M., Narita, M., Ichisaka, T., Tomoda, K. and Yamanaka, S. (2007). Induction of pluripotent stem cells from adult human fibroblasts by defined factors. *Cell,* **131**, 1-12.

Takao, Y., Yokota, Y. and Koide, H. (2007). Beta-catenin up-regulates Nanog expression through interaction with Oct-3/4 in embryonic stem cells. *Biochemical and Biophysical Research Communications,* **353**, 699-705.

Tamm, C., Galitó, S. and Annerén, C. (2013). A comparative study for mouse embryonic stem cell culturing. *PLOS One*, **8**(2), 81156-81166.

Tanimoto, Y., Yokozeki, M., Hiura, K., Matsumoto, K., Nakanishi, H., Matsumoto, T., Marie, P. and Moriyama, K. (2004). A soluble form of fibroblast growth factor receptor 2 (FGFR2) with a S252W mutation acts as an efficient inhibitor for the advanced osteoblastic fifferentiation caused by FGFR2 in Apert syndrome. *The Journal of Biological Chemistry,* **279**(44), 45926-45434.

Taveggla, C., Zanazzi, G., Petrylak, A., Yano, H., Rosenbiuth, J., Einheber, R., Xu, X., Esper, R., Loeb, J., Shrager, P., Chao, M., Fallis, D., Role, L. and Saizer, J. (2005). Neuregulin-1 type III determines the ensheathment fate of axons. *Neuron,* 47, 681-694.

Teng., L. and Labosky. P. (2006). *Neural Crest Induction and Differentiation*. *Advances in Experimental Medicine and Biology Vol. 589.* Edited by Saint-Jeannett, J-P. Springer Science and Business Media LLC, New York, USA, pp 206-212.

Theveneau, E. and Mayer, R. (2012). Neural crest delamination and migration: From epithelium-to-mesenchymal transition to collective cell migration. *Developmental Biology*, **366**, 34-54.

Thompson, K., Pine, P., Rosenzweig, B., Turpaz, Y. and Retief, J. (2007). Characterization of the effect of sample quality on high density oligonucleotide microarray data using progressively degraded rat liver RNA.

Tien, C-L., jones, A., Wang, H., Gerigk, M., Nozell, S. and Chang, C. (2015). Snail2/Slug cooperates with Polycomb repressive complex 2 (PRC2) to regulate neural crest development. *Development*, **142**, 722-731.

Thomson, J., Itskovitz-Eldor, J., Shapiro, S., Waknitz, M., Swiergiel, J., Marshall, V. and Jones, J. (1998). Embryonic stem cell lines derived from human blastocysts. *Science,* **282**(5395), 1145-1147.

Tortora, G. and Derrickson, B. (2006). Principles of Anatomy and Physiology 11th Edition. JohnWiley and Sons Inc. Danvers, USA. p70, 414-424.

Torres, J., Prieto, J., Durupt, F., Broad, S. and Watt, F. (2012). Efficient differentiation of embryonic stem cells into mesodermal precursors by BMP, retinoic acid and notch signalling. *PLoS One*, **7**(4), e36405.

Trainor, P. (2010). Craniofacial birth defects; The role of neural crest cells in the etiology and pathogenesis of Treacher-Collins syndrome and the potential for prevention. *American Journal of Medical Genetics,* Volume **152**(12), 2984-2993.

Tung, P-Y., Variakhanova, N., and Knoepfler, P. (2013) Identification of DPPA4 and DPPA2 as a novel family of pluripotency-related oncogenes. *Stem Cells*, **31**(11), 2330-2342.

Uriu, K., Morelli, L. and Oates, A. (2014). Interplay between cellular signalling and cell movement in development. *Seminars in Cell and Developmental Biology*, **35,** 66-72.

van Bezooijen, R., Roelan, B., Visser, A., van der Wee-Pals, L., de Wilt, E., Karperien, M., Hamersma, H., Papapoulos, S., ten Dijke, P. and Löwick, W. (2005). Sclerostin is an osteocyte-expressed negative regulator of bone formation but not a classical BMP-4 antagonist. *The Journal of Experimental Medicine*, **199**(6), 805-814.

van De Putte, T., Maruhashi, M., Francis, A., Nelles, L., Kondoh, H., Huylebroeck, D and Higashi, Y. (2003). Mice lacking Zfhx1b, the gene that codes for SMAD-interacting protein-1, reveal a role for multiple neural crest cell defect in the etiology of Hirschsprung disease-mental retardation syndrome. *American Journal of Human Genetics,* **72**, 465-470.

van Noostrand, J., Brady, C., Jung, H., Fuentes, D., Kozak., Johnson, T., Lin., C-Y., Lin, C-J., Swiderski, D., Vogel, H., Bernstein, J., Attié-Bitach, T., Chang, C-P., Wysoka, J., Martin, D and Attard, L. (2015). Inappropriate p53 activation during development induces features of CHARGE syndrome. *Nature*, **514**(7521), 228-232.

Varga, A. and Wrana, (2005). The disparate role of BMP-4 in stem cell biology. *Oncogene*, (**24**), 37, 5713-5721.

Wakayama, T., Rodriguez, I., Perry, A., Yanagimachi, R. and Mombaerts, P. (1999). Mice cloned from embryonic stem cells. *PNAS, **96**(26), 14984-14989.*

Wang, A., Tang, Z., Park. I-H., Zhu, Y., Patel, S., Daley, G. and Song, L. (2011). Induced pluripotent stem cells for neural tissue engineering. *Biomaterials*, **32**(22), 5023-5032.

Wang, C., Huang, Y. and dai, W. (2015). Tumour suppression function of FoxD3 in lung cancer. *Irish journal of Medical Science*, (article in press, available on-line ahead of publication)

Wang, W., Tan, X., Zhou, L., Gao, F. and Dai, X. (2010). Involvement of the expression and redistribution of *claudin-23* in pancreatic cancer cell dissociation. *Molecular Medicine Reports*, **3**, 845-850.

Wang, Y., Xiao, R., Yang, F., Karim, B., Iacovelli, A., Cai, J., Lerner, C., Richtsmeier, J., Leszi, J., Hill, C., Yu, K., Ornitz, D., Eliseeff, J., Huso, D. and Jabs, E. (2005). Abnormalities in cartilage and bone development in the Apert syndrome FGFR2$^{+/S252W}$ mouse. *Development and Disease*, **132**(15), 3537-3548.

Wang, Z., Oron, E., Nelson, B. Razis, S. and Ivanova, N. (2012) Distinct lineage specification roles for Nanog, Oct4 and Sox2 in human embryonic stem cells. *Cell Stem Cell*, **10**, 440-454.

Weinstein, D., Laeninger, J., Hamby, C. and Safai, B. (2014) Diagnostic and prognostic biomarkers in melanoma. *Journal of Clinical and Aesthetic Dermatology*, **7**(6), 13-24.

Wegner, N. and Stolt, C. (2005). From stem cells to neurons and glia: a Soxist's view of neural development. *Trends in Neurosciences,* **28**(11), 583-588.

Wijgerde, M., Karp, S., Mcmahon, J. and Mcmahon, A. (2005). Noggin antagonism of BMP4 controls the development of the axial skeleton in the mouse. *Developmental Biology*. **286**, 149-157.

Williams, R., Hilton, D., Pease, S., Wilson, T., Stewart, C., Gearing, D., Wagner, E., Metcalf, D., Nicola, N. and Gough, N. (1988). Myeloid leukaemia inhibitory factor maintains the developmental potential of embryonic stem cells. *Nature*, **366** (2000), 684-686.

Wiszniak, S., Kabbara, S., Lumb, R., Schera, M., Secker, G., Harvey, N., Kumar, S. and Schwarz, Q. (2013). The ubiquitin ligase Nedd4 regulates craniofacial development by promoting cranial neural crest cell survival and stem cell-like properties. *Developmental Biology*, **383**, 186-200.

Wiszniak, S. and Schwartz, Q. (2014) Neural crest cells in vascular development. *Neural Crest Cells. Evolution Development and Disease.* Edited by Trainor, P. Elsevier, London, UK. pp314-331.

Wolffe, A., Jones, P. and Wade, P. (1999). DNA demethylation. *PNAS,* **96**(11), 5894-5896.

Wong, C., Paratore, C., Dours-Zimmerma, M., Rochat, A., Pietri, T., Suter, U., Zimmerman, D., Dufour, S., Thiery, J., Meijer, D., Beermann, F., Barrandon, Y.and Somer, L. (2006). Neural-crest derived cells with stem cell features can be traced back to multiple lineages in the adult skin. *The Journal of Cell Biology*, **175**(6), 1005-1015.

Wrighton, K., Lin, X. and Feng, X-H. (2009). Phospho-control of TGF-β superfamily signalling. *Cell Research*, 19(1), 8-20.

Wu, C. (1997). Chromatin remodelling and the control of gene expression. *The Journal of Biological Chemistry*, **272**(45), 28710-28714.

Wu, M., Li, J., Engleka, K., Zhou, B., Lu, M., Plotkin, J. and Epstein, J. (2008). Persistent expression of Pax3 in the neural crest causes cleft palate and defective osteogenesis in mice. *The Journal of Clinical Investigation*, **118**(6), 2076-2087.

Wynn, M., Rupp, P., Trainor, P., Schnell, S.and Kulesa, P. (2013). Follow-the-leader cell migration requires biased cell-cell contact and local microenvironmental signals. *Physical Biology*, **10**(3), 1-17.

Xu, R-H., Sampsell-Barron, T., Gu, F., Root, S., Peck, R., Pan, G., Yu, J., Antosiewicz-Bourget, J., Tian, S., Stewart, R. and Thomson, J. (2008). NANOG is a direct target of TGFβ/Activin-mediated SMAD signalling in human ESCs. *Cell Stem Cell*, **3**, 196-206.

Xu, X., Smorag, L., Nakamura, T., Kimura, T., Dressel, R., Fitzner, A., Tan, X., Linke, M., Zechne, U., Engel, W. and Pantakani, D. (2015) *Dppa3* expression is critical for generation of fully reprogrammed iPS cells and maintenance of *Dlk-Dio3* imprinting. *Nature Communications*, **6**, 1-11.

Yang, F.-C., Tan, T., Huang, T., Christianson, J., Samad, O., Liu, Y., *et al*. (2013). Genetic control of the segregation of pain-related sensory neurons innervating the cutaneious versus deep tissues . *Cell Reports,**5***, 1353-1364.

Ybot-Gonzalez, P., Gaston-Massuet, C., Girdler, G., Klingersmith, J., Arkell, R., Greene, N. and Copp, A. (2007). Neural plate morphogenesis during mouse neurulation is regulated by antagonism of Bmp signalling. *Development,* **134**, 3203-3211.

Ying, Q-L., Nichols, J., Chambers, I. and Smith, A. (2003). BMP induction of Id proteins supresses differentiation and sustains embryonic stem cell self-renewal in collaboration with Stat3. *Cell,* **115**, 281-292.

Yoshida-Noro, C., Heasman, J., Goldstone, K., Vickers, L. and Wylie, C. (1999). Expression of the Lewis group carbohydrate antigens during Xenopus development. *Glycobiology,* **9**(12), 1323-1330.

Young, H., Bergner, A., Simpson, M., McKeown, S., Hao, M., Anderson, C. and Enomoto, H.(2014). Colonising while migrating: How do individual enteric neural crest cells behave? *BMC Biology,* **12**(23), 1-18.

Zanin, J., Battiato, L. and Rovasio, R. (2013). Neurotrophic factor NT-3 displays a non-canonical cell guidance signalling function for cephalic neural crest stem cells.. *European Journal of Cell Biology,* **92**(8-9), 264-279.

Zhang, C., Atasoy, D., Arac, D., Yang, X., Fucillo. M., Robinson, A., Ko, J., Brunger, A. and Südhof, T. (2010). Neurexins physically and functionally interact with GABA(A) receptors. *Neuron*, **66**(13), 403-416.

Zhang, J and Li, L. (2005). BMP signalling and stem cell regulation. *Developmental Biology*, **284**, 1-11.

Zhang, J., Fei, T., Li, Z., Zhu, G. Wang, L. and Chen, Y-G. (2013). BMP induces cochlin expression to facilitate self-renewal and suppress neural differentiation of mouse embryonic stem cells. *The Journal of Biological Chemistry*, **288** (12), 8053-8060.

Zhang, Y., Pak, C., Han, Y., Ahlenius, H., Zhang, Z., Chanda, S., Marro, S., Patzke, C., Acuna, C., Covy, J., Xu, W., Yang, N., Danko, T., Chen, L., Wernig, N. and Südhof, T. (2014). Rapid single-step induction of functional neurons from human pluripotent stem cells. *Neuron*, **78**(5), 785-798.

Zhou, Z., Qin, J., Tang, J., Li, B., Geng, Q., Jiang, W., Wu, W., Rehan, V., Tang, W., Xu, X. and Xia, Y. (2013). Down-regulation of MeCP2 in Hirchsprung's disease. *Journal of Pediatric Surgery,* **48**, 2099-2105.

# Appendix 1: Buffers and Solutions

**6x DNA loading Dye**
10 mM Tris-HCl (pH 7.6)
0.03% bromophenol blue
0.03% xylene cyanol FF
0.15% orange G
60% (v/v in deionised water) glycerol
60 mM EDTA.
Dilute to 2x with deionised water for usage

**Electrophoresis buffer**
6.01g Tris Base
2.0 g SDS
28.84 g glycine
Add deionised water to a final volume of 2 l

**Laemmli sample buffer (2x)**
1.51 g Tris-base
20 ml glycerol
4g SDS
0.02g bromophenol blue
Add 70 ml deionised water, adjust pH to 6.8. Add deoinised water to a final volume of 100 ml

**MACS Washing Buffer**
100 ml sterile PBS
0.5 g bovine serum albumin
0.12 g EDTA

**PBS**
Add 1 PBS tablet per 100 ml deionised water and autoclave for 10 minutes at 115°C

**PBS-Tween**
To 1 l of PBS, add 0.5 ml of Tween-20 and mix on a magnetic stirrer at room temperature

**RIPA lysis buffer**
3.94g Tris-HCl
8.77 NaCl
5g Sodium deoxycholate
5g SDS
0.37 g EDTA
0.18 g EGTA
10 ml Triton X-100
Add 800 ml of deionised water, adjust pH to 7.5 add 0.17g PMSF. Before use, add protease inhibitor cocktail (1:100)

**Separating buffer**
45.5g Tris-base
1g SDS
Add 200 ml deionised water, adjust pH to 8.8. Add deionised water to a final volume of 250 ml

**Stacking buffer**
15 g Tris-base
1g SDS
Add 200 ml deionised water. Adjust pH to 6.8. Add deionised water to 250 ml

**TBE Buffer (10x)**
54.5 g Tris base
27.5 g Boric acid
2.375g EDTA
Add 400 ml deionised water, adjust pH to 8.3. Add deionised water for a final volume of 500 ml

**TBS-Tween**
1.211 Tris-base
8.18 NaCl
1 ml Tween-20
Add 900 ml deionised water, adjust pH to 7.4. Add deionised water to a final volume of 1 l

**Towbin buffer**
1.51 g Tris-base
7.2 g Glycine
0.167 g SDS
Add to 400 ml of deionised water, add 75 ml methanol. Adjust pH to 8.3. Add deionised water to a final volume of 500 m

## Appendix 2: PCR Primer Sets

| Gene | Forward 5'-3' | Reverse 5'-3' | Amplicon size (bp) | Annealing temp. (°C)/time (s) | Number of cycles |
|---|---|---|---|---|---|
| *NCAM* | cgccgctgacagaacccgaaa | ccagagtgccacactccgca | 806 | 61/15 | 32 |
| *CD325* | gctcactgctcaggaccccg | ggcgctctttatcccgccgt | 707 | 61/15 | 32 |
| *Tudor domain containing 12* | agcacacggagaagtgtactg | agccgttcttctcgtcacag | 165 | 61/30 | 35 |
| *Oct-4* | ggatggcatactgtggacct | tttcatgtcctgggactcctcg | 200 | 60/30 | 35 |
| *Dppa2* | tgagtacggatggcaagaaagt | ggcccgattcctctgaagac | 151 | 61/30 | 35 |
| *Dppa3* | gccgtacctgtggagaacaa | tcactgtcccgttcaaactca | 182 | 60/30 | 35 |
| *Dppa4* | tgagcagcaaaggccagaaat | ctgtcttcaacctggcgtct | 120 | 61/30 | 35 |
| *Dppa5* | ccgtgggtgaaagttcctga | ccctgtgggccaaacagata | 89 | 61/30 | 35 |
| *Nanog* | gacaagggccctgaggaggagg | ccgttccaggactgagcggt | 150 | 61/30 | 35 |
| *Nestin* | tttcctgaccccaagctgaag | aggctgtcacaggagtctca | 136 | 62/30 | 36 |
| *Pax3* | aggaaacaagctggagccaa | gatctgacacggcttgtgga | 148 | 62/15 | 40 |
| *Sox9* | gccacggaacagactcacat | cctgagattgcccagagtgc | 124 | 63/15 | 40 |
| *Musashi-1* | gttccaagccacgacctacg | cacggaattcggggaactgg | 80 | 62/30 | 36 |
| *E-Cadherin* | aacccaagcacgtatcaggg | gagtgttgggggcatcatca | 94 | 60/30 | 40 |
| *Sonic hedgehog* | agctgacccctttagc | ttgcacctctgagtcatcagc | 196 | 61/30 | 40 |
| *SMAD1* | cagaggagatgttcaggcagt | ccggttaacgttggagagca | 190 | 60/30 | 32 |
| *Neuroligin1* | cctggtctgacatccggaac | cccgaatatcatcttcagttggg | 195 | 61/30 | 40 |
| *Neuroligin3* | gaagatggatccggcgctaa | acgatgacgttgccgtaact | 185 | 61/30 | 40 |
| *Pou3f4* | gtatggcaacgtgttctcgc | cgggcttcctgtggatgaat | 133 | 61/30 | 40 |
| *Pou4f2* | ttccaaccccaccgagcaat | tactctgggagacgatgtcca | 96 | 61/30 | 40 |
| *Claudin1** | actccttgctgaatctgaacagt | ggacacaaagattgcgatcag | 92 | 61/30 | 35 |
| *Claudin23** | aggtcaagccttcctttctg | ccttaaaagataaatgaacccaacc | 71 | 61/30 | 35 |

| Gene | Forward 5'-3' | Reverse 5'-3' | Amplicon size (bp) | Annealing temp. (°C)/time (s) | Number of cycles |
|---|---|---|---|---|---|
| *TrKA* | acaacgggaactacaccctg | tgtgctgttaccgtccactg | 146 | 60/30 | 35 |
| *TrKC* | tggcttcccagcactttgta | gtgtgtcctcccaccctgta | 139 | 60/30 | 35 |
| *Runx1* | agtcgttcatgagagatgcca | gtggtcagctagtacctccac | 173 | 63/15 | 35 |
| *Runx3* | atggcttccaacagcatcttt | ctggtgctcgggtctcgtat | 71 | 60/30 | 35 |
| β-*Actin* ** | agagaagctgtgctatgttg | ctcgttgccaatagtgatga | 150 | 61/30 | 25 |
| 18s Ribosomal RNA* | aaatcagttatggttcttttggtc | gctctagaattaccacagttattcaa | 100 | 61/30 | 25 |

Primers marked * were donated by Dr. Qiuyu Wang (School of Healthcare Sciences, Manchester Metropolitan University), Sequences for primers marked ** were developed and provided by the real time primer database (http://www.rtprimerdb.org) (accessed 25-7-12). All other primer sets were designed using the NCBI primer design tool (http://www.ncbi.nlm.nih.gov/tools/primer-blast) (accessed between 7-12 and 9-14).

## Appendix 3: Cell Representative Cell Cycle Histograms and Calculations

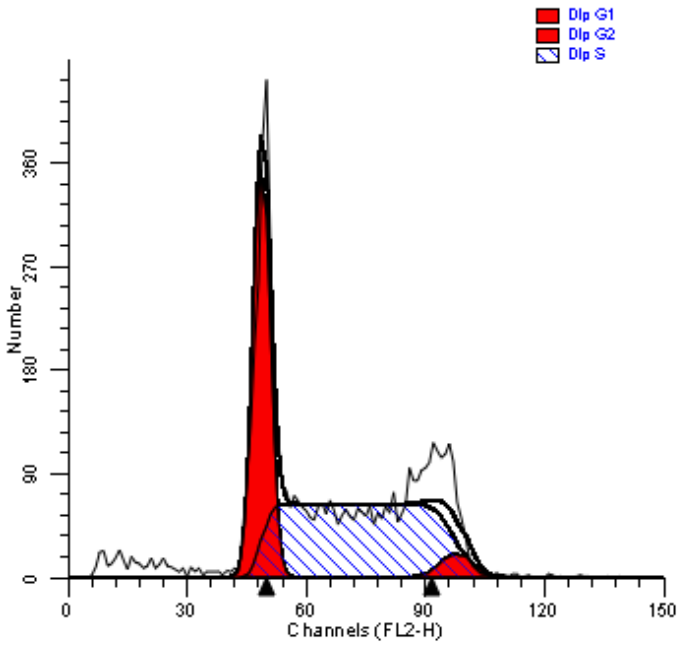


Cells after stage 2 (14 days total treatment). Stage 2 was carried out with PIM

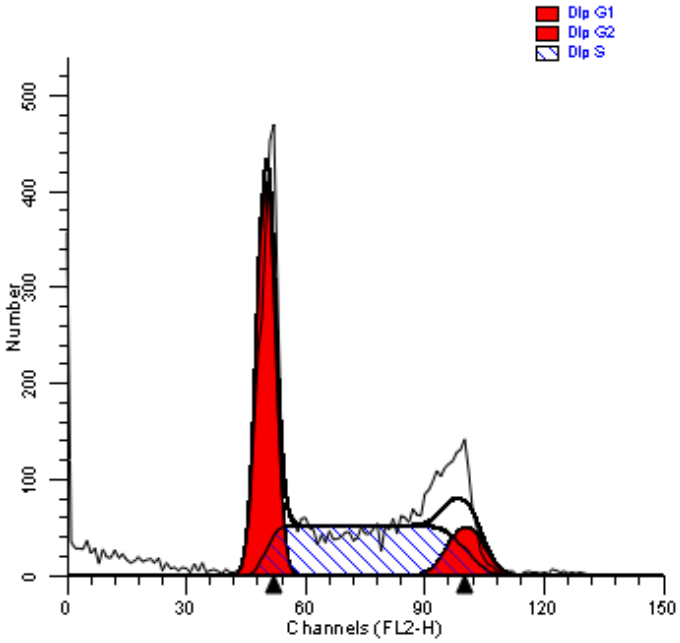


Cells after stage 2 (14 days total treatment). Stage 2 was carried out with SIM

**Example Doubling Time Calculation:**

Doubling time is calculated using the formula:

$$\frac{t_2 - t_1}{(\log(n_2) - \log(n_1)) \times 3.32}$$

Where: $n_1$ = cell count time point 1, $n_2$ = cell count time point 2, $t_1$ = time point 1 (days) $t_2$ = time point 2 (days).

If cell counts at 0 and 3 days were determined to be 25000 and 139000 cells respectively doubling time would equate to:

$$\frac{3\text{-}0}{(\log(139000) - \log(25000)) \times 3.32} =$$

$$\frac{3}{(5.14 - 4.40)*3.32} =$$

$$\frac{3}{2.47} = 1.21 \text{ days}$$

# Appendix 4: Microarray Analysis of *Claudin* and *Cadherin* Expression

Gene expression was measured by microarray analysis (section 2.16). Expression of selected gene families was calculated compared to embryonic stem cells at three stages; stage 1 (initially differentiating cells), stage 2 (neural crest cells) and stage 3. The effects of BMP-4 during differentiation between stage 1 and 2 was assessed at the start (1 hour) and end (10 days) of this stage. Expression level analyses of the *Claudin* and *Cadherin* families of adhesion protein coding genes was carried out. Differential expression was observed in a number of genes from both families, both across the differentiation program and mediated by BMP-4 during stage 2 (Figs A1-A4). The regulation of adhesion molecules by BMP-4 appears to be intrinsic to neural crest patterning and migration and further studies to examine these effects in greater detail would be beneficial.

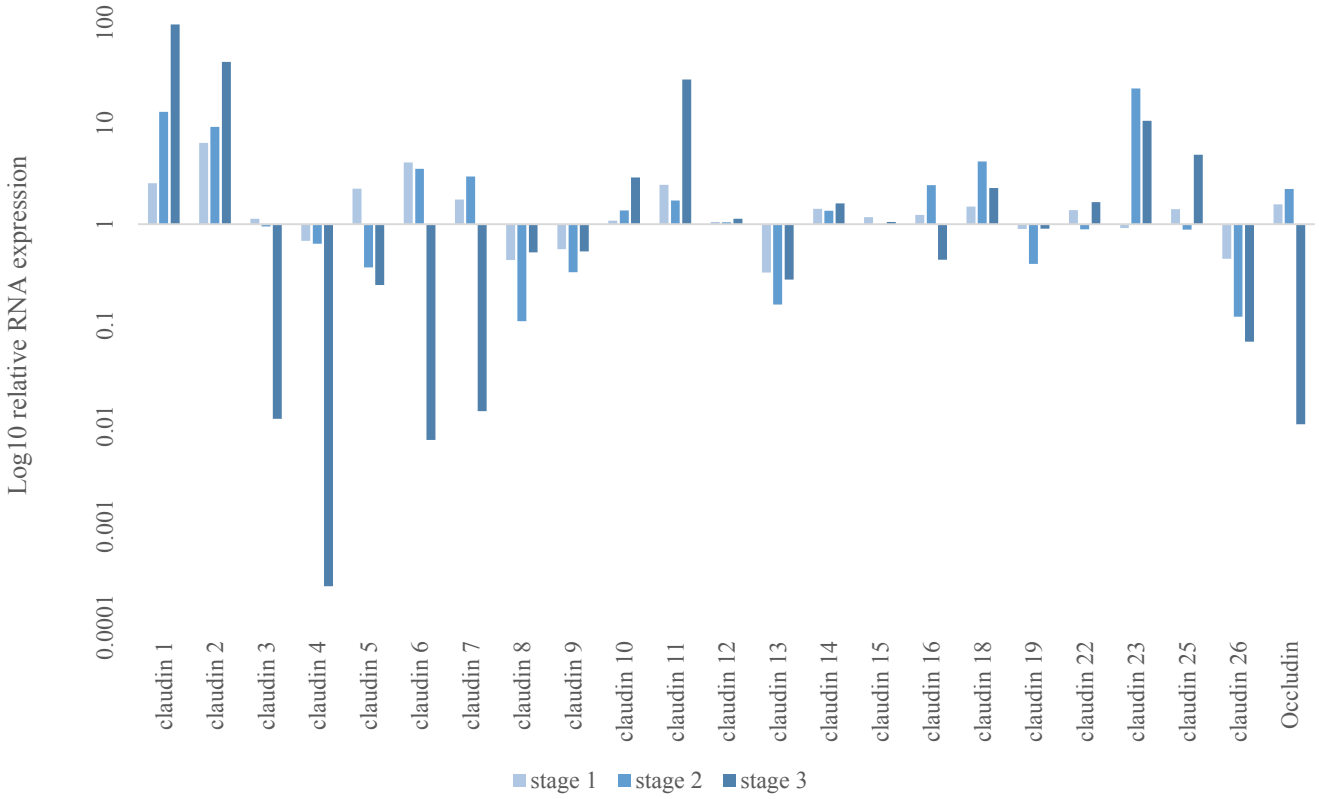


**Figure A1. *Claudin* expression during peripheral neuron differentiation from mouse embryonic stem cells**. Expression profiles of the tight junction associated *Claudin* genes and the closely related *Occludin* showed high levels of variability following microarray analysis.

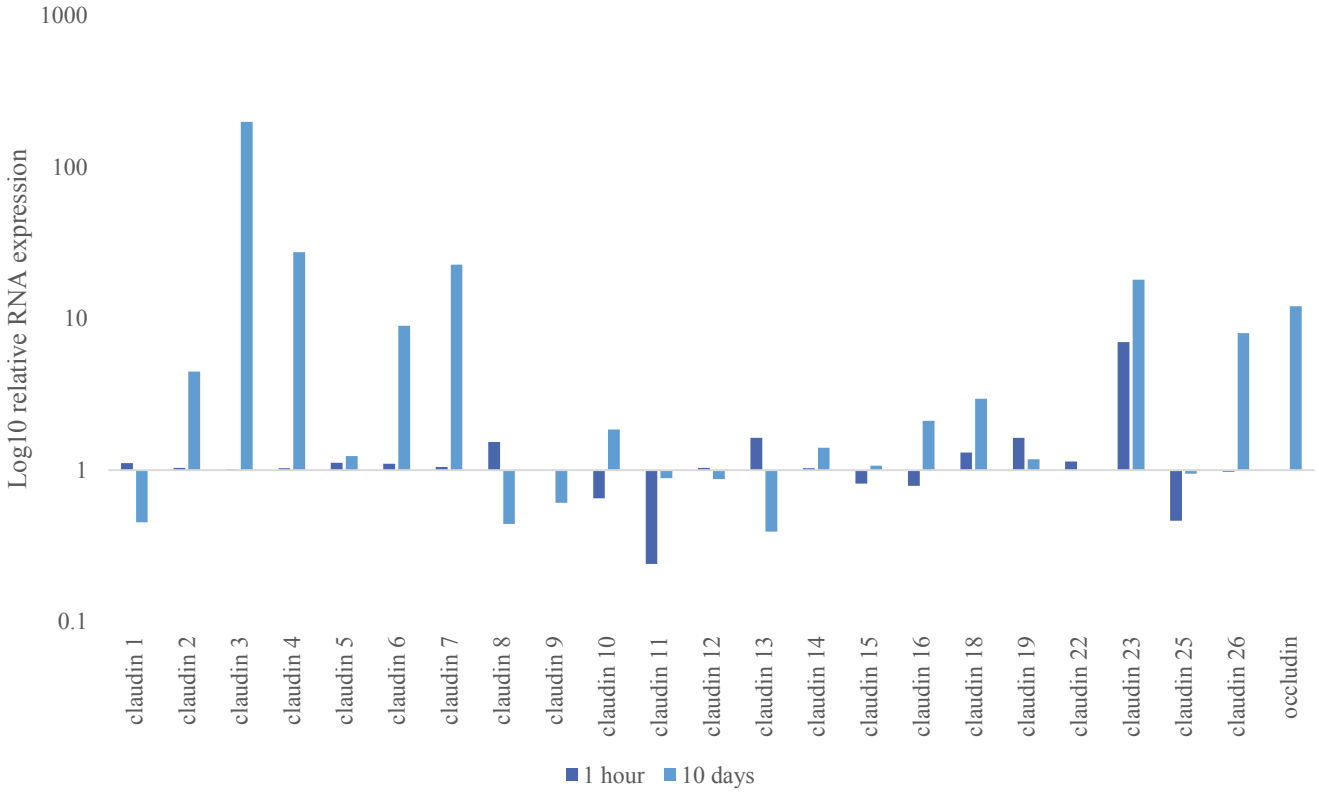


**Figure A2. BMP-4 supplementation altered expression of *Claudins* in stage 2 differentiating cells.** Supplementation positively regulated 12 of 23 genes assayed after 10 days while negatively regulating 3.

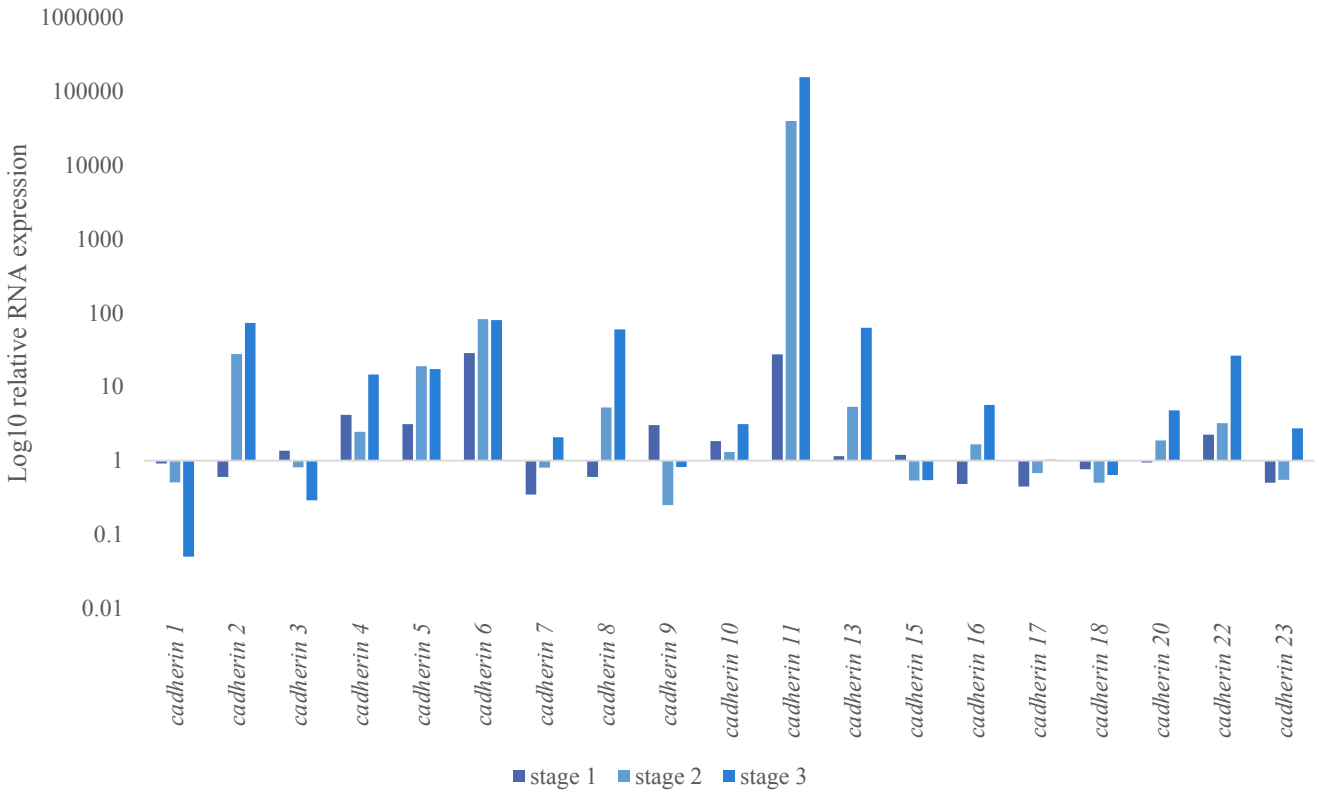


**Figure A3. *Cadherin* expression during peripheral neuron differentiation from mouse embryonic stem cells**. Expression profiles of the adhesion protein coding *Cadherin* gene family were positively regulated in 11 of 19 probes tested.

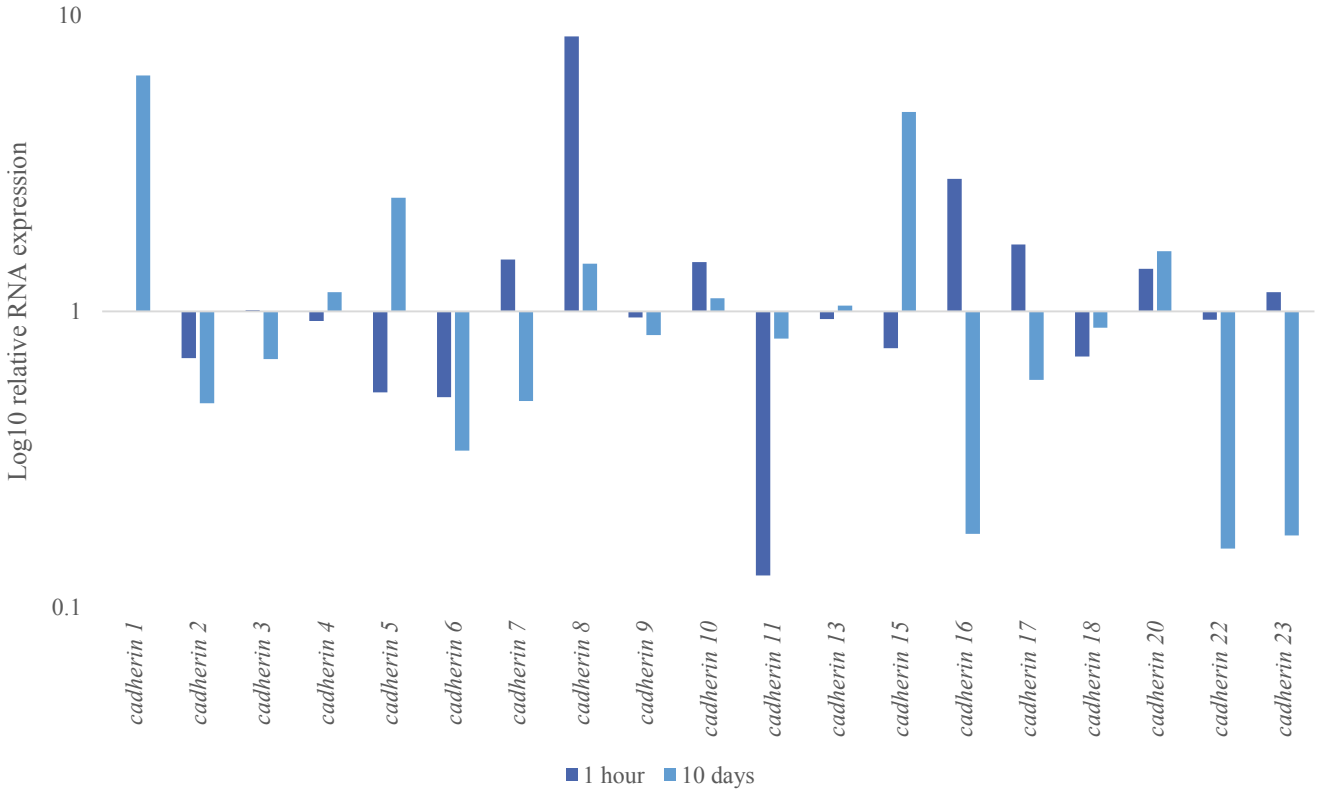


**Figure A2. BMP-4 supplementation altered expression of *Cadherins* in stage 2 differentiating cells.** Supplementation positively regulated 3 of 19 genes assayed after 10 days while negatively regulating 10.

## Appendix 5: Microarray Analysis of Trunk and Cranial Neural Crest Markers

**Table A1**. **Cranial and trunk neural crest biomarker expression.** Neuronal associated markers were upregulated during differentiation of E14 murine embryonic stem cells into peripheral neurons. Gene expression of cranial neural crest associated genes did not change. Trunk neural crest biomarkers

| Gene | Region | Upregulated by BMP-4 | Downregulated by BMP-4 | Unchanged by BMP-4 | Upregulated after BMP-4 withdrawal | Downregulated after BMP-4 withdrawal | Unchanged by BMP-4 withdrawal |
|---|---|---|---|---|---|---|---|
| *Hox genes* | Cranial | | | x | | | x |
| *Melan-A* | Crainial | | | x | | | x |
| *Mitf* | Cranial | | | x | | | x |
| *Vimentin* | Trunk | x | | | | | x |
| *GFAP* | Trunk | | | x | x | | |
| *p0* | Trunk | x | | | x | | |
| *S100β* | Trunk | x | | | x | | |
| *GAP43* | Trunk | x | | | x | | |
| *F-spondin* | Trunk | x | | | x | | |
| *Lbx1* | Trunk | | | x | | x | |
| *ET-1* | Trunk | | | x | | x | |
| *ET-A* | Trunk | | | x | | x | |

d